Hybrid High-Order methods for complex problems in fluid mechanics

André Harnist

THÈSE POUR OBTENIR LE GRADE DE DOCTEUR DE L'UNIVERSITÉ DE MONTPELLIER

En Mathématiques et Modélisation

École doctorale I2S - Information, Structures, Systèmes

Unité de recherche IMAG - Institut Montpelliérain Alexander Grothendieck

Méthodes Hybrid High-Order pour des problèmes complexes en mécanique des fluides

Présentée par André HARNIST

Le 11 octobre 2021

Sous la direction de Daniele A. DI PIETRO

Devant le jury composé de

Daniele A. DI PIETRO	Professeur des universités	Université de Montpellier	Directeur
Jérôme DRONIOU	Professeur des universités	Monash University	Examinateur
Stella KRELL	Maître de conférences	Université de Nice	Examinatrice
Pauline LAFITTE	Professeure des universités	Université Paris-Saclay	Présidente du jury
Marco VERANI	Full Professor	Politecnico di Milano	Rapporteur
Martin VOHRALÍK	Directeur de recherche	INRIA de Paris	Rapporteur

UNIVERSITÉ DE MONTPELLIER

Résumé

Les travaux de cette thèse portent sur le développement et l'analyse de méthodes de discrétisation Hybrides d'Ordre Élevé (HHO : Hybrid High-Order, en anglais) pour des problèmes complexes en mécanique des fluides. Les méthodes HHO sont une nouvelle classe de méthodes de discrétisation des EDPs, capable de gérer des maillages polytopiques généraux. Nous nous intéressons aux problèmes faisant intervenir des fluides non-newtoniens, plus précisément dans un cadre non-hilbertien. L'objectif est de généraliser des théorèmes d'analyse fonctionnelle discrète au cas non-hilbertien afin d'établir des résultats de bonne position, de convergence par compacité, et des estimations d'erreur pour les méthodes HHO. Trois problèmes principaux sont étudiés pour lesquels nous développons, analysons et illustrons numériquement une méthode HHO. Le premier porte sur les équations de Stokes généralisées aux fluides non-newtoniens, pouvant considérer des fluides caractérisés par des lois en puissance ou de Carreau–Yasuda. Dans l'analyse, nous introduisons la notion de fonction encadrée permettant de gérer la non-linéarité du problème. De plus, nous généralisons au cadre non-hilbertien une inégalité de Korn discrète afin d'obtenir la bonne position du problème, ainsi qu'une estimation d'erreur. Le second problème concerne les problèmes de Leray–Lions, dont un exemple classique est celui du p-Laplacien. Dans le cas où $p < 2$, des dégénérescences locales peuvent apparaître lorsque le gradient de la solution s'annule ou explose. Dans ce travail, nous établissons de nouvelles estimations d'erreur offrant des ordres de convergence allant de $(k+1)(p-1)$ à $k+1$ selon la dégénérescence du problème, où k correspond au degré polynomial de la méthode. Le troisième problème porte sur les équations de Navier–Stokes, généralisées aux fluides non-newtoniens incompressibles, dont leur convection peut suivre une loi en puissance. Nous introduisons deux exposants de Sobolev caractérisant le comportement de loi en puissance des lois de viscosité et de convection du fluide. Dans ce travail, une analyse du problème continu permet de faire apparaître des relations entre ces exposants de Sobolev qui se répercutent au niveau discret. Nous établissons ainsi des résultats de convergence sous l'hypothèse de régularité minimale, ainsi qu'une estimation d'erreur pour les fluides pseudoplastiques. Enfin, nous appliquons la méthode sur le problème de la cavité entraînée, permettant d'illustrer les phénomènes engendrés par l'introduction des lois en puissances dans les termes de visqueux et convectif.

Mots-clés : méthodes Hybrides d'Ordre Élevé, fluides non-newtoniens, loi en puissance, loi de Carreau–Yasuda, fonctions encadrées, équations de Stokes généralisées, problèmes de Leray–Lions, équations de Navier–Stokes généralisées, convection régit par une loi en puissance, estimations d'erreur, convergence par compacité, problème de la cavité entraînée

Abstract

The work of this thesis focuses on the development and analysis of Hybrid High-Order (HHO) discretization methods for complex problems in fluid mechanics. HHO methods are a new class of PDEs discretization methods, capable of handling general polytopic meshes. We are interested in problems involving non-Newtonian fluids, more precisely in a non-Hilbertian structure. The objective is to generalize discrete functional analysis theorems to the non-Hilbertian case in order to establish results of good position, convergence by compactness, and error estimates for HHO methods. Three main problems are studied for which we develop, analyze and numerically illustrate a HHO method. The first concerns the Stokes equations generalized to non-Newtonian fluids, which can consider fluids characterized by power-laws or Carreau–Yasuda laws. In this analysis, we introduce the notion of power-framed function, making it possible to handle the non-linearity of the problem. In addition, we generalize a discrete Korn inequality to the non-Hilbertian case in order to obtain the good position of the problem, as well as an error estimate. The second problem concerns the Leray–Lions problems, a classic example of which is that of the p-Laplacian. In the case of $p < 2$, local degenerations can appear when the gradient of the solution vanishes or explodes. In this work, we establish new error estimates offering orders of convergence ranging from $(k+1)(p-1)$ to $k+1$ depending on the degeneration of the problem, where k corresponds to the polynomial degree of the method. The third problem concerns the Navier–Stokes equations, generalized to incompressible non-Newtonian fluids, whose convection may follow a power-law. We introduce two Sobolev exponents characterizing the power-law behavior of the viscosity and convection laws of the fluid. In this work, an analysis of the continuous problem leads to relations between these Sobolev exponents which have repercussions at the discrete level. We thus establish convergence results under minimal regularity assumptions, as well as an error estimate for pseudoplastic fluids. Finally, we apply this method to the lid-driven cavity problem, illustrating the phenomena engendered by the introduction of the power-laws in the viscous and convective terms.

Keywords: Hybrid High-Order methods, non-Newtonian fluids, power-law, Carreau–Yasuda law, framed functions, generalized Stokes equations, Leray–Lions problems, generalized Navier–Stokes equations, power-like convective behaviour, error estimates, convergence by compactness, lid-driven cavity problem

Acknowledgments

J'aimerais avant tout remercier Daniele A. Di Pietro, mon directeur de thèse, pour son soutien, son savoir et sa patience. Depuis mon stage de Master, son encadrement et ses encouragements étaient une source de motivation constante. Je lui suis profondément reconnaissant pour sa gentillesse et sa bienveillance qui ont rendu ces années exceptionnelles.

Je remercie grandement l'école doctorale I2S pour avoir financé ma thèse, en particulier Pascal Nouet pour les échanges intéressants que nous avons eus lors des conseils.

I wish to personally thank each member of the jury of my Ph.D. defense. I warmly thank Marco Verani and Martin Vohralík for accepting the heavy task of being referees, and their precious remarks which enriched this manuscript. Furthermore, I would like to thank Pauline Lafitte for accepting to preside the jury, as well as Stella Krell and Jérôme Droniou for their insightful questions and remarks.

Un grand merci à Michele Botti, Daniel Castanon Quiroz et à nouveau Jérôme Droniou, avec qui j'ai eu l'opportunité de collaborer durant cette thèse, pour leur contribution et tout ce qu'ils m'ont appris.

Je remercie chaleureusement les enseignants avec qui j'ai eu l'occasion de faire équipe lors de mes missions d'enseignement, notamment Sylvain Brochard et Matthieu Hillairet pour leur aide et précieux conseils. J'exprime également toute ma gratitude envers Gwladys Toulemonde pour m'avoir confié la responsabilité d'un enseignement et guidé dans cette expérience très enrichissante qui renforça mon désir d'enseigner.

Merci aux membres permanents de l'IMAG, Pascal Azerad, Moulay Tahar Benameur, Jean-François Crouzet, Vanessa Lleras, Bijan Mohammadi, François Vilar et bien d'autres, qui m'ont chaleureusement accueilli.

Merci aux doctorants et post-doctorants pour leur bonne humeur, leurs discussions et camaraderie, notamment Alain Berod, Francesco Bonaldi, Matthieu Faitg, Tom

Ferragut, Ilaria Fontana, Florian Miralles, Thiziri Moulla, Meriem Zefzouf, et en particulier mes co-bureaux Abdoulrahim Ibrahim, Gwenaël Peltier et Robert Rapadamnaba pour avoir entretenu une bonne ambiance pendant toutes ces années. Je remercie aussi les anciens, Jocelyn Chauvet, Gautier Dietrich et Mario Veruete, avec une mention spéciale à Florent Chave pour son aide précieuse lors du concours doctoral.

Enfin, un grand merci au personnel administratif de l'IMAG pour leur contribution indispensable au laboratoire et leur gentillesse, notamment Sophie Cazanave Pin et Brigitte Labric, ainsi que Baptiste Chapuisat, toujours présent pour résoudre mes problèmes informatiques.

J'aimerais désormais remercier les enseignants que j'ai rencontrés durant mes études et qui alimentèrent ma passion pour les Mathématiques. Je remercie les enseignants de l'Université de La Rochelle, Gilles Bailly-Maitre, Michel Berthier, Laurence Cherfils, Catherine Choquet, Antoine Colin, Abdallah El Hamidi, Noël Fraisseix, Mokhtar Kirane, Nadir Sari et Catherine Stenger ; ainsi que ceux de l'Université de Montpellier, Stéphane Baseilhac, Michele Bolognesi, Terence Bayen, Rémi Carles, Kleber Carrapatoso, Françoise Krasucki, Fabien Marche et Berardo Ruffini ; en concluant avec les formateurs du collège doctoral de l'Université de Montpellier, Sébastien Balme, Marc Dumas et Sylvain Rouanet, qui m'ont appris tout ce qu'il fallait pour pouvoir enseigner à mon tour. Merci pour vos cours, votre temps, votre pédagogie et vos conseils.

Merci à mes amis, Marwa et Mohammad, pour nos moments passés ensemble. Je vous souhaite une très bonne continuation à vous et votre adorable famille.

J'aimerais à présent remercier ma famille, mes parents bien sûr, pour tout ce qu'ils ont fait pour moi, mamie Jo, mamie Isabelle et papi François pour leurs encouragements. Enfin, je remercie du fond du cœur tonton Philippe, tata Brigitte et tonton Christophe, qui se sont portés garants pour mes logements pendant toutes ces années.

A big thank you to Lee and Louise, my awesome parents-in-law, for your unconditional support during all these years and for making me feel like a part of the family!

Finally, I would like to express all my gratitude and love to my fiancée Megan for all your help and support since our first year of university. This manuscript would not have been possible without you. I can't wait to continue our adventure together!

Contents

Introduction

Dans ce manuscrit de thèse, nous développons, analysons, et implémentons des méthodes de discrétisation Hybrides d'Ordre Élevé (HHO : Hybrid High-Order, en anglais) dans le cadre de problèmes généralisés aux fluides non-newtoniens. Par la suite, nous allons présenter l'état de l'art de la méthode HHO, ainsi qu'une introduction à sa construction et ses outils. Puis, nous décrirons le contenu et les contributions principales de chacun des chapitres de ce manuscrit.

1 Méthodes Hybrid High-Order

Les méthodes HHO, dont la construction est détaillée dans [50], sont une nouvelle famille de méthodes de discrétisation pour les Équations aux Dérivées Partielles (EDPs) ayant récemment fait leur apparition.

1.1 État de l'art

Le terme *Hybrid* fait référence au fait que la méthode possède deux types d'inconnues de polynômes localisées sur les éléments et sur les faces du maillage. Le terme *High-Order* indique la possibilité de choisir un ordre d'approximation élevé, c'est-à-dire des inconnues de polynômes de haut degré, afin d'augmenter la précision du schéma. Les deux éléments clés des méthodes HHO sont :

(i) des opérateurs différentiels discrets, définis de manière implicite à travers une intégration par parties discrètes faisant intervenir les inconnues sur les éléments et les faces;

(ii) des fonctions de stabilisation, obtenues par pénalisation de résidus d'ordre élevé, et assurant la stabilité du schéma.

Cette construction offre de nombreux avantages qui les distinguent des méthodes classiques comme les Éléments Finis et les Volumes Finis, les plus remarquables étant :

(i) la possibilité de traiter des maillages polytopiques généraux;

(ii) la possibilité d'utiliser un ordre d'approximation arbitraire;

(iii) une stabilité de la forme inf-sup pour les problèmes mixtes;

(iv) la fidélité à la physique;

(v) un coût de calcul réduit grâce à l'hybridation, la condensation statique et leur stencil compact;

(vi) une implémentation intuitive et indépendante de la dimension.

Les méthodes HHO ont connu une expansion remarquable et, depuis leurs débuts, cf. [55], de nombreux problèmes faisant intervenir des EDPs furent étudiés. Nous pouvons citer les applications traitant des écoulements incompressibles de fluides newtoniens gouvernés par les équations d'Oseen [2], de Stokes [1, 23] et de Navier–Stokes [28, 50, 62], possiblement dirigé par des forces volumétriques irrotationnelles élevées [34, 60].

Nous retrouvons également des études portant sur le problème de Brinkman [25], les équations d'advection-diffusion-réaction [51], les problèmes d'élasticité linéaire quasi-incompressible [55, 57] et non-linéaire [30], les problèmes de poroélasticité linéaire [20] et non-linéaire [29], la magnétostatique [39, 40], le problème de fracture en milieu poreux [37, 38], le problème de Cahn-Hilliard [41, 42], l'électrostatique [61, 63], les problèmes elliptiques aux interfaces [31] ou hautement oscillant [43], l'approximation spectrale d'opérateurs elliptiques [32].

Les méthodes HHO s'étendent aussi vers de nouveaux horizons avec une suite polynomiale exacte de de Rham [49, 54], des maillages courbés [24], ou encore une version hp pour diffusion variable [3].

Enfin, l'analyse de convergence du problème non-linéaire de Leray–Lions [48], ainsi que son estimation d'erreur établie dans [47], ont offert de nombreux outils aux travaux réalisés durant cette thèse.

1.2 Définitions et propriétés

Soit $d \in \mathbb{N}$, $d \geq 2$. Pour tout $X \subset \mathbb{R}^d$, nous notons h_X son *diamètre*, ∂X sa *frontière*, et $\overline{X}$ sa *fermeture*. Pour lever toute ambiguïté, nous définissons un *polytope* comme l'intérieur d'une union finie de fermetures de *simplexes* de $\mathbb{R}^d$. Dans la suite, nous considérons un polytope Ω de $\mathbb{R}^d$.

1.2.1 Suite de maillage régulière

Définition 1 (Maillage polytopal)**.** Un *maillage polytopal* de Ω est un couple $\mathcal{M}_h := (\mathcal{T}_h, \mathcal{F}_h)$ où :

(i) L'ensemble des *éléments* $\mathcal{T}_h$ est une famille finie de polytopes non vides, disjoints deux à deux, vérifiant

$$h = \max_{T\in\mathcal{T}_h} h_T, \qquad \overline{\Omega} = \bigcup_{T\in\mathcal{T}_h} \overline{T}.$$

(ii) L'ensemble des *faces du maillage* $\mathcal{F}_h$ est une famille finie de sous-ensembles non vides d'hyperplans de $\mathbb{R}^d$, ouverts, disjoints deux à deux, tel que

$$\bigcup_{T\in\mathcal{T}_h} \partial T = \bigcup_{F\in\mathcal{F}_h} \overline{F}.$$

De plus, nous distinguerons les faces en définissant les deux sous-ensembles suivants de $\mathcal{F}_h$:

- L'ensemble des *faces de bord* $\mathcal{F}_h^{\mathrm{b}} := \{F \in \mathcal{F}_h \mid F \subset \partial\Omega\}$;
- L'ensemble des *faces intérieures* $\mathcal{F}_h^{\mathrm{i}} := \mathcal{F}_h \backslash \mathcal{F}_h^{\mathrm{b}}$.

Nous définissons aussi les sous-ensembles suivants de $\mathcal{T}_h$ et $\mathcal{F}_h$:

- L'ensemble des éléments $\mathcal{T}_F := \{T \in \mathcal{T}_h \mid F \subset \partial T\}$ de toute face $F \in \mathcal{F}_h$;
- L'ensemble des faces $\mathcal{F}_T := \{F \in \mathcal{F}_h \mid F \subset \partial T\}$ de tout élément $T \in \mathcal{T}_h$.

Enfin nous noterons $\boldsymbol{n}_{TF}$ le vecteur normal unitaire de F pointant vers l'extérieur de T.

La taille d'un maillage polytopal $\mathcal{M}_h$ est donc caractérisée par le réel $h \in]0, +\infty[$. On définit alors l'ensemble des tailles de maillage $\mathcal{H} \subset \mathbb{R}_+^*$, dénombrable et ayant 0 comme unique point d'accumulation, et on considère une suite de maillages $(\mathcal{M}_h)_{h\in\mathcal{H}} = (\mathcal{T}_h, \mathcal{F}_h)_{h\in\mathcal{H}}$. Nous supposerons dans la suite que la suite $(\mathcal{M}_h)_{h\in\mathcal{H}}$ est *régulière* au sens de [50, Définition 1.9]. Cela implique, qu'il existe un *paramètre de régularité du maillage* $\rho \in]0, 1[$ permettant de borner uniformément par rapport à h le nombre de faces de chaque élément du maillage, ainsi que le rapport entre son diamètre et celui de chacune de ses faces. Dans la suite, on fixera un certain $h \in \mathcal{H}$.

1.2.2 Projecteurs orthogonaux

Pour tout élément ou face $X \in \mathcal{T}_h \cup \mathcal{F}_h$ et $l \in \mathbb{N}$, on note *l'espace polynomial local* $\mathbb{P}^l(X)$ (resp. $\mathbb{P}^l(X)^d$, $\mathbb{P}^l(X)^{d\times d}$) comme l'espace engendré par la restriction à X des polynômes à d variables, à valeur dans $\mathbb{R}$ (resp. $\mathbb{R}^d$, $\mathbb{R}^{d\times d}$), et de degré total inférieur à l.

Définition 2 (Projecteur L^2-orthogonal local)**.** On définit le *projecteur L^2-orthogonal local* $\pi_X^l : L^1(X) \to \mathbb{P}^l(X)$ tel que, pour tout $v \in L^1(X)$,

$$\int_X (\pi_X^l v - v) w = 0 \qquad \forall w \in \mathbb{P}^l(X). \tag{1}$$

On utilisera la notation en gras pour définir coordonnée par coordonnée le projecteur L^2-orthogonal local $\boldsymbol{\pi}_X^l$ sur les espaces polynomiaux $\mathbb{P}^l(X)^d$ et $\mathbb{P}^l(X)^{d\times d}$.

Pour éviter l'accumulation de constantes génériques, nous noterons dans la suite, $a \lesssim b$ (resp., $a \gtrsim b$) pour signifier $a \le Cb$ (resp., $a \ge Cb$) où $C > 0$ est un réel indépendant de h, et de tout élément ou face intervenant dans le cas d'une inégalité locale. On notera aussi $a \simeq b$ lorsque $a \lesssim b \lesssim a$.

Proposition 3 (Propriétés d'approximation du projecteur L^2-orthogonal)**.** *Soit $T \in \mathcal{T}_h$, $p \in [1, +\infty[$, $n \in [0, l+1]$, et $m \in [0, n]$. On a la propriété d'approximation de π_T^l suivante : Pour tout $v \in W^{n,p}(T)$,*

$$|v - \pi_T^l v|_{W^{m,p}(T)} \lesssim h_T^{n-m} |v|_{W^{n,p}(T)}. \tag{2a}$$

Si de plus, $n \ge 1$, on a la propriété d'approximation de trace de π_T^l suivante : Pour tout $v \in W^{n,p}(T)$,

$$\|v - \pi_T^l v\|_{L^p(\partial T)} \lesssim h_T^{n-\frac{1}{p}} |v|_{W^{n,p}(T)}. \tag{2b}$$

A l'échelle globale, on définit, pour tout $l \in \mathbb{N}$, *l'espace polynomial brisé*

$$\mathbb{P}^l(\mathcal{T}_h) \coloneqq \left\{ v \in L^1(\Omega) \mid v_{|T} \in \mathbb{P}^l(T) \quad \forall T \in \mathcal{T}_h \right\},$$

ainsi que le *projecteur L^2-orthogonal global* $\pi_h^l : L^1(\Omega) \to \mathbb{P}^l(\mathcal{T}_h)$ tel que, pour tout $v \in L^1(\Omega)$ et tout $T \in \mathcal{T}_h$,

$$(\pi_h^l v)_{|T} \coloneqq \pi_T^l v_{|T}.$$

A nouveau, on notera en gras le projecteur L^2-orthogonal global $\boldsymbol{\pi}_h^l$ appliqué sur des champs vectoriels de $L^1(\Omega)^d$ dans $\mathbb{P}^l(\mathcal{T}_h)^d$, ou des champs tensoriels de $L^1(\Omega)^{d\times d}$ dans $\mathbb{P}^l(\mathcal{T}_h)^{d\times d}$, et obtenu en appliquant π_h^l coordonnée par coordonnée.

1.2.3 Espaces de Sobolev brisés

Pour tout $n \in [0, +\infty]$ et $p \in [1, +\infty]$, on définit *l'espace de Sobolev brisé*

$$W^{n,p}(\mathcal{T}_h) \coloneqq \left\{ v \in L^p(\Omega) \ : \ v_{|T} \in W^{n,p}(T) \quad \forall T \in \mathcal{T}_h \right\}, \tag{3}$$

et on le munit de la semi-norme définie par $|v|_{W^{n,p}(\mathcal{T}_h)} \coloneqq \left(\sum_{T\in\mathcal{T}_h} |v|^p_{W^{n,p}(T)} \right)^{\frac{1}{p}}$ pour tout $v \in W^{n,p}(\mathcal{T}_h)$. De même, on note respectivement, $W^{n,p}(\mathcal{T}_h)^d$ et $W^{n,p}(\mathcal{T}_h)^{d\times d}$, les espaces de Sobolev brisés vectoriel et tensoriel, munis de leur semi-norme $|\cdot|_{W^{n,p}(\mathcal{T}_h)^d}$ et $|\cdot|_{W^{n,p}(\mathcal{T}_h)^{d\times d}}$.

2 Une méthode HHO pour des fluides non-newtoniens rampants

Cette section est un résumé du Chapitre 1, portant sur une méthode HHO pour des fluides non-newtoniens vérifiant les équations de Stokes. Les travaux de ce chapitre sont consacrés à l'étude des équations de Stokes pour des fluides non-newtoniens, dans un cadre non-hilbertien. Cette analyse généralise les travaux existants pour le cas newtonien et hilbertien. Dans le contexte de cette étude, de nouveaux résultats d'analyse fonctionnelle discrète furent démontrés afin d'analyser la méthode HHO, notamment la bonne position du problème discret et la convergence du schéma. Ces résultats couvrent la généralisation au cas non-hilbertien de l'inégalité de Korn discrète [28, Lemme 1], ainsi que des propriétés d'opérateur de Fortin et de stabilité inf-sup, qui jusqu'à présent ne s'appliquaient qu'au cas hilbertien. Ces outils nous permirent ainsi d'établir une estimation d'erreur a priori entre les solutions continue et discrète, offrant des ordres de convergence coïncidant avec ceux de [47] pour la vélocité. De plus, en introduisant les notions de fonction encadrée et d'exposant singulier, nous pouvons fusionner l'analyse des deux catégories de fluides non-newtonien, i.e. les fluides pseudo-plastiques et dilatants.

La suite de cette section sera d'abord consacrée à présenter les fluides non-newtoniens et la notion de fonction encadrée, puis nous résumerons le Chapitre 1. Nous commencerons par une présentation du problème continu, puis la construction de la méthode HHO en introduisant les opérateurs et fonctions discrets. Puis, nous analysons cette méthode, à l'aide de l'inégalité de Korn discrète, cf. Lemme 13. La bonne position du problème discret sera donnée dans le Théorème 2, et nous énonçons l'estimation d'erreur dans le Théorème 3. Nous avons illustré cette étude avec des simulations numériques au Chapitre 1, afin de valider les résultats théoriques.

Ces travaux ont donné lieu à un article complet paru dans la revue internationale ESAIM: Mathematical Modelling and Numerical Analysis, cf. [27].

2.1 Fluides newtoniens et non-newtoniens

La rhéologie d'un fluide peut se caractériser en fonction de sa viscosité. Lorsque la viscosité est indépendante des forces appliquées, on dit que le fluide est *newtonien*. L'eau et l'air sont des fluides newtoniens par exemple. Les fluides non-newtoniens se définissent donc par une viscosité qui varie selon la force extérieure appliquée pour devenir "plus liquides" ou "plus solides". On discerne ainsi deux catégories de fluides non-newtoniens : les fluides dits *pseudoplastiques*, dont la viscosité diminue avec une contrainte accrue, et les fluides appelés *dilatants*, dont la viscosité augmente avec une contrainte accrue. Le sang et le ketchup se liquéfient lorsqu'ils sont agités, ce sont donc des fluides pseudoplastiques. À l'inverse, le miel et l'oobleck (composé d'amidon de

maïs et d'eau) se solidifient face aux forces externes et sont donc des fluides dilatants.

Les rhéologies non-linéaires sont notamment rencontrées dans de nombreux domaines comme la dynamique des glaces et la modélisation des glaciers [4, 78], la convection mantellique [101], le génie chimique [80] ou encore les fluides biologiques [69, 85].

2.1.1 Tenseur des contraintes

On note $(\mathbb{R}^{d\times d}_{\mathrm{s}}, :)$ l'ensemble des matrices carrées symétriques de taille $d \times d$ munit du produit scalaire de Frobenius défini tel que, pour tout $\boldsymbol{\tau} = (\tau_{ij})_{1\le i,j\le d}$ et tout $\boldsymbol{\eta} = (\eta_{ij})_{1\le i,j\le d}$ dans $\mathbb{R}^{d\times d}$, $\boldsymbol{\tau} : \boldsymbol{\eta} \coloneqq \sum_{i,j=1}^{d} \tau_{ij}\eta_{ij}$, avec la norme correspondante définie par $|\boldsymbol{\tau}|_{d\times d} \coloneqq \sqrt{\boldsymbol{\tau} : \boldsymbol{\tau}}$.

Le mouvement d'un fluide occupant un ensemble Ω est défini et quantifié par une loi $\boldsymbol{\sigma} : \Omega \times \mathbb{R}^{d\times d}_{\mathrm{s}} \to \mathbb{R}^{d\times d}_{\mathrm{s}}$ que l'on appelle *tenseur des contraintes*. Un fluide newtonien se caractérise par le fait que son tenseur des contraintes est linéaire en son second argument, i.e., pour presque tout $\boldsymbol{x} \in \Omega$ et tout $\boldsymbol{\tau} \in \mathbb{R}^{d\times d}_{\mathrm{s}}$,

$$\boldsymbol{\sigma}(\boldsymbol{x}, \boldsymbol{\tau}) \coloneqq \mu(\boldsymbol{x})\boldsymbol{\tau}, \tag{4}$$

où $\mu : \Omega \to]0, +\infty[$ correspond à la viscosité locale du fluide. Les fluides non-newtoniens possèdent, en revanche, un tenseur des contraintes non-linéaire. Un exemple classique est la loi en puissance.

Exemple 4 (Loi en puissance)**.** Un fluide décrit par une loi en puissance (aussi appelée loi d'Ostwald–de Waele) est défini tel que, pour presque tout $\boldsymbol{x} \in \Omega$ et tout $\boldsymbol{\tau} \in \mathbb{R}^{d\times d}_{\mathrm{s}}$,

$$\boldsymbol{\sigma}(\boldsymbol{x}, \boldsymbol{\tau}) = \mu(\boldsymbol{x})|\boldsymbol{\tau}|^{p-2}_{d\times d}\boldsymbol{\tau}, \tag{5}$$

où $p \in]1, +\infty[$ est *l'indice d'écoulement* et $\mu : \Omega \to [\mu_-, \mu_+] \subset]0, +\infty[$ est une fonction mesurable correspondant à *l'indice local de consistance du flux*.

La valeur de p permet de quantifier la nature du fluide :

(i) Si $p > 2$, le fluide est dilatant;

(ii) Si $p < 2$ le fluide est pseudoplastique;

(iii) Si $p = 2$, le fluide est newtonien, et on retrouve (4).

Il existe des lois permettant de caractériser un fluide non-newtonien avec plus de précision.

Exemple 5 (Carreau–Yasuda)**.** Un fluide de Carreau–Yasuda, introduit dans [105] et généralisé dans [76, Eq. (1.2)], est défini tel que, pour presque tout $\boldsymbol{x} \in \Omega$ et tout $\boldsymbol{\tau} \in \mathbb{R}^{d\times d}_{\mathrm{s}}$,

$$\boldsymbol{\sigma}(\boldsymbol{x}, \boldsymbol{\tau}) = \mu(\boldsymbol{x}) \left(\delta(\boldsymbol{x})^{a(\boldsymbol{x})} + |\boldsymbol{\tau}|^{a(\boldsymbol{x})}_{d\times d}\right)^{\frac{p-2}{a(\boldsymbol{x})}} \boldsymbol{\tau}, \tag{6}$$

où p et μ ont le même rôle que dans l'Exemple 4 et où

(i) $a : \Omega \to [a_-, a_+] \subset]0, +\infty[$ est une fonction mesurable correspondant à *l'indice de transition d'écoulement local*;

(ii) $\delta : \Omega \to [0, +\infty[$ est le *paramètre de dégénérescence*.

La loi de Carreau–Yasuda est une généralisation de la loi de Carreau (correspondant à $a_\pm = 2$) qui permet de prendre en compte les différents niveaux locaux de l'écoulement du fluide. Le cas dégénéré $\delta \equiv 0$ correspond à la loi en puissance (5).

2.1.2 Fonction (p, δ)-encadrée

On considère une partie mesurable U de $\mathbb{R}^n$, $n \in \mathbb{N}^*$, et $(W, (\cdot,\cdot)_W)$ un espace préhilbertien avec pour norme induite $\|\cdot\|_W$.

Définition 6 (Fonction (p, δ)-encadrée)**.** Soit $p \in]1, +\infty[$ et $\delta : U \to [0, +\infty[$ une fonction mesurable. On dit qu'une fonction mesurable $\boldsymbol{\sigma} : U \times W \to W$ est (p, δ)-*encadrée* s'il existe $\sigma_{\mathrm{hc}}, \sigma_{\mathrm{hm}} \in]0, +\infty[$ tel que, pour tout $(\boldsymbol{\tau}, \boldsymbol{\eta}) \in W^2$ avec $\boldsymbol{\tau} \neq \boldsymbol{\eta}$ et presque tout $\boldsymbol{x} \in U$, la fonction $\boldsymbol{\sigma}$ vérifie les propriétés de *continuité hölderienne*

$$\|\boldsymbol{\sigma}(\boldsymbol{x}, \boldsymbol{\tau}) - \boldsymbol{\sigma}(\boldsymbol{x}, \boldsymbol{\eta})\|_W \leq \sigma_{\mathrm{hc}} \left(\delta(\boldsymbol{x})^p + \|\boldsymbol{\tau}\|_W^p + \|\boldsymbol{\eta}\|_W^p\right)^{\frac{p-2}{p}} \|\boldsymbol{\tau} - \boldsymbol{\eta}\|_W, \tag{7a}$$

et de *monotonicité hölderienne*

$$(\boldsymbol{\sigma}(\boldsymbol{x}, \boldsymbol{\tau}) - \boldsymbol{\sigma}(\boldsymbol{x}, \boldsymbol{\eta}), \boldsymbol{\tau} - \boldsymbol{\eta})_W \geq \sigma_{\mathrm{hm}} \left(\delta(\boldsymbol{x})^p + \|\boldsymbol{\tau}\|_W^p + \|\boldsymbol{\eta}\|_W^p\right)^{\frac{p-2}{p}} \|\boldsymbol{\tau} - \boldsymbol{\eta}\|_W^2. \tag{7b}$$

Afin de pouvoir vérifier que le tenseur des contraintes d'un fluide newtonien est (p, δ)-encadré, le théorème suivant permet de se ramener à la démonstration de deux inégalités dans $\mathbb{R}$.

Théorème 1 (Fonction (p, δ)-encadrée)**.** *Soit $\boldsymbol{\sigma} : U \times W \to W$. On suppose qu'il existe une fonction de Carathéodory $\varsigma : U \times [0, +\infty) \to \mathbb{R}$ tel que, pour tout $\boldsymbol{\tau} \in W$ et presque tout $\boldsymbol{x} \in U$,*

$$\boldsymbol{\sigma}(\boldsymbol{x}, \boldsymbol{\tau}) = \varsigma(\boldsymbol{x}, \|\boldsymbol{\tau}\|_W)\boldsymbol{\tau}. \tag{8a}$$

On suppose aussi que $\varsigma(\boldsymbol{x}, \cdot)$ est dérivable sur $]0, +\infty[$ pour presque tout $\boldsymbol{x} \in U$, et qu'il existe $\varsigma_{\mathrm{hc}}, \varsigma_{\mathrm{hm}} \in]0, +\infty[$ et $\delta : U \to [0, +\infty[$ mesurable tel que, pour tout $\alpha \in]0, +\infty[$ et presque tout $\boldsymbol{x} \in U$,

$$\varsigma_{\mathrm{hm}}(\delta(\boldsymbol{x})^p + \alpha^p)^{\frac{p-2}{p}} \leq \frac{\partial(\alpha\varsigma(\boldsymbol{x}, \alpha))}{\partial\alpha} \leq \varsigma_{\mathrm{hc}}(\delta(\boldsymbol{x})^p + \alpha^p)^{\frac{p-2}{p}}. \tag{8b}$$

Alors, $\boldsymbol{\sigma}$ est (p, δ)-encadrée.

Preuve 1. Voir Section 1.A.

Corollaire 7 (Lois en puissance et de Carreau–Yasuda)**.** *Le tenseur des contraintes du (μ, δ, a, p)-fluide de Carreau–Yasuda défini dans l'Exemple 5 est (p, δ)-encadré. Par conséquent, la loi en puissance de l'Exemple 4 est $(p, 0)$-encadrée.*

Preuve 2. Voir Section 1.A.

L'exposant p d'une fonction (p, δ)-encadrée deviendra naturellement l'exposant de Sobolev de l'espace où vit la vélocité du fluide. Remarquons que dans les deux exemples de lois citées dans le Corollaire 7, le cas hilbertien $p = 2$ correspond aux fluides newtoniens. Cependant, il est possible de considérer des lois de fluides non-newtoniens vivant dans un cadre hilbertien comme dans l'exemple ci-dessous.

Exemple 8 (Yeleswarapu)**.** Un fluide de Yeleswarapu, introduit dans [106], est défini tel que, pour presque tout $\boldsymbol{x} \in \Omega$ et tout $\boldsymbol{\tau} \in \mathbb{R}^{d\times d}_{\mathrm{s}}$,

$$\boldsymbol{\sigma}(\boldsymbol{\tau}) = \left(\mu_\infty + (\mu_0 - \mu_\infty)\frac{1 + \ln(1 + \lambda|\boldsymbol{\tau}|_{d\times d})}{1 + \lambda|\boldsymbol{\tau}|_{d\times d}}\right)\boldsymbol{\tau}, \tag{9}$$

où $\mu_0, \lambda \in]0, +\infty[$ et $\mu_\infty \in [0, \mu_0[$. On peut montrer grâce au Théorème 1 que la fonction $\boldsymbol{\sigma}$ est $(2, 0)$-encadrée, bien qu'elle ne soit pas linéaire.

2.1.3 Fonction singulièrement (p, δ)-encadrée

La formulation faible des futurs problèmes considérés faisant intervenir le tenseur des contraintes dans des intégrales, les propriétés des fonctions (p, δ)-encadrées doivent parfois être allégées afin de pouvoir appliquer des inégalités de Hölder. Pour cela, on introduit l'exposant singulier de p défini par

$$\tilde{p} = \min(p, 2) \in]1, 2]. \tag{10}$$

Définition 9 (Fonction singulièrement (p, δ)-encadrée)**.** Soit $p \in]1, +\infty[$ et $\delta : U \to [0, +\infty[$ une fonction mesurable. On dit qu'une fonction mesurable $\boldsymbol{\sigma} : U \times W \to W$ est singulièrement (p, δ)-*encadrée* s'il existe $\sigma_{\mathrm{hc}}, \sigma_{\mathrm{hm}} \in]0, +\infty[$ tel que, pour tout $(\boldsymbol{\tau}, \boldsymbol{\eta}) \in W^2$ et presque tout $\boldsymbol{x} \in U$, la fonction $\boldsymbol{\sigma}$ vérifie les propriétés de *continuité hölderienne singulière*

$$\|\boldsymbol{\sigma}(\boldsymbol{x}, \boldsymbol{\tau}) - \boldsymbol{\sigma}(\boldsymbol{x}, \boldsymbol{\eta})\|_W \leq \sigma_{\mathrm{hc}} \left(\delta(\boldsymbol{x})^p + \|\boldsymbol{\tau}\|_W^p + \|\boldsymbol{\eta}\|_W^p\right)^{\frac{p-\tilde{p}}{p}} \|\boldsymbol{\tau} - \boldsymbol{\eta}\|_W^{\tilde{p}-1}, \tag{11a}$$

et de *monotonicité hölderienne singulière*

$$(\boldsymbol{\sigma}(\boldsymbol{x}, \boldsymbol{\tau}) - \boldsymbol{\sigma}(\boldsymbol{x}, \boldsymbol{\eta}), \boldsymbol{\tau} - \boldsymbol{\eta})_W \left(\delta(\boldsymbol{x})^p + \|\boldsymbol{\tau}\|_W^p + \|\boldsymbol{\eta}\|_W^p\right)^{\frac{2-\tilde{p}}{p}} \geq \sigma_{\mathrm{hm}} \|\boldsymbol{\tau} - \boldsymbol{\eta}\|_W^{p+2-\tilde{p}}. \tag{11b}$$

Nous précisons que la terminologie définie dans la Définition 9 n'est pas celle employée dans [27, 35, 52] mais est plus appropriée pour différencier les propriétés hölderiennes et hölderiennes singulières.

Une inégalité triangulaire permet de montrer qu'une fonction (p,δ)-encadrée est aussi singulièrement (p,δ)-encadrée. De plus on a les égalités suivantes :

$$\frac{p-\tilde{p}}{p}+\frac{\tilde{p}-1}{p}=1,\quad \frac{p}{p+2-\tilde{p}}+\frac{2-\tilde{p}}{p+2-\tilde{p}}=1, \tag{12}$$

où chaque fraction est positive quelle que soit la valeur de $p\in\,]1,+\infty[$. On peut donc appliquer des inégalités de Hölder pour obtenir des inégalités analogues à (11) après intégration.

2.2 Problème de Stokes généralisé

Soit $\Omega\subset\mathbb{R}^d$, $d\in\{2,3\}$, un polyèdre ouvert connexe à frontière lipschitzienne $\partial\Omega$. On considère un fluide possiblement non-newtonien occupant Ω et soumis à une *force volumétrique* $\boldsymbol{f}:\Omega\to\mathbb{R}^d$. Son écoulement est régi par le problème de Stokes généralisé, qui consiste à trouver la vélocité $\boldsymbol{u}:\Omega\to\mathbb{R}^d$ et la pression $p:\Omega\to\mathbb{R}$ tel que

$$-\boldsymbol{\nabla}\cdot\boldsymbol{\sigma}(\cdot,\boldsymbol{\nabla}_{\mathrm{s}}\boldsymbol{u})+\boldsymbol{\nabla}p=\boldsymbol{f}\qquad\text{in }\Omega, \tag{13a}$$

$$\boldsymbol{\nabla}\cdot\boldsymbol{u}=0\qquad\text{in }\Omega, \tag{13b}$$

$$\boldsymbol{u}=\boldsymbol{0}\qquad\text{on }\partial\Omega, \tag{13c}$$

$$\int_\Omega p(\boldsymbol{x})\,\mathrm{d}\boldsymbol{x}=0, \tag{13d}$$

où $\boldsymbol{\sigma}:\Omega\times\mathbb{R}^{d\times d}_{\mathrm{s}}\to\mathbb{R}^{d\times d}_{\mathrm{s}}$ est le tenseur des contraintes du fluide, $\boldsymbol{\nabla}\cdot$ est l'opérateur de divergence appliqué aux champs vectoriels et tensoriels, $\boldsymbol{\nabla}_{\mathrm{s}}$ est la partie symétrique de l'opérateur gradient $\boldsymbol{\nabla}$ appliqué aux champs vectoriels, et on notera aussi $\boldsymbol{\nabla}_{\mathrm{ss}}$ la partie anti-symétrique de $\boldsymbol{\nabla}$.

2.2.1 Hypothèses sur le tenseur des contraintes

Pour tout $m\in[1,\infty]$, on définit *l'exposant conjugué* de m par

$$m':=\begin{cases}\frac{m}{m-1} & \text{si } m\in(1,\infty)\\ \infty & \text{si } m=1\\ 1 & \text{si } m=\infty\end{cases}\in[1,\infty]. \tag{14}$$

Hypothèse 1 (Tenseur des contraintes)**.** Soit $r\in\,]1,+\infty[$ un réel fixé. On suppose que

$$\boldsymbol{\sigma}(\cdot,\boldsymbol{0})\in L^{r'}(\Omega,\mathbb{R}^{d\times d}_{\mathrm{s}})\text{ pour presque tout }\boldsymbol{x}\in\Omega, \tag{15a}$$

$$\boldsymbol{\sigma}:\Omega\times\mathbb{R}^{d\times d}_{\mathrm{s}}\to\mathbb{R}^{d\times d}_{\mathrm{s}}\text{ est singulièrement }(r,\delta)\text{-encadrée}, \tag{15b}$$

avec $\delta \in [0, +\infty[$ et où $\sigma_{\mathrm{hc}}, \sigma_{\mathrm{hm}} \in]0, +\infty[$ sont les constantes respectives de continuité et monotonicité hölderiennes singulières.

On pose δ constant dans l'Hypothèse 1 pour alléger la lecture mais il est possible de considérer $\delta \in L^r(\Omega, [0, +\infty[)$. Sous cette hypothèse de régularité, la loi de Carreau–Yasuda (6) vérifie l'Hypothèse 1, cf. Corollaire 7.

2.2.2 Formulation faible

Dans la suite, on omettra les variables d'intégration et mesures des intégrales afin d'alléger la lecture, et on posera $|\Omega|_d = 1$, la mesure de Ω.

On définit les espaces discrets de la vélocité et la pression prenant en compte les conditions aux bords et de moyenne nulle respectivement :

$$\boldsymbol{U} \coloneqq \left\{ \boldsymbol{v} \in W^{1,r}(\Omega)^d \ : \ \boldsymbol{v}_{|\partial\Omega} = \boldsymbol{0} \right\}, \quad P \coloneqq \left\{ q \in L^{r'}(\Omega) \ : \ \int_\Omega q = 0 \right\}. \tag{16}$$

En supposant $\boldsymbol{f} \in L^{r'}(\Omega)^d$, la formulation faible continue du problème (13) consiste à : Trouver $(\boldsymbol{u}, p) \in \boldsymbol{U} \times P$ tel que

$$a(\boldsymbol{u}, \boldsymbol{v}) + b(\boldsymbol{v}, p) = \int_\Omega \boldsymbol{f} \cdot \boldsymbol{v} \qquad \forall \boldsymbol{v} \in \boldsymbol{U}, \tag{17a}$$

$$-b(\boldsymbol{u}, q) = 0 \qquad \forall q \in P, \tag{17b}$$

où la fonction $a : \boldsymbol{U} \times \boldsymbol{U} \to \mathbb{R}$ et la forme bilinéaire $b : \boldsymbol{U} \times L^{r'}(\Omega) \to \mathbb{R}$ sont telles que, pour tout $\boldsymbol{v}, \boldsymbol{w} \in \boldsymbol{U}$ et tout $q \in L^{r'}(\Omega)$,

$$a(\boldsymbol{w}, \boldsymbol{v}) \coloneqq \int_\Omega \boldsymbol{\sigma}(\cdot, \boldsymbol{\nabla}_{\mathrm{s}} \boldsymbol{w}) : \boldsymbol{\nabla}_{\mathrm{s}} \boldsymbol{v}, \qquad b(\boldsymbol{v}, q) \coloneqq -\int_\Omega (\boldsymbol{\nabla} \cdot \boldsymbol{v}) q. \tag{18}$$

2.2.3 Inégalité de Korn et bonne position du problème continu

Grâce aux propriétés de continuité et monotonicité hölderiennes singulières (11) de $\boldsymbol{\sigma}$, et en rappelant (12), on obtient des propriétés analogues pour a.

Proposition 10 (Continuité et monotonicité hölderiennes singulières de a)**.** *Sous l'Hypothèse 1, pour tout $\boldsymbol{u}, \boldsymbol{v}, \boldsymbol{w} \in \boldsymbol{U}$, on a*

$$\begin{aligned} &|a(\boldsymbol{u}, \boldsymbol{v}) - a(\boldsymbol{w}, \boldsymbol{v})| \\ &\qquad \le \sigma_{\mathrm{hc}} \left(\delta + \|\boldsymbol{\nabla}_{\mathrm{s}} \boldsymbol{u}\|^r_{L^r(\Omega)^{d\times d}} + \|\boldsymbol{\nabla}_{\mathrm{s}} \boldsymbol{w}\|^r_{L^r(\Omega)^{d\times d}} \right)^{\frac{r-\tilde{r}}{r}} \|\boldsymbol{\nabla}_{\mathrm{s}}(\boldsymbol{u} - \boldsymbol{w})\|^{\tilde{r}-1}_{L^r(\Omega)^{d\times d}}, \end{aligned} \tag{19}$$

$$\begin{aligned} &(a(\boldsymbol{u}, \boldsymbol{u} - \boldsymbol{w}) - a(\boldsymbol{w}, \boldsymbol{u} - \boldsymbol{w})) \left(\delta + \|\boldsymbol{\nabla}_{\mathrm{s}} \boldsymbol{u}\|^r_{L^r(\Omega)^{d\times d}} + \|\boldsymbol{\nabla}_{\mathrm{s}} \boldsymbol{w}\|^r_{L^r(\Omega)^{d\times d}} \right)^{\frac{2-\tilde{r}}{r}} \\ &\qquad \ge \sigma_{\mathrm{hm}} \|\boldsymbol{\nabla}_{\mathrm{s}}(\boldsymbol{u} - \boldsymbol{w})\|^{r+2-\tilde{r}}_{L^r(\Omega)^{d\times d}}. \end{aligned} \tag{20}$$

Preuve 3. La preuve s'obtient avec le même raisonnement qu'en Section 1.7.2.1.

Au niveau continu, l'inégalité de Korn (cf. [72, Théorème 1]) affirme qu'il existe $C_{\mathrm{K},r} \in]0,+\infty[$, dépendant uniquement de Ω et r, tel que, pour tout $\boldsymbol{v} \in \boldsymbol{U}$,

$$\|\boldsymbol{v}\|_{W^{1,r}(\Omega)^d} \le C_{\mathrm{K},r} \|\boldsymbol{\nabla}_{\mathrm{s}} \boldsymbol{v}\|_{L^r(\Omega)^{d\times d}}. \tag{21}$$

Ainsi, sous l'Hypothèse 1, la formulation faible continue (17) admet une unique solution $(\boldsymbol{u}, p) \in \boldsymbol{U} \times P$ (cf. [76, Section 2.4]). De plus, elle vérifie la majoration suivante :

$$|\boldsymbol{u}|_{W^{1,r}(\Omega)^d} \le C_{\mathrm{vel}} \left(\left(\sigma_{\mathrm{hm}}^{-1} \|\boldsymbol{f}\|_{L^{r'}(\Omega)^d} \right)^{\frac{1}{r-1}} + \left(\delta^{2-\tilde{r}} \sigma_{\mathrm{hm}}^{-1} \|\boldsymbol{f}\|_{L^{r'}(\Omega)^d} \right)^{\frac{1}{r+1-\tilde{r}}} \right), \tag{22a}$$

où $C_{\mathrm{vel}} > 0$ dépend uniquement de Ω et r.

2.3 Méthode Hybrid High-Order

On considère une suite de maillages régulière $(\mathcal{M}_h)_{h\in\mathcal{H}}$ définie comme dans le paragraphe 1.2.1.

2.3.1 Espaces et normes discrets

On fixe un entier $k \ge 1$ correspondant au degré de la méthode et on définit l'espace discret de la vélocité contenant les inconnues discrètes par

$$\underline{\boldsymbol{U}}_h^k := \left\{ \underline{\boldsymbol{v}}_h := ((\boldsymbol{v}_T)_{T\in\mathcal{T}_h}, (\boldsymbol{v}_F)_{F\in\mathcal{F}_h}) \;\middle|\; \begin{array}{l} \boldsymbol{v}_T \in \mathbb{P}^k(T)^d \quad \forall T \in \mathcal{T}_h \\ \boldsymbol{v}_F \in \mathbb{P}^k(F)^d \quad \forall F \in \mathcal{F}_h \end{array} \right\}. \tag{23}$$

On définit *l'opérateur d'interpolation* $\underline{\boldsymbol{I}}_h^k : W^{1,1}(\Omega)^d \to \underline{\boldsymbol{U}}_h^k$ renvoyant une fonction de $\boldsymbol{v} \in W^{1,1}(\Omega)^d$ sur le vecteur d'inconnues discrètes $\underline{\boldsymbol{I}}_h^k \boldsymbol{v}$ défini par :

$$\underline{\boldsymbol{I}}_h^k \boldsymbol{v} := ((\boldsymbol{\pi}_T^k \boldsymbol{v}_{|T})_{T\in\mathcal{T}_h}, (\boldsymbol{\pi}_F^k \boldsymbol{v}_{|F})_{F\in\mathcal{F}_h}). \tag{24}$$

Pour tout $T \in \mathcal{T}_h$, on note $\underline{\boldsymbol{U}}_T^k$ et $\underline{\boldsymbol{I}}_T^k$, les restrictions de $\underline{\boldsymbol{U}}_h^k$ et $\underline{\boldsymbol{I}}_h^k$ sur T, respectivement. De plus, pour tout $\underline{\boldsymbol{v}}_h \in \underline{\boldsymbol{U}}_h^k$, on note $\underline{\boldsymbol{v}}_T := (\boldsymbol{v}_T, (\boldsymbol{v}_F)_{F\in\mathcal{F}_T}) \in \underline{\boldsymbol{U}}_T^k$ le vecteur contenant les inconnues liées à T et ses faces, et $\boldsymbol{v}_h \in \mathbb{P}^k(\mathcal{T}_h)^d$ le champ polynomial brisé obtenu en accolant les inconnues d'éléments, i.e.,

$$(\boldsymbol{v}_h)_{|T} := \boldsymbol{v}_T \qquad \forall T \in \mathcal{T}_h. \tag{25}$$

On définit sur $\underline{\boldsymbol{U}}_h^k$ la $W^{1,r}(\Omega)^d$-semi-norme $\|\cdot\|_{\boldsymbol{\varepsilon},r,h}$ telle que, pour tout $\underline{\boldsymbol{v}}_h \in \underline{\boldsymbol{U}}_h^k$,

$$\|\underline{\boldsymbol{v}}_h\|_{\boldsymbol{\varepsilon},r,h} := \left(\sum_{T\in\mathcal{T}_h} \|\underline{\boldsymbol{v}}_T\|_{\boldsymbol{\varepsilon},r,T}^r \right)^{\frac{1}{r}}, \tag{26a}$$

où pour tout $T \in \mathcal{T}_h$,

$$\|\underline{\boldsymbol{v}}_T\|_{\boldsymbol{\varepsilon},r,T} \coloneqq \left(\|\boldsymbol{\nabla}_{\mathrm{s}} \boldsymbol{v}_T\|_{L^r(T)^{d\times d}}^r + \sum_{F\in\mathcal{F}_T} h_F^{1-r} \|\boldsymbol{v}_F - \boldsymbol{v}_T\|_{L^r(F)^d}^r \right)^{\frac{1}{r}}. \tag{26b}$$

Pour tout $T \in \mathcal{T}_h$ et tout $\boldsymbol{v} \in W^{1,r}(T)^d$,

$$\|\underline{\boldsymbol{I}}_T^k \boldsymbol{v}\|_{\boldsymbol{\varepsilon},r,T} \le C_{\mathrm{I}} |\boldsymbol{v}|_{W^{1,r}(T)^d}, \tag{27}$$

où $C_{\mathrm{I}} > 0$ est indépendant de T et h.

On définit, enfin, les espaces des vélocités et pressions discrètes qui prennent en compte les conditions de bord et de moyenne nulle, respectivement :

$$\underline{\boldsymbol{U}}_{h,0}^k \coloneqq \left\{ \underline{\boldsymbol{v}}_h \in \underline{\boldsymbol{U}}_h^k \ : \ \boldsymbol{v}_F = \boldsymbol{0} \quad \forall F \in \mathcal{F}_h^{\mathrm{b}} \right\}, \quad P_h^k \coloneqq \mathbb{P}^k(\mathcal{T}_h) \cap P. \tag{28}$$

2.3.2 Opérateurs discrets

Soit $\otimes$, le produit tensoriel tel que, pour tout $\boldsymbol{x} = (x_i)_{1\le i\le d}$ et $\boldsymbol{y} = (y_i)_{1\le i\le d}$ dans $\mathbb{R}^d$, $\boldsymbol{x}\otimes\boldsymbol{y} \coloneqq (x_i y_j)_{1\le i,j\le d} \in \mathbb{R}^{d\times d}$.

Pour tout $T \in \mathcal{T}_h$, on définit la *reconstruction locale du gradient* $\mathbf{G}_T^k : \underline{\boldsymbol{U}}_T^k \to \mathbb{P}^k(T)^{d\times d}$ telle que, pour tout $\underline{\boldsymbol{v}}_T \in \underline{\boldsymbol{U}}_T^k$ et $\boldsymbol{\tau} \in \mathbb{P}^k(T)^{d\times d}$,

$$\int_T \mathbf{G}_T^k \underline{\boldsymbol{v}}_T : \boldsymbol{\tau} = \int_T \boldsymbol{\nabla}\boldsymbol{v}_T : \boldsymbol{\tau} + \sum_{F\in\mathcal{F}_T} \int_F (\boldsymbol{v}_F - \boldsymbol{v}_T)\cdot(\boldsymbol{\tau}\boldsymbol{n}_{TF}). \tag{29}$$

Cet opérateur est construit de telle sorte que, pour tout $\boldsymbol{v} \in W^{1,1}(T)^d$,

$$\mathbf{G}_T^k(\underline{\boldsymbol{I}}_T^k \boldsymbol{v}) = \boldsymbol{\pi}_T^k(\boldsymbol{\nabla}\boldsymbol{v}), \tag{30}$$

et possède ainsi des propriétés d'approximation provenant de (2). De plus, on définit les reconstructions locales du gradient symétrique $\mathbf{G}_{\mathrm{s},T}^k : \underline{\boldsymbol{U}}_T^k \to \mathbb{P}^k(T, \mathbb{R}_{\mathrm{s}}^{d\times d})$ et de la divergence $\mathrm{D}_T^k : \underline{\boldsymbol{U}}_T^k \to \mathbb{P}^k(T)$ telles que,

$$\mathbf{G}_{\mathrm{s},T}^k = \frac{1}{2}\left(\mathbf{G}_T^k + (\mathbf{G}_T^k)^{\mathrm{T}}\right), \quad \mathrm{D}_T^k \coloneqq \mathrm{tr}(\mathbf{G}_T^k). \tag{31}$$

On obtient les reconstructions globales du gradient $\mathbf{G}_h^k : \underline{\boldsymbol{U}}_h^k \to \mathbb{P}^k(\mathcal{T}_h)^{d\times d}$ et du gradient symétrique $\mathbf{G}_{\mathrm{s},h}^k : \underline{\boldsymbol{U}}_h^k \to \mathbb{P}^k(\mathcal{T}_h, \mathbb{R}_{\mathrm{s}}^{d\times d})$ en accolant les contributions locales :

$$(\mathbf{G}_h^k)_{|T} \coloneqq \mathbf{G}_T^k, \quad (\mathbf{G}_{\mathrm{s},h}^k)_{|T} \coloneqq \mathbf{G}_{\mathrm{s},T}^k, \quad \forall T \in \mathcal{T}_h. \tag{32}$$

Enfin, pour tout $T \in \mathcal{T}_h$, nous définissons le *résidu de bord* $\boldsymbol{\Delta}_{\partial T}^k : \underline{\boldsymbol{U}}_T^k \to L^r(\partial T)^d$ tel que, pour tout $\underline{\boldsymbol{v}}_T \in \underline{\boldsymbol{U}}_T^k$,

$$(\boldsymbol{\Delta}_{\partial T}^k \underline{\boldsymbol{v}}_T)_{|F} \coloneqq \frac{1}{h_T}\left(\boldsymbol{\pi}_F^k(\mathbf{r}_T^{k+1}\underline{\boldsymbol{v}}_T - \boldsymbol{v}_F) - \boldsymbol{\pi}_T^k(\mathbf{r}_T^{k+1}\underline{\boldsymbol{v}}_T - \boldsymbol{v}_T)\right) \qquad \forall F \in \mathcal{F}_T,$$

avec *reconstruction de la vélocité* $\mathbf{r}_T^{k+1} : \underline{\boldsymbol{U}}_T^k \to \mathbb{P}^{k+1}(T)^d$ telle que

$$\int_T (\boldsymbol{\nabla}_{\mathrm{s}}\mathbf{r}_T^{k+1}\underline{\boldsymbol{v}}_T - \mathbf{G}_{\mathrm{s},T}^k\underline{\boldsymbol{v}}_T) : \boldsymbol{\nabla}_{\mathrm{s}}\boldsymbol{w} = 0 \qquad \forall \boldsymbol{w} \in \mathbb{P}^{k+1}(T)^d,$$

$$\int_T \mathbf{r}_T^{k+1}\underline{\boldsymbol{v}}_T = \int_T \boldsymbol{v}_T \quad \text{et} \quad \int_T \boldsymbol{\nabla}_{\mathrm{ss}}\mathbf{r}_T^{k+1}\underline{\boldsymbol{v}}_T = \frac{1}{2}\sum_{F\in\mathcal{F}_T}\int_F (\boldsymbol{v}_F \otimes \boldsymbol{n}_{TF} - \boldsymbol{n}_{TF} \otimes \boldsymbol{v}_F).$$

2.3.3 Terme visqueux discret

Dans la suite, on utilisera la notation $|\cdot|$ pour la valeur absolue ainsi que pour la norme euclidienne des vecteurs de $\mathbb{R}^d$.

La version discrète de la fonction visqueuse a est donnée par $\mathrm{a}_h : \underline{\boldsymbol{U}}_h^k \times \underline{\boldsymbol{U}}_h^k \to \mathbb{R}$ et définie telle que, pour tout $\underline{\boldsymbol{v}}_h, \underline{\boldsymbol{w}}_h \in \underline{\boldsymbol{U}}_h^k$,

$$\mathrm{a}_h(\underline{\boldsymbol{w}}_h, \underline{\boldsymbol{v}}_h) \coloneqq \int_\Omega \boldsymbol{\sigma}(\cdot, \mathbf{G}_{\mathrm{s},h}^k\underline{\boldsymbol{w}}_h) : \mathbf{G}_{\mathrm{s},h}^k\underline{\boldsymbol{v}}_h + \gamma\sum_{T\in\mathcal{T}_h}\mathrm{s}_T(\underline{\boldsymbol{w}}_T, \underline{\boldsymbol{v}}_T), \tag{33}$$

où $\gamma \in [\sigma_{\mathrm{hm}}, \sigma_{\mathrm{hc}}]$ est un *paramètre de stabilisation* et où les *fonctions de stabilisation locales* $\mathrm{s}_T : \underline{\boldsymbol{U}}_T^k \times \underline{\boldsymbol{U}}_T^k \to \mathbb{R}, T \in \mathcal{T}_h$, peuvent être définies telle que, pour tout $\underline{\boldsymbol{v}}_h, \underline{\boldsymbol{w}}_h \in \underline{\boldsymbol{U}}_h^k$,

$$\mathrm{s}_T(\underline{\boldsymbol{w}}_T, \underline{\boldsymbol{v}}_T) \coloneqq \int_{\partial T} |\boldsymbol{\Delta}_{\partial T}^k\underline{\boldsymbol{w}}_T|^{r-2}\boldsymbol{\Delta}_{\partial T}^k\underline{\boldsymbol{w}}_T \cdot \boldsymbol{\Delta}_{\partial T}^k\underline{\boldsymbol{v}}_T. \tag{34}$$

Remarquons qu'en (34) se trouve la fonction singulièrement $(r,0)$-encadrée $\mathbb{R}^d \ni \boldsymbol{x} \mapsto |\boldsymbol{x}|^{r-2}\boldsymbol{x} \in \mathbb{R}^d$. On obtient ainsi des propriétés analogues aux continuité et monotonicité hölderiennes singulières de a pour les fonctions de stabilisation locales, et donc pour a_h.

Lemme 11 (Continuité et monotonicité hölderiennes singulières de a_h)**.** *Sous l'Hypothèse 1, pour tout $\underline{\boldsymbol{u}}_h, \underline{\boldsymbol{v}}_h, \underline{\boldsymbol{w}}_h \in \underline{\boldsymbol{U}}_h^k$, on a*

$$\begin{aligned}\left|\mathrm{a}_h(\underline{\boldsymbol{u}}_h, \underline{\boldsymbol{v}}_h) - \mathrm{a}_h(\underline{\boldsymbol{w}}_h, \underline{\boldsymbol{v}}_h)\right| \\ \lesssim \sigma_{\mathrm{hc}}\left(\delta^r + \|\underline{\boldsymbol{u}}_h\|_{\boldsymbol{\varepsilon},r,h}^r + \|\underline{\boldsymbol{w}}_h\|_{\boldsymbol{\varepsilon},r,h}^r\right)^{\frac{r-\tilde{r}}{r}}\|\underline{\boldsymbol{u}}_h - \underline{\boldsymbol{w}}_h\|_{\boldsymbol{\varepsilon},r,h}^{\tilde{r}-1}\|\underline{\boldsymbol{v}}_h\|_{\boldsymbol{\varepsilon},r,h},\end{aligned} \tag{35a}$$

$$\begin{aligned}\left(\mathrm{a}_h(\underline{\boldsymbol{u}}_h, \underline{\boldsymbol{u}}_h - \underline{\boldsymbol{w}}_h) - \mathrm{a}_h(\underline{\boldsymbol{w}}_h, \underline{\boldsymbol{u}}_h - \underline{\boldsymbol{w}}_h)\right)\left(\delta^r + \|\underline{\boldsymbol{u}}_h\|_{\boldsymbol{\varepsilon},r,h}^r + \|\underline{\boldsymbol{w}}_h\|_{\boldsymbol{\varepsilon},r,h}^r\right)^{\frac{2-\tilde{r}}{r}} \\ \gtrsim \sigma_{\mathrm{hm}}\|\underline{\boldsymbol{u}}_h - \underline{\boldsymbol{w}}_h\|_{\boldsymbol{\varepsilon},r,h}^{r+2-\tilde{r}}.\end{aligned} \tag{35b}$$

Preuve 4. Voir Section 1.7.2.1.

2.3.4 Couplage pression-vélocité discret

Le couplage pression-vélocité discret est donné par la forme bilinéaire $\mathrm{b}_h : \underline{\boldsymbol{U}}_h^k \times \mathbb{P}^k(\mathcal{T}_h) \to \mathbb{R}$ telle que, pour tout $(\underline{\boldsymbol{v}}_h, q_h) \in \underline{\boldsymbol{U}}_h^k \times \mathbb{P}^k(\mathcal{T}_h)$,

$$\mathrm{b}_h(\underline{\boldsymbol{v}}_h, q_h) \coloneqq -\sum_{T\in\mathcal{T}_h} \int_T \mathrm{D}_T^k \underline{\boldsymbol{v}}_T \, q_T, \tag{36}$$

où $q_T \coloneqq (q_h)_{|T}$ pour tout $T \in \mathcal{T}_h$. On obtient pour b_h, la propriété inf-sup suivante.

Lemme 12 (Propriété inf-sup de b_h)**.** *Pour tout $q_h \in P_h^k$, on a*

$$\|q_h\|_{L^{r'}(\Omega)} \lesssim \sup_{\underline{\boldsymbol{v}}_h \in \underline{\boldsymbol{U}}_{h,0}^k, \|\underline{\boldsymbol{v}}_h\|_{\boldsymbol{\varepsilon},r,h}=1} \mathrm{b}_h(\underline{\boldsymbol{v}}_h, q_h). \tag{37}$$

Preuve 5. Voir Section 1.7.2.2.

2.4 Problème discret et résultats principaux

Le problème discret est défini par : Trouver $(\underline{\boldsymbol{u}}_h, p_h) \in \underline{\boldsymbol{U}}_{h,0}^k \times P_h^k$ tel que

$$\mathrm{a}_h(\underline{\boldsymbol{u}}_h, \underline{\boldsymbol{v}}_h) + \mathrm{b}_h(\underline{\boldsymbol{v}}_h, p_h) = \int_\Omega \boldsymbol{f}\cdot\boldsymbol{v}_h \qquad \forall \underline{\boldsymbol{v}}_h \in \underline{\boldsymbol{U}}_{h,0}^k, \tag{38a}$$

$$-\mathrm{b}_h(\underline{\boldsymbol{u}}_h, q_h) = 0 \qquad \forall q_h \in P_h^k. \tag{38b}$$

2.4.1 Inégalité de Korn discrète et bonne position du problème discret

Dualement à (21), on reproduit une inégalité de Korn discrète pour la semi-norme $\|\cdot\|_{\boldsymbol{\varepsilon},r,h}$, qui devient alors une norme sur $\underline{\boldsymbol{U}}_{h,0}^k$.

Lemme 13. *(Inégalité de Korn discrète) Pour tout $\underline{\boldsymbol{v}}_h \in \underline{\boldsymbol{U}}_{h,0}^k$, on a*

$$\|\boldsymbol{v}_h\|_{L^r(\Omega)^d}^r + |\boldsymbol{v}_h|_{W^{1,r}(\mathcal{T}_h)^d}^r \lesssim \|\underline{\boldsymbol{v}}_h\|_{\boldsymbol{\varepsilon},r,h}^r. \tag{39}$$

Preuve 6. Voir Section 1.6.

On obtient ainsi la bonne position du problème discret.

Théorème 2 (Bonne position)**.** *Il existe une unique solution $(\underline{\boldsymbol{u}}_h, p_h) \in \underline{\boldsymbol{U}}_{h,0}^k \times P_h^k$ au problème discret (38). De plus, elle vérifie les majorations suivantes :*

$$\|\underline{\boldsymbol{u}}_h\|_{\boldsymbol{\varepsilon},r,h} \lesssim \left(\sigma_{\mathrm{hm}}^{-1}\|\boldsymbol{f}\|_{L^{r'}(\Omega)^d}\right)^{\frac{1}{r-1}} + \left(\delta^{2-\tilde{r}}\sigma_{\mathrm{hm}}^{-1}\|\boldsymbol{f}\|_{L^{r'}(\Omega)^d}\right)^{\frac{1}{r+1-\tilde{r}}}, \tag{40a}$$

$$\|p_h\|_{L^{r'}(\Omega)} \lesssim \sigma_{\mathrm{hc}}\left(\sigma_{\mathrm{hm}}^{-1}\|\boldsymbol{f}\|_{L^{r'}(\Omega)^d} + \delta^{|r-2|(\tilde{r}-1)}\left(\sigma_{\mathrm{hm}}^{-1}\|\boldsymbol{f}\|_{L^{r'}(\Omega)^d}\right)^{\frac{\tilde{r}-1}{r+1-\tilde{r}}}\right). \tag{40b}$$

Preuve 7. Voir Section 1.7.2.3.

2.4.2 Estimation d'erreur

Sous l'hypothèse de régularité supplémentaire sur la solution du problème continu, on peut établir une estimation d'erreur a priori de la méthode.

Théorème 3 (Estimation d'erreur)**.** *Soit* $(\boldsymbol{u}, p) \in \boldsymbol{U} \times P$ *et* $(\underline{\boldsymbol{u}}_h, p_h) \in \underline{\boldsymbol{U}}_{h,0}^k \times P_h^k$ *les solutions respectives des problèmes* (17) *et* (38)*. On suppose que*

(i) $\boldsymbol{u} \in W^{k+2,r}(\mathcal{T}_h)^d$,

(ii) $\boldsymbol{\sigma}(\cdot, \boldsymbol{\nabla}_{\mathrm{s}}\boldsymbol{u}) \in W^{1,r'}(\Omega, \mathbb{R}_{\mathrm{s}}^{d\times d}) \cap W^{(k+1)(\tilde{r}-1),r'}(\mathcal{T}_h, \mathbb{R}_{\mathrm{s}}^{d\times d})$,

(iii) $p \in W^{1,r'}(\Omega) \cap W^{(k+1)(\tilde{r}-1),r'}(\mathcal{T}_h)$.

Alors, sous l'Hypothèse 1, on a

$$\|\underline{\boldsymbol{u}}_h - \underline{\boldsymbol{I}}_h^k \boldsymbol{u}\|_{\boldsymbol{\varepsilon},r,h} \leq \mathcal{N}_1 h^{\frac{(k+1)(\tilde{r}-1)}{r+1-\tilde{r}}}, \tag{41a}$$

$$\|p_h - \pi_h^k p\|_{L^{r'}(\Omega)} \lesssim \mathcal{N}_2 h^{(k+1)(\tilde{r}-1)} + \mathcal{N}_3 h^{\frac{(k+1)(\tilde{r}-1)^2}{r+1-\tilde{r}}}, \tag{41b}$$

où $\mathcal{N}_1, \mathcal{N}_2, \mathcal{N}_3 \in [0, +\infty[$ *dépendent uniquement de* $r, \sigma_{\mathrm{hc}}, \sigma_{\mathrm{hm}}, \delta$ *et des normes* $|\boldsymbol{u}|_{W^{1,r}(\Omega)^d}$, $|\boldsymbol{u}|_{W^{k+2,r}(\mathcal{T}_h)^d}$, $|\boldsymbol{\sigma}(\cdot, \boldsymbol{\nabla}_{\mathrm{s}}\boldsymbol{u})|_{W^{(k+1)(\tilde{r}-1),r'}(\mathcal{T}_h)^{d\times d}}$, $|p|_{W^{(k+1)(\tilde{r}-1),r'}(\mathcal{T}_h)}$, $\|\boldsymbol{f}\|_{L^{r'}(\Omega)^d}$.

Preuve 8. Voir Section 1.7.3.3.

On en déduit les ordres de convergence respectifs suivants pour la vélocité et la pression :

$$O_{\mathrm{vel}}^k := \frac{(k+1)(\tilde{r}-1)}{r+1-\tilde{r}} \quad \text{et} \quad O_{\mathrm{pre}}^k := \frac{(k+1)(\tilde{r}-1)^2}{r+1-\tilde{r}}. \tag{42}$$

Remarquons que, suite à la présence de termes d'ordres plus élevés dans l'estimation d'erreur (41), on pourrait observer des taux de convergence plus élevés avant d'atteindre les ordres de convergence asymptotiques. De plus, les ordres de convergence obtenus pour la vélocité coïncident avec ceux démontrés dans [47, Théorème 3.2] pour des discrétisations HHO sur des problèmes scalaires de Leray–Lions. Une panoplie de tests démontre la stabilité et la précision de la méthode.

3 Amélioration des estimations d'erreur pour des méthodes HHO sur les problèmes de Leray–Lions

Cette section résume le Chapitre 2, où nous construisons et analysons une méthode HHO pour les problèmes de Leray–Lions. L'objectif de ces travaux est d'apporter une amélioration des estimations d'erreur démontrées dans [47], pour les problèmes de Leray–Lions dans $W^{1,p}$ dans le cas $p \leq 2$. Une des nouveautés repose sur l'introduction

de la notion de dégénérescence. En effet, de par la nature du problème, des puissances négatives de la norme du gradient de la solution peuvent apparaître dans le flux. Cela peut avoir pour conséquence de créer des dégénérescences locales du problème. Les autres contributions incluent l'adoption d'hypothèses plus large sur la fonction flux, qui permettent notamment de considérer des flux de type Carreau–Yasuda, en faisant intervenir la notion de fonction encadrée. Des hypothèses analogues sont supposées pour la fonction de stabilisation, dans le but de traiter en parallèle avec la fonction flux, l'analyse du schéma. Ces nouveautés permettent de démontrer des estimations d'erreur qui prennent en compte l'influence de la dégénérescence du problème sur les taux de convergence. L'analyse dépend de la nature de la fonction flux et traite simultanément les deux cas de dégénérescence, selon si la norme du gradient de la solution s'annule ou explose.

Après avoir présenté le problème de Leray–Lions, avec les nouvelles hypothèses de fonction encadrée sur la fonction flux, nous construisons la méthode HHO avec la nouvelle fonction de stabilisation. Nous énonçons ensuite dans le Théorème 4, l'estimation d'erreur; en posant k, le degré polynomial de la méthode, on obtient des taux de convergence entre $k+1$, pour le cas globalement non-dégénéré, et $(k+1)(p-1)$, pour le cas globalement dégénéré, ce qui coïncide avec l'estimation d'erreur originellement prouvée dans [47, Théorème 3.2]. Pour y parvenir, nous utilisons à la fois les propriétés hölderiennes et hölderiennes singulières que possèdent les fonctions flux et de stabilisation, cf. Hypothèses 2 et 3. Des tests numériques furent effectués pour confirmer ces estimations d'erreur.

Ces travaux ont donné lieu à un article complet paru dans la revue internationale Calcolo, cf. [52].

3.1 Problème de Leray–Lions

Soit $\Omega \subset \mathbb{R}^d$ un polytope borné connexe à frontière lipschitzienne $\partial\Omega$. Le problème de Leray–Lions consiste à : Trouver $u : \Omega \to \mathbb{R}$ tel que

$$-\boldsymbol{\nabla}\cdot\boldsymbol{\sigma}(\cdot,\boldsymbol{\nabla}u) = f \qquad \text{in } \Omega, \tag{43a}$$
$$u = 0 \qquad \text{on } \partial\Omega, \tag{43b}$$

où $f : \Omega \to \mathbb{R}$ représente une *force volumétrique*, tandis que $\boldsymbol{\sigma} : \Omega \times \mathbb{R}^d \to \mathbb{R}^d$ est la *fonction flux* qui peut dépendre de la variable d'espace et qui intervient à travers le gradient du *potentiel* $u : \Omega \to \mathbb{R}$.

Hypothèse 2 (Fonction flux)**.** Soit $p \in]1,2]$ un réel fixé. On suppose que

$$\boldsymbol{\sigma}(\cdot,\mathbf{0}) \in L^{p'}(\Omega)^d \text{ pour presque tout } \boldsymbol{x} \in \Omega, \tag{44a}$$
$$\boldsymbol{\sigma} : \Omega \times \mathbb{R}^d \to \mathbb{R}^d \text{ est } (p,\delta)\text{-encadrée}, \tag{44b}$$

avec $\delta \in L^p(\Omega, [0,+\infty[)$ et où on note $\sigma_{\mathrm{hc}}, \sigma_{\mathrm{hm}} \in]0,+\infty[$ les constantes respectives de continuité et monotonicité hölderiennes.

Exemple 14 (Carreau–Yasuda)**.** Un exemple de fonction flux vérifiant l'Hypothèse 2 est la fonction de Carreau–Yasuda définie pour presque tout $\boldsymbol{x} \in \Omega$ et tout $\boldsymbol{\tau} \in \mathbb{R}^d$ par

$$\boldsymbol{\sigma}(\boldsymbol{x}, \boldsymbol{\tau}) = \mu(\boldsymbol{x}) \left(\delta(\boldsymbol{x})^{a(\boldsymbol{x})} + |\boldsymbol{\tau}|^{a(\boldsymbol{x})}\right)^{\frac{p-2}{a(\boldsymbol{x})}} \boldsymbol{\tau}, \tag{45}$$

correspondant à la version vectorielle de (6), où $\mu : \Omega \to [\mu_-, \mu_+] \subset]0,+\infty[$ et $a : \Omega \to [a_-, a_+] \subset]0,+\infty[$ sont des fonctions mesurables et $\delta \in L^p(\Omega, [0,+\infty[)$. Remarquons que lorsque $\delta \equiv 0$ et $\mu \equiv 1$, (43) devient le problème du p-laplacien $-\boldsymbol{\nabla}\cdot(|\boldsymbol{\nabla} u|^{p-2}\boldsymbol{\nabla} u) = f$.

On définit l'espace du potentiel incluant les conditions aux limites par :

$$U \coloneqq \{v \in W^{1,p}(\Omega) \mid v_{|\partial\Omega} = 0\}.$$

En suppose maintenant que $f \in L^{p'}(\Omega)$, la formulation faible du problème (43) est définie par : Trouver $u \in U$ tel que

$$a(u, v) = \int_\Omega f v \qquad \forall v \in U, \tag{46}$$

où la *fonction de diffusion* $a : U \times U \to \mathbb{R}$ est définie telle que, pour tout $v, w \in U$,

$$a(w, v) \coloneqq \int_\Omega \boldsymbol{\sigma}(\cdot, \boldsymbol{\nabla} w) \cdot \boldsymbol{\nabla} v. \tag{47}$$

Proposition 15 (Bonne position et majoration)**.** *Sous l'Hypothèse 2, la formulation faible (46) admet une unique solution $u \in U$. De plus, elle vérifie l'inégalité suivante :*

$$\begin{aligned} \|\boldsymbol{\nabla} u\|_{L^p(\Omega)^d} \le{}& \left(2^{\frac{2-p}{p}} C_{\mathrm{P}} \sigma_{\mathrm{hm}}^{-1} \|f\|_{L^{p'}(\Omega)}\right)^{\frac{1}{p-1}} \\ &+ \min\left(\|\delta\|_{L^p(\Omega)}; 2^{\frac{2-p}{p}} C_{\mathrm{P}} \sigma_{\mathrm{hm}}^{-1} \|\delta\|_{L^p(\Omega)}^{2-p} \|f\|_{L^{p'}(\Omega)}\right). \end{aligned} \tag{48}$$

où $C_{\mathrm{P}} > 0$ dépend seulement de Ω et p, et provient de l'inégalité de Poincaré telle que, pour tout $v \in U$, $\|v\|_{L^p(\Omega)} \le C_{\mathrm{P}} \|\boldsymbol{\nabla} v\|_{L^p(\Omega)^d}$.

Preuve 9. Voir Section 2.2.2.

3.2 Méthode Hybrid High-Order

On considère une suite de maillages régulière $(\mathcal{M}_h)_{h\in\mathcal{H}}$ de Ω définie comme dans le paragraphe 1.2.1.

3.2.1 Espace hybride et semi-norme

Posons $k \in \mathbb{N}$, le degré de la méthode. On définit l'espace hybride

$$\underline{U}_h^k \coloneqq \left\{ \underline{v}_h \coloneqq ((v_T)_{T\in\mathcal{T}_h}, (v_F)_{F\in\mathcal{F}_h}) \;\middle|\; \begin{array}{l} v_T \in \mathbb{P}^k(T) \quad \forall T \in \mathcal{T}_h \\ v_F \in \mathbb{P}^k(F) \quad \forall F \in \mathcal{F}_h \end{array} \right\}. \tag{49}$$

Cet espace est la version scalaire de celui défini par (23). On introduit l'opérateur d'interpolation $\underline{I}_h^k : W^{1,1}(\Omega) \to \underline{U}_h^k$ qui projette une fonction $v \in W^{1,1}(\Omega)$ sur le vecteur d'inconnues discrètes $\underline{I}_h^k v$ tel que :

$$\underline{I}_h^k v \coloneqq ((\pi_T^k v_{|_T})_{T\in\mathcal{T}_h}, (\pi_F^k v_{|_F})_{F\in\mathcal{F}_h}).$$

Au niveau local, pour tout $T \in \mathcal{T}_h$, on note $\underline{U}_T^k$ et $\underline{I}_T^k$ les restrictions de $\underline{U}_h^k$ et $\underline{I}_h^k$ sur T, respectivement. De plus, pour tout $\underline{v}_h \in \underline{U}_h^k$, on note $\underline{v}_T \coloneqq (v_T, (v_F)_{F\in\mathcal{F}_T}) \in \underline{U}_T^k$ le vecteur collectant les inconnues discrètes rattachées à l'élément T et ses faces. Enfin, pour tout $\underline{v}_h \in \underline{U}_h^k$, on définit le polynôme brisé $v_h \in \mathbb{P}^k(\mathcal{T}_h)$ par :

$$(v_h)_{|_T} \coloneqq v_T \qquad \forall T \in \mathcal{T}_h.$$

Pour tout $q \in (1, +\infty)$, on définit sur $\underline{U}_h^k$ la semi-norme $\|\cdot\|_{1,q,h}$ telle que, pour tout $\underline{v}_h \in \underline{U}_h^k$,

$$\|\underline{v}_h\|_{1,q,h} \coloneqq \left(\sum_{T\in\mathcal{T}_h} \|\underline{v}_T\|_{1,q,T}^q \right)^{\frac{1}{q}}, \tag{50a}$$

où, pour tout $T \in \mathcal{T}_h$,

$$\|\underline{v}_T\|_{1,q,T} \coloneqq \left(\|\boldsymbol{\nabla} v_T\|_{L^q(T)^d}^q + \sum_{F\in\mathcal{F}_T} h_F^{1-q} \|v_F - v_T\|_{L^q(F)}^q \right)^{\frac{1}{q}}. \tag{50b}$$

On définit à présent l'espace du potentiel discret comme le sous-espace de $\underline{U}_h^k$ incluant les conditions aux bords :

$$\underline{U}_{h,0}^k \coloneqq \left\{ \underline{v}_h \in \underline{U}_h^k \;:\; v_F = 0 \quad \forall F \in \mathcal{F}_h^{\mathrm{b}} \right\}.$$

On a l'inégalité de Poincaré discrète suivante, cf. [48, Proposition 5.4] : Pour tout $\underline{v}_h \in \underline{U}_{h,0}^k$,

$$\|v_h\|_{L^q(\Omega)} \lesssim \|\underline{v}_h\|_{1,q,h}. \tag{51}$$

Cette inégalité implique que $\|\cdot\|_{1,q,h}$ est une norme sur $\underline{U}_{h,0}^k$.

3.2.2 Opérateurs discrets

Pour tout $T \in \mathcal{T}_h$, on définit le *gradient discret local* $\mathbf{G}_T^k : \underline{U}_T^k \to \mathbb{P}^k(T)^d$ tel que, pour tout $\underline{v}_T \in \underline{U}_T^k$,

$$\int_T \mathbf{G}_T^k \underline{v}_T \cdot \boldsymbol{\tau} = \int_T \boldsymbol{\nabla} v_T \cdot \boldsymbol{\tau} + \sum_{F \in \mathcal{F}_T} \int_F (v_F - v_T)\, (\boldsymbol{\tau} \cdot \boldsymbol{n}_{TF}) \qquad \forall \boldsymbol{\tau} \in \mathbb{P}^k(T)^d. \tag{52}$$

De plus, nous définissons *l'opérateur de bord résiduel* $\Delta_{\partial T}^k : \underline{U}_T^k \to L^p(\partial T)$ tel que, pour tout $\underline{v}_T \in \underline{U}_T^k$,

$$(\Delta_{\partial T}^k \underline{v}_T)_{|F} \coloneqq \frac{1}{h_T} \left[\pi_F^k (\mathrm{r}_T^{k+1} \underline{v}_T - v_F) - \pi_T^k (\mathrm{r}_T^{k+1} \underline{v}_T - v_T) \right] \qquad \forall F \in \mathcal{F}_T, \tag{53}$$

où on a introduit le *potentiel discret local* $\mathrm{r}_T^{k+1} : \underline{U}_T^k \to \mathbb{P}^{k+1}(T)$ définit tel que, pour tout $\underline{v}_T \in \underline{U}_T^k$,

$$\int_T (\boldsymbol{\nabla} \mathrm{r}_T^{k+1} \underline{v}_T - \mathbf{G}_T^k \underline{v}_T) \cdot \boldsymbol{\nabla} w = 0 \qquad \forall w \in \mathbb{P}^{k+1}(T), \tag{54}$$

$$\int_T \mathrm{r}_T^{k+1} \underline{v}_T = \int_T v_T. \tag{55}$$

3.2.3 Fonctions de diffusion discrète et de stabilisations locales

On peut à présent définir la *fonction de diffusion discrète* $\mathrm{a}_h : \underline{U}_h^k \times \underline{U}_h^k \to \mathbb{R}$ telle que, pour tout $\underline{v}_h, \underline{w}_h \in \underline{U}_h^k$,

$$\mathrm{a}_h(\underline{w}_h, \underline{v}_h) \coloneqq \sum_{T \in \mathcal{T}_h} \left(\int_T \boldsymbol{\sigma}(\cdot, \mathbf{G}_T^k \underline{w}_T) \cdot \mathbf{G}_T^k \underline{v}_T + h_T \int_{\partial T} \mathrm{S}_T(\cdot, \Delta_{\partial T}^k \underline{w}_T) \Delta_{\partial T}^k \underline{v}_T \right), \tag{56}$$

où pour tout $T \in \mathcal{T}_h$, S_T est une *fonction de stabilisation locale* pour laquelle nous émettrons des hypothèses analogues à l'Hypothèse 2 de la fonction flux $\boldsymbol{\sigma}$. Tout d'abord, nous définissons le squelette du maillage $\partial\mathcal{M}_h \coloneqq \bigcup_{F \in \mathcal{F}_h} \overline{F}$ et posons

$$\begin{aligned} L^p(\partial\mathcal{M}_h) &\coloneqq \left\{ \mu \,:\, \partial\mathcal{M}_h \to \mathbb{R} \,:\, \mu_{|F} \in L^p(F) \quad \forall F \in \mathcal{F}_h \right\}, \\ \|\mu\|_{L^p(\partial\mathcal{M}_h)} &\coloneqq \left(\sum_{T \in \mathcal{T}_h} h_T \sum_{F \in \mathcal{F}_T} \|\mu_{|F}\|_{L^p(F)}^p \right)^{\frac{1}{p}} \quad \forall \mu \in L^p(\partial\mathcal{M}_h). \end{aligned} \tag{57}$$

Hypothèse 3 (Fonction de stabilisation locale)**.** Pour tout $T \in \mathcal{T}_h$,

$$\mathrm{S}_T(\boldsymbol{x}, 0) = 0 \text{ pour presque tout } \boldsymbol{x} \in \Omega, \tag{58a}$$

$$\mathrm{S}_T : \partial T \times \mathbb{R} \to \mathbb{R} \text{ est } (\zeta, p)\text{-encadrée}, \tag{58b}$$

avec $\zeta \in L^p(\partial\mathcal{M}_h; [0, +\infty[)$ et où les constantes respectives de continuité et monotonicité hölderiennes singulières sont σ_{hc} et σ_{hm}.

Le caractère de fonction encadrée n'avait jusqu'à présent, jamais été appliqué aux fonctions de stabilisation. Il permet de considérer une classe plus large de fonctions de stabilisation, notamment grâce à l'introduction de la fonction de dégénérescence ζ. De plus, des résultats analogues entre les fonctions de stabilisation et le tenseur des contraintes peuvent être établis.

Exemple 16 (Fonction de stabilisation)**.** Une fonction de stabilisation locale vérifiant l'Hypothèse 3 peut être obtenue en posant, pour tout $T \in \mathcal{T}_h$, tout $w \in \mathbb{R}$, et tout $\boldsymbol{x} \in \partial T$,

$$\mathrm{S}_T(\boldsymbol{x}, w) := \tfrac{\sigma_{\mathrm{hc}}+\sigma_{\mathrm{hm}}}{2} \left(\zeta(\boldsymbol{x})^p + |w|^p\right)^{\frac{p-2}{p}} w. \tag{59}$$

On obtient ainsi une monotonicité hölderienne pour a_h, analogue à (35b) pour $p \leq 2$.

Lemme 17 (Monotonicité hölderienne de a_h)**.** *Sous les Hypothèses 2 et 3, pour tout* $\underline{v}_h, \underline{w}_h \in \underline{U}_h^k$, *on a*

$$\begin{aligned}\sigma_{\mathrm{hm}}\|\underline{v}_h - \underline{w}_h\|_{1,p,h}^2 \lesssim \left(\|\delta\|_{L^p(\Omega)}^p + \|\zeta\|_{L^p(\partial\mathcal{M}_h)}^p + \|\underline{v}_h\|_{1,p,h}^p + \|\underline{w}_h\|_{1,p,h}^p\right)^{\frac{2-p}{p}} \\ \times \left(\mathrm{a}_h(\underline{v}_h, \underline{v}_h - \underline{w}_h) - \mathrm{a}_h(\underline{w}_h, \underline{v}_h - \underline{w}_h)\right).\end{aligned} \tag{60}$$

Preuve 10. Voir Section 2.5.1.

3.3 Problème discret et résultat principaux

Nous définissons la version discrète de la formulation faible (46) par : Trouver $\underline{u}_h \in \underline{U}_{h,0}^k$ tel que

$$\mathrm{a}_h(\underline{u}_h, \underline{v}_h) = \int_\Omega f v_h \qquad \forall \underline{v}_h \in \underline{U}_{h,0}^k. \tag{61}$$

3.3.1 Bonne position du problème discret

On énonce l'existence et unicité d'une solution au problème (61).

Proposition 18 (Bonne position et majoration)**.** *Sous les Hypothèses 2 et 3, la formulation faible discrète* (61) *admet une unique solution* $\underline{u}_h \in \underline{U}_{h,0}^k$. *De plus, elle vérifie l'inégalité suivante :*

$$\|\underline{u}_h\|_{1,p,h} \lesssim C_1 \|f\|_{L^{p'}(\Omega)}^{\frac{1}{p-1}} + C_2 \min\left(\|\delta\|_{L^p(\mathcal{T}_h)}^{p-1} + \|\zeta\|_{L^p(\partial\mathcal{M}_h)}^{p-1}; \sigma_{\mathrm{hm}}^{-1}\|f\|_{L^{p'}(\Omega)}\right), \tag{62}$$

où $C_1, C_2 \in [0, +\infty[$ *dépendent uniquement de* $p, \sigma_{\mathrm{hm}}, \|\delta\|_{L^p(\mathcal{T}_h)}$ *et* $\|\zeta\|_{L^p(\partial\mathcal{M}_h)}$.

Preuve 11. Voir Section 58.

3.3.2 Estimation d'erreur adaptée à la dégénérescence

On énonce finalement l'estimation d'erreur ci-dessous.

Théorème 4 (Estimation d'erreur)**.** *Soit $u \in U$ et $\underline{u}_h \in \underline{U}_{h,0}^k$ les solutions des formulations faibles (46) et (61), respectivement. On suppose l'hypothèse de régularité supplémentaire $u \in W^{k+2,p}(\mathcal{T}_h)$ et $\boldsymbol{\sigma}(\cdot, \boldsymbol{\nabla} u) \in W^{1,p'}(\Omega)^d \cap W^{k+1,p'}(\mathcal{T}_h)^d$. Alors, sous les Hypothèses 2 et 3, on a*

$$\|\underline{u}_h - \underline{I}_h^k u\|_{1,p,h} \lesssim \mathcal{N}_1 h^{k+1} + \mathcal{N}_2 \min(\eta_h; 1)^{2-p}\, h^{(k+1)(p-1)}, \tag{63}$$

où l'on définit le paramètre de dégénérescence du flux

$$\mathfrak{D}_h \coloneqq \min\left(\operatorname*{ess\,inf}_{\Omega} (\delta + |\boldsymbol{\nabla} u|)\,; \operatorname*{ess\,inf}_{\partial \mathcal{M}_h} \zeta \right), \tag{64}$$

que l'on introduit dans le nombre sans dimension

$$\eta_h \coloneqq \begin{cases} h^{k+1} \max_{T \in \mathcal{T}_h} \left(|T|^{-\frac{1}{p}} |u|_{W^{k+2,p}(T)} \right) \mathfrak{D}_h^{-1} & \text{si } \mathfrak{D}_h \neq 0 \neq |u|_{W^{k+2,p}(\mathcal{T}_h)} \\ +\infty & \text{si } \mathfrak{D}_h = 0 \neq |u|_{W^{k+2,p}(\mathcal{T}_h)} \\ 0 & \text{si } \mathfrak{D}_h = 0 = |u|_{W^{k+2,p}(\mathcal{T}_h)} \end{cases} \tag{65}$$

et où $\mathcal{N}_1, \mathcal{N}_2 \in [0, +\infty[$ dépendent uniquement de $p, \sigma_{\mathrm{hc}}, \sigma_{\mathrm{hm}}, \|\delta\|_{L^p(\Omega)}$, $\|\zeta\|_{L^p(\partial \mathcal{M}_h)}$, $\|f\|_{L^{p'}(\Omega)}$, $|\boldsymbol{\sigma}(\cdot, \boldsymbol{\nabla} u)|_{W^{k+1,p'}(\mathcal{T}_h)^d}$ et $|u|_{W^{k+2,p}(\mathcal{T}_h)}$.

Preuve 12. Voir Section 2.5.2.

Le paramètre $\mathfrak{D}_h$ permet de mesurer localement la dégénérescence du flux et de la fonction de stabilisation : plus il est proche de zéro, plus le modèle est dégénéré. Le nombre sans dimension η_h permet, quant à lui, de déterminer le taux de convergence de la méthode :

(i) Si $\eta_h \geq 1$, on est dans le cas *globalement dégénéré* avec pour taux de convergence $(k+1)(p-1)$;

(ii) Si $\eta_h \leq h^{k+1} |u|_{W^{k+2,p}(\mathcal{T}_h)}$, i.e. $\mathfrak{D}_h \geq 1$, on est dans le cas *globalement non-dégénéré* avec pour taux de convergence $k+1$;

(iii) Le cas $\eta_h \in]h^{k+1} |u|_{W^{k+2,p}(\mathcal{T}_h)}, 1[$ correspond à des taux de convergence intermédiaires entre $(k+1)(p-1)$ et $k+1$.

Dans le chapitre 2, nous énonçons une version locale du Théorème 4. Une série de résultats numériques permettent de confirmer les prédictions du théorème.

4 Méthode HHO pour des fluides non-newtoniens avec convection suivant une loi en puissance

Dans le Chapitre 3, nous étendons les travaux du Chapitre 1, qui portent sur l'écoulement de fluides non-newtoniens gouverné par les équations de Stokes, aux équations de Navier–Stokes. La différence entre ces deux problèmes réside dans l'introduction d'un terme convectif. Dans la littérature, le terme convectif du problème de Navier–Stokes a connu peu d'évolution à l'instar du terme visqueux. Récemment, une variante du terme convectif trilinéaire classique fut considérée dans [86], en relation avec le calcul de la distance de Wasserstein dans le contexte de l'application au transport optimal. Pour aller plus loin, nous avons développé une nouvelle façon de définir le terme convectif en introduisant la notion de loi de convection. Dès lors, il est possible de considérer des termes convectifs différents du cas classique. Par exemple, on peut choisir un terme convectif suivant une loi en puissance, et dans ce cas, on retrouve celui décrit dans [86]. De plus, cette nouvelle loi satisfait des relations de non-dissipativité et une propriété de continuité hölderienne singulière, et a pour atout de faciliter l'étude du problème continu ainsi que l'analyse de la méthode HHO. Ainsi dans ces travaux, nous construisons et étudions une méthode HHO appliquée au problème de Navier–Stokes stationnaire, généralisé aux fluides non-newtoniens incompressibles. Ces travaux ont également l'avantage d'inclure une généralisation du terme convectif.

Dans la suite de cette section, nous résumons les travaux réalisés dans le Chapitre 3. Premièrement, nous énonçons le problème continu de Navier–Stokes stationnaire pour des fluides incompressibles avec les hypothèses susmentionnées sur le terme convectif, cf. Hypothèse 5, admettant un comportement de loi en puissance, tout comme le terme visqueux, cf. Hypothèse 4. Les comportements de loi en puissance des termes visqueux et convectifs sont caractérisés par des exposants de Sobolev $r \in]1, \infty[$ et $s \in]1, \infty[$, possiblement distincts. Ensuite, nous énonçons dans le Théorème 5, la bonne position du problème continu afin de mettre en exergue des relations entre ces exposants, qui déterminent l'existence et l'unicité de la solution. Nous construisons ensuite la méthode HHO qui nécessite en outre le développement d'une fonction convective discrète. La bonne position du problème discret fut également établie dans le Théorème 6. Puis, nous énonçons dans le Théorème 7 des résultats de convergence sous l'hypothèse de régularités minimales des solutions par un argument de compacité. Enfin, nous donnons dans le Théorème 8, une estimation d'erreur pour des fluides pseudoplastiques impliquant différents ordres de convergence selon la dégénérescence du problème dans le même esprit que la Section 3, i.e. entre $(k+1)(r-1)$ et $k+1$ pour la vélocité et entre $(k+1)(r-1)^2$ et $(k+1)(r-1)$ pour la pression, où k est le degré polynomial de la méthode. Plusieurs simulations numériques figurent dans le Chapitre 3, dont le problème de la cavité entraînée, dans le but de valider les résultats théoriques.

Ces travaux ont été soumis pour publication, cf. [35].

4.1 Problème de Navier–Stokes généralisé

Soit $\Omega \subset \mathbb{R}^d$, $d \in \{2,3\}$, un polyèdre ouvert connexe à frontière lipschitzienne $\partial\Omega$. On considère un fluide incompressible possiblement non-newtonien occupant Ω et soumis à une *force volumétrique* $\boldsymbol{f} : \Omega \to \mathbb{R}^d$. Son écoulement est régi par le *problème de Navier–Stokes généralisé*, qui consiste à trouver la *vélocité* $\boldsymbol{u} : \Omega \to \mathbb{R}^d$ et la *pression* $p : \Omega \to \mathbb{R}$ tel que

$$-\boldsymbol{\nabla}\cdot\boldsymbol{\sigma}(\cdot,\boldsymbol{\nabla}_{\mathrm{s}}\boldsymbol{u}) + (\boldsymbol{u}\cdot\boldsymbol{\nabla})\boldsymbol{\chi}(\cdot,\boldsymbol{u}) + \boldsymbol{\nabla}p = \boldsymbol{f} \qquad \text{in } \Omega, \tag{66a}$$
$$\boldsymbol{\nabla}\cdot\boldsymbol{u} = 0 \qquad \text{in } \Omega, \tag{66b}$$
$$\boldsymbol{u} = \boldsymbol{0} \qquad \text{on } \partial\Omega, \tag{66c}$$
$$\int_\Omega p = 0, \tag{66d}$$

où $\boldsymbol{\sigma} : \Omega \times \mathbb{R}^{d\times d}_{\mathrm{s}} \to \mathbb{R}^{d\times d}_{\mathrm{s}}$ est la *loi de viscosité* et $\boldsymbol{\chi} : \Omega \times \mathbb{R}^d \to \mathbb{R}^d$ est la *loi de convection*.

4.1.1 Hypothèses sur les lois de viscosité et de convection

Hypothèse 4 (Loi de viscosité)**.** Soit $r \in]1,+\infty[$ un réel fixé. On suppose que

$$\boldsymbol{\sigma}(\cdot,\boldsymbol{0}) \in L^{r'}(\Omega,\mathbb{R}^{d\times d}_{\mathrm{s}}) \text{ pour presque tout } \boldsymbol{x} \in \Omega, \tag{67a}$$
$$\boldsymbol{\sigma} : \Omega \times \mathbb{R}^{d\times d}_{\mathrm{s}} \to \mathbb{R}^{d\times d}_{\mathrm{s}} \text{ est } (r,\delta)\text{-encadrée}, \tag{67b}$$

avec $\delta \in [0,+\infty[$ et où on note $\sigma_{\mathrm{hc}}, \sigma_{\mathrm{hm}} \in]0,+\infty[$ les constantes respectives de continuité et monotonicité hölderiennes.

Contrairement à l'Hypothèse 1 établie pour le problème de Stokes, où on suppose que $\boldsymbol{\sigma}$ n'est que singulièrement encadrée, on suppose ici l'hypothèse plus large de fonction encadrée afin d'obtenir une meilleure estimation d'erreur dans le cas des fluides pseudoplastiques, de manière analogue à celle développée dans l'analyse de Leray–Lions du Chapitre 2. Comme pour le problème de Stokes en Section 2.2.1, la loi de Carreau–Yasuda (6) vérifie l'Hypothèse 4.

Hypothèse 5 (Loi de convection)**.** Soit $s \in]1,\infty[$ fixé. On suppose que

$$\boldsymbol{\chi} : \Omega \times \mathbb{R}^d \to \mathbb{R}^d \text{ est mesurable}, \tag{68a}$$
$$\boldsymbol{\chi}(\boldsymbol{x},\boldsymbol{0}) = \boldsymbol{0} \text{ pour presque tout } \boldsymbol{x} \in \Omega. \tag{68b}$$

On suppose aussi les relations de non-dissipativité suivantes : pour tout $\boldsymbol{w} \in \mathbb{R}^d$,

$$(\boldsymbol{w}\cdot\boldsymbol{\nabla})\boldsymbol{\chi}(\cdot,\boldsymbol{w}) = (\boldsymbol{\chi}(\cdot,\boldsymbol{w})\cdot\boldsymbol{\nabla})\boldsymbol{w} + (s-2)|\boldsymbol{w}|^{-2}[(\boldsymbol{\chi}(\cdot,\boldsymbol{w})\cdot\boldsymbol{\nabla})\boldsymbol{w}\cdot\boldsymbol{w}]\boldsymbol{w}, \tag{68c}$$
$$\boldsymbol{w}\otimes\boldsymbol{\chi}(\cdot,\boldsymbol{w}) = \boldsymbol{\chi}(\cdot,\boldsymbol{w})\otimes\boldsymbol{w}. \tag{68d}$$

De plus, il existe $\chi_{\mathrm{hc}} \in]0,\infty[$ tel que, pour tout $\boldsymbol{v},\boldsymbol{w} \in \mathbb{R}^d$ et presque tout $\boldsymbol{x} \in \Omega$, on a la propriété de continuité hölderienne singulière

$$|\chi(\boldsymbol{x},\boldsymbol{w}) - \chi(\boldsymbol{x},\boldsymbol{v})| \leq \chi_{\mathrm{hc}} \left(|\boldsymbol{w}|^s + |\boldsymbol{v}|^s\right)^{\frac{s-\tilde{s}}{s}} |\boldsymbol{w}-\boldsymbol{v}|^{\tilde{s}-1}. \tag{68e}$$

Exemple 19 (Loi de convection de Laplace)**.** Un exemple de loi de convection vérifiant l'Hypothèse 5 est la fonction de Laplace considérée dans [86] dans le contexte de l'application au transport optimal et définie telle que, pour presque tout $\boldsymbol{x} \in \Omega$ et tout $\boldsymbol{w} \in \mathbb{R}^d$,

$$\chi(\boldsymbol{x},\boldsymbol{w}) = \nu(\boldsymbol{x})|\boldsymbol{w}|^{s-2}\boldsymbol{w}, \tag{69}$$

où $s \in]1,+\infty[$ est *l'indice de convection* et $\nu : \Omega \to [0,\nu_+] \subset [0,+\infty[$ est une fonction mesurable correspondant à *l'indice local de convection du flux*.

On peut choisir la loi de convection standard en posant $s = 2$ et $\nu \equiv 1$. Remarquons aussi que poser $\nu \equiv 0$ nous ramène au problème de Stokes (13).

4.1.2 Formulation faible continue

On considère les mêmes espaces $\boldsymbol{U}$ et P de vélocité et pression définis pour le problème de Stokes généralisé en Section 2.2.

En supposant $\boldsymbol{f} \in L^{r'}(\Omega)^d$, on définit la formulation faible du problème continu (66) par : Trouver $(\boldsymbol{u},p) \in \boldsymbol{U} \times P$ tel que

$$a(\boldsymbol{u},\boldsymbol{v}) + c(\boldsymbol{u},\boldsymbol{v}) + b(\boldsymbol{v},p) = \int_\Omega \boldsymbol{f}\cdot\boldsymbol{v} \qquad \forall \boldsymbol{v} \in \boldsymbol{U}, \tag{70a}$$

$$-b(\boldsymbol{u},q) = 0 \qquad \forall q \in P, \tag{70b}$$

où $a : \boldsymbol{U}\times\boldsymbol{U} \to \mathbb{R}$ et $b : \boldsymbol{U} \times L^{r'}(\Omega) \to \mathbb{R}$ sont définies comme dans la formulation faible du problème de Stokes (18), et où la *fonction convective* $c : \boldsymbol{U}\times\boldsymbol{U} \to \mathbb{R}$ est définie telle que, pour tout $\boldsymbol{v},\boldsymbol{w} \in \boldsymbol{U}$,

$$\begin{aligned} c(\boldsymbol{w},\boldsymbol{v}) \coloneqq \frac{1}{s}\int_\Omega (\chi(\cdot,\boldsymbol{w})\cdot\boldsymbol{\nabla})\boldsymbol{w}\cdot\boldsymbol{v} - \frac{1}{s'}\int_\Omega (\chi(\cdot,\boldsymbol{w})\cdot\boldsymbol{\nabla})\boldsymbol{v}\cdot\boldsymbol{w} \\ + \frac{s-2}{s}\int_\Omega \frac{\boldsymbol{v}\cdot\boldsymbol{w}}{|\boldsymbol{w}|^2}(\chi(\cdot,\boldsymbol{w})\cdot\boldsymbol{\nabla})\boldsymbol{w}\cdot\boldsymbol{w}. \end{aligned} \tag{71}$$

Sous l'Hypothèse 5, on a par construction la propriété de *non-dissipativité* suivante : Pour tout $\boldsymbol{w} \in \boldsymbol{U}$,

$$c(\boldsymbol{w},\boldsymbol{w}) = 0. \tag{72}$$

4.1.3 Inégalité de Sobolev et bonne position du problème continu

Avec la seule Hypothèse 4, l'unicité de la solution du problème (70) n'est pas garantie pour toute valeur de r et s, et en particulier lorsque $r > 2$ dans le cas dégénéré $\delta = 0$. Le cas non-dégénéré peut néanmoins être traité à l'aide de la continuité hölderienne singulière de a suivante.

Lemme 20 (Continuité hölderienne singulière de a)**.** *Sous l'Hypothèse 4, pour tout $m \in \{\tilde{r}, r\}$ et tout $\boldsymbol{u}, \boldsymbol{w} \in \boldsymbol{U}$, on a*

$$a(\boldsymbol{u}, \boldsymbol{u}-\boldsymbol{w}) - a(\boldsymbol{w}, \boldsymbol{u}-\boldsymbol{w}) \geq C_{\mathrm{a}}\sigma_{\mathrm{hm}} \left(\delta^r + |\boldsymbol{u}|^r_{W^{1,r}(\Omega)^d} + |\boldsymbol{w}|^r_{W^{1,r}(\Omega)^d}\right)^{\frac{\tilde{r}-2}{r}} \delta^{r-m} |\boldsymbol{u}-\boldsymbol{w}|^{m+2-\tilde{r}}_{W^{1,m}(\Omega)^d}, \quad (73)$$

où $C_{\mathrm{a}} > 0$ dépend uniquement de r et Ω.

Preuve 13. Voir Section 3.2.3.

Pour tout $m \in [1, +\infty]$, on définit *l'exposant de Sobolev* de m par

$$m^* := \begin{cases} \frac{dm}{d-m} & \text{if } m < d \\ +\infty & \text{if } m \geq d \end{cases} \in [m, +\infty]. \quad (74)$$

De plus, on rappelle l'inégalité de Sobolev continue suivante : Pour tout $m \in [1, +\infty[$ tel que $m \leq r^*$ et tout $\boldsymbol{v} \in \boldsymbol{U}$,

$$\|\boldsymbol{v}\|_{L^m(\Omega)^d} \leq C_{\mathrm{S},m} |\boldsymbol{v}|_{W^{1,r}(\Omega)^d}, \quad (75)$$

où $C_{\mathrm{S},m} > 0$ dépend uniquement de m, r, d et Ω. Cette inégalité est à l'origine des hypothèses sur s pour la continuité hölderienne singulière suivante de c_h.

Lemme 21 (Continuité hölderienne singulière de c)**.** *Sous l'Hypothèse 5, pour tout $m \in [1, r]$ tel que $s \leq \frac{m^*}{m'}$, et tout $\boldsymbol{u}, \boldsymbol{v}, \boldsymbol{w} \in \boldsymbol{U}$, on a*

$$|c(\boldsymbol{u}, \boldsymbol{v}) - c(\boldsymbol{w}, \boldsymbol{v})| \leq C_{\mathrm{c},m}\chi_{\mathrm{hc}} \left(|\boldsymbol{u}|^r_{W^{1,r}(\Omega)^d} + |\boldsymbol{w}|^r_{W^{1,r}(\Omega)^d}\right)^{\frac{s+1-\tilde{s}}{r}} |\boldsymbol{u}-\boldsymbol{w}|^{\tilde{s}-1}_{W^{1,m}(\Omega)^d} |\boldsymbol{v}|_{W^{1,m}(\Omega)^d}, \quad (76)$$

où $C_{\mathrm{c},m} > 0$ dépend uniquement de m, r, s, d et Ω.

Preuve 14. Voir Section 3.2.3.

Le lemme précédent est un résultat essentiel dans l'étude de la bonne position du problème continu de Navier–Stokes où le terme convectif suit un comportement de loi en puissance, cf. Théorème 5. En effet, puisque c n'est pas la fonction trilinéaire classique, nous avons besoin d'établir ce nouvel outil. Un résultat analogue est énoncé dans le cadre discret, cf. Lemme 23.

Théorème 5 (Bonne position)**.** *Sous les Hypothèses 4 et 5, il existe une solution* $(\boldsymbol{u}, p) \in \boldsymbol{U} \times P$ *à la formulation faible* (70)*, et toute solution satisfait*

$$|\boldsymbol{u}|_{W^{1,r}(\Omega)^d} \le C_{\mathrm{v}} \left[\left(\sigma_{\mathrm{hm}}^{-1} \|\boldsymbol{f}\|_{L^{r'}(\Omega)^d} \right)^{r'} + \min \left(\delta^r ; \left(\delta^{2-\tilde{r}} \sigma_{\mathrm{hm}}^{-1} \|\boldsymbol{f}\|_{L^{r'}(\Omega)^d} \right)^{\frac{r}{r+1-\tilde{r}}} \right) \right]^{\frac{1}{r}} \tag{77}$$

avec $C_{\mathrm{v}} > 0$ *dépendant uniquement de* Ω*,* d *et* r*. De plus, si on a* $2 \le s \le \frac{\tilde{r}^*}{\tilde{r}'}$ *ainsi que l'hypothèse de petites données suivante :*

$$\delta^r + \left(\sigma_{\mathrm{hm}}^{-1} \|\boldsymbol{f}\|_{L^{r'}(\Omega)^d} \right)^{r'} < \left(1 + 2C_{\mathrm{v}}^r \right)^{-1} \left(C_{\mathrm{c},\tilde{r}}^{-1} \chi_{\mathrm{hc}}^{-1} C_{\mathrm{a}} \sigma_{\mathrm{hm}} \delta^{r-\tilde{r}} \right)^{\frac{r}{s+1-\tilde{r}}}, \tag{78}$$

alors la solution de (70) *est unique.*

Preuve 15. Voir Section 3.2.3.

L'unicité de la solution n'est pas garantie pour tout $r, s \in]1, +\infty[$. En effet, en plus de l'hypothèse $s \le \frac{\tilde{r}^*}{\tilde{r}'}$ provenant de la continuité hölderienne singulière (76), des problèmes surgissent lorsque $s < 2$ ou $r > 2$. Toutefois, dans le cas non-dégénéré $\delta \neq 0$, l'unicité de la solution peut être étendue au cas $r > 2$.

4.2 Méthode Hybrid High-Order

On considère une suite de maillages régulière $(\mathcal{M}_h)_{h \in \mathcal{H}}$ définie comme dans le paragraphe 1.2.1. On fixe un degré $k \ge 1$ pour la méthode et on utilisera les espaces et normes discrets définis pour le problème de Stokes en Section 2.3.1.

4.2.1 Terme visqueux et couplage pression-vitesse discrets

En rappelant les définitions des opérateurs discrets en Section 2.3.2, on redéfinit la fonction visqueuse discrète $\mathrm{a}_h : \underline{\boldsymbol{U}}_h^k \times \underline{\boldsymbol{U}}_h^k \to \mathbb{R}$ telle que, pour tout $\underline{\boldsymbol{v}}_h, \underline{\boldsymbol{w}}_h \in \underline{\boldsymbol{U}}_h^k$,

$$\mathrm{a}_h(\underline{\boldsymbol{w}}_h, \underline{\boldsymbol{v}}_h) \coloneqq \int_\Omega \boldsymbol{\sigma}(\cdot, \mathbf{G}_{\mathrm{s},h}^k \underline{\boldsymbol{w}}_h) : \mathbf{G}_{\mathrm{s},h}^k \underline{\boldsymbol{v}}_h + \sum_{T \in \mathcal{T}_h} h_T \int_{\partial T} \mathbf{S}_T(\cdot, \boldsymbol{\Delta}_{\partial T}^k \underline{\boldsymbol{w}}_T) \cdot \boldsymbol{\Delta}_{\partial T}^k \underline{\boldsymbol{v}}_T, \tag{79}$$

où pour tout $T \in \mathcal{T}_h$, $\mathbf{S}_T : \Omega \times \mathbb{R}^d \to \mathbb{R}^d$ est une fonction de stabilisation locale (r, δ)-encadrée par les mêmes constantes hölderiennes σ_{hc} et σ_{hm} de $\boldsymbol{\sigma}$. Le choix des fonctions de stabilisation dans la définition de la fonction a_h est inspiré du Chapitre 2, concernant les problèmes de Leray–Lions. Ce choix marque l'unique changement avec la fonction visqueuse discrète (33), apparaissant dans le Chapitre 1. Comme pour l'étude du problème de Leray–Lions, on peut considérer pour $\mathbf{S}_T$ une fonction de dégénérescence différente de δ. On conservera le choix δ pour alléger la lecture.

On obtient la propriété hölderienne singulière (35a) pour a_h. De plus, dualement à a, on a la monotonicité hölderienne singulière suivante.

Lemme 22 (Monotonicité hölderienne singulière de a_h)**.** *Sous l'Hypothèse 4, pour tout* $m \in \{\tilde{r}, r\}$ *et tout* $\underline{\boldsymbol{u}}_h, \underline{\boldsymbol{w}}_h \in \underline{\boldsymbol{U}}_h^k$*, on a*

$$\begin{aligned}&\mathrm{a}_h(\underline{\boldsymbol{u}}_h, \underline{\boldsymbol{u}}_h - \underline{\boldsymbol{w}}_h) - \mathrm{a}_h(\underline{\boldsymbol{w}}_h, \underline{\boldsymbol{u}}_h - \underline{\boldsymbol{w}}_h)\\ &\qquad \geq C_{\mathrm{da}}\sigma_{\mathrm{hm}}\left(\delta^r + \|\underline{\boldsymbol{u}}_h\|_{\boldsymbol{\varepsilon},r,h}^r + \|\underline{\boldsymbol{w}}_h\|_{\boldsymbol{\varepsilon},r,h}^r\right)^{\frac{\tilde{r}-2}{r}} \delta^{r-m}\|\underline{\boldsymbol{u}}_h - \underline{\boldsymbol{w}}_h\|_{\boldsymbol{\varepsilon},m,h}^{m+2-\tilde{r}}, \quad (80)\end{aligned}$$

où $C_{\mathrm{da}} > 0$ *est indépendant de* h*.*

Preuve 16. Voir Section 3.4.4.

On considère le couplage pression-vélocité discret $\mathrm{b}_h : \underline{\boldsymbol{U}}_h^k \times \mathbb{P}^k(\mathcal{T}_h) \to \mathbb{R}$ défini en (36).

4.2.2 Terme convectif discret

On définit la *fonction convective discrète* $\mathrm{c}_h : \underline{\boldsymbol{U}}_h^k \times \underline{\boldsymbol{U}}_h^k \to \mathbb{R}$ telle que, pour tout $(\underline{\boldsymbol{w}}_h, \underline{\boldsymbol{v}}_h) \in \underline{\boldsymbol{U}}_h^k \times \underline{\boldsymbol{U}}_h^k$,

$$\begin{aligned}\mathrm{c}_h(\underline{\boldsymbol{w}}_h, \underline{\boldsymbol{v}}_h) \coloneqq \frac{1}{s}\int_\Omega (\boldsymbol{\chi}(\cdot, \boldsymbol{w}_h)\cdot \mathbf{G}_h^k)\underline{\boldsymbol{w}}_h \cdot \boldsymbol{v}_h - \frac{1}{s'}\int_\Omega (\boldsymbol{\chi}(\cdot, \boldsymbol{w}_h)\cdot \mathbf{G}_h^k)\underline{\boldsymbol{v}}_h \cdot \boldsymbol{w}_h \quad (81)\\ + \frac{s-2}{s}\int_\Omega \frac{\boldsymbol{v}_h \cdot \boldsymbol{w}_h}{|\boldsymbol{w}_h|^2}(\boldsymbol{\chi}(\cdot, \boldsymbol{w}_h)\cdot \mathbf{G}_h^k)\underline{\boldsymbol{w}}_h \cdot \boldsymbol{w}_h.\end{aligned}$$

Cette expression s'obtient en remplaçant le gradient continu par sa version discrète et les fonctions par leur version polynomiale brisée. De même que pour c, on a par construction la propriété de non-dissipativité suivante : Pour tout $\underline{\boldsymbol{w}}_h \in \underline{\boldsymbol{U}}_h^k$,

$$\mathrm{c}_h(\underline{\boldsymbol{w}}_h, \underline{\boldsymbol{w}}_h) = 0. \quad (82)$$

De plus, on a la continuité hölderienne singulière de c_h suivante.

Lemme 23 (Continuité hölderienne singulière de c_h)**.** *Sous l'Hypothèse 5, pour tout* $m \in [1, r]$ *tel que* $s \leq \frac{m^*}{m'}$*, et tout* $\underline{\boldsymbol{u}}_h, \underline{\boldsymbol{v}}_h, \underline{\boldsymbol{w}}_h \in \underline{\boldsymbol{U}}_{h,0}^k$*, on a*

$$\begin{aligned}&\left|\mathrm{c}_h(\underline{\boldsymbol{u}}_h, \underline{\boldsymbol{v}}_h) - \mathrm{c}_h(\underline{\boldsymbol{w}}_h, \underline{\boldsymbol{v}}_h)\right|\\ &\qquad \leq C_{\mathrm{dc},m}\chi_{\mathrm{hc}}\left(\|\underline{\boldsymbol{u}}_h\|_{\boldsymbol{\varepsilon},r,h}^r + \|\underline{\boldsymbol{w}}_h\|_{\boldsymbol{\varepsilon},r,h}^r\right)^{\frac{s+1-\tilde{s}}{r}} \|\underline{\boldsymbol{u}}_h - \underline{\boldsymbol{w}}_h\|_{\boldsymbol{\varepsilon},m,h}^{\tilde{s}-1}\|\underline{\boldsymbol{v}}_h\|_{\boldsymbol{\varepsilon},m,h}, \quad (83)\end{aligned}$$

où $C_{\mathrm{dc},m} > 0$ *est indépendant de* h*.*

Preuve 17. Voir Section 3.4.3.

De manière analogue au Lemme 21, le lemme précédent est un résultat essentiel dans l'étude de la méthode HHO. Tout comme le cas continu, la fonction convective discrète c_h n'est pas la fonction trilinéaire classique, donc un outil supplémentaire a dû être développé. Ce lemme intervient de manière significative dans la démonstration de l'unicité de la solution du problème discret, cf. Théorème 6 , ainsi que dans l'estimation d'erreur pour la pression, cf. Théorème 8.

4.2.3 Inégalité de Sobolev discrète

On rappelle l'inégalité de Sobolev discrète (cf. [48, Proposition 5.4]): Pour tout $m \in [1, \infty[$ tel que $m \leq r^*$, et tout $\underline{\boldsymbol{v}}_h \in \underline{\boldsymbol{U}}_{h,0}^k$,

$$\|\boldsymbol{v}_h\|_{L^m(\Omega)^d} \lesssim \|\underline{\boldsymbol{v}}_h\|_{\boldsymbol{\varepsilon},r,h}. \tag{84}$$

4.3 Problème discret et résultats principaux

Le problème discret est défini par : Trouver $(\underline{\boldsymbol{u}}_h, p_h) \in \underline{\boldsymbol{U}}_{h,0}^k \times P_h^k$ tel que

$$\mathrm{a}_h(\underline{\boldsymbol{u}}_h, \underline{\boldsymbol{v}}_h) + \mathrm{c}_h(\underline{\boldsymbol{u}}_h, \underline{\boldsymbol{v}}_h) + \mathrm{b}_h(\underline{\boldsymbol{v}}_h, p_h) = \int_\Omega \boldsymbol{f} \cdot \boldsymbol{v}_h \qquad \forall \underline{\boldsymbol{v}}_h \in \underline{\boldsymbol{U}}_{h,0}^k, \tag{85a}$$

$$-\mathrm{b}_h(\underline{\boldsymbol{u}}_h, q_h) = 0 \qquad \forall q_h \in P_h^k. \tag{85b}$$

4.3.1 Bonne position du problème discret

On établit l'existence d'une solution pour le problème discret (85) avec des propriétés de majoration. Sous l'hypothèse de petites données, on peut établir l'unicité de la solution selon la valeur de l'exposant convectif s.

Théorème 6 (Bonne position)**.** *Sous les Hypothèses 4 et 5, il existe une solution $(\underline{\boldsymbol{u}}_h, p_h) \in \underline{\boldsymbol{U}}_{h,0}^k \times P_h^k$ au problème discret (85). De plus, elle vérifie les majorations suivantes :*

$$\|\underline{\boldsymbol{u}}_h\|_{\boldsymbol{\varepsilon},r,h} \leq C_{\mathrm{dv}} \left[\mathcal{N}_f^{r'} + \min\left(\delta^r ; \left(\delta^{2-\tilde{r}} \mathcal{N}_f \right)^{\frac{r}{r+1-\tilde{r}}} \right) \right]^{\frac{1}{r}}, \tag{86a}$$

$$\|p_h\|_{L^{r'}(\Omega)} \lesssim \sigma_{\mathrm{hc}} \left[\mathcal{N}_f + \delta^{|r-2|(\tilde{r}-1)} \mathcal{N}_f^{\frac{\tilde{r}-1}{r+1-\tilde{r}}} \right], \tag{86b}$$

avec $\mathcal{N}_f := \sigma_{\mathrm{hm}}^{-1} \|\boldsymbol{f}\|_{L^{r'}(\Omega)^d}$ et où $C_{\mathrm{dv}} > 0$ est indépendant de h. De plus, si on a $2 \leq s \leq \frac{\tilde{r}^*}{\tilde{r}'}$, ainsi que l'hypothèse de petites données suivante :

$$\delta^r + \mathcal{N}_f^{r'} < \left(1 + 2C_{\mathrm{dv}}^r\right)^{-1} \left(C_{\mathrm{dc},\tilde{r}}^{-1} \chi_{\mathrm{hc}}^{-1} C_{\mathrm{da}} \sigma_{\mathrm{hm}} \delta^{r-\tilde{r}} \right)^{\frac{r}{s+1-\tilde{r}}}, \tag{87}$$

alors la solution de (85) est unique.

Preuve 18. Voir Section 3.2.3.

4.3.2 Convergence avec régularité minimale

On énonce des résultats de convergence sous l'hypothèse de régularité minimale des solutions du problème continu (70).

Théorème 7 (Convergence avec régularité minimale)**.** *On suppose $s < \frac{r^*}{r'}$. Soit $((\underline{\boldsymbol{u}}_h, p_h))_{h\in\mathcal{H}}$ une suite de $(\underline{\boldsymbol{U}}_{h,0}^k \times P_h^k)_{h\in\mathcal{H}}$ telle que, pour tout $h \in \mathcal{H}$, $(\underline{\boldsymbol{u}}_h, p_h)$ est solution du problème (85). Alors, sous les Hypothèses 4 et 5, il existe une solution $(\boldsymbol{u}, p) \in \boldsymbol{U} \times P$ de (70) telle que, à une sous-suite près :*

- $\boldsymbol{u}_h \xrightarrow[h\to 0]{} \boldsymbol{u}$ *fortement dans* $L^{[1,r^*)}(\Omega)^d$;
- $\mathbf{G}_{\mathrm{s},h}^k \underline{\boldsymbol{u}}_h \xrightarrow[h\to 0]{} \boldsymbol{\nabla}_{\mathrm{s}}\boldsymbol{u}$ *fortement dans* $L^r(\Omega)^{d\times d}$;
- $|\underline{\boldsymbol{u}}_h|_{r,h} \xrightarrow[h\to 0]{} 0$;
- $p_h \xrightarrow[h\to 0]{} p$ *fortement dans* $L^{r'}(\Omega)$.

Si de plus, la solution de (70) est unique, la convergence s'étend à la suite entière.

Preuve 19. Voir Section 3.6.2.

4.3.3 Estimation d'erreur a priori

On énonce l'estimation d'erreur suivante pour les fluides pseudoplastiques sous l'hypothèse d'unicité, de régularité supplémentaire, et de petites données de la solution du problème continu (70).

Théorème 8 (Estimation d'erreur)**.** *On suppose $r \le 2 \le s \le \frac{r^*}{r'}$. Soit $(\boldsymbol{u}, p) \in \boldsymbol{U} \times P$ et $(\underline{\boldsymbol{u}}_h, p_h) \in \underline{\boldsymbol{U}}_{h,0}^k \times P_h^k$ les solutions respectives des problèmes (70) et (85). On suppose qu'il y a unicité des solutions, ainsi que l'hypothèse de régularité supplémentaire suivante :*

(i) $\boldsymbol{u} \in W^{k+2,r}(\mathcal{T}_h)^d \cap W^{k+1,sr'}(\mathcal{T}_h)^d$,

(ii) $\boldsymbol{\sigma}(\cdot, \boldsymbol{\nabla}_{\mathrm{s}}\boldsymbol{u}) \in W^{1,r'}(\Omega)^{d\times d} \cap W^{k+1,r'}(\mathcal{T}_h)^{d\times d}$,

(iii) $p \in W^{1,r'}(\Omega) \cap W^{k+1,r'}(\mathcal{T}_h)$.

On suppose aussi l'hypothèse de petites données suivante :

$$\delta^r + \left(\sigma_{\mathrm{hm}}^{-1}\|\boldsymbol{f}\|_{L^{r'}(\Omega)^d}\right)^{r'} \le \left(1 + C_{\mathrm{v}}^r + C_{\mathrm{I}}^r C_{\mathrm{dv}}^r\right)^{-1} \left(\frac{C_{\mathrm{da}}\sigma_{\mathrm{hm}}}{2C_{\mathrm{dc},r}\chi_{\mathrm{hc}}}\right)^{\frac{r}{s+1-r}}. \tag{88}$$

Alors, sous les Hypothèses 4 et 5, on a

$$\|\underline{\boldsymbol{u}}_h - \underline{I}_h^k \boldsymbol{u}\|_{\boldsymbol{\varepsilon},r,h} \lesssim \mathcal{N}_1 \left(h^{(k+1)(r-1)} \min\left(\zeta_h(\boldsymbol{u}); 1\right)^{2-r} + h^{k+1}\right), \tag{89a}$$

$$\begin{aligned}\|p_h - \pi_h^k p\|_{L^{r'}(\Omega)} \lesssim{}& \mathcal{N}_2 \left(h^{(k+1)(r-1)} \min\left(\zeta_h(\boldsymbol{u}); 1\right)^{2-r} + h^{k+1}\right) \\ &+ \mathcal{N}_3 \left(h^{(k+1)(r-1)} \min\left(\zeta_h(\boldsymbol{u}); 1\right)^{2-r} + h^{k+1}\right)^{r-1},\end{aligned} \tag{89b}$$

avec $\zeta_h(\boldsymbol{w}) \coloneqq \delta^{-1} \max_{T\in\mathcal{T}_h} \big(|T|^{-\frac{1}{p}} |\boldsymbol{w}|_{W^{k+2,r}(T)^d}\big) h^{k+1}$ *si* $\delta \neq 0$, $\zeta_h(\boldsymbol{w}) \coloneqq \infty$ *sinon, et où* $\mathcal{N}_1, \mathcal{N}_2, \mathcal{N}_3 \in [0, +\infty[$ *dépendent seulement des constantes* $r, s, \sigma_{\mathrm{hc}}, \sigma_{\mathrm{hm}}, \delta, \chi_{\mathrm{hc}}$ *et de normes globales de* $\boldsymbol{u}, \boldsymbol{\sigma}, p$ *et* $\boldsymbol{f}$.

Preuve 20. Voir Section 3.6.3.

On en déduit des intervalles pour les ordres de convergence asymptotiques de la vélocité et de la pression qui sont respectivement

$$O^k_{\mathrm{vel}} \in \big[(k+1)(r-1), k+1\big], \quad O^k_{\mathrm{pre}} \in \big[(k+1)(r-1)^2, (k+1)(r-1)\big]. \tag{90}$$

Leur position dans l'intervalle dépend du nombre sans dimension $\zeta_h(\boldsymbol{u})$.

Le théorème précédent ne permet pas de connaître les ordres de convergence pour $r > 2$ ou $s < 2$. En effet, l'estimation d'erreur nécessite l'unicité des solutions continue et discrète. Or, les théorèmes de bonne position 5 et 6 assurent l'unicité que lorsque $r \leq 2 \leq s$ (avec parfois $r > 2$, dans le cas non-dégénéré). L'analyse des cas $r > 2$ ou $s < 2$ nécessite des résultats supplémentaires, ce qui pourrait faire l'objet d'une future étude.

Cependant, la consistance de c_h suivante permet de supposer que les ordres de convergence deviennent plus bas lorsque $s < 2$ puisqu'un terme en $h^{(k+1)(s-1)}$ apparaît.

Lemme 24 (Consistance de c_h)**.** *Sous l'Hypothèse 5, si* $s \leq \frac{r^*}{r'}$, *alors pour tout* $\boldsymbol{w} \in \boldsymbol{U} \cap W^{k+2,r}(\mathcal{T}_h)^d \cap W^{k+1,sr'}(\mathcal{T}_h)^d$ *tel que* $\boldsymbol{\nabla}\cdot\boldsymbol{w} = 0$, *on a*

$$\sup_{\underline{\boldsymbol{v}}_h \in \underline{\boldsymbol{U}}^k_{h,0}, \|\underline{\boldsymbol{v}}_h\|_{\varepsilon,r,h}=1} \left| \int_\Omega (\boldsymbol{w}\cdot\boldsymbol{\nabla})\boldsymbol{\chi}(\cdot,\boldsymbol{w})\cdot\boldsymbol{v}_h - \mathrm{c}_h(\underline{I}^k_h \boldsymbol{w}, \underline{\boldsymbol{v}}_h) \right| \lesssim \mathcal{N}_1 h^{k+1} + \mathcal{N}_2 h^{(k+1)(\tilde{s}-1)}, \tag{91}$$

où $\mathcal{N}_1, \mathcal{N}_2 \in [0, +\infty[$ *dépendent uniquement des réels* r, s, χ_{hc} *et des normes* $|\boldsymbol{u}|_{W^{1,r}(\Omega)^d}$, $|\boldsymbol{u}|_{W^{k+2,r}(\mathcal{T}_h)^d}$, $|\boldsymbol{u}|_{W^{1,sr'}(\Omega)^d}$, $|\boldsymbol{u}|_{W^{k+1,sr'}(\mathcal{T}_h)^d}$.

Preuve 21. Voir Section 3.6.1.

Des résultats numériques permettent de confirmer les résultats de la méthode. On considérera aussi le problème de la cavité entraînée pour mettre en évidence l'influence des lois en puissances choisies pour les lois de viscosité et de convection.

5 Conclusion et perspectives

Ce travail de thèse a porté sur le développement et l'analyse de nouveaux schémas Hybrid High-Order pour des problèmes complexes en mécanique des fluides. Les

méthodes HHO sont une nouvelle classe de méthodes de discrétisation des EDPs qui surmonte les obstacles que peuvent rencontrer les méthodes classiques telles que les Volumes Finis et les Éléments Finis.

L'objectif de cette thèse fut de s'appuyer sur la littérature de HHO pour étudier des problèmes faisant intervenir des fluides non-newtoniens. Dans ce contexte, des résultats d'analyse fonctionnelle discrète furent généralisés au cas non-hilbertien afin de pouvoir fournir des résultats de bonne position, des estimations d'erreur et des résultats de convergence par compacité.

Trois problèmes furent étudiés pour lesquels une méthode HHO fut développée, implémentée et illustrée par des résultats numériques. Le premier porte sur les équations de Stokes généralisées aux fluides non-newtoniens. Les fluides caractérisés par les lois en puissance ou de Carreau–Yasuda font partie du champ d'application de cette étude. Afin d'analyser la bonne position et la convergence de la méthode, on introduit la notion de fonction encadrée. De plus, la généralisation au cadre non-hilbertien d'une inégalité de Korn discrète permit de démontrer la bonne position du problème ainsi qu'une estimation d'erreur.

La deuxième étude vise à développer une nouvelle estimation d'erreur dans le cadre des problèmes de Leray–Lions, relatifs au p-Laplacien. Dans le cas $p \in]1, 2]$, des dégénérescences locales peuvent apparaître. Dans cette nouvelle estimation d'erreur, on en déduit des ordres de convergence variant de $(k + 1)(p - 1)$ pour le cas globalement dégénéré, à $k + 1$ pour le cas globalement non-dégénéré, où k correspond au degré polynomial de la méthode. L'ordre de convergence optimal $k + 1$, correspondant au cas linéaire hilbertien $p = 2$, peut donc être atteint pour des problèmes non-linéaires vivant dans des espaces de Sobolev d'exposant variable $p \in]1, 2]$.

La troisième étude est consacrée au développement et l'analyse d'une méthode HHO pour des équations de Navier–Stokes généralisées aux fluides incompressibles non-newtoniens dont le comportement convectif peut suivre une loi en puissance. Deux exposants de Sobolev furent introduits pour caractériser les lois de viscosité et de convection du fluide. Des relations de non-dissipativité permettent de considérer des lois de convection suivant une loi en puissance. Ces dernières ont permis d'écrire une formulation faible du problème continu ainsi qu'une étude sur la bonne position du problème faisant apparaître des relations entre les exposants de Sobolev des lois de viscosité et de convection. À partir de ces résultats, une méthode HHO fut développée pour obtenir des résultats de convergence sous l'hypothèse de régularité minimale. On énonça aussi une estimation d'erreur pour les fluides pseudoplastiques. Une application sur le problème de la cavité entraînée permit d'illustrer les phénomènes provenant des lois en puissance introduites dans les lois de viscosité et de convection.

5.1 Perspectives

Suite à ces travaux, plusieurs perspectives peuvent être envisagées.

5.1.1 Amélioration des estimations d'erreur

Très récemment, une estimation d'erreur pour les problèmes de Leray–Lions dans le cas $p \leq 2$, impliquant des taux de convergence de $\frac{k+1}{3-p}$, fut démontrée dans [33] pour une méthode Hybrid High-Order sur des maillages simpliciaux standards, basé sur un gradient stable inspiré de [53]. Une prochaine étape serait d'obtenir ces taux de convergence pour la méthode HHO concernant le problème de Leray–Lions, mais aussi pour l'estimation d'erreur de la vélocité dans l'étude des équations de Stokes et Navier–Stokes généralisées. De plus, dans le cadre du problème de Navier–Stokes, nous pouvons envisager de généraliser les estimations aux cas où les exposants des lois de viscosité et de convection vérifient respectivement $r < 2$ et $s > 2$.

5.1.2 Adaptivité de maillage pour les problèmes de Leray–lions

Pour chaque méthode HHO développée dans cette thèse, une estimation d'erreur fut démontrée pour des solutions suffisamment régulières. Une prochaine étape pourrait être de faire de l'adaptation de maillage basée sur des estimateurs a posteriori, permettant d'exploiter la montée en ordre même pour des solutions peu régulières. Une adaptation de maillage fut développée dans [36] pour le problème de Stokes, utilisant des algorithmes itératifs appliqués sur une discrétisation par Éléments Finis. Une estimation d'erreur a posteriori fut démontrée, faisant intervenir différentes composantes de l'erreur. Une étude analogue pourrait être envisagée dans le contexte du Chapitre 1, pour la discrétisation HHO du problème de Stokes, afin d'obtenir une estimation d'erreur a posteriori. Aussi, cette approche pourrait être appliquée dans le cadre du problème de Leray–Lions et des équations de Navier–Stokes.

5.1.3 Équations de Navier–Stokes instationnaires généralisées

Dans ce manuscrit, nous avons étudié le problème stationnaire de Navier–Stokes généralisé aux fluides non-newtoniens, avec convection suivant une loi en puissance. Un prolongement naturel de cette étude serait de considérer ce problème dans le cas instationnaire. Outre l'ajout de la dérivée en temps de la vélocité dans les équations de Navier–Stokes, les modifications peuvent concerner la dépendance en temps des lois de viscosité et de convection. Ceci permettrait de considérer d'autres catégories de fluides tels que, les fluides thixotropes, dont la viscosité diminue avec la durée de la contrainte, et rhéopectiques, où la viscosité augmente avec la durée de la contrainte. Des exemples de fluides thixotropes incluent la peinture [7], le yaourt [100], et les gels de pectine [88]. D'autre part, le liquide synovial [102], et la majorité des encres d'imprimante [108] sont des fluides rhéopectiques.

5.1.4 Équations de Navier–Stokes étendues aux fluides viscoélastiques et viscoplastiques

D'autres types de fluide non-newtonien, qui peuvent faire l'objet d'une étude dans le cadre du problème de Stokes ou encore de Navier–Stokes, sont les fluides dits viscoélastiques. Associés souvent aux polymères, ces fluides possèdent un comportement à la fois visqueux et élastique sous l'effet d'une déformation. Certains fluides biologiques sont de nature viscoélastique, cf. [99]. Inversement, nous pouvons aussi considérer les fluides viscoplastiques, qui présentent un comportement de solide au repos et un comportement liquide lorsque la déformation dépasse un certain seuil. Comme exemples, nous pouvons citer les mousses, les pâtes et les huiles, cf. [95].

5.1.5 Application des équations de Navier–Stokes généralisées au transport optimal

Les travaux de [86] soulignent le lien étroit entre les équations de Navier–Stokes pour les fluides non-newtoniens et le transport optimal associé aux distances de Wasserstein. Pour ce faire, le moment de la vélocité est décrit par une loi en puissance. Ainsi, une possible application de la discrétisation HHO du Chapitre 3 portant sur le problème de Navier–Stokes pour les fluides non-newtoniens avec un terme convectif généralisé serait dans une étude du transport optimal faisant intervenir les distances de Wasserstein. De plus, nous proposons une généralisation du terme convectif qui, dans [86], est défini par une loi en puissance. Cette généralisation permettrait de définir d'autres types de moments liés à la vélocité.

5.1.6 Formulation tourbillon-vitesse-pression du problème de Stokes

Dans [5], une formulation variationnelle fut proposée pour le problème de Stokes, capable d'intégrer à la fois des variables de tourbillon, de vitesse et de pression. Cette formulation triple permet en outre de prendre naturellement en compte les différents types de conditions limites. Une méthode de discrétisation fut développée et a nécessité l'introduction d'un terme de stabilisation, ce qui laisse penser qu'une approximation par méthode HHO serait prometteuse. Nous pouvons ainsi envisager de construire une méthode HHO pour le problème de tourbillon-vitesse-pression de Stokes, avec une généralisation possible aux fluides non-newtoniens.

Chapter 1

A HHO method for creeping flows of non-Newtonian fluids

This chapter has been published in the following international journal (see [27]):

ESAIM: Mathematical Modelling and Numerical Analysis, 2021.
Volume 55, Issue 5, Pages 2045–2073.

Abstract

In this paper, we design and analyze a Hybrid High-Order discretization method for the steady motion of non-Newtonian, incompressible fluids in the Stokes approximation of small velocities. The proposed method has several appealing features including the support of general meshes and high-order, unconditional inf-sup stability, and orders of convergence that match those obtained for scalar Leray–Lions problems. A complete well-posedness and convergence analysis of the method is carried out under new, general assumptions on the strain rate-shear stress law, which encompass several common examples such as the power-law and Carreau–Yasuda models. Numerical examples complete the exposition.

1.1 Introduction

In this paper, we design and analyze a Hybrid High-Order (HHO) discretization method for the steady motion of a non-Newtonian, incompressible fluid in the Stokes approximation of small velocities. Notable applications include ice sheet dynamics [78], mantle convection [101], chemical engineering [80], and biological fluids rheology [69, 85]. We focus on fluids with shear-rate-dependent viscosity, whose behavior is characterized by a nonlinear strain rate-shear stress function. Physical interpretations and discussions of non-Newtonian fluid models can be found, e.g., in [19, 93]. Typical examples that are

frequently used in the applications include the power-law and Carreau–Yasuda model, covered by the present analysis.

The earliest investigations of fluids with shear-dependent viscosity date back to the pioneering work of Ladyzhenskaya [84]. For a detailed mathematical study of the well-posedness and regularity of the continuous problem, see also [13, 18, 64, 92, 96] and references therein. Early results on the numerical analysis of non-Newtonian fluid flow problems were given in [9, 75, 98]. Later, these results were improved in [16] and [76] by proving error estimates that are optimal for fluids with shear thinning behavior (described by a power-law exponent $r \leq 2$). In [16], the authors considered a conforming inf-sup stable finite element discretization, while in [76] a low-order scheme with local projection stabilization was proposed. In both works, the use of Orlicz functions is instrumental to unify the treatment of the shear thinning and shear thickening cases (also called pseudoplastic and dilatant, respectively; cf. Example 28). More recently, a finite element method based on a four-field formulation of the nonlinear Stokes equations has been analyzed in [97]. Other notable contributions on the numerical approximation of generalized Stokes problems include [65, 78, 81, 82].

The main issues to be accounted for in the numerical solution of non-Newtonian fluid flow problems are the presence of local features emerging from the nonlinear strain rate-shear stress relation, the incompressibility condition leading to indefinite systems, the roughly varying model coefficients, and, possibly, complex geometries requiring unstructured and highly-adapted meshes. The HHO method provides several advantages to deal with the complex nature of the problem, such as the support of general polygonal or polyhedral meshes, the possibility to select the approximation order, and unconditional inf-sup stability. Moreover, HHO schemes can be efficiently implemented thanks to the possibility of statically condensing a large subset of the unknowns for linearized versions of the problem encountered, e.g., when solving the nonlinear system by the Newton method. Hybrid High-Order methods have been successfully applied to the simulation of incompressible flows of Newtonian fluids governed by the Stokes [1] and Navier–Stokes equations [28, 62], possibly driven by large irrotational volumetric forces [34, 60]. Works related to the problem of creeping flows of non-Newtonian fluids are [30] and [47, 48], respectively dealing with nonlinear elasticity and Leray–Lions problems. Going from nonlinear coercive elliptic equations to the nonlinear Stokes system involves additional difficulties arising from the pressure and the divergence constraint. Finally, we mention that HHO methods are members of a wider family of polytopal methods that also includes, e.g., Virtual Element methods (cf., e.g., [14, 15] for their application to Newtonian incompressible flows) and can fit within general frameworks for the approximation of nonlinear problems such as the one provided by the Gradient Discretisation Method (see [53, 66]).

The HHO discretization presented in this paper hinges on discontinuous polynomial unknowns on the mesh and on its skeleton, from which discrete differential operators are

reconstructed. These operators are used to formulate discrete counterparts of the viscous and pressure-velocity coupling terms. For the former, stability is ensured by a cleverly designed stabilization contribution involving the penalization of boundary differences. We carry out a complete analysis of the proposed method. In particular, under general assumptions on the strain rate-shear stress function, we derive error estimates for the velocity and pressure approximations. The energy-norm error estimate for the velocity given in Theorem 36 yields the same convergence orders established in [47, Theorem 3.2] for the scalar Leray–Lions elliptic problem. A key tool in our analysis is provided by Lemma 39, in which we prove a generalization of the discrete Korn inequality of [28, Lemma 1] to the non-Hilbertian case. The other main contributions are a novel formulation of the requirements on the strain rate-shear stress function allowing a unified treatment of pseudoplastic and dilatant fluids and the identification of a set of general assumptions on the nonlinear stabilization function ensuring the desired consistency properties along with the well-posedness of the discrete problem.

The rest of the paper is organized as follows. In Section 1.2 we introduce the strong and weak formulations of the nonlinear Stokes problem and present the assumptions on the strain rate-shear stress function. The discrete setting is established in Section 1.3, including the definition of the discrete spaces for the velocity and the pressure. The HHO scheme along with the main theoretical results are stated in Section 1.4, and a numerical validation is provided in Section 1.5. In Section 1.6 we prove the discrete counterpart of the Korn inequality needed in the analysis of the method. Section 1.7 contains the proof of the main results (well-posedness and error estimates). Finally, in Appendix 1.A we provide a sufficient condition for the strain rate-shear stress law to fulfil the assumptions presented in Section 1.2. The paper is structured so as to offer two levels of reading. In particular, the reader mainly interested in the formulation of the method and its numerical performance can focus on Section 1.2–1.5. The remaining sections cover technical aspects of the analysis, and can be skipped at first reading.

1.2 Continuous setting

Let $\Omega \subset \mathbb{R}^d$, $d \in \{2, 3\}$, denote a bounded, connected, polyhedral open set with Lipschitz boundary $\partial\Omega$. We consider a possibly non-Newtonian fluid occupying Ω and subjected to a volumetric force field $\boldsymbol{f} : \Omega \to \mathbb{R}^d$. Its flow is governed by the generalized Stokes problem, which consists in finding the velocity field $\boldsymbol{u} : \Omega \to \mathbb{R}^d$ and the pressure field

$p : \Omega \to \mathbb{R}$ such that

$$-\boldsymbol{\nabla}\cdot\boldsymbol{\sigma}(\cdot, \boldsymbol{\nabla}_{\mathrm{s}}\boldsymbol{u}) + \boldsymbol{\nabla} p = \boldsymbol{f} \qquad \text{in } \Omega, \tag{1.1a}$$

$$\boldsymbol{\nabla}\cdot\boldsymbol{u} = 0 \qquad \text{in } \Omega, \tag{1.1b}$$

$$\boldsymbol{u} = \boldsymbol{0} \qquad \text{on } \partial\Omega, \tag{1.1c}$$

$$\int_\Omega p(\boldsymbol{x})\,\mathrm{d}\boldsymbol{x} = 0, \tag{1.1d}$$

where $\boldsymbol{\nabla}\cdot$ denotes the divergence operator applied to vector or tensor fields, $\boldsymbol{\nabla}_{\mathrm{s}}$ is the symmetric part of the gradient operator $\boldsymbol{\nabla}$ applied to vector fields, and, denoting by $\mathbb{R}^{d\times d}_{\mathrm{s}}$ the set of square, symmetric, real-valued $d \times d$ matrices, $\boldsymbol{\sigma} : \Omega \times \mathbb{R}^{d\times d}_{\mathrm{s}} \to \mathbb{R}^{d\times d}_{\mathrm{s}}$ is the strain rate-shear stress law. In what follows, we formulate assumptions on $\boldsymbol{\sigma}$ that encompass common models for non-Newtonian fluids and state a weak formulation for problem (1.1) that will be used as a starting point for its discretization.

1.2.1 Strain rate-shear stress law

We define the Frobenius inner product such that, for all $\boldsymbol{\tau} = (\tau_{ij})_{1\le i,j\le d}$ and $\boldsymbol{\eta} = (\eta_{ij})_{1\le i,j\le d}$ in $\mathbb{R}^{d\times d}$, $\boldsymbol{\tau} : \boldsymbol{\eta} \coloneqq \sum_{i,j=1}^d \tau_{ij}\eta_{ij}$, and we denote by $|\boldsymbol{\tau}|_{d\times d} \coloneqq \sqrt{\boldsymbol{\tau} : \boldsymbol{\tau}}$ the corresponding norm.

Assumption 1 (Strain rate-shear stress law)**.** Let a real number $r \in (1, \infty)$ be fixed, denote by $r' \coloneqq \frac{r}{r-1} \in (1, \infty)$ the conjugate exponent of r, and define the singular exponent of r by

$$\tilde{r} \coloneqq \min(r, 2) \in (1, 2]. \tag{1.2}$$

The strain rate-shear stress law satisfies

$$\boldsymbol{\sigma}(\boldsymbol{x}, \boldsymbol{0}) = \boldsymbol{0} \text{ for almost every } \boldsymbol{x} \in \Omega, \tag{1.3a}$$

$$\boldsymbol{\sigma} : \Omega \times \mathbb{R}^{d\times d}_{\mathrm{s}} \to \mathbb{R}^{d\times d}_{\mathrm{s}} \text{ is measurable.} \tag{1.3b}$$

Moreover, there exist real numbers $\delta \in [0, \infty)$ and $\sigma_{\mathrm{hc}}, \sigma_{\mathrm{hm}} \in (0, \infty)$ such that, for all $\boldsymbol{\tau}, \boldsymbol{\eta} \in \mathbb{R}^{d\times d}_{\mathrm{s}}$ and almost every $\boldsymbol{x} \in \Omega$, we have the Hölder continuity property

$$|\boldsymbol{\sigma}(\boldsymbol{x}, \boldsymbol{\tau}) - \boldsymbol{\sigma}(\boldsymbol{x}, \boldsymbol{\eta})|_{d\times d} \le \sigma_{\mathrm{hc}} \left(\delta^r + |\boldsymbol{\tau}|^r_{d\times d} + |\boldsymbol{\eta}|^r_{d\times d}\right)^{\frac{r-\tilde{r}}{r}} |\boldsymbol{\tau} - \boldsymbol{\eta}|^{\tilde{r}-1}_{d\times d}, \tag{1.3c}$$

and the Hölder monotonicity property

$$(\boldsymbol{\sigma}(\boldsymbol{x}, \boldsymbol{\tau}) - \boldsymbol{\sigma}(\boldsymbol{x}, \boldsymbol{\eta})) : (\boldsymbol{\tau} - \boldsymbol{\eta}) \left(\delta^r + |\boldsymbol{\tau}|^r_{d\times d} + |\boldsymbol{\eta}|^r_{d\times d}\right)^{\frac{2-\tilde{r}}{r}} \ge \sigma_{\mathrm{hm}} |\boldsymbol{\tau} - \boldsymbol{\eta}|^{r+2-\tilde{r}}_{d\times d}. \tag{1.3d}$$

Some remarks are in order.

Remark 25 (Residual shear stress). Assumption (1.3a) can be relaxed by taking $\boldsymbol{\sigma}(\cdot, \mathbf{0}) \in L^{r'}(\Omega, \mathbb{R}^{d\times d}_{\mathrm{s}})$. This modification requires only minor changes in the analysis, not detailed for the sake of conciseness.

Remark 26 (Singular exponent). Inequalities (1.3c)–(1.3d) can be proved starting from the following assumptions, which correspond to the conditions (1.78) below characterizing an (r, δ)-power-framed function: For all $\boldsymbol{\tau}, \boldsymbol{\eta} \in \mathbb{R}^{d\times d}_{\mathrm{s}}$ with $\boldsymbol{\tau} \neq \boldsymbol{\eta}$ and almost every $\boldsymbol{x} \in \Omega$,

$$|\boldsymbol{\sigma}(\boldsymbol{x}, \boldsymbol{\tau}) - \boldsymbol{\sigma}(\boldsymbol{x}, \boldsymbol{\eta})|_{d\times d} \leq \sigma_{\mathrm{hc}} \left(\delta^r + |\boldsymbol{\tau}|^r_{d\times d} + |\boldsymbol{\eta}|^r_{d\times d}\right)^{\frac{r-2}{r}} |\boldsymbol{\tau} - \boldsymbol{\eta}|_{d\times d},$$
$$(\boldsymbol{\sigma}(\boldsymbol{x}, \boldsymbol{\tau}) - \boldsymbol{\sigma}(\boldsymbol{x}, \boldsymbol{\eta})) : (\boldsymbol{\tau} - \boldsymbol{\eta}) \geq \sigma_{\mathrm{hm}} \left(\delta^r + |\boldsymbol{\tau}|^r_{d\times d} + |\boldsymbol{\eta}|^r_{d\times d}\right)^{\frac{r-2}{r}} |\boldsymbol{\tau} - \boldsymbol{\eta}|^2_{d\times d}.$$

These relations are reminiscent of the ones used in [47] in the context of scalar Leray–Lions problems. The advantage of assumptions (1.3c)-(1.3d), expressed in terms of the singular index $\tilde{r}$, is that they enable a unified treatment of the cases $r < 2$ and $r \geq 2$ in the proofs of Lemma 42, Theorem 35, Lemma 44, and Theorem 36 below.

Remark 27 (Relations between the Hölder and monotonicity constants). Inequalities (1.3c) and (1.3d) give

$$\sigma_{\mathrm{hm}} \leq \sigma_{\mathrm{hc}}. \tag{1.4}$$

Indeed, let $\boldsymbol{\tau} \in \mathbb{R}^{d\times d}_{\mathrm{s}}$ be such that $|\boldsymbol{\tau}|_{d\times d} > 0$. Using the Hölder monotonicity (1.3d) (with $\boldsymbol{\eta} = \mathbf{0}$), the Cauchy–Schwarz inequality, and the Hölder continuity (1.3c) (again with $\boldsymbol{\eta} = \mathbf{0}$), we infer that

$$\begin{aligned}\sigma_{\mathrm{hm}} \left(\delta^r + |\boldsymbol{\tau}|^r_{d\times d}\right)^{\frac{\tilde{r}-2}{r}} |\boldsymbol{\tau}|^{r+2-\tilde{r}}_{d\times d} \leq \boldsymbol{\sigma}(\cdot, \boldsymbol{\tau}) : \boldsymbol{\tau} &\leq |\boldsymbol{\sigma}(\cdot, \boldsymbol{\tau})|_{d\times d} |\boldsymbol{\tau}|_{d\times d} \\ &\leq \sigma_{\mathrm{hc}} \left(\delta^r + |\boldsymbol{\tau}|^r_{d\times d}\right)^{\frac{r-\tilde{r}}{r}} |\boldsymbol{\tau}|^{\tilde{r}}_{d\times d}\end{aligned}$$

almost everywhere in Ω. Hence, $\frac{\sigma_{\mathrm{hm}}}{\sigma_{\mathrm{hc}}} \leq \left(\frac{\delta^r + |\boldsymbol{\tau}|^r_{d\times d}}{|\boldsymbol{\tau}|^r_{d\times d}}\right)^{\frac{|r-2|}{r}}$. Letting $|\boldsymbol{\tau}|_{d\times d} \to \infty$ gives (1.4).

Example 28 (Carreau–Yasuda fluids)**.** (μ, δ, a, r)-Carreau–Yasuda fluids, introduced in [105] and later generalized in [76, Eq. (1.2)], are fluids for which it holds, for almost every $\boldsymbol{x} \in \Omega$ and all $\boldsymbol{\tau} \in \mathbb{R}^{d\times d}_{\mathrm{s}}$,

$$\boldsymbol{\sigma}(\boldsymbol{x}, \boldsymbol{\tau}) = \mu(\boldsymbol{x}) \left(\delta^{a(\boldsymbol{x})} + |\boldsymbol{\tau}|^{a(\boldsymbol{x})}_{d\times d}\right)^{\frac{r-2}{a(\boldsymbol{x})}} \boldsymbol{\tau}, \tag{1.5}$$

where $\mu : \Omega \to [\mu_-, \mu_+]$ is a measurable function with $\mu_-, \mu_+ \in (0, \infty)$ corresponding to the local flow consistency index, $\delta \in [0, \infty)$ is the degeneracy parameter, $a : \Omega \to [a_-, a_+]$ is a measurable function with $a_-, a_+ \in (0, \infty)$ expressing the local transition flow behavior index, and $r \in (1, \infty)$ is the flow behavior index. The Carreau–Yasuda law is a generalization of the Carreau law (corresponding to $a_- = a_+ = 2$) that takes

into account the different local levels of flow behavior in the fluid. The degenerate case $\delta = 0$ corresponds to the power-law model. Non-Newtonian fluids described by constitutive laws with a (μ, δ, a, r)-structure exhibit a different behavior according to the value of r. If $r > 2$, then the fluid shows shear thickening behavior and is called *dilatant*. Examples of dilatant fluids are wet sand and oobleck. The case $r < 2$, on the other hand, corresponds to *pseudoplastic* fluids having shear thinning behavior, such as blood. Finally, if $r = 2$, then the fluid is Newtonian and (1.1) becomes the classical (linear) Stokes problem. We show in Appendix 1.A that the strain rate-shear stress law (1.5) is an (r, δ)-power-framed function with,

$$\sigma_{\mathrm{hc}} = \begin{cases} \frac{\mu_+}{r-1} 2^{\left[-\left(\frac{1}{a_+}-\frac{1}{r}\right)^{\ominus}-1\right](r-2)+\frac{1}{r}} & \text{if } r < 2, \\ \mu_+(r-1)2^{\left(\frac{1}{a_-}-\frac{1}{r}\right)^{\oplus}(r-2)} & \text{if } r \geq 2, \end{cases}$$

and

$$\sigma_{\mathrm{hm}} = \begin{cases} \mu_-(r-1)2^{\left(\frac{1}{a_-}-\frac{1}{r}\right)^{\oplus}(r-2)} & \text{if } r \leq 2, \\ \frac{\mu_-}{r-1} 2^{\left[-\left(\frac{1}{a_+}-\frac{1}{r}\right)^{\ominus}-1\right](r-2)-1} & \text{if } r > 2, \end{cases}$$

where $\xi^{\oplus} := \max(0, \xi)$ and $\xi^{\ominus} := -\min(0, \xi)$ denote, respectively, the positive and negative parts of a real number ξ. As a consequence, it matches Assumption 1.

1.2.2 Weak formulation

From this point on, we omit both the integration variable and the measure from integrals, as they can be in all cases inferred from the context. We define the following velocity and pressure spaces embedding, respectively, the homogeneous boundary condition and the zero-average constraint:

$$\boldsymbol{U} := \left\{ \boldsymbol{v} \in W^{1,r}(\Omega)^d \ : \ \boldsymbol{v}_{|\partial\Omega} = \boldsymbol{0} \right\}, \quad P := L_0^{r'}(\Omega) := \left\{ q \in L^{r'}(\Omega) \ : \ \int_\Omega q = 0 \right\}.$$

Assuming $\boldsymbol{f} \in L^{r'}(\Omega)^d$, the weak formulation of problem (1.1) reads: Find $(\boldsymbol{u}, p) \in \boldsymbol{U} \times P$ such that

$$a(\boldsymbol{u}, \boldsymbol{v}) + b(\boldsymbol{v}, p) = \int_\Omega \boldsymbol{f} \cdot \boldsymbol{v} \qquad \forall \boldsymbol{v} \in \boldsymbol{U}, \tag{1.6a}$$

$$-b(\boldsymbol{u}, q) = 0 \qquad \forall q \in P, \tag{1.6b}$$

where the function $a : \boldsymbol{U} \times \boldsymbol{U} \to \mathbb{R}$ and the bilinear form $b : \boldsymbol{U} \times L^{r'}(\Omega) \to \mathbb{R}$ are defined such that, for all $\boldsymbol{v}, \boldsymbol{w} \in \boldsymbol{U}$ and all $q \in L^{r'}(\Omega)$,

$$a(\boldsymbol{w}, \boldsymbol{v}) := \int_\Omega \boldsymbol{\sigma}(\cdot, \boldsymbol{\nabla}_{\mathrm{s}} \boldsymbol{w}) : \boldsymbol{\nabla}_{\mathrm{s}} \boldsymbol{v}, \qquad b(\boldsymbol{v}, q) := -\int_\Omega (\boldsymbol{\nabla} \cdot \boldsymbol{v}) q. \tag{1.7}$$

Remark 29 (Mass equation). The test space in (1.6b) can be extended to $L^{r'}(\Omega)$ since, for all $\boldsymbol{v} \in \boldsymbol{U}$, the divergence theorem and the fact that $\boldsymbol{v}_{|\partial\Omega} = \boldsymbol{0}$ yield $b(\boldsymbol{v}, 1) = -\int_\Omega \boldsymbol{\nabla}\cdot\boldsymbol{v} = -\int_{\partial\Omega} \boldsymbol{v}\cdot\boldsymbol{n}_{\partial\Omega} = 0$, with $\boldsymbol{n}_{\partial\Omega}$ denoting the unit vector normal to $\partial\Omega$ and pointing out of Ω.

Remark 30 (Well-posedness and a priori estimates). It can be checked that, under Assumption 1, the continuous problem (1.6) admits a unique solution $(\boldsymbol{u}, p) \in \boldsymbol{U}\times P$; see, e.g., [76, Section 2.4], where slightly stronger assumptions are considered. For future use, we also note the following a priori bound on the velocity:

$$|\boldsymbol{u}|_{W^{1,r}(\Omega)^d} \le \left(2^{\frac{2-\tilde r}{r}} C_{\mathrm K}\sigma_{\mathrm{hm}}^{-1}\|\boldsymbol{f}\|_{L^{r'}(\Omega)^d}\right)^{\frac{1}{r-1}} + \left(2^{\frac{2-\tilde r}{r}} C_{\mathrm K}|\Omega|_d^{\frac{2-\tilde r}{r}}\delta^{2-\tilde r}\sigma_{\mathrm{hm}}^{-1}\|\boldsymbol{f}\|_{L^{r'}(\Omega)^d}\right)^{\frac{1}{r+1-\tilde r}}, \quad (1.8)$$

where $C_{\mathrm K} > 0$ comes from the Korn inequality given at (1.34) below. To prove (1.8), use the Hölder monotonicity (1.3d) of $\boldsymbol{\sigma}$, sum (1.6a) written for $\boldsymbol{v} = \boldsymbol{u}$ to (1.6b) written for $q = p$, and use the Hölder inequality together with the Korn inequality (1.34) to write

$$\sigma_{\mathrm{hm}}\left(|\Omega|_d\delta^r + \|\boldsymbol{\nabla}_{\mathrm s}\boldsymbol{u}\|_{L^r(\Omega)^{d\times d}}^r\right)^{\frac{\tilde r-2}{r}}\|\boldsymbol{\nabla}_{\mathrm s}\boldsymbol{u}\|_{L^r(\Omega)^{d\times d}}^{r+2-\tilde r} \le a(\boldsymbol{u},\boldsymbol{u}) = \int_\Omega \boldsymbol{f}\cdot\boldsymbol{u} \le C_{\mathrm K}\|\boldsymbol{f}\|_{L^{r'}(\Omega)^d}\|\boldsymbol{\nabla}_{\mathrm s}\boldsymbol{u}\|_{L^r(\Omega)^{d\times d}}, \quad (1.9)$$

where $|\Omega|_d$ is the measure of Ω, that is,

$$\mathcal N \coloneqq \left(|\Omega|_d\delta^r + \|\boldsymbol{\nabla}_{\mathrm s}\boldsymbol{u}\|_{L^r(\Omega)^{d\times d}}^r\right)^{\frac{\tilde r-2}{r}}\|\boldsymbol{\nabla}_{\mathrm s}\boldsymbol{u}\|_{L^r(\Omega)^{d\times d}}^{r+1-\tilde r} \le C_{\mathrm K}\sigma_{\mathrm{hm}}^{-1}\|\boldsymbol{f}\|_{L^{r'}(\Omega)^d}. \quad (1.10)$$

Observing that $\|\boldsymbol{\nabla}_{\mathrm s}\boldsymbol{u}\|_{L^r(\Omega)^{d\times d}}^{r+1-\tilde r} \le 2^{\frac{2-\tilde r}{r}}\max\left(\|\boldsymbol{\nabla}_{\mathrm s}\boldsymbol{u}\|_{L^r(\Omega)^{d\times d}}^r, |\Omega|_d\delta^r\right)^{\frac{2-\tilde r}{r}}\mathcal N$, we obtain, enumerating the cases for the maximum and summing the corresponding bounds, $\|\boldsymbol{\nabla}_{\mathrm s}\boldsymbol{u}\|_{L^r(\Omega)^{d\times d}} \le (2^{\frac{2-\tilde r}{r}}\mathcal N)^{\frac{1}{r-1}} + \left(2^{\frac{2-\tilde r}{r}}|\Omega|_d^{\frac{2-\tilde r}{r}}\delta^{2-\tilde r}\mathcal N\right)^{\frac{1}{r+1-\tilde r}}$. Combining this inequality with (1.10) gives (1.8).

1.3 Discrete setting

1.3.1 Mesh and notation for inequalities up to a multiplicative constant

We define a mesh as a couple $\mathcal M_h \coloneqq (\mathcal T_h, \mathcal F_h)$, where $\mathcal T_h$ is a finite collection of polyhedral elements T such that $h = \max_{T\in\mathcal T_h} h_T$ with h_T denoting the diameter of T, while $\mathcal F_h$ is

a finite collection of planar faces F with diameter h_F. Notice that, here and in what follows, we use the three-dimensional nomenclature also when $d = 2$, i.e., we speak of polyhedra and faces rather than polygons and edges. It is assumed henceforth that the mesh $\mathcal{M}_h$ matches the geometrical requirements detailed in [50, Definition 1.7]. In order to have the boundedness property (1.15) for the interpolator, we additionally assume that the mesh elements are star-shaped with respect to every point of a ball of radius uniformly comparable to the element diameter; see [50, Lemma 7.12] for the Hilbertian case. Boundary faces lying on $\partial\Omega$ and internal faces contained in Ω are collected in the sets $\mathcal{F}_h^{\mathrm{b}}$ and $\mathcal{F}_h^{\mathrm{i}}$, respectively. For every mesh element $T \in \mathcal{T}_h$, we denote by $\mathcal{F}_T$ the subset of $\mathcal{F}_h$ containing the faces that lie on the boundary ∂T of T. For every face $F \in \mathcal{F}_h$, we denote by $\mathcal{T}_F$ the subset of $\mathcal{T}_h$ containing the one (if $F \in \mathcal{F}_h^{\mathrm{b}}$) or two (if $F \in \mathcal{F}_h^{\mathrm{i}}$) elements on whose boundary F lies. Finally, for each mesh element $T \in \mathcal{T}_h$ and face $F \in \mathcal{F}_T$, $\boldsymbol{n}_{TF}$ denotes the (constant) unit vector normal to F pointing out of T.

Our focus is on the h-convergence analysis, so we consider a sequence of refined meshes that is regular in the sense of [50, Definition 1.9] with regularity parameter uniformly bounded away from zero. The mesh regularity assumption implies, in particular, that the diameter of a mesh element and those of its faces are comparable uniformly in h and that the number of faces of one element is bounded above by an integer independent of h.

To avoid the proliferation of generic constants, we write henceforth $a \lesssim b$ (resp., $a \gtrsim b$) for the inequality $a \le Cb$ (resp., $a \ge Cb$) with real number $C > 0$ independent of h, of the constants δ, σ_{hc}, σ_{hm} in Assumption 1, and, for local inequalities, of the mesh element or face on which the inequality holds. We also write $a \simeq b$ to mean $a \lesssim b$ and $b \lesssim a$. The dependencies of the hidden constants are further specified when needed.

1.3.2 Projectors and broken spaces

Given $X \in \mathcal{T}_h \cup \mathcal{F}_h$ and $l \in \mathbb{N}$, we denote by $\mathbb{P}^l(X)$ the space spanned by the restriction to X of scalar-valued, d-variate polynomials of total degree $\le l$. The local L^2-orthogonal projector $\pi_X^l : L^1(X) \to \mathbb{P}^l(X)$ is defined such that, for all $v \in L^1(X)$,

$$\int_X (\pi_X^l v - v) w = 0 \qquad \forall w \in \mathbb{P}^l(X). \tag{1.11}$$

When applied to vector-valued fields in $L^1(X)^d$ (resp., tensor-valued fields in $L^1(X)^{d\times d}$), the L^2-orthogonal projector mapping on $\mathbb{P}^l(X)^d$ (resp., $\mathbb{P}^l(X)^{d\times d}$) acts component-wise and is denoted in boldface font. Let $T \in \mathcal{T}_h$, $n \in [0, l+1]$ and $m \in [0, n]$. The following (n, r, m)-approximation properties of π_T^l hold: For any $v \in W^{n,r}(T)$,

$$|v - \pi_T^l v|_{W^{m,r}(T)} \lesssim h_T^{n-m} |v|_{W^{n,r}(T)}. \tag{1.12a}$$

The above property will also be used in what follows with r replaced by its conjugate exponent r'. If, additionally, $n \ge 1$, we have the following (n, r')-trace approximation

property:

$$\|v - \pi_T^l v\|_{L^{r'}(\partial T)} \lesssim h_T^{n-\frac{1}{r'}} |v|_{W^{n,r'}(T)}. \tag{1.12b}$$

The hidden constants in (1.12) are independent of h and T, but possibly depend on d, the mesh regularity parameter, l, n, and r. The approximation properties (1.12) are proved for integer n and m in [48, Appendix A.2] (see also [50, Theorem 1.45]), and can be extended to non-integer values using standard interpolation techniques (see, e.g., [89, Theorem 5.1]).

At the global level, for a given integer $l \geq 0$, we define the broken polynomial space $\mathbb{P}^l(\mathcal{T}_h)$ spanned by functions in $L^1(\Omega)$ whose restriction to each mesh element $T \in \mathcal{T}_h$ lies in $\mathbb{P}^l(T)$, and we define the global L^2-orthogonal projector $\pi_h^l : L^1(\Omega) \to \mathbb{P}^l(\mathcal{T}_h)$ such that, for all $v \in L^1(\Omega)$ and all $T \in \mathcal{T}_h$,

$$(\pi_h^l v)_{|T} \coloneqq \pi_T^l v_{|T}.$$

Broken polynomial spaces are subspaces of the broken Sobolev spaces

$$W^{n,r}(\mathcal{T}_h) \coloneqq \left\{ v \in L^r(\Omega) \ : \ v_{|T} \in W^{n,r}(T) \quad \forall T \in \mathcal{T}_h \right\}.$$

We define the broken gradient operator $\boldsymbol{\nabla}_h : W^{1,1}(\mathcal{T}_h) \to L^1(\Omega)^d$ such that, for all $v \in W^{1,1}(\mathcal{T}_h)$ and all $T \in \mathcal{T}_h$, $(\boldsymbol{\nabla}_h v)_{|T} \coloneqq \boldsymbol{\nabla} v_{|T}$. We define similarly the broken gradient acting on vector fields along with its symmetric part $\boldsymbol{\nabla}_{\mathrm{s},h}$, as well as the broken divergence operator $\boldsymbol{\nabla}_h \cdot$ acting on tensor fields. The global L^2-orthogonal projector $\boldsymbol{\pi}_h^l$ mapping vector-valued fields in $L^1(\Omega)^d$ (resp., tensor-valued fields in $L^1(\Omega)^{d\times d}$) on $\mathbb{P}^l(\mathcal{T}_h)^d$ (resp., $\mathbb{P}^l(\mathcal{T}_h)^{d\times d}$) is obtained applying π_h^l component-wise.

1.3.3 Discrete spaces and norms

Let an integer $k \geq 1$ be fixed. The HHO space of discrete velocity unknowns is

$$\underline{\boldsymbol{U}}_h^k \coloneqq \left\{ \underline{\boldsymbol{v}}_h \coloneqq ((\boldsymbol{v}_T)_{T\in\mathcal{T}_h}, (\boldsymbol{v}_F)_{F\in\mathcal{F}_h}) \;\middle|\; \begin{array}{ll} \boldsymbol{v}_T \in \mathbb{P}^k(T)^d & \forall T \in \mathcal{T}_h \\ \boldsymbol{v}_F \in \mathbb{P}^k(F)^d & \forall F \in \mathcal{F}_h \end{array} \right\}.$$

The interpolation operator $\underline{\boldsymbol{I}}_h^k : W^{1,1}(\Omega)^d \to \underline{\boldsymbol{U}}_h^k$ maps a function $\boldsymbol{v} \in W^{1,1}(\Omega)^d$ on the vector of discrete unknowns $\underline{\boldsymbol{I}}_h^k \boldsymbol{v}$ defined as follows:

$$\underline{\boldsymbol{I}}_h^k \boldsymbol{v} \coloneqq ((\boldsymbol{\pi}_T^k \boldsymbol{v}_{|T})_{T\in\mathcal{T}_h}, (\boldsymbol{\pi}_F^k \boldsymbol{v}_{|F})_{F\in\mathcal{F}_h}).$$

For all $T \in \mathcal{T}_h$, we denote by $\underline{\boldsymbol{U}}_T^k$ and $\underline{\boldsymbol{I}}_T^k$ the restrictions of $\underline{\boldsymbol{U}}_h^k$ and $\underline{\boldsymbol{I}}_h^k$ to T, respectively and, for all $\underline{\boldsymbol{v}}_h \in \underline{\boldsymbol{U}}_h^k$, we let $\underline{\boldsymbol{v}}_T \coloneqq (\boldsymbol{v}_T, (\boldsymbol{v}_F)_{F\in\mathcal{F}_T}) \in \underline{\boldsymbol{U}}_T^k$ denote the vector collecting the discrete unknowns attached to T and its faces. Furthermore, for all $\underline{\boldsymbol{v}}_h \in \underline{\boldsymbol{U}}_h^k$, we define the broken polynomial field $\boldsymbol{v}_h \in \mathbb{P}^k(\mathcal{T}_h)^d$ obtained patching element unknowns, that is,

$$(\boldsymbol{v}_h)_{|T} \coloneqq \boldsymbol{v}_T \qquad \forall T \in \mathcal{T}_h. \tag{1.13}$$

We define on $\underline{\boldsymbol{U}}_h^k$ the $W^{1,r}(\Omega)^d$-like strain seminorm $\|\cdot\|_{\boldsymbol{\varepsilon},r,h}$ such that, for all $\underline{\boldsymbol{v}}_h \in \underline{\boldsymbol{U}}_h^k$,

$$\|\underline{\boldsymbol{v}}_h\|_{\boldsymbol{\varepsilon},r,h} \coloneqq \left(\sum_{T\in\mathcal{T}_h} \|\underline{\boldsymbol{v}}_T\|_{\boldsymbol{\varepsilon},r,T}^r\right)^{\frac{1}{r}} \tag{1.14a}$$

with for all $T \in \mathcal{T}_h$,

$$\|\underline{\boldsymbol{v}}_T\|_{\boldsymbol{\varepsilon},r,T} \coloneqq \left(\|\boldsymbol{\nabla}_{\mathrm{s}}\boldsymbol{v}_T\|_{L^r(T)^{d\times d}}^r + \sum_{F\in\mathcal{F}_T} h_F^{1-r}\|\boldsymbol{v}_F - \boldsymbol{v}_T\|_{L^r(F)^d}^r\right)^{\frac{1}{r}}. \tag{1.14b}$$

The following boundedness property for $\underline{\boldsymbol{I}}_T^k$ can be proved adapting the arguments of [50, Proposition 6.24] and requires the star-shaped assumption on the mesh elements: For all $T \in \mathcal{T}_h$ and all $\boldsymbol{v} \in W^{1,r}(T)^d$,

$$\|\underline{\boldsymbol{I}}_T^k\boldsymbol{v}\|_{\boldsymbol{\varepsilon},r,T} \lesssim |\boldsymbol{v}|_{W^{1,r}(T)^d}, \tag{1.15}$$

where the hidden constant depends only on d, the mesh regularity parameter, r, and k.

The discrete velocity and pressure are sought in the following spaces, which embed, respectively, the homogeneous boundary condition for the velocity and the zero-average constraint for the pressure:

$$\underline{\boldsymbol{U}}_{h,0}^k \coloneqq \left\{\underline{\boldsymbol{v}}_h = ((\boldsymbol{v}_T)_{T\in\mathcal{T}_h}, (\boldsymbol{v}_F)_{F\in\mathcal{F}_h}) \in \underline{\boldsymbol{U}}_h^k \;:\; \boldsymbol{v}_F = \boldsymbol{0} \quad \forall F \in \mathcal{F}_h^{\mathrm{b}}\right\},$$
$$P_h^k \coloneqq \mathbb{P}^k(\mathcal{T}_h) \cap P.$$

By the discrete Korn inequality proved in Lemma 39 below, $\|\cdot\|_{\boldsymbol{\varepsilon},r,h}$ is a norm on $\underline{\boldsymbol{U}}_{h,0}^k$ (the proof is obtained reasoning as in [50, Corollary 2.16]).

1.4 HHO scheme

In this section, after introducing the discrete counterparts of the viscous and pressure-velocity coupling terms, we state the discrete problem along with the main results.

1.4.1 Viscous term

1.4.1.1 Local symmetric gradient reconstruction

For all $T \in \mathcal{T}_h$, we define the local symmetric gradient reconstruction $\mathbf{G}_{\mathrm{s},T}^k : \underline{\boldsymbol{U}}_T^k \to \mathbb{P}^k(T, \mathbb{R}_{\mathrm{s}}^{d\times d})$ such that, for all $\underline{\boldsymbol{v}}_T \in \underline{\boldsymbol{U}}_T^k$, and all $\boldsymbol{\tau} \in \mathbb{P}^k(T, \mathbb{R}_{\mathrm{s}}^{d\times d})$,

$$\int_T \mathbf{G}_{\mathrm{s},T}^k\underline{\boldsymbol{v}}_T : \boldsymbol{\tau} = \int_T \boldsymbol{\nabla}_{\mathrm{s}}\boldsymbol{v}_T : \boldsymbol{\tau} + \sum_{F\in\mathcal{F}_T}\int_F (\boldsymbol{v}_F - \boldsymbol{v}_T)\cdot(\boldsymbol{\tau}\boldsymbol{n}_{TF}). \tag{1.16}$$

This symmetric gradient reconstruction, originally introduced in [30, Section 4.2], is designed so that the following relation holds (see, e.g., [29, Proposition 5] or [50, Section 7.2.5]): For all $\boldsymbol{v} \in W^{1,1}(T)^d$,

$$\mathbf{G}_{\mathrm{s},T}^k(\underline{\boldsymbol{I}}_T^k \boldsymbol{v}) = \boldsymbol{\pi}_T^k(\boldsymbol{\nabla}_{\mathrm{s}} \boldsymbol{v}). \tag{1.17}$$

The global symmetric gradient reconstruction $\mathbf{G}_{\mathrm{s},h}^k : \underline{\boldsymbol{U}}_h^k \to \mathbb{P}^k(\mathcal{T}_h, \mathbb{R}_{\mathrm{s}}^{d\times d})$ is obtained patching the local contributions, that is, for all $\underline{\boldsymbol{v}}_h \in \underline{\boldsymbol{U}}_h^k$, we set

$$(\mathbf{G}_{\mathrm{s},h}^k \underline{\boldsymbol{v}}_h)_{|T} \coloneqq \mathbf{G}_{\mathrm{s},T}^k \underline{\boldsymbol{v}}_T \qquad \forall T \in \mathcal{T}_h. \tag{1.18}$$

1.4.1.2 Discrete viscous function

The discrete counterpart of the function a defined by (1.7) is $\mathrm{a}_h : \underline{\boldsymbol{U}}_h^k \times \underline{\boldsymbol{U}}_h^k \to \mathbb{R}$ such that, for all $\underline{\boldsymbol{v}}_h, \underline{\boldsymbol{w}}_h \in \underline{\boldsymbol{U}}_h^k$,

$$\mathrm{a}_h(\underline{\boldsymbol{w}}_h, \underline{\boldsymbol{v}}_h) \coloneqq \int_\Omega \boldsymbol{\sigma}(\cdot, \mathbf{G}_{\mathrm{s},h}^k \underline{\boldsymbol{w}}_h) : \mathbf{G}_{\mathrm{s},h}^k \underline{\boldsymbol{v}}_h + \gamma \mathrm{s}_h(\underline{\boldsymbol{w}}_h, \underline{\boldsymbol{v}}_h). \tag{1.19}$$

In the above definition, recalling (1.4), γ is a stabilization parameter such that

$$\gamma \in [\sigma_{\mathrm{hm}}, \sigma_{\mathrm{hc}}], \tag{1.20}$$

while the stabilization function $\mathrm{s}_h : \underline{\boldsymbol{U}}_h^k \times \underline{\boldsymbol{U}}_h^k \to \mathbb{R}$ is such that, for all $\underline{\boldsymbol{v}}_h, \underline{\boldsymbol{w}}_h \in \underline{\boldsymbol{U}}_h^k$,

$$\mathrm{s}_h(\underline{\boldsymbol{w}}_h, \underline{\boldsymbol{v}}_h) \coloneqq \sum_{T\in\mathcal{T}_h} \mathrm{s}_T(\underline{\boldsymbol{w}}_T, \underline{\boldsymbol{v}}_T), \tag{1.21}$$

where the local contributions are assumed to satisfy the following assumption.

Assumption 2 (Local stabilization function)**.** For all $T \in \mathcal{T}_h$, the local stabilization function $\mathrm{s}_T : \underline{\boldsymbol{U}}_T^k \times \underline{\boldsymbol{U}}_T^k \to \mathbb{R}$ is linear in its second argument and satisfies the following properties, with hidden constants independent of both h and T:

1. *Stability and boundedness.* Recalling the definition (1.14b) of the local $\|\cdot\|_{\boldsymbol{\varepsilon},r,T}$-seminorm, for all $\underline{\boldsymbol{v}}_T \in \underline{\boldsymbol{U}}_T^k$ it holds:

$$\|\mathbf{G}_{\mathrm{s},T}^k \underline{\boldsymbol{v}}_T\|_{L^r(T)^{d\times d}}^r + \mathrm{s}_T(\underline{\boldsymbol{v}}_T, \underline{\boldsymbol{v}}_T) \eqsim \|\underline{\boldsymbol{v}}_T\|_{\boldsymbol{\varepsilon},r,T}^r. \tag{1.22}$$

2. *Polynomial consistency.* For all $\boldsymbol{w} \in \mathbb{P}^{k+1}(T)^d$ and all $\underline{\boldsymbol{v}}_T \in \underline{\boldsymbol{U}}_T^k$,

$$\mathrm{s}_T(\underline{\boldsymbol{I}}_T^k \boldsymbol{w}, \underline{\boldsymbol{v}}_T) = 0. \tag{1.23}$$

3. *Hölder continuity.* For all $\underline{\boldsymbol{u}}_T, \underline{\boldsymbol{v}}_T, \underline{\boldsymbol{w}}_T \in \underline{\boldsymbol{U}}_T^k$, it holds, setting $\underline{\boldsymbol{e}}_T \coloneqq \underline{\boldsymbol{u}}_T - \underline{\boldsymbol{w}}_T$,

$$\begin{aligned}\left|\mathrm{s}_T(\underline{\boldsymbol{u}}_T, \underline{\boldsymbol{v}}_T) - \mathrm{s}_T(\underline{\boldsymbol{w}}_T, \underline{\boldsymbol{v}}_T)\right| \\ \lesssim \left(\mathrm{s}_T(\underline{\boldsymbol{u}}_T, \underline{\boldsymbol{u}}_T) + \mathrm{s}_T(\underline{\boldsymbol{w}}_T, \underline{\boldsymbol{w}}_T)\right)^{\frac{r-\tilde{r}}{r}} \mathrm{s}_T(\underline{\boldsymbol{e}}_T, \underline{\boldsymbol{e}}_T)^{\frac{\tilde{r}-1}{r}} \mathrm{s}_T(\underline{\boldsymbol{v}}_T, \underline{\boldsymbol{v}}_T)^{\frac{1}{r}}. \quad (1.24)\end{aligned}$$

4. *Hölder monotonicity.* For all $\underline{\boldsymbol{u}}_T, \underline{\boldsymbol{w}}_T \in \underline{\boldsymbol{U}}_T^k$, it holds, setting again $\underline{\boldsymbol{e}}_T \coloneqq \underline{\boldsymbol{u}}_T - \underline{\boldsymbol{w}}_T$,

$$\begin{aligned}\left(\mathrm{s}_T(\underline{\boldsymbol{u}}_T, \underline{\boldsymbol{e}}_T) - \mathrm{s}_T(\underline{\boldsymbol{w}}_T, \underline{\boldsymbol{e}}_T)\right) \left(\mathrm{s}_T(\underline{\boldsymbol{u}}_T, \underline{\boldsymbol{u}}_T) + \mathrm{s}_T(\underline{\boldsymbol{w}}_T, \underline{\boldsymbol{w}}_T)\right)^{\frac{2-\tilde{r}}{r}} \\ \gtrsim \mathrm{s}_T(\underline{\boldsymbol{e}}_T, \underline{\boldsymbol{e}}_T)^{\frac{r+2-\tilde{r}}{r}}. \quad (1.25)\end{aligned}$$

Remark 31 (Comparison with the linear case). If $r = 2$, s_T can be any symmetric bilinear form satisfying (1.22)–(1.23). Indeed, property (1.24) coincides in this case with the Cauchy–Schwarz inequality, while, by linearity of s_T, property (1.25) holds with the equal sign.

1.4.1.3 An example of viscous stabilization function

Taking inspiration from the scalar case (cf., e.g., [48, Eq. (4.11c)]), a local stabilization function that matches Assumption 2 can be obtained setting, for all $\underline{\boldsymbol{v}}_T, \underline{\boldsymbol{w}}_T \in \underline{\boldsymbol{U}}_T^k$,

$$\mathrm{s}_T(\underline{\boldsymbol{w}}_T, \underline{\boldsymbol{v}}_T) \coloneqq \int_{\partial T} |\boldsymbol{\Delta}_{\partial T}^k \underline{\boldsymbol{w}}_T|^{r-2} \boldsymbol{\Delta}_{\partial T}^k \underline{\boldsymbol{w}}_T \cdot \boldsymbol{\Delta}_{\partial T}^k \underline{\boldsymbol{v}}_T, \quad (1.26)$$

where, denoting by $\mathbb{P}^k(\mathcal{F}_T)^d$ the space of vector-valued broken polynomials of total degree $\le k$ on $\mathcal{F}_T$, the boundary residual operator $\boldsymbol{\Delta}_{\partial T}^k : \underline{\boldsymbol{U}}_T^k \to \mathbb{P}^k(\mathcal{F}_T)^d$ is such that, for all $\underline{\boldsymbol{v}}_T \in \underline{\boldsymbol{U}}_T^k$,

$$(\boldsymbol{\Delta}_{\partial T}^k \underline{\boldsymbol{v}}_T)_{|F} \coloneqq h_F^{-\frac{1}{r'}} \left(\boldsymbol{\pi}_F^k(\mathbf{r}_T^{k+1} \underline{\boldsymbol{v}}_T - \boldsymbol{v}_F) - \boldsymbol{\pi}_T^k(\mathbf{r}_T^{k+1} \underline{\boldsymbol{v}}_T - \boldsymbol{v}_T)\right) \qquad \forall F \in \mathcal{F}_T,$$

with velocity reconstruction $\mathbf{r}_T^{k+1} : \underline{\boldsymbol{U}}_T^k \to \mathbb{P}^{k+1}(T)^d$ such that

$$\int_T (\boldsymbol{\nabla}_{\mathrm{s}} \mathbf{r}_T^{k+1} \underline{\boldsymbol{v}}_T - \mathbf{G}_{\mathrm{s},T}^k \underline{\boldsymbol{v}}_T) : \boldsymbol{\nabla}_{\mathrm{s}} \boldsymbol{w} = 0 \qquad \forall \boldsymbol{w} \in \mathbb{P}^{k+1}(T)^d,$$

$$\int_T \mathbf{r}_T^{k+1} \underline{\boldsymbol{v}}_T = \int_T \boldsymbol{v}_T, \text{ and } \int_T \boldsymbol{\nabla}_{\mathrm{ss}} \mathbf{r}_T^{k+1} \underline{\boldsymbol{v}}_T = \frac{1}{2} \sum_{F \in \mathcal{F}_T} \int_F (\boldsymbol{v}_F \otimes \boldsymbol{n}_{TF} - \boldsymbol{n}_{TF} \otimes \boldsymbol{v}_F).$$

Above, $\boldsymbol{\nabla}_{\mathrm{ss}}$ denotes the skew-symmetric part of the gradient operator $\boldsymbol{\nabla}$ applied to vector fields and $\otimes$ is the tensor product such that, for all $\boldsymbol{x} = (x_i)_{1 \le i \le d}$ and $\boldsymbol{y} = (y_i)_{1 \le i \le d}$ in $\mathbb{R}^d$, $\boldsymbol{x} \otimes \boldsymbol{y} \coloneqq (x_i y_j)_{1 \le i,j \le d} \in \mathbb{R}^{d \times d}$.

Lemma 32 (Stabilization function (1.26))**.** *The local stabilization function defined by* (1.26) *satisfies Assumption 2.*

Proof. The proof of (1.22) for $r = 2$ is given in [30, Eq. (25)]. The result can be generalized to $r \neq 2$ using the same arguments of [48, Lemma 5.2]. Property (1.23) is an immediate consequence of the fact that $\boldsymbol{\Delta}_{\partial T}^k(\underline{\boldsymbol{I}}_T^k \boldsymbol{w}) = \boldsymbol{0}$ for any $\boldsymbol{w} \in \mathbb{P}^{k+1}(T)^d$, which can be proved reasoning as in [50, Proposition 2.6].

Let us prove (1.24). First, we remark that, since the function $\alpha \mapsto \alpha^{r-2}$ verifies the conditions in (1.77b) below, we can apply Theorem 46 to infer that the function $\mathbb{R}^d \ni \boldsymbol{x} \mapsto |\boldsymbol{x}|^{r-2}\boldsymbol{x}$ satisfies for all $\boldsymbol{x}, \boldsymbol{y} \in \mathbb{R}^d$,

$$\left||\boldsymbol{x}|^{r-2}\boldsymbol{x} - |\boldsymbol{y}|^{r-2}\boldsymbol{y}\right| \lesssim \left(|\boldsymbol{x}|^r + |\boldsymbol{y}|^r\right)^{\frac{r-\tilde{r}}{r}} |\boldsymbol{x}-\boldsymbol{y}|^{\tilde{r}-1}, \tag{1.27a}$$

$$\left(|\boldsymbol{x}|^{r-2}\boldsymbol{x} - |\boldsymbol{y}|^{r-2}\boldsymbol{y}\right)\cdot(\boldsymbol{x}-\boldsymbol{y})\left(|\boldsymbol{x}|^r + |\boldsymbol{y}|^r\right)^{\frac{2-\tilde{r}}{r}} \gtrsim |\boldsymbol{x}-\boldsymbol{y}|^{r+2-\tilde{r}}. \tag{1.27b}$$

Recalling (1.26), we can write

$$\begin{aligned}
\left|\mathrm{s}_T(\underline{\boldsymbol{u}}_T, \underline{\boldsymbol{v}}_T) - \mathrm{s}_T(\underline{\boldsymbol{w}}_T, \underline{\boldsymbol{v}}_T)\right| &\le \int_{\partial T} \left||\boldsymbol{\Delta}_{\partial T}^k \underline{\boldsymbol{u}}_T|^{r-2}\boldsymbol{\Delta}_{\partial T}^k \underline{\boldsymbol{u}}_T - |\boldsymbol{\Delta}_{\partial T}^k \underline{\boldsymbol{w}}_T|^{r-2}\boldsymbol{\Delta}_{\partial T}^k \underline{\boldsymbol{w}}_T\right| |\boldsymbol{\Delta}_{\partial T}^k \underline{\boldsymbol{v}}_T| \\
&\lesssim \int_{\partial T} \left(|\boldsymbol{\Delta}_{\partial T}^k \underline{\boldsymbol{u}}_T|^r + |\boldsymbol{\Delta}_{\partial T}^k \underline{\boldsymbol{w}}_T|^r\right)^{\frac{r-\tilde{r}}{r}} |\boldsymbol{\Delta}_{\partial T}^k \underline{\boldsymbol{e}}_T|^{\tilde{r}-1} |\boldsymbol{\Delta}_{\partial T}^k \underline{\boldsymbol{v}}_T| \\
&\le \left(\mathrm{s}_T(\underline{\boldsymbol{u}}_T, \underline{\boldsymbol{u}}_T) + \mathrm{s}_T(\underline{\boldsymbol{w}}_T, \underline{\boldsymbol{w}}_T)\right)^{\frac{r-\tilde{r}}{r}} \mathrm{s}_T(\underline{\boldsymbol{e}}_T, \underline{\boldsymbol{e}}_T)^{\frac{\tilde{r}-1}{r}} \mathrm{s}_T(\underline{\boldsymbol{v}}_T, \underline{\boldsymbol{v}}_T)^{\frac{1}{r}},
\end{aligned}$$

where we have used (1.27a) to pass to the second line and the $(1; \frac{r}{r-\tilde{r}}, \frac{r}{\tilde{r}-1}, r)$-Hölder inequality to conclude.

Moving to (1.25), (1.27b) and the $(1; \frac{r+2-\tilde{r}}{2-\tilde{r}}, \frac{r+2-\tilde{r}}{r})$-Hölder inequality yield

$$\begin{aligned}
\mathrm{s}_T(\underline{\boldsymbol{e}}_T, \underline{\boldsymbol{e}}_T) &= \int_{\partial T} |\boldsymbol{\Delta}_{\partial T}^k \underline{\boldsymbol{u}}_T - \boldsymbol{\Delta}_{\partial T}^k \underline{\boldsymbol{w}}_T|^r \\
&\lesssim \int_{\partial T} \left(|\boldsymbol{\Delta}_{\partial T}^k \underline{\boldsymbol{u}}_T|^r + |\boldsymbol{\Delta}_{\partial T}^k \underline{\boldsymbol{w}}_T|^r\right)^{\frac{2-\tilde{r}}{r+2-\tilde{r}}} \\
&\qquad \times \left[\left(|\boldsymbol{\Delta}_{\partial T}^k \underline{\boldsymbol{u}}_T|^{r-2}\boldsymbol{\Delta}_{\partial T}^k \underline{\boldsymbol{u}}_T - |\boldsymbol{\Delta}_{\partial T}^k \underline{\boldsymbol{w}}_T|^{r-2}\boldsymbol{\Delta}_{\partial T}^k \underline{\boldsymbol{w}}_T\right)\cdot \boldsymbol{\Delta}_{\partial T}^k \underline{\boldsymbol{e}}_T\right]^{\frac{r}{r+2-\tilde{r}}} \\
&\le \left(\mathrm{s}_T(\underline{\boldsymbol{u}}_T, \underline{\boldsymbol{u}}_T) + \mathrm{s}_T(\underline{\boldsymbol{w}}_T, \underline{\boldsymbol{w}}_T)\right)^{\frac{2-\tilde{r}}{r+2-\tilde{r}}} \left(\mathrm{s}_T(\underline{\boldsymbol{u}}_T, \underline{\boldsymbol{e}}_T) - \mathrm{s}_T(\underline{\boldsymbol{w}}_T, \underline{\boldsymbol{e}}_T)\right)^{\frac{r}{r+2-\tilde{r}}}. \qquad \square
\end{aligned}$$

1.4.2 Pressure-velocity coupling

For all $T \in \mathcal{T}_h$, we define the local divergence reconstruction $\mathrm{D}_T^k : \underline{\boldsymbol{U}}_T^k \to \mathbb{P}^k(T)$ by setting, for all $\underline{\boldsymbol{v}}_T \in \underline{\boldsymbol{U}}_T^k$, $\mathrm{D}_T^k \underline{\boldsymbol{v}}_T \coloneqq \mathrm{tr}(\mathbf{G}_{\mathrm{s},T}^k \underline{\boldsymbol{v}}_T)$. We have the following characterization of D_T^k: For all $\underline{\boldsymbol{v}}_T \in \underline{\boldsymbol{U}}_T^k$,

$$\int_T \mathrm{D}_T^k \underline{\boldsymbol{v}}_T \, q = \int_T (\boldsymbol{\nabla}\cdot\boldsymbol{v}_T) \, q + \sum_{F\in\mathcal{F}_T} \int_F (\boldsymbol{v}_F - \boldsymbol{v}_T)\cdot\boldsymbol{n}_{TF} \, q \qquad \forall q \in \mathbb{P}^k(T), \tag{1.28}$$

as can be checked writing (1.16) for $\boldsymbol{\tau} = q\mathrm{I}_d$. Taking the trace of (1.17), it is inferred that, for all $T \in \mathcal{T}_h$ and all $\boldsymbol{v} \in W^{1,1}(T)^d$, $\mathrm{D}_T^k(\underline{\boldsymbol{I}}_T^k \boldsymbol{v}) = \pi_T^k(\boldsymbol{\nabla}\cdot\boldsymbol{v})$. The pressure-velocity coupling is realized by the bilinear form $\mathrm{b}_h : \underline{\boldsymbol{U}}_h^k \times \mathbb{P}^k(\mathcal{T}_h) \to \mathbb{R}$ such that, for all $(\underline{\boldsymbol{v}}_h, q_h) \in \underline{\boldsymbol{U}}_h^k \times \mathbb{P}^k(\mathcal{T}_h)$, setting $q_T \coloneqq (q_h)_{|T}$ for all $T \in \mathcal{T}_h$,

$$\mathrm{b}_h(\underline{\boldsymbol{v}}_h, q_h) \coloneqq -\sum_{T\in\mathcal{T}_h} \int_T \mathrm{D}_T^k \underline{\boldsymbol{v}}_T \, q_T. \tag{1.29}$$

1.4.3 Discrete problem and main results

The discrete problem reads: Find $(\underline{\boldsymbol{u}}_h, p_h) \in \underline{\boldsymbol{U}}_{h,0}^k \times P_h^k$ such that

$$\mathrm{a}_h(\underline{\boldsymbol{u}}_h, \underline{\boldsymbol{v}}_h) + \mathrm{b}_h(\underline{\boldsymbol{v}}_h, p_h) = \int_\Omega \boldsymbol{f}\cdot\boldsymbol{v}_h \qquad \forall \underline{\boldsymbol{v}}_h \in \underline{\boldsymbol{U}}_{h,0}^k, \tag{1.30a}$$

$$-\mathrm{b}_h(\underline{\boldsymbol{u}}_h, q_h) = 0 \qquad \forall q_h \in P_h^k. \tag{1.30b}$$

Remark 33 (Discrete mass equation). The space of test functions in (1.30b) can be extended to $\mathbb{P}^k(\mathcal{T}_h)$ since, for all $\underline{\boldsymbol{v}}_h \in \underline{\boldsymbol{U}}_{h,0}^k$, the divergence theorem together with the fact that $\boldsymbol{v}_F = \boldsymbol{0}$ for all $F \in \mathcal{F}_h^{\mathrm{b}}$ and $\sum_{T\in\mathcal{T}_F} \int_F \boldsymbol{v}_F \cdot \boldsymbol{n}_{TF} = 0$ for all $F \in \mathcal{F}_h^{\mathrm{i}}$, yield

$$\mathrm{b}_h(\underline{\boldsymbol{v}}_h, 1) = -\sum_{T\in\mathcal{T}_h}\sum_{F\in\mathcal{F}_T} \int_F \boldsymbol{v}_F\cdot\boldsymbol{n}_{TF} = -\sum_{F\in\mathcal{F}_h^{\mathrm{i}}}\sum_{T\in\mathcal{T}_F} \int_F \boldsymbol{v}_F\cdot\boldsymbol{n}_{TF} = 0.$$

Remark 34 (Efficient implementation). When solving the system of nonlinear algebraic equations corresponding to (1.30) by, e.g., the Newton algorithm, all element-based velocity unknowns and all but one pressure unknown per element can be locally eliminated at each iteration by static condensation. As all the computations are local, this procedure is an embarrassingly parallel task which can fully benefit from multi-thread and multi-processor architectures. This implementation strategy has been described for the linear Stokes problem in [60, Section 6.2]. After further eliminating the boundary unknowns by strongly enforcing the boundary condition (1.1c), we end up solving, at each iteration of the nonlinear solver, a linear system of size $d\mathrm{card}(\mathcal{F}_h^{\mathrm{i}})\binom{k+d-1}{d-1} + \mathrm{card}(\mathcal{T}_h)$. Concerning the interplay between the static condensation strategy and the performance of p-multilevel linear solvers, we refer to [23].

In what follows, we state the main results for the HHO scheme (1.30). The proofs are postponed to Section 1.7.

Theorem 35 (Well-posedness)**.** *There exists a unique solution* $(\underline{\boldsymbol{u}}_h, p_h) \in \underline{\boldsymbol{U}}_{h,0}^k \times P_h^k$ *to the discrete problem* (1.30)*. Additionally, the following a priori bounds hold:*

$$\|\underline{\boldsymbol{u}}_h\|_{\boldsymbol{\varepsilon},r,h} \lesssim \left(\sigma_{\mathrm{hm}}^{-1}\|\boldsymbol{f}\|_{L^{r'}(\Omega)^d}\right)^{\frac{1}{r-1}} + \left(\delta^{2-\tilde{r}}\sigma_{\mathrm{hm}}^{-1}\|\boldsymbol{f}\|_{L^{r'}(\Omega)^d}\right)^{\frac{1}{r+1-\tilde{r}}}, \tag{1.31a}$$

$$\|p_h\|_{L^{r'}(\Omega)} \lesssim \sigma_{\mathrm{hc}}\left(\sigma_{\mathrm{hm}}^{-1}\|\boldsymbol{f}\|_{L^{r'}(\Omega)^d} + \delta^{|r-2|(\tilde{r}-1)}\left(\sigma_{\mathrm{hm}}^{-1}\|\boldsymbol{f}\|_{L^{r'}(\Omega)^d}\right)^{\frac{\tilde{r}-1}{r+1-\tilde{r}}}\right). \tag{1.31b}$$

Proof. See Section 1.7.2. □

Theorem 36 (Error estimate)**.** *Let* $(\boldsymbol{u}, p) \in \boldsymbol{U} \times P$ *and* $(\underline{\boldsymbol{u}}_h, p_h) \in \underline{\boldsymbol{U}}_{h,0}^k \times P_h^k$ *solve* (1.6) *and* (1.30)*, respectively. Assume the additional regularity* $\boldsymbol{u} \in W^{k+2,r}(\mathcal{T}_h)^d$*,* $\boldsymbol{\sigma}(\cdot, \boldsymbol{\nabla}_{\mathrm{s}}\boldsymbol{u}) \in W^{1,r'}(\Omega, \mathbb{R}_{\mathrm{s}}^{d\times d}) \cap W^{(k+1)(\tilde{r}-1),r'}(\mathcal{T}_h, \mathbb{R}_{\mathrm{s}}^{d\times d})$*, and* $p \in W^{1,r'}(\Omega) \cap W^{(k+1)(\tilde{r}-1),r'}(\mathcal{T}_h)$*. Then, under Assumptions 1 and 2,*

$$\|\underline{\boldsymbol{u}}_h - \underline{\boldsymbol{I}}_h^k\boldsymbol{u}\|_{\boldsymbol{\varepsilon},r,h} \lesssim h^{\frac{(k+1)(\tilde{r}-1)}{r+1-\tilde{r}}}\left(\sigma_{\mathrm{hm}}^{-1}\mathcal{N}_f^{2-\tilde{r}}\mathcal{N}_{\boldsymbol{\sigma},\boldsymbol{u},p}\right)^{\frac{1}{r+1-\tilde{r}}}, \tag{1.32a}$$

$$\begin{aligned}\|p_h - \pi_h^k p\|_{L^{r'}(\Omega)} &\lesssim h^{(k+1)(\tilde{r}-1)}\mathcal{N}_{\boldsymbol{\sigma},\boldsymbol{u},p} \\ &\quad + h^{\frac{(k+1)(\tilde{r}-1)^2}{r+1-\tilde{r}}}\sigma_{\mathrm{hc}}\mathcal{N}_f^{|r-2|(\tilde{r}-1)}\left(\sigma_{\mathrm{hm}}^{-1}\mathcal{N}_{\boldsymbol{\sigma},\boldsymbol{u},p}\right)^{\frac{\tilde{r}-1}{r+1-\tilde{r}}},\end{aligned} \tag{1.32b}$$

where we have set, for the sake of brevity,

$$\begin{aligned}\mathcal{N}_{\boldsymbol{\sigma},\boldsymbol{u},p} &\coloneqq \sigma_{\mathrm{hc}}\left(\delta^r + |\boldsymbol{u}|_{W^{1,r}(\Omega)^d}^r\right)^{\frac{r-\tilde{r}}{r}}|\boldsymbol{u}|_{W^{k+2,r}(\mathcal{T}_h)^d}^{\tilde{r}-1} \\ &\quad + |\boldsymbol{\sigma}(\cdot, \boldsymbol{\nabla}_{\mathrm{s}}\boldsymbol{u})|_{W^{(k+1)(\tilde{r}-1),r'}(\mathcal{T}_h)^{d\times d}} + |p|_{W^{(k+1)(\tilde{r}-1),r'}(\mathcal{T}_h)}, \\ \mathcal{N}_f &\coloneqq \delta + \left(\sigma_{\mathrm{hm}}^{-1}\|\boldsymbol{f}\|_{L^{r'}(\Omega)^d}\right)^{\frac{1}{r-1}} + \left(\delta^{2-\tilde{r}}\sigma_{\mathrm{hm}}^{-1}\|\boldsymbol{f}\|_{L^{r'}(\Omega)^d}\right)^{\frac{1}{r+1-\tilde{r}}}.\end{aligned}$$

Proof. See Section 1.7.3. □

Remark 37 (Orders of convergence). From (1.32), neglecting higher-order terms, we infer asymptotic convergence rates of $O_{\mathrm{vel}}^k \coloneqq \frac{(k+1)(\tilde{r}-1)}{r+1-\tilde{r}}$ for the velocity and $O_{\mathrm{pre}}^k \coloneqq \frac{(k+1)(\tilde{r}-1)^2}{r+1-\tilde{r}}$ for the pressure, that is,

$$\begin{aligned}O_{\mathrm{vel}}^k &= \begin{cases}(k+1)(r-1) & \text{if } r < 2,\\ \frac{k+1}{r-1} & \text{if } r \geq 2,\end{cases} \\ O_{\mathrm{pre}}^k &= \begin{cases}(k+1)(r-1)^2 & \text{if } r < 2,\\ \frac{k+1}{r-1} & \text{if } r \geq 2.\end{cases}\end{aligned} \tag{1.33}$$

Notice that, owing to the presence of higher-order terms in the right-hand sides of (1.32), higher convergence rates may be observed before attaining the asymptotic ones;

see Section 1.5. The asymptotic order of convergence for the velocity coincides with the one proved in [47, Theorem 3.2] for HHO discretizations of scalar Leray–Lions problems. We refer to [52] for recent improvements on these estimates depending on the degeneracy of the problem.

1.5 Numerical examples

In this section, we evaluate the numerical performance of the HHO method on a complete panel of numerical test cases. We focus on the $(\mu, 0, 1, r)$-Carreau–Yasuda law (1.5) (corresponding to the power-law model) with values of the exponent r ranging from 1.25 to 2.75. Our implementation relies on the SpaFEDTe library (cf. `https://spafedte.github.io`).

1.5.1 Trigonometric solution

We begin by considering a manufactured solution to problem (1.1) in order to assess the convergence of the method. We take $\Omega = (0,1)^2$ and exact velocity $\boldsymbol{u}$ and pressure p given by, respectively,

$$\begin{aligned}\boldsymbol{u}(x_1,x_2) &= \left(\sin\left(\tfrac{\pi}{2}x_1\right)\cos\left(\tfrac{\pi}{2}x_2\right), -\cos\left(\tfrac{\pi}{2}x_1\right)\sin\left(\tfrac{\pi}{2}x_2\right)\right),\\ p(x_1,x_2) &= \sin\left(\tfrac{\pi}{2}x_1\right)\sin\left(\tfrac{\pi}{2}x_2\right) - \tfrac{4}{\pi^2}.\end{aligned}$$

The volumetric load $\boldsymbol{f}$ and the Dirichlet boundary condition are inferred from the exact solution. Considering $\mu = 1$ and $r \in \{1.5, 1.75, \ldots, 2.75\}$, this solution matches the assumptions required in Theorem 36 for $k = 1$, except the case $r = 1.5$ for which $\boldsymbol{\sigma}(\cdot, \boldsymbol{\nabla}_{\mathrm{s}}\boldsymbol{u}) \notin W^{1,r'}(\Omega, \mathbb{R}^{d\times d}_{\mathrm{s}})$. We consider the HHO scheme for $k = 1$ on three mesh families, namely Cartesian orthogonal, distorted triangular, and distorted Cartesian; see Figure 1.1. Overall, the results are in agreement with the theoretical predictions, and in some cases the expected asymptotic orders of convergence are exceeded. Specifically, for $r \neq 2$, the convergence rates computed on the last refinement surpass in some cases the theoretical ones. As noticed in Remark 37, this suggests that the asymptotic order is still not attained. A similar phenomenon has been observed on certain meshes for the p-Laplace problem; see [47, Section 3.5.2] and [53, Section 3.7]. In some cases, we observe a better convergence for the velocity on distorted triangular meshes than on Cartesian meshes. This phenomenon possibly results from the combination of two factors: on one hand, the improved robustness of HHO methods with respect to elongated elements when compared to classical discretization methods; on the other hand, the fact that unstructured triangular meshes have more elements than Cartesian meshes for a given meshsize and lack privileged directions, which reduces mesh bias. Further investigation is postponed to a future work.

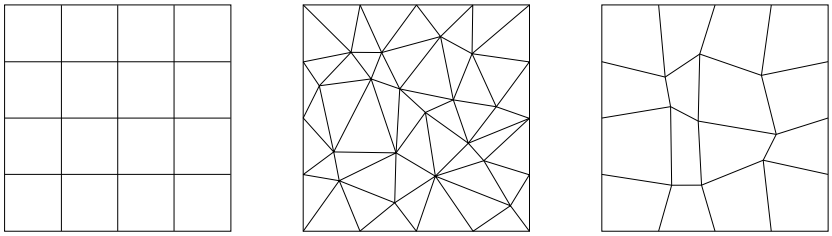

Figure 1.1: Coarsest Cartesian, distorted triangular, and distorted Cartesian meshes used in Section 1.5.

1.5.2 Lid-driven cavity flow

We next consider the lid-driven cavity flow, a well-known problem in fluid mechanics. The domain is the unit square $\Omega = (0,1)^2$, and we enforce a unit tangential velocity $\boldsymbol{u} = (1,0)$ on the top edge (of equation $x_2 = 1$) and wall boundary conditions on the other edges. This boundary condition is incompatible with the formulation (1.6), even generalized to non-homogeneous boundary conditions, since $\boldsymbol{u} \notin W^{1,r}(\Omega)^d$. However, this is a very classical test that demonstrates the quality of the method. We consider a low Reynolds number $\mathrm{Re} := \frac{2}{\mu} = 1$. For $r \in \{1.25, 2, 2.75\}$, we solve the discrete problem on Cartesian and distorted triangular meshes (cf. Figure 1.1) of approximate size 128×128 for $k = 1$, and 16×16 for $k = 5$. This choice is meant to compare the low-order version of the method on a fine mesh with the high-order version on a very coarse one. The corresponding total number of degrees of freedom is: 130048 for the fine Cartesian mesh with $k = 1$; 5760 for the coarse Cartesian mesh with $k = 5$; 298676 for the fine triangular mesh with $k = 1$; and 14196 for the coarse triangular mesh with $k = 5$. In Figure 1.4 we display the velocity magnitude, while in Figure 1.5 we plot the horizontal component u_1 of the velocity along the vertical centreline $x_1 = \frac{1}{2}$ (resp., vertical component u_2 along the horizontal centreline $x_2 = \frac{1}{2}$). The lines corresponding to $k = 1$ on the fine mesh and to $k = 5$ on the coarse mesh are perfectly superimposed, regardless of the mesh family and of the value of r. This shows that, despite the lack of regularity of the exact solution, high-order versions of the scheme on very coarse meshes deliver similar results as low-order versions on very fine grids. Furthermore, we observe significant differences in the behavior of the flow according to r, coherent with the expected physical behavior. In particular, the viscous effects increase with r, as reflected by the size of the central vortex.

1.6 Discrete Korn inequality

We prove in this section a discrete counterpart of the following Korn inequality (see [72, Theorem 1]) that will be needed in the analysis: There is $C_{\mathrm{K}} > 0$ depending only on Ω

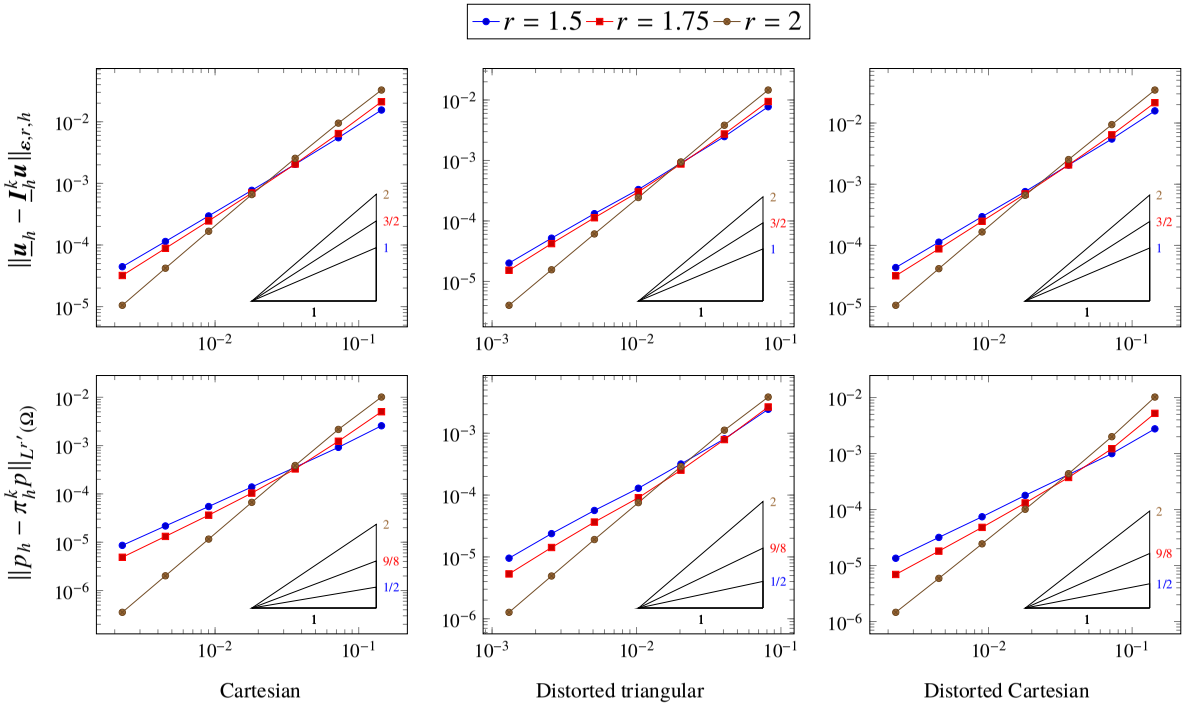

Figure 1.2: Numerical results for the test case of Section 1.5.1 when $r \leq 2$. The slopes indicate the order of convergence expected from Theorem 36, i.e. $O^1_{\text{vel}} = 2(r-1)$ and $O^1_{\text{pre}} = 2(r-1)^2$ for $r \in \{1.5, 1.75, 2\}$.

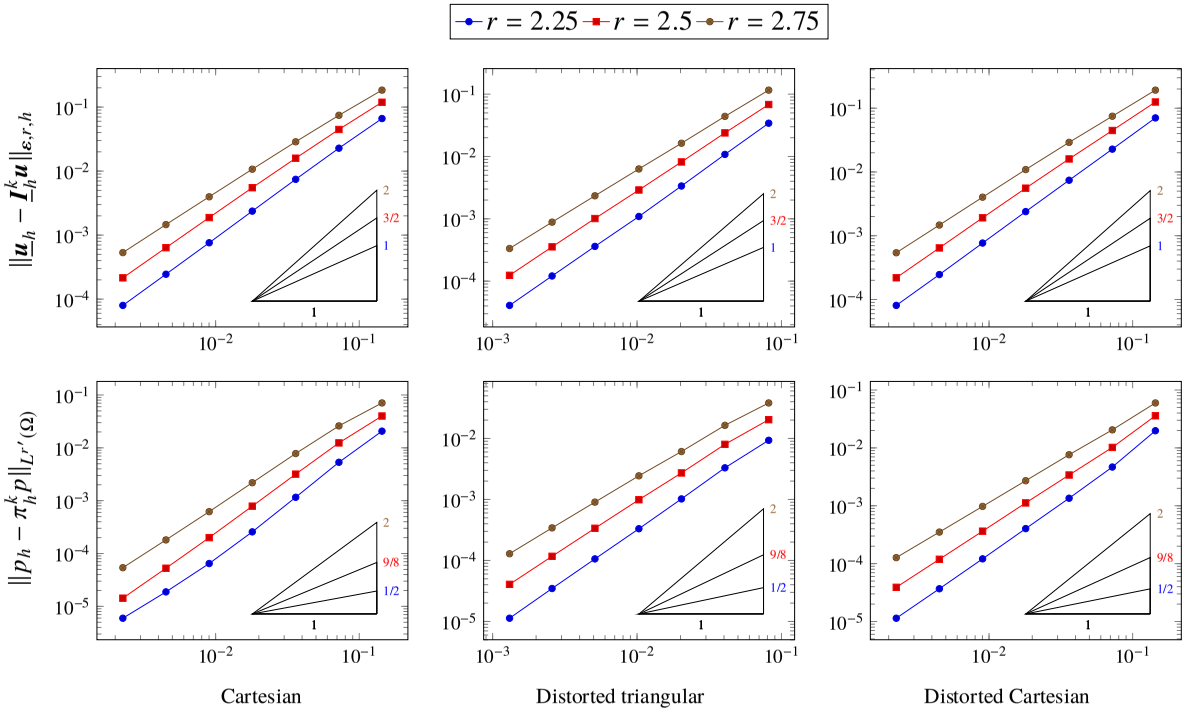

Figure 1.3: Numerical results for the test case of Section 1.5.1 when $r > 2$. The slopes indicate the order of convergence expected from Theorem 36, i.e. $O^1_{\text{vel}} = O^1_{\text{pre}} = \frac{2}{r-1}$.

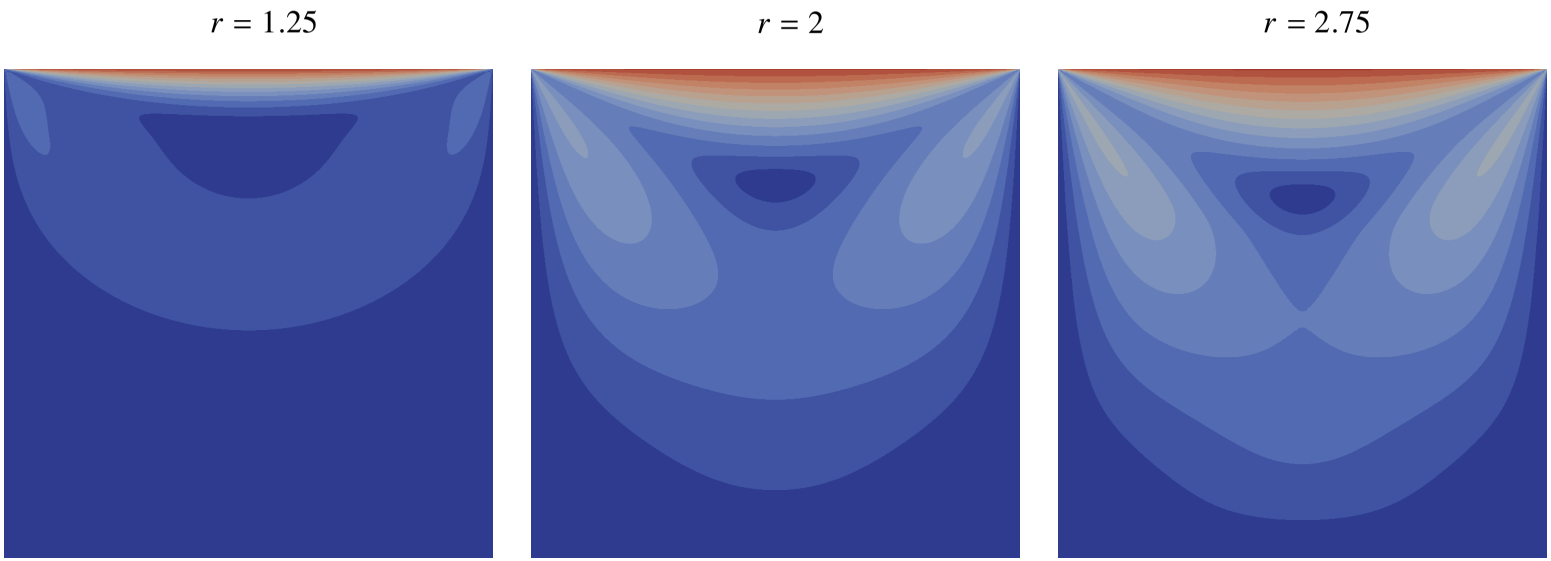

Figure 1.4: Numerical results for the test case of Section 1.5.2: lid-driven cavity flow. Velocity magnitude contours (15 equispaced values in the range $[0, 1]$). Computations on a Cartesian mesh of size 128×128 with $k = 5$.

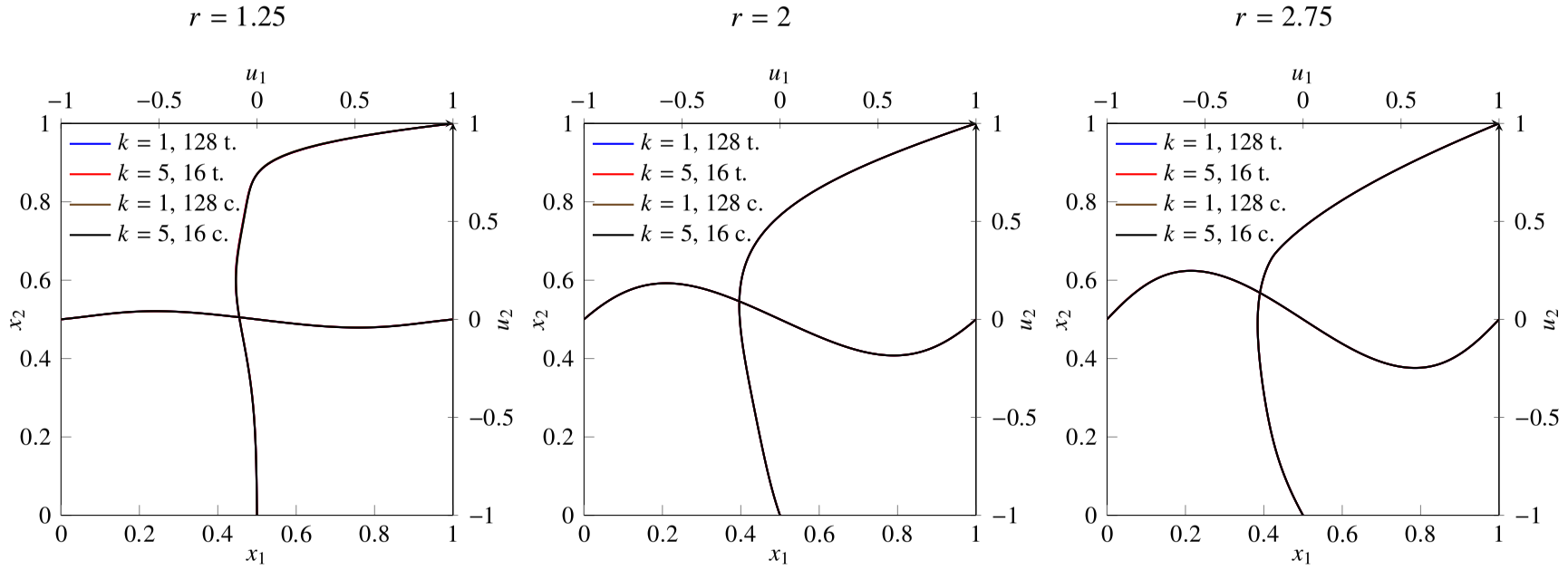

Figure 1.5: Numerical results for the test case of Section 1.5.2: lid-driven cavity flow. Horizontal component u_1 of the velocity along the vertical centreline $x_1 = \frac{1}{2}$ and vertical component u_2 of the velocity along the horizontal centreline $x_2 = \frac{1}{2}$.

and r such that for all $\boldsymbol{v} \in \boldsymbol{U}$,

$$\|\boldsymbol{v}\|_{W^{1,r}(\Omega)^d} \le C_{\mathrm{K}} \|\boldsymbol{\nabla}_{\mathrm{s}} \boldsymbol{v}\|_{L^r(\Omega)^{d\times d}}. \tag{1.34}$$

We start by recalling the following preliminary result concerning the node-averaging interpolator (sometimes called Oswald interpolator). Let $\mathfrak{T}_h$ be a matching simplicial submesh of $\mathcal{M}_h$ in the sense of [50, Definition 1.8]. The node-averaging operator $\boldsymbol{I}^k_{\mathrm{av},h} : \mathbb{P}^k(\mathcal{T}_h)^d \to \mathbb{P}^k(\mathfrak{T}_h)^d \cap W^{1,r}(\Omega)^d$ is such that, for all $\boldsymbol{v}_h \in \mathbb{P}^k(\mathcal{T}_h)^d$ and all Lagrange node V of $\mathfrak{T}_h$, denoting by $\mathfrak{T}_V$ the set of simplices sharing V,

$$(\boldsymbol{I}^k_{\mathrm{av},h} \boldsymbol{v}_h)(V) \coloneqq \begin{cases} \frac{1}{\mathrm{card}(\mathfrak{T}_V)} \sum_{\tau\in\mathfrak{T}_V} \boldsymbol{v}_{h|_\tau}(V) & \text{if } V \in \Omega, \\ \boldsymbol{0} & \text{if } V \in \partial\Omega. \end{cases}$$

For all $F \in \mathcal{F}_h^{\mathrm{i}}$, denote by $T_1, T_2 \in \mathcal{T}_h$ the elements sharing F, taken in an arbitrary but fixed order. We define the jump operator such that, for any function $\boldsymbol{v} \in W^{1,1}(\mathcal{T}_h)^d$, $[\boldsymbol{v}]_F \coloneqq (\boldsymbol{v}_{|_{T_1}})_{|_F} - (\boldsymbol{v}_{|_{T_2}})_{|_F}$. This definition is extended to boundary faces $F \in \mathcal{F}_h^{\mathrm{b}}$ by setting $[\boldsymbol{v}]_F \coloneqq \boldsymbol{v}_{|_F}$.

Proposition 38 (Boundedness of the node-averaging operator)**.** *For all $\boldsymbol{v}_h \in \mathbb{P}^k(\mathcal{T}_h)^d$, it holds*

$$|\boldsymbol{v}_h - \boldsymbol{I}^k_{\mathrm{av},h} \boldsymbol{v}_h|^r_{W^{1,r}(\mathcal{T}_h)^d} \lesssim \sum_{F\in\mathcal{F}_h} h_F^{1-r} \|[\boldsymbol{v}_h]_F\|^r_{L^r(F)^d}. \tag{1.35}$$

Proof. Combining [50, Eq. (4.13)] (which corresponds to (1.35) for $r = 2$) with the local Lebesgue embeddings of [50, Lemma 1.25] (see also [48, Lemma 5.1]) gives, for any $T \in \mathcal{T}_h$,

$$\|\boldsymbol{v}_h - \boldsymbol{I}^k_{\mathrm{av},h} \boldsymbol{v}_h\|^r_{L^r(T)^d} \lesssim \sum_{F\in\mathcal{F}_{\mathcal{V},T}} h_F \|[\boldsymbol{v}_h]_F\|^r_{L^r(F)^d}, \tag{1.36}$$

where $\mathcal{F}_{\mathcal{V},T}$ collects the faces whose closure has non-empty intersection with $\overline{T}$. Using the local inverse inequality of [50, Lemma 1.28] (see also [48, Eq. (A.1)]), we can write

$$\begin{aligned} |\boldsymbol{v}_h - \boldsymbol{I}^k_{\mathrm{av},h} \boldsymbol{v}_h|^r_{W^{1,r}(\mathcal{T}_h)^d} &\lesssim \sum_{T\in\mathcal{T}_h} h_T^{-r} \|\boldsymbol{v}_h - \boldsymbol{I}^k_{\mathrm{av},h} \boldsymbol{v}_h\|^r_{L^r(T)^d} \\ &\lesssim \sum_{T\in\mathcal{T}_h} \sum_{F\in\mathcal{F}_{\mathcal{V},T}} h_F^{1-r} \|[\boldsymbol{v}_h]_F\|^r_{L^r(F)^d} \\ &\lesssim \sum_{F\in\mathcal{F}_h} \sum_{T\in\mathcal{T}_{\mathcal{V},F}} h_F^{1-r} \|[\boldsymbol{v}_h]_F\|^r_{L^r(F)^d} \\ &\le \max_{F\in\mathcal{F}_h} \mathrm{card}(\mathcal{T}_{\mathcal{V},F}) \sum_{F\in\mathcal{F}_h} h_F^{1-r} \|[\boldsymbol{v}_h]_F\|^r_{L^r(F)^d}, \end{aligned}$$

where we have used the fact that $h_T^{-r} \le h_F^{-r}$ along with inequality (1.36) to pass to the second line, and we have exchanged the sums after setting $\mathcal{T}_{\mathcal{V},F} \coloneqq \{T \in \mathcal{T}_h : \overline{F} \cap \overline{T} \neq \emptyset\}$

for all $F \in \mathcal{F}_h$ to pass to the third line. Observing that $\max_{F\in\mathcal{F}_h} \mathrm{card}(\mathcal{T}_{\mathcal{V},F}) \lesssim 1$ (since, for any $F \in \mathcal{F}_h$, $\mathrm{card}(\mathcal{T}_{\mathcal{V},F})$ is bounded by the left-hand side of [50, Eq. (4.23)] written for any $T \in \mathcal{T}_h$ to which F belongs), (1.35) follows. □

The following inequalities between sums of powers will be often used in what follows without necessarily recalling this fact explicitly each time. Let an integer $n \geq 1$ and a real number $m \in (0,\infty)$ be given. Then, for all $a_1,\dots,a_n \in (0,\infty)$, we have

$$n^{-(m-1)^\ominus}\sum_{i=1}^n a_i^m \leq \left(\sum_{i=1}^n a_i\right)^m \leq n^{(m-1)^\oplus}\sum_{i=1}^n a_i^m. \tag{1.37}$$

If $m = 1$, then (1.37) holds with the equal sign. If $m < 1$, [103, Eqs. (5) and (3)] with $\alpha = 1$ and $\beta = m$ give $n^{m-1}\sum_{i=1}^n a_i^m \leq \left(\sum_{i=1}^n a_i\right)^m \leq \sum_{i=1}^n a_i^m$. If, on the other hand, $m > 1$, [103, Eqs. (3) and (5)] with $\alpha = m$ and $\beta = 1$ give $\sum_{i=1}^n a_i^m \leq \left(\sum_{i=1}^n a_i\right)^m \leq n^{m-1}\sum_{i=1}^n a_i^m$. Gathering the above cases yields (1.37).

Lemma 39. *(Discrete Korn inequality) We have, for all $\underline{\boldsymbol{v}}_h \in \underline{\boldsymbol{U}}_{h,0}^k$, recalling the notation (1.13),*

$$\|\boldsymbol{v}_h\|_{L^r(\Omega)^d}^r + |\boldsymbol{v}_h|_{W^{1,r}(\mathcal{T}_h)^d}^r \lesssim \|\underline{\boldsymbol{v}}_h\|_{\boldsymbol{\varepsilon},r,h}^r. \tag{1.38}$$

Proof. Let $\underline{\boldsymbol{v}}_h \in \underline{\boldsymbol{U}}_{h,0}^k$. Using a triangle inequality followed by (1.37), we can write

$$\begin{aligned}
|\boldsymbol{v}_h|_{W^{1,r}(\mathcal{T}_h)^d}^r &\lesssim |\boldsymbol{I}_{\mathrm{av},h}^k\boldsymbol{v}_h|_{W^{1,r}(\mathcal{T}_h)^d}^r + |\boldsymbol{v}_h - \boldsymbol{I}_{\mathrm{av},h}^k\boldsymbol{v}_h|_{W^{1,r}(\mathcal{T}_h)^d}^r\\
&\lesssim \|\boldsymbol{\nabla}_{\mathrm{s}}(\boldsymbol{I}_{\mathrm{av},h}^k\boldsymbol{v}_h)\|_{L^r(\Omega)^{d\times d}}^r + |\boldsymbol{v}_h - \boldsymbol{I}_{\mathrm{av},h}^k\boldsymbol{v}_h|_{W^{1,r}(\mathcal{T}_h)^d}^r\\
&\lesssim \|\boldsymbol{\nabla}_{\mathrm{s},h}\boldsymbol{v}_h\|_{L^r(\Omega)^{d\times d}}^r + |\boldsymbol{v}_h - \boldsymbol{I}_{\mathrm{av},h}^k\boldsymbol{v}_h|_{W^{1,r}(\mathcal{T}_h)^d}^r\\
&\lesssim \|\boldsymbol{\nabla}_{\mathrm{s},h}\boldsymbol{v}_h\|_{L^r(\Omega)^{d\times d}}^r + \sum_{F\in\mathcal{F}_h} h_F^{1-r}\|[\boldsymbol{v}_h]_F\|_{L^r(F)^d}^r,
\end{aligned}$$

where we have used the continuous Korn inequality (1.34) to pass to the second line, we have inserted $\pm\boldsymbol{\nabla}_{\mathrm{s},h}\boldsymbol{v}_h$ into the first norm and used a triangle inequality followed by (1.37) to pass to the third line, and we have invoked the bound (1.35) to conclude. Observing that, for any $F \in \mathcal{F}_h$, $|[\boldsymbol{v}_h]_F| \leq \sum_{T\in\mathcal{T}_F} |\boldsymbol{v}_F - \boldsymbol{v}_T|$ by a triangle inequality, and using (1.37), we can continue writing

$$|\boldsymbol{v}_h|_{W^{1,r}(\mathcal{T}_h)^d}^r \lesssim \|\boldsymbol{\nabla}_{\mathrm{s},h}\boldsymbol{v}_h\|_{L^r(\Omega)^{d\times d}}^r + \sum_{F\in\mathcal{F}_h}\sum_{T\in\mathcal{T}_F} h_F^{1-r}\|\boldsymbol{v}_F - \boldsymbol{v}_T\|_{L^r(F)^d}^r = \|\underline{\boldsymbol{v}}_h\|_{\boldsymbol{\varepsilon},r,h}^r,$$

where we have exchanged the sums over faces and elements and recalled definition (1.14a) to conclude. This proves the bound for the second term in the left-hand side of (1.38). Combining this result with the global discrete Sobolev embeddings of [48, Proposition 5.4] yields the bound for the first term in (1.38). □

1.7 Well-posedness and convergence analysis

In this section, after studying the stabilization function s_h, we prove the main results stated in Section 1.4.3.

1.7.1 Properties of the stabilization function

Lemma 40 (Consistency of s_T)**.** *For any $T \in \mathcal{T}_h$ and any s_T satisfying Assumption 2, it holds, for all $\boldsymbol{w} \in W^{k+2,r}(T)^d$ and all $\underline{\boldsymbol{v}}_T \in \underline{\boldsymbol{U}}_T^k$,*

$$|s_T(\underline{\boldsymbol{I}}_T^k \boldsymbol{w}, \underline{\boldsymbol{v}}_T)| \lesssim h_T^{(k+1)(\tilde{r}-1)} |\boldsymbol{w}|_{W^{1,r}(T)^d}^{r-\tilde{r}} |\boldsymbol{w}|_{W^{k+2,r}(T)^d}^{\tilde{r}-1} \|\underline{\boldsymbol{v}}_T\|_{\boldsymbol{\varepsilon},r,T}, \tag{1.39}$$

where the hidden constant is independent of h, T, and $\boldsymbol{w}$.

Proof. The proof adapts the arguments of [50, Propositon 2.14]. Using the polynomial consistency property (1.23), we can write

$$\begin{aligned}
|s_T(\underline{\boldsymbol{I}}_T^k \boldsymbol{w}, \underline{\boldsymbol{v}}_T)| &= |s_T(\underline{\boldsymbol{I}}_T^k \boldsymbol{w}, \underline{\boldsymbol{v}}_T) - s_T(\underline{\boldsymbol{I}}_T^k(\boldsymbol{\pi}_T^{k+1}\boldsymbol{w}), \underline{\boldsymbol{v}}_T)| \\
&\lesssim s_T(\underline{\boldsymbol{I}}_T^k \boldsymbol{w}, \underline{\boldsymbol{I}}_T^k \boldsymbol{w})^{\frac{r-\tilde{r}}{r}} s_T(\underline{\boldsymbol{I}}_T^k(\boldsymbol{w} - \boldsymbol{\pi}_T^{k+1}\boldsymbol{w}), \underline{\boldsymbol{I}}_T^k(\boldsymbol{w} - \boldsymbol{\pi}_T^{k+1}\boldsymbol{w}))^{\frac{\tilde{r}-1}{r}} s_T(\underline{\boldsymbol{v}}_T, \underline{\boldsymbol{v}}_T)^{\frac{1}{r}} \\
&\lesssim \|\underline{\boldsymbol{I}}_T^k \boldsymbol{w}\|_{\boldsymbol{\varepsilon},r,T}^{r-\tilde{r}} \|\underline{\boldsymbol{I}}_T^k(\boldsymbol{w} - \boldsymbol{\pi}_T^{k+1}\boldsymbol{w})\|_{\boldsymbol{\varepsilon},r,T}^{\tilde{r}-1} \|\underline{\boldsymbol{v}}_T\|_{\boldsymbol{\varepsilon},r,T} \\
&\lesssim |\boldsymbol{w}|_{W^{1,r}(T)^d}^{r-\tilde{r}} |\boldsymbol{w} - \boldsymbol{\pi}_T^{k+1}\boldsymbol{w}|_{W^{1,r}(T)^d}^{\tilde{r}-1} \|\underline{\boldsymbol{v}}_T\|_{\boldsymbol{\varepsilon},r,T} \\
&\lesssim h_T^{(k+1)(\tilde{r}-1)} |\boldsymbol{w}|_{W^{1,r}(T)^d}^{r-\tilde{r}} |\boldsymbol{w}|_{W^{k+2,r}(T)^d}^{\tilde{r}-1} \|\underline{\boldsymbol{v}}_T\|_{\boldsymbol{\varepsilon},r,T},
\end{aligned}$$

where we have used the Hölder continuity (1.24) and observed that, by the consistency property (1.23), $s_T(\underline{\boldsymbol{I}}_T^k(\boldsymbol{\pi}_T^{k+1}\boldsymbol{w}), \underline{\boldsymbol{I}}_T^k(\boldsymbol{\pi}_T^{k+1}\boldsymbol{w})) = 0$ to pass to the second line, we have used the boundedness property (1.22) to pass to the third line, the boundedness (1.15) of $\underline{\boldsymbol{I}}_T^k$ to pass to the fourth line, and the $(k+2, r, 1)$-approximation property (1.12a) of $\boldsymbol{\pi}_T^{k+1}$ to conclude. □

In what follows, we will need generalized versions of the continuous and discrete Hölder inequalities, recalled hereafter for the sake of convenience. Let $X \subset \mathbb{R}^d$ be measurable, $n \in \mathbb{N}^*$, and let $t, p_1, \ldots, p_n \in (0, \infty]$ be such that $\sum_{i=1}^n \frac{1}{p_i} = \frac{1}{t}$. The continuous $(t; p_1, \ldots, p_n)$-Hölder inequality reads: For any $(f_1, \ldots, f_n) \in \bigtimes_{i=1}^n L^{p_i}(X)$,

$$\left\| \prod_{i=1}^n f_i \right\|_{L^t(X)} \le \prod_{i=1}^n \|f_i\|_{L^{p_i}(X)}. \tag{1.40}$$

Let $m \in \mathbb{N}^*$. For all $f : \{1, \ldots, m\} \to \mathbb{R}$ and all $q \in [1, \infty)$, setting $\|f\|_q := \left(\sum_{i=1}^m |f(i)|^q\right)^{\frac{1}{q}}$, and $\|f\|_\infty := \max_{1 \le i \le m} |f(i)|$, the discrete $(t; p_1, \ldots, p_n)$-Hölder inequality reads: For any $f_1, \ldots, f_n : \{1, \ldots, m\} \to \mathbb{R}$,

$$\left\| \prod_{i=1}^n f_i \right\|_t \le \prod_{i=1}^n \|f_i\|_{p_i}. \tag{1.41}$$

Proposition 41 (Properties of s_h)**.** *Let s_h be given by (1.21) with, for all $T \in \mathcal{T}_h$, s_T satisfying Assumption 2. Then it holds, for all $\underline{\boldsymbol{v}}_h \in \underline{\boldsymbol{U}}_h^k$,*

$$\|\mathbf{G}_{\mathrm{s},h}^k \underline{\boldsymbol{v}}_h\|_{L^r(\Omega)^{d\times d}}^r + \mathrm{s}_h(\underline{\boldsymbol{v}}_h, \underline{\boldsymbol{v}}_h) \simeq \|\underline{\boldsymbol{v}}_h\|_{\boldsymbol{\varepsilon},r,h}^r. \tag{1.42}$$

Furthermore, for all $\underline{\boldsymbol{u}}_h, \underline{\boldsymbol{v}}_h, \underline{\boldsymbol{w}}_h \in \underline{\boldsymbol{U}}_h^k$ it holds, setting $\underline{\boldsymbol{e}}_h \coloneqq \underline{\boldsymbol{u}}_h - \underline{\boldsymbol{w}}_h$,

$$\begin{aligned}
&\left|\mathrm{s}_h(\underline{\boldsymbol{u}}_h, \underline{\boldsymbol{v}}_h) - \mathrm{s}_h(\underline{\boldsymbol{w}}_h, \underline{\boldsymbol{v}}_h)\right| \\
&\qquad \lesssim \left(\mathrm{s}_h(\underline{\boldsymbol{u}}_h, \underline{\boldsymbol{u}}_h) + \mathrm{s}_h(\underline{\boldsymbol{w}}_h, \underline{\boldsymbol{w}}_h)\right)^{\frac{r-\tilde{r}}{r}} \mathrm{s}_h(\underline{\boldsymbol{e}}_h, \underline{\boldsymbol{e}}_h)^{\frac{\tilde{r}-1}{r}} \mathrm{s}_h(\underline{\boldsymbol{v}}_h, \underline{\boldsymbol{v}}_h)^{\frac{1}{r}}, \qquad (1.43)\\
&\left(\mathrm{s}_h(\underline{\boldsymbol{u}}_h, \underline{\boldsymbol{e}}_h) - \mathrm{s}_h(\underline{\boldsymbol{w}}_h, \underline{\boldsymbol{e}}_h)\right)\left(\mathrm{s}_h(\underline{\boldsymbol{u}}_h, \underline{\boldsymbol{u}}_h) + \mathrm{s}_h(\underline{\boldsymbol{w}}_h, \underline{\boldsymbol{w}}_h)\right)^{\frac{2-\tilde{r}}{r}} \\
&\qquad \gtrsim \mathrm{s}_h(\underline{\boldsymbol{e}}_h, \underline{\boldsymbol{e}}_h)^{\frac{r+2-\tilde{r}}{r}}. \qquad (1.44)
\end{aligned}$$

Finally, for any $\boldsymbol{w} \in \boldsymbol{U} \cap W^{k+2,r}(\mathcal{T}_h)^d$, it holds

$$\sup_{\underline{\boldsymbol{v}}_h \in \underline{\boldsymbol{U}}_{h,0}^k, \|\underline{\boldsymbol{v}}_h\|_{\boldsymbol{\varepsilon},r,h}=1} \mathrm{s}_h(\underline{\boldsymbol{I}}_h^k \boldsymbol{w}, \underline{\boldsymbol{v}}_h) \lesssim h^{(k+1)(\tilde{r}-1)} |\boldsymbol{w}|_{W^{1,r}(\Omega)^d}^{r-\tilde{r}} |\boldsymbol{w}|_{W^{k+2,r}(\mathcal{T}_h)^d}^{\tilde{r}-1}. \tag{1.45}$$

Above, the hidden constants are independent of h and of the arguments of s_h.

Proof. For the sake of conciseness, we only sketch the proof and leave the details to the reader. Summing (1.22) over $T \in \mathcal{T}_h$ immediately yields (1.42). The Hölder continuity property (1.43) follows applying to the quantity in the left-hand side triangle inequalities, using (1.24), and concluding with a discrete $(1; \frac{r}{r-\tilde{r}}, \frac{r}{\tilde{r}-1}, r)$-Hölder inequality. Moving to (1.44), starting from $|\mathrm{s}_h(\underline{\boldsymbol{e}}_h, \underline{\boldsymbol{e}}_h)|$, we use (1.25) and apply a discrete $(1; \frac{r+2-\tilde{r}}{2-\tilde{r}}, \frac{r+2-\tilde{r}}{r})$-Hölder inequality to conclude. Finally, to prove (1.45) we start from $\mathrm{s}_h(\underline{\boldsymbol{I}}_h^k \boldsymbol{w}, \underline{\boldsymbol{v}}_h)$, expand this quantity according to (1.21), use, for all $T \in \mathcal{T}_h$, the local consistency property (1.39) together with $h_T \le h$, invoke the discrete $(1; \frac{r}{r-\tilde{r}}, \frac{r}{\tilde{r}-1}, r)$-Hölder inequality, and pass to the supremum to conclude. □

1.7.2 Well-posedness

In this section, after proving Hölder continuity and Hölder monotonicity properties for the discrete viscous function a_h and the inf-sup stability of the pressure-velocity coupling bilinear form b_h, we prove Theorem 35.

1.7.2.1 Hölder continuity and Hölder monotonicity of the viscous function

Lemma 42 (Hölder continuity and Hölder monotonicity of a_h)**.** *For all $\underline{\boldsymbol{u}}_h, \underline{\boldsymbol{v}}_h, \underline{\boldsymbol{w}}_h \in \underline{\boldsymbol{U}}_h^k$, setting $\underline{\boldsymbol{e}}_h \coloneqq \underline{\boldsymbol{u}}_h - \underline{\boldsymbol{w}}_h$, it holds*

$$\begin{aligned}
&\left|\mathrm{a}_h(\underline{\boldsymbol{u}}_h, \underline{\boldsymbol{v}}_h) - \mathrm{a}_h(\underline{\boldsymbol{w}}_h, \underline{\boldsymbol{v}}_h)\right| \\
&\qquad \lesssim \sigma_{\mathrm{hc}} \left(\delta^r + \|\underline{\boldsymbol{u}}_h\|_{\boldsymbol{\varepsilon},r,h}^r + \|\underline{\boldsymbol{w}}_h\|_{\boldsymbol{\varepsilon},r,h}^r\right)^{\frac{r-\tilde{r}}{r}} \|\underline{\boldsymbol{e}}_h\|_{\boldsymbol{\varepsilon},r,h}^{\tilde{r}-1} \|\underline{\boldsymbol{v}}_h\|_{\boldsymbol{\varepsilon},r,h}, \qquad (1.46)
\end{aligned}$$

$$\big(\mathrm{a}_h(\underline{\boldsymbol{u}}_h,\underline{\boldsymbol{e}}_h)-\mathrm{a}_h(\underline{\boldsymbol{w}}_h,\underline{\boldsymbol{e}}_h)\big)\left(\delta^r+\|\underline{\boldsymbol{u}}_h\|_{\boldsymbol{\varepsilon},r,h}^r+\|\underline{\boldsymbol{w}}_h\|_{\boldsymbol{\varepsilon},r,h}^r\right)^{\frac{2-\tilde r}{r}} \gtrsim \sigma_{\mathrm{hm}}\|\underline{\boldsymbol{e}}_h\|_{\boldsymbol{\varepsilon},r,h}^{r+2-\tilde r}. \quad (1.47)$$

Proof. (i) *Hölder continuity.* Using a Cauchy–Schwarz inequality followed by the Hölder continuity (1.3c) of $\boldsymbol{\sigma}$, we can write

$$\begin{aligned}
&\left|\int_\Omega\big(\boldsymbol{\sigma}(\cdot,\mathbf{G}_{\mathrm{s},h}^k\underline{\boldsymbol{u}}_h)-\boldsymbol{\sigma}(\cdot,\mathbf{G}_{\mathrm{s},h}^k\underline{\boldsymbol{w}}_h)\big):\mathbf{G}_{\mathrm{s},h}^k\underline{\boldsymbol{v}}_h\right|\\
&\le\sigma_{\mathrm{hc}}\int_\Omega\left(\delta^r+|\mathbf{G}_{\mathrm{s},h}^k\underline{\boldsymbol{u}}_h|_{d\times d}^r+|\mathbf{G}_{\mathrm{s},h}^k\underline{\boldsymbol{w}}_h|_{d\times d}^r\right)^{\frac{r-\tilde r}{r}}|\mathbf{G}_{\mathrm{s},h}^k\underline{\boldsymbol{e}}_h|_{d\times d}^{\tilde r-1}|\mathbf{G}_{\mathrm{s},h}^k\underline{\boldsymbol{v}}_h|_{d\times d}\\
&\lesssim\sigma_{\mathrm{hc}}\left(|\Omega|_d\delta^r+\|\mathbf{G}_{\mathrm{s},h}^k\underline{\boldsymbol{u}}_h\|_{L^r(\Omega)^{d\times d}}^r+\|\mathbf{G}_{\mathrm{s},h}^k\underline{\boldsymbol{w}}_h\|_{L^r(\Omega)^{d\times d}}^r\right)^{\frac{r-\tilde r}{r}}\\
&\qquad\times\|\mathbf{G}_{\mathrm{s},h}^k\underline{\boldsymbol{e}}_h\|_{L^r(\Omega)^{d\times d}}^{\tilde r-1}\|\mathbf{G}_{\mathrm{s},h}^k\underline{\boldsymbol{v}}_h\|_{L^r(\Omega)^{d\times d}}\\
&\lesssim\sigma_{\mathrm{hc}}\left(\delta^r+\|\underline{\boldsymbol{u}}_h\|_{\boldsymbol{\varepsilon},r,h}^r+\|\underline{\boldsymbol{w}}_h\|_{\boldsymbol{\varepsilon},r,h}^r\right)^{\frac{r-\tilde r}{r}}\|\underline{\boldsymbol{e}}_h\|_{\boldsymbol{\varepsilon},r,h}^{\tilde r-1}\|\underline{\boldsymbol{v}}_h\|_{\boldsymbol{\varepsilon},r,h},
\end{aligned}\quad (1.48)$$

where we have used the $(1;\frac{r}{r-\tilde r},\frac{r}{\tilde r-1},r)$-Hölder inequality (1.40) in the second bound and the global seminorm equivalence (1.42) together with the fact that $|\Omega|_d\lesssim 1$ (since Ω is bounded) to conclude. For the stabilization term, combining the Hölder continuity (1.43) of s_h and the seminorm equivalence (1.42) readily gives

$$\big|\mathrm{s}_h(\underline{\boldsymbol{u}}_h,\underline{\boldsymbol{v}}_h)-\mathrm{s}_h(\underline{\boldsymbol{w}}_h,\underline{\boldsymbol{v}}_h)\big| \lesssim\left(\delta^r+\|\underline{\boldsymbol{u}}_h\|_{\boldsymbol{\varepsilon},r,h}^r+\|\underline{\boldsymbol{w}}_h\|_{\boldsymbol{\varepsilon},r,h}^r\right)^{\frac{r-\tilde r}{r}}\|\underline{\boldsymbol{e}}_h\|_{\boldsymbol{\varepsilon},r,h}^{\tilde r-1}\|\underline{\boldsymbol{v}}_h\|_{\boldsymbol{\varepsilon},r,h}, \quad (1.49)$$

where we have additionally noticed that $\delta^r\ge 0$ to add this term to the quantity inside parentheses. Using the definition (1.19) of a_h, a triangle inequality followed by (1.48) and (1.49), and recalling that $\gamma\le\sigma_{\mathrm{hc}}$ (cf. (1.20)), (1.46) follows.

(ii) *Hölder monotonicity.* Using the Hölder monotonicity (1.3d) of $\boldsymbol{\sigma}$ and the $(1;\frac{r+2-\tilde r}{2-\tilde r},\frac{r+2-\tilde r}{r})$-

Hölder inequality (1.40), we get

$$\begin{aligned}
\sigma_{\mathrm{hm}}^{\frac{r}{r+2-\tilde{r}}} \|\mathbf{G}_{\mathrm{s},h}^k \underline{\boldsymbol{e}}_h\|_{L^r(\Omega)^{d\times d}}^r &\leq \int_\Omega \left(\delta^r + |\mathbf{G}_{\mathrm{s},h}^k \underline{\boldsymbol{u}}_h|_{d\times d}^r + |\mathbf{G}_{\mathrm{s},h}^k \underline{\boldsymbol{w}}_h|_{d\times d}^r\right)^{\frac{2-\tilde{r}}{r+2-\tilde{r}}} \\
&\quad \times \left(\left(\boldsymbol{\sigma}(\cdot, \mathbf{G}_{\mathrm{s},h}^k \underline{\boldsymbol{u}}_h) - \boldsymbol{\sigma}(\cdot, \mathbf{G}_{\mathrm{s},h}^k \underline{\boldsymbol{w}}_h)\right) : \mathbf{G}_{\mathrm{s},h}^k \underline{\boldsymbol{e}}_h\right)^{\frac{r}{r+2-\tilde{r}}} \\
&\lesssim \left(\delta^r + \|\mathbf{G}_{\mathrm{s},h}^k \underline{\boldsymbol{u}}_h\|_{L^r(\Omega)^{d\times d}}^r + \|\mathbf{G}_{\mathrm{s},h}^k \underline{\boldsymbol{w}}_h\|_{L^r(\Omega)^{d\times d}}^r\right)^{\frac{2-\tilde{r}}{r+2-\tilde{r}}} \\
&\quad \times \left(\int_\Omega \left(\boldsymbol{\sigma}(\cdot, \mathbf{G}_{\mathrm{s},h}^k \underline{\boldsymbol{u}}_h) - \boldsymbol{\sigma}(\cdot, \mathbf{G}_{\mathrm{s},h}^k \underline{\boldsymbol{w}}_h)\right) : \mathbf{G}_{\mathrm{s},h}^k \underline{\boldsymbol{e}}_h\right)^{\frac{r}{r+2-\tilde{r}}} \\
&\lesssim \left(\delta^r + \|\underline{\boldsymbol{u}}_h\|_{\boldsymbol{\varepsilon},r,h}^r + \|\underline{\boldsymbol{w}}_h\|_{\boldsymbol{\varepsilon},r,h}^r\right)^{\frac{2-\tilde{r}}{r+2-\tilde{r}}} \\
&\quad \times \left(\int_\Omega \left(\boldsymbol{\sigma}(\cdot, \mathbf{G}_{\mathrm{s},h}^k \underline{\boldsymbol{u}}_h) - \boldsymbol{\sigma}(\cdot, \mathbf{G}_{\mathrm{s},h}^k \underline{\boldsymbol{w}}_h)\right) : \mathbf{G}_{\mathrm{s},h}^k \underline{\boldsymbol{e}}_h\right)^{\frac{r}{r+2-\tilde{r}}},
\end{aligned} \tag{1.50}$$

where the conclusion follows from the global seminorm equivalence (1.42). Additionally, using the Hölder monotonicity (1.44) of s_h together with the fact that $\sigma_{\mathrm{hm}} \leq \gamma$ (cf. (1.20)) and invoking again the seminorm equivalence (1.42), we readily obtain

$$\begin{aligned}
&\sigma_{\mathrm{hm}}^{\frac{r}{r+2-\tilde{r}}} \mathrm{s}_h(\underline{\boldsymbol{e}}_h, \underline{\boldsymbol{e}}_h) \\
&\qquad \lesssim \left(\delta^r + \|\underline{\boldsymbol{u}}_h\|_{\boldsymbol{\varepsilon},r,h}^r + \|\underline{\boldsymbol{w}}_h\|_{\boldsymbol{\varepsilon},r,h}^r\right)^{\frac{2-\tilde{r}}{r+2-\tilde{r}}} \left(\gamma \mathrm{s}_h(\underline{\boldsymbol{u}}_h, \underline{\boldsymbol{e}}_h) - \gamma \mathrm{s}_h(\underline{\boldsymbol{w}}_h, \underline{\boldsymbol{e}}_h)\right)^{\frac{r}{r+2-\tilde{r}}}.
\end{aligned} \tag{1.51}$$

Finally, combining again the norm equivalence (1.42) with (1.50) and (1.51), and using (1.37) yields

$$\sigma_{\mathrm{hm}}^{\frac{r}{r+2-\tilde{r}}} \|\underline{\boldsymbol{e}}_h\|_{\boldsymbol{\varepsilon},r,h}^r \lesssim \left(\delta^r + \|\underline{\boldsymbol{u}}_h\|_{\boldsymbol{\varepsilon},r,h}^r + \|\underline{\boldsymbol{w}}_h\|_{\boldsymbol{\varepsilon},r,h}^r\right)^{\frac{2-\tilde{r}}{r+2-\tilde{r}}} \left(\mathrm{a}_h(\underline{\boldsymbol{u}}_h, \underline{\boldsymbol{e}}_h) - \mathrm{a}_h(\underline{\boldsymbol{w}}_h, \underline{\boldsymbol{e}}_h)\right)^{\frac{r}{r+2-\tilde{r}}}.$$

Raising this inequality to the power $\frac{r-2-\tilde{r}}{r}$ yields (1.47). □

1.7.2.2 Stability of the pressure-velocity coupling

Lemma 43 (Inf-sup stability of b_h)**.** *It holds, for all $q_h \in P_h^k$,*

$$\|q_h\|_{L^{r'}(\Omega)} \lesssim \sup_{\underline{\boldsymbol{v}}_h \in \underline{\boldsymbol{U}}_{h,0}^k, \|\underline{\boldsymbol{v}}_h\|_{\varepsilon,r,h}=1} \mathrm{b}_h(\underline{\boldsymbol{v}}_h, q_h), \tag{1.52}$$

with hidden constant depending only on d, k, r, Ω, and the mesh regularity parameter.

Proof. The proof follows the classical Fortin argument (cf., e.g., [21, Section 8.4]), adapted here to the non-Hilbertian setting.

(i) *Fortin operator.* We need to prove that the following properties hold for any $\boldsymbol{v} \in W^{1,r}(\Omega)^d$:

$$\|\underline{\boldsymbol{I}}_h^k \boldsymbol{v}\|_{\boldsymbol{\varepsilon},r,h} \lesssim |\boldsymbol{v}|_{W^{1,r}(\Omega)^d}, \tag{1.53a}$$

$$\mathrm{b}_h(\underline{\boldsymbol{I}}_h^k \boldsymbol{v}, q_h) = b(\boldsymbol{v}, q_h) \qquad \forall q_h \in \mathbb{P}^k(\mathcal{T}_h). \tag{1.53b}$$

Property (1.53a) is obtained by raising both sides of (1.15) to the power r, summing over $T \in \mathcal{T}_h$, then taking the rth root of the resulting inequality. The proof of (1.53b) is given, e.g., in [50, Lemma 8.12].

(ii) *Inf-sup condition on* b_h. Let $q_h \in P_h^k$ and set $c_h \coloneqq \int_\Omega |q_h|^{r'-2} q_h$. Using the triangle and Hölder inequalities, we get

$$\begin{aligned} \||q_h|^{r'-2}q_h - c_h\|_{L^r(\Omega)} &\le \|q_h\|_{L^{r'}(\Omega)}^{r'-1} + |c_h||\Omega|_d^{\frac{1}{r}} \\ &\le (1 + |\Omega|_d)\, \|q_h\|_{L^{r'}(\Omega)}^{r'-1} \lesssim \|q_h\|_{L^{r'}(\Omega)}^{r'-1}, \end{aligned} \tag{1.54}$$

where we have used the fact that $|c_h| \le \|q_h\|_{L^{r'}(\Omega)}^{r'-1} |\Omega|_d^{\frac{1}{r'}}$ along with $\frac{1}{r} + \frac{1}{r'} = 1$ in the second bound and the fact that $|\Omega|_d \lesssim 1$ to conclude. Thus, using the surjectivity of the continuous divergence operator $\boldsymbol{\nabla}\cdot : \boldsymbol{U} \to L_0^r(\Omega) \coloneqq \{q \in L^r(\Omega) : \int_\Omega q = 0\}$, (c.f. [67] and also [22, Theorem 1]), we infer that there exists $\boldsymbol{v}_{q_h} \in \boldsymbol{U}$ such that

$$-\boldsymbol{\nabla}\cdot\boldsymbol{v}_{q_h} = |q_h|^{r'-2}q_h - c_h \quad \text{and} \quad |\boldsymbol{v}_{q_h}|_{W^{1,r}(\Omega)^d} \lesssim \||q_h|^{r'-2}q_h - c_h\|_{L^r(\Omega)}. \tag{1.55}$$

Denote by \$ the supremum in (1.52). Using the fact that q_h has zero mean value over Ω, the equality in (1.55) together with the definition (1.7) of b, and the second Fortin property (1.53b), we have

$$\begin{aligned} \|q_h\|_{L^{r'}(\Omega)}^{r'} = \int_\Omega \big(|q_h|^{r'-2}q_h - c_h\big)q_h &= b(\boldsymbol{v}_{q_h}, q_h) \\ &= \mathrm{b}_h(\underline{\boldsymbol{I}}_h^k \boldsymbol{v}_{q_h}, q_h) \le \$\|\underline{\boldsymbol{I}}_h^k \boldsymbol{v}_{q_h}\|_{\boldsymbol{\varepsilon},r,h} \lesssim \$\|q_h\|_{L^{r'}(\Omega)}^{r'-1}, \end{aligned}$$

where, to conclude, we have used (1.53a) followed by (1.55) and (1.54). Simplifying yields (1.52). □

1.7.2.3 Proof of Theorem 35

Proof of Theorem 35. (i) *Existence.* Denote by $P_h^{k,*}$ the dual space of P_h^k and let $B_h : \underline{\boldsymbol{U}}_{h,0}^k \to P_h^{k,*}$ be such that, for all $\underline{\boldsymbol{v}}_h \in \underline{\boldsymbol{U}}_{h,0}^k$,

$$\langle B_h \underline{\boldsymbol{v}}_h, q_h \rangle \coloneqq -\mathrm{b}_h(\underline{\boldsymbol{v}}_h, q_h) \qquad \forall q_h \in P_h^k.$$

Here and in what follows, $\langle\cdot,\cdot\rangle$ denotes the appropriate duality pairing as inferred from its arguments. Define the following subspace of $\underline{\boldsymbol{U}}_{h,0}^k$ spanned by vectors of discrete unknowns with zero discrete divergence:

$$\underline{\boldsymbol{W}}_h^k \coloneqq \mathrm{Ker}(B_h) = \left\{\underline{\boldsymbol{v}}_h \in \underline{\boldsymbol{U}}_{h,0}^k : \mathrm{b}_h(\underline{\boldsymbol{v}}_h, q_h) = 0 \quad \forall q_h \in P_h^k\right\}, \tag{1.56}$$

and consider the following problem: Find $\underline{\boldsymbol{u}}_h \in \underline{\boldsymbol{W}}_h^k$ such that

$$\mathrm{a}_h(\underline{\boldsymbol{u}}_h, \underline{\boldsymbol{v}}_h) = \int_\Omega \boldsymbol{f}\cdot\boldsymbol{v}_h \qquad \forall \underline{\boldsymbol{v}}_h \in \underline{\boldsymbol{W}}_h^k. \tag{1.57}$$

Existence of a solution to this problem for a fixed h can be proved adapting the arguments of [48, Theorem 4.5]. Specifically, equip $\underline{\boldsymbol{W}}_h^k$ with an inner product $(\cdot,\cdot)_{\boldsymbol{W},h}$ (which need not be further specified), denote by $\|\cdot\|_{\boldsymbol{W},h}$ the induced norm, and let $\boldsymbol{\Phi}_h : \underline{\boldsymbol{W}}_h^k \to \underline{\boldsymbol{W}}_h^k$ be such that, for all $\underline{\boldsymbol{w}}_h \in \underline{\boldsymbol{W}}_h^k$, $(\boldsymbol{\Phi}_h(\underline{\boldsymbol{w}}_h), \underline{\boldsymbol{v}}_h)_{\boldsymbol{W},h} = \mathrm{a}_h(\underline{\boldsymbol{w}}_h, \underline{\boldsymbol{v}}_h)$ for all $\underline{\boldsymbol{v}}_h \in \underline{\boldsymbol{W}}_h^k$. The Hölder monotonicity (1.47) of a_h yields, for any $\underline{\boldsymbol{v}}_h \in \underline{\boldsymbol{W}}_h^k$ such that $\|\underline{\boldsymbol{v}}_h\|_{\boldsymbol{\varepsilon},r,h} \geq \delta$,

$$\begin{aligned}(\boldsymbol{\Phi}_h(\underline{\boldsymbol{v}}_h), \underline{\boldsymbol{v}}_h)_{\boldsymbol{W},h} &\geq \sigma_{\mathrm{hm}}(\delta^r + \|\underline{\boldsymbol{v}}_h\|_{\boldsymbol{\varepsilon},r,h}^r)^{\frac{\tilde{r}-2}{r}}\|\underline{\boldsymbol{v}}_h\|_{\boldsymbol{\varepsilon},r,h}^{r+2-\tilde{r}}\\ &\gtrsim \sigma_{\mathrm{hm}}\|\underline{\boldsymbol{v}}_h\|_{\boldsymbol{\varepsilon},r,h}^r \geq C^r\sigma_{\mathrm{hm}}\|\underline{\boldsymbol{v}}_h\|_{\boldsymbol{W},h}^r,\end{aligned}$$

where C denotes the constant (possibly depending on h) in the equivalence of the norms $\|\cdot\|_{\boldsymbol{\varepsilon},r,h}$ and $\|\cdot\|_{\boldsymbol{W},h}$ (which holds since $\underline{\boldsymbol{W}}_h^k$ is finite-dimensional). This shows that $\boldsymbol{\Phi}_h$ is coercive hence, by [46, Theorem 3.3], surjective. Let now $\underline{\boldsymbol{w}}_h \in \underline{\boldsymbol{W}}_h^k$ be such that $(\underline{\boldsymbol{w}}_h, \underline{\boldsymbol{v}}_h)_{\boldsymbol{W},h} = \int_\Omega \boldsymbol{f}\cdot\boldsymbol{v}_h$ for all $\underline{\boldsymbol{v}}_h \in \underline{\boldsymbol{W}}_h^k$. By the surjectivity of $\boldsymbol{\Phi}_h$, there exists $\underline{\boldsymbol{u}}_h \in \underline{\boldsymbol{W}}_h^k$ such that $\boldsymbol{\Phi}_h(\underline{\boldsymbol{u}}_h) = \underline{\boldsymbol{w}}_h$ which, by definition of $\underline{\boldsymbol{w}}_h$ and $\boldsymbol{\Phi}_h$, is a solution to the discrete problem (1.57).

The proof of existence now continues as in the linear case; see, e.g., [21, Theorem 4.2.1]. Denote by $\underline{\boldsymbol{U}}_{h,0}^{k,*}$ the dual space of $\underline{\boldsymbol{U}}_{h,0}^k$ and consider the linear mapping $\ell_h \in \underline{\boldsymbol{U}}_{h,0}^{k,*}$ such that, for all $\underline{\boldsymbol{v}}_h \in \underline{\boldsymbol{U}}_{h,0}^k$,

$$\langle \ell_h, \underline{\boldsymbol{v}}_h\rangle \coloneqq \int_\Omega \boldsymbol{f}\cdot\boldsymbol{v}_h - \mathrm{a}_h(\underline{\boldsymbol{u}}_h, \underline{\boldsymbol{v}}_h).$$

Thanks to (1.57), ℓ_h vanishes identically for every $\underline{\boldsymbol{v}}_h \in \underline{\boldsymbol{W}}_h^k$, that is to say, ℓ_h lies in the polar space of $\underline{\boldsymbol{W}}_h^k$ which, denoting by $B_h^* : P_h^k \to \underline{\boldsymbol{U}}_{h,0}^{k,*}$ the adjoint operator of B_h, coincides in our case with $\mathrm{Im}(B_h^*)$ (see, e.g., [21, Theorem 4.14]). Hence, $\ell_h \in \mathrm{Im}(B_h^*)$, and there exists therefore a $p_h \in P_h^k$ such that $B_h^* p_h = \ell_h$. This means that, for all $\underline{\boldsymbol{v}}_h \in \underline{\boldsymbol{U}}_{h,0}^k$,

$$\mathrm{b}_h(\underline{\boldsymbol{v}}_h, p_h) = \langle B_h^* p_h, \underline{\boldsymbol{v}}_h\rangle = \langle \ell_h, \underline{\boldsymbol{v}}_h\rangle = \int_\Omega \boldsymbol{f}\cdot\boldsymbol{v}_h - \mathrm{a}_h(\underline{\boldsymbol{u}}_h, \underline{\boldsymbol{v}}_h),$$

i.e., the $(\underline{\boldsymbol{u}}_h, p_h)$ satisfies the discrete momentum equation (1.30a). On the other hand, since $\underline{\boldsymbol{u}}_h \in \underline{\boldsymbol{W}}_h^k$, we also have, by the definition (1.56) of $\underline{\boldsymbol{W}}_h^k$, $\mathrm{b}_h(\underline{\boldsymbol{u}}_h, q_h) = 0$ for all $q_h \in P_h^k$, which shows that the discrete mass equation (1.30b) is also verified. In conclusion, $(\underline{\boldsymbol{u}}_h, p_h) \in \underline{\boldsymbol{U}}_{h,0}^k \times P_h^k$ solves (1.30).

(ii) *Uniqueness.* We start by proving uniqueness for the velocity. Let $(\underline{\boldsymbol{u}}_h, p_h), (\underline{\boldsymbol{u}}_h', p_h') \in \underline{\boldsymbol{U}}_{h,0}^k \times P_h^k$ be two solutions of (1.30). Making $\underline{\boldsymbol{v}}_h = \underline{\boldsymbol{u}}_h - \underline{\boldsymbol{u}}_h'$ in (1.30a) written first for $(\underline{\boldsymbol{u}}_h, p_h)$ then for $(\underline{\boldsymbol{u}}_h', p_h')$, then taking the difference and observing that $\mathrm{b}_h(\underline{\boldsymbol{u}}_h - \underline{\boldsymbol{u}}_h', p_h) = \mathrm{b}_h(\underline{\boldsymbol{u}}_h - \underline{\boldsymbol{u}}_h', p_h') = 0$ by (1.30b), we infer that

$$\mathrm{a}_h(\underline{\boldsymbol{u}}_h, \underline{\boldsymbol{u}}_h - \underline{\boldsymbol{u}}_h') - \mathrm{a}_h(\underline{\boldsymbol{u}}_h', \underline{\boldsymbol{u}}_h - \underline{\boldsymbol{u}}_h') = 0.$$

Thus, the Hölder monotonicity (1.47) of a_h yields $\|\underline{\boldsymbol{u}}_h - \underline{\boldsymbol{u}}_h'\|_{\boldsymbol{\varepsilon},r,h} = 0$, which implies $\underline{\boldsymbol{u}}_h = \underline{\boldsymbol{u}}_h'$ since $\|\cdot\|_{\boldsymbol{\varepsilon},r,h}$ is a norm on $\underline{\boldsymbol{U}}_{h,0}^k$. Moreover, using the inf-sup stability (1.52) of b_h and (1.30a) written first for $\underline{\boldsymbol{u}}_h$ then for $\underline{\boldsymbol{u}}_h'$, we get

$$\begin{aligned}\|p_h - p_h'\|_{L^{r'}(\Omega)} &\lesssim \sup_{\underline{\boldsymbol{v}}_h \in \underline{\boldsymbol{U}}_{h,0}^k, \|\underline{\boldsymbol{v}}_h\|_{\boldsymbol{\varepsilon},r,h}=1} \mathrm{b}_h(\underline{\boldsymbol{v}}_h, p_h - p_h') \\ &= \sup_{\underline{\boldsymbol{v}}_h \in \underline{\boldsymbol{U}}_{h,0}^k, \|\underline{\boldsymbol{v}}_h\|_{\boldsymbol{\varepsilon},r,h}=1} \big(\mathrm{a}_h(\underline{\boldsymbol{u}}_h', \underline{\boldsymbol{v}}_h) - \mathrm{a}_h(\underline{\boldsymbol{u}}_h, \underline{\boldsymbol{v}}_h)\big) = 0,\end{aligned}$$

hence $p_h = p_h'$.

(iii) *A priori estimates.* Using the Hölder monotonicity (1.47) of a_h (with $\underline{\boldsymbol{w}}_h = \underline{\boldsymbol{0}}$), equation (1.30a) together with (1.30b), and the Hölder inequality together with the discrete Korn inequality (1.38), we obtain

$$\sigma_{\mathrm{hm}}\big(\delta^r + \|\underline{\boldsymbol{u}}_h\|_{\boldsymbol{\varepsilon},r,h}^r\big)^{\frac{\tilde{r}-2}{r}} \|\underline{\boldsymbol{u}}_h\|_{\boldsymbol{\varepsilon},r,h}^{r+2-\tilde{r}} \lesssim \mathrm{a}_h(\underline{\boldsymbol{u}}_h, \underline{\boldsymbol{u}}_h) = \int_\Omega \boldsymbol{f}\cdot\boldsymbol{u}_h \lesssim \|\boldsymbol{f}\|_{L^{r'}(\Omega)^d} \|\underline{\boldsymbol{u}}_h\|_{\boldsymbol{\varepsilon},r,h}. \tag{1.58}$$

We then conclude as in the continuous case to infer (1.31a) (see Remark 30). To prove the bound (1.31b) on the pressure, we use the inf-sup stability (1.52) of b_h to write

$$\begin{aligned}\|p_h\|_{L^{r'}(\Omega)} &\lesssim \sup_{\underline{\boldsymbol{v}}_h \in \underline{\boldsymbol{U}}_{h,0}^k, \|\underline{\boldsymbol{v}}_h\|_{\boldsymbol{\varepsilon},r,h}=1} \mathrm{b}_h(\underline{\boldsymbol{v}}_h, p_h) \\ &= \sup_{\underline{\boldsymbol{v}}_h \in \underline{\boldsymbol{U}}_{h,0}^k, \|\underline{\boldsymbol{v}}_h\|_{\boldsymbol{\varepsilon},r,h}=1} \left(\int_\Omega \boldsymbol{f}\cdot\boldsymbol{v}_h - \mathrm{a}_h(\underline{\boldsymbol{u}}_h, \underline{\boldsymbol{v}}_h)\right) \\ &\lesssim \|\boldsymbol{f}\|_{L^{r'}(\Omega)^d} + \sigma_{\mathrm{hc}}\big(\delta^r + \|\underline{\boldsymbol{u}}_h\|_{\boldsymbol{\varepsilon},r,h}^r\big)^{\frac{r-\tilde{r}}{r}} \|\underline{\boldsymbol{u}}_h\|_{\boldsymbol{\varepsilon},r,h}^{\tilde{r}-1} \\ &\lesssim \sigma_{\mathrm{hc}}\left(\sigma_{\mathrm{hm}}^{-1}\|\boldsymbol{f}\|_{L^{r'}(\Omega)^d} + \delta^{|r-2|(\tilde{r}-1)}\left(\sigma_{\mathrm{hm}}^{-1}\|\boldsymbol{f}\|_{L^{r'}(\Omega)^d}\right)^{\frac{\tilde{r}-1}{r+1-\tilde{r}}}\right),\end{aligned}$$

where we have used the discrete momentum equation (1.30a) to pass to the second line, the Hölder and discrete Korn (1.38) inequalities together with the Hölder continuity (1.46) of a_h to pass to the third line, and the a priori bound (1.31a) on the velocity together with $\frac{\sigma_{\mathrm{hc}}}{\sigma_{\mathrm{hm}}} \geq 1$ (see (1.4)) to conclude. □

1.7.3 Error estimate

In this section, after studying the consistency of the viscous and pressure-velocity coupling terms, we prove Theorem 36.

1.7.3.1 Consistency of the viscous function

Lemma 44 (Consistency of a_h)**.** *Let $\boldsymbol{w} \in \boldsymbol{U} \cap W^{k+2,r}(\mathcal{T}_h)^d$ be such that $\boldsymbol{\sigma}(\cdot, \boldsymbol{\nabla}_{\mathrm{s}}\boldsymbol{w}) \in W^{1,r'}(\Omega, \mathbb{R}^{d\times d}_{\mathrm{s}}) \cap W^{(k+1)(\tilde{r}-1),r'}(\mathcal{T}_h, \mathbb{R}^{d\times d}_{\mathrm{s}})$. Define the viscous consistency error linear form $\mathcal{E}_{\mathrm{a},h}(\boldsymbol{w};\cdot) : \underline{\boldsymbol{U}}^k_h \to \mathbb{R}$ such that, for all $\underline{\boldsymbol{v}}_h \in \underline{\boldsymbol{U}}^k_h$,*

$$\mathcal{E}_{\mathrm{a},h}(\boldsymbol{w};\underline{\boldsymbol{v}}_h) \coloneqq \int_\Omega (\boldsymbol{\nabla}\cdot\boldsymbol{\sigma}(\cdot,\boldsymbol{\nabla}_{\mathrm{s}}\boldsymbol{w}))\cdot\boldsymbol{v}_h + \mathrm{a}_h(\underline{\boldsymbol{I}}^k_h\boldsymbol{w},\underline{\boldsymbol{v}}_h). \tag{1.59}$$

Then, under Assumptions 1 and 2, we have

$$\begin{aligned}\sup_{\underline{\boldsymbol{v}}_h\in\underline{\boldsymbol{U}}^k_{h,0},\|\underline{\boldsymbol{v}}_h\|_{\varepsilon,r,h}=1} \mathcal{E}_{\mathrm{a},h}(\boldsymbol{w};\underline{\boldsymbol{v}}_h) \lesssim h^{(k+1)(\tilde{r}-1)}\Bigg[\sigma_{\mathrm{hc}}\left(\delta^r + |\boldsymbol{w}|^r_{W^{1,r}(\Omega)^d}\right)^{\frac{r-\tilde{r}}{r}}\\ \times |\boldsymbol{w}|^{\tilde{r}-1}_{W^{k+2,r}(\mathcal{T}_h)^d} + |\boldsymbol{\sigma}(\cdot,\boldsymbol{\nabla}_{\mathrm{s}}\boldsymbol{w})|_{W^{(k+1)(\tilde{r}-1),r'}(\mathcal{T}_h)^{d\times d}}\Bigg].\end{aligned} \tag{1.60}$$

Proof. Let $\hat{\underline{\boldsymbol{w}}}_h \coloneqq \underline{\boldsymbol{I}}^k_h\boldsymbol{w}$ and $\underline{\boldsymbol{v}}_h \in \underline{\boldsymbol{U}}^k_{h,0}$. Expanding a_h according to its definition (1.19) in the expression (1.59) of $\mathcal{E}_{\mathrm{a},h}$, inserting $\pm\int_\Omega \boldsymbol{\sigma}(\cdot,\boldsymbol{\nabla}_{\mathrm{s}}\boldsymbol{w}) : \mathbf{G}^k_{\mathrm{s},h}\underline{\boldsymbol{v}}_h \pm \int_\Omega \boldsymbol{\pi}^k_h\boldsymbol{\sigma}(\cdot,\boldsymbol{\nabla}_{\mathrm{s}}\boldsymbol{w}) : \mathbf{G}^k_{\mathrm{s},h}\underline{\boldsymbol{v}}_h$, and rearranging, we obtain

$$\begin{aligned}\mathcal{E}_{\mathrm{a},h}(\boldsymbol{w};\underline{\boldsymbol{v}}_h) = \underbrace{\int_\Omega (\boldsymbol{\nabla}\cdot\boldsymbol{\sigma}(\cdot,\boldsymbol{\nabla}_{\mathrm{s}}\boldsymbol{w}))\cdot\boldsymbol{v}_h + \int_\Omega \boldsymbol{\pi}^k_h\boldsymbol{\sigma}(\cdot,\boldsymbol{\nabla}_{\mathrm{s}}\boldsymbol{w}) : \mathbf{G}^k_{\mathrm{s},h}\underline{\boldsymbol{v}}_h}_{\mathcal{T}_1}\\ + \cancel{\int_\Omega \left(\boldsymbol{\sigma}(\cdot,\boldsymbol{\nabla}_{\mathrm{s}}\boldsymbol{w}) - \boldsymbol{\pi}^k_h\boldsymbol{\sigma}(\cdot,\boldsymbol{\nabla}_{\mathrm{s}}\boldsymbol{w})\right) : \mathbf{G}^k_{\mathrm{s},h}\underline{\boldsymbol{v}}_h}\\ + \underbrace{\int_\Omega \left(\boldsymbol{\sigma}(\cdot,\mathbf{G}^k_{\mathrm{s},h}\hat{\underline{\boldsymbol{w}}}_h) - \boldsymbol{\sigma}(\cdot,\boldsymbol{\nabla}_{\mathrm{s}}\boldsymbol{w})\right) : \mathbf{G}^k_{\mathrm{s},h}\underline{\boldsymbol{v}}_h}_{\mathcal{T}_2} + \underbrace{\gamma\mathrm{s}_h(\hat{\underline{\boldsymbol{w}}}_h,\underline{\boldsymbol{v}}_h)}_{\mathcal{T}_3},\end{aligned} \tag{1.61}$$

where have used the definition (1.11) of $\boldsymbol{\pi}^k_h$ together with the fact that $\mathbf{G}^k_{\mathrm{s},h}\underline{\boldsymbol{v}}_h \in \mathbb{P}^k(\mathcal{T}_h, \mathbb{R}^{d\times d}_{\mathrm{s}})$ in the cancellation. We proceed to estimate the terms in the right-hand side. For the first term, we start by noticing that

$$\sum_{T\in\mathcal{T}_h}\sum_{F\in\mathcal{F}_T}\int_F \boldsymbol{v}_F\cdot(\boldsymbol{\sigma}(\cdot,\boldsymbol{\nabla}_{\mathrm{s}}\boldsymbol{w})\boldsymbol{n}_{TF}) = 0 \tag{1.62}$$

as a consequence of the continuity of the normal trace of $\boldsymbol{\sigma}(\cdot,\boldsymbol{\nabla}_{\mathrm{s}}\boldsymbol{w})$ together with the single-valuedness of $\boldsymbol{v}_F$ across each interface $F\in\mathcal{F}_h^{\mathrm{i}}$ and of the fact that $\boldsymbol{v}_F=\boldsymbol{0}$ for every boundary face $F\in\mathcal{F}_h^{\mathrm{b}}$. Using an element by element integration by parts on the first term of $\mathcal{T}_1$ along with the definitions (1.18) of $\mathbf{G}_{\mathrm{s},h}^k$ and (1.16) of $\mathbf{G}_{\mathrm{s},T}^k$, we can write

$$\begin{aligned}\mathcal{T}_1&=\cancel{\int_\Omega\Big(\boldsymbol{\pi}_h^k\boldsymbol{\sigma}(\cdot,\boldsymbol{\nabla}_{\mathrm{s}}\boldsymbol{w})-\boldsymbol{\sigma}(\cdot,\boldsymbol{\nabla}_{\mathrm{s}}\boldsymbol{w})\Big):\boldsymbol{\nabla}_{\mathrm{s},h}\boldsymbol{v}_h}\\&\quad+\sum_{T\in\mathcal{T}_h}\sum_{F\in\mathcal{F}_T}\left(\int_F(\boldsymbol{v}_F-\boldsymbol{v}_T)\cdot(\boldsymbol{\pi}_T^k\boldsymbol{\sigma}(\cdot,\boldsymbol{\nabla}_{\mathrm{s}}\boldsymbol{w}))\boldsymbol{n}_{TF}+\int_F\boldsymbol{v}_T\cdot(\boldsymbol{\sigma}(\cdot,\boldsymbol{\nabla}_{\mathrm{s}}\boldsymbol{w})\boldsymbol{n}_{TF})\right)\\&=\sum_{T\in\mathcal{T}_h}\sum_{F\in\mathcal{F}_T}\int_F(\boldsymbol{v}_F-\boldsymbol{v}_T)\cdot\Big(\boldsymbol{\pi}_T^k\boldsymbol{\sigma}(\cdot,\boldsymbol{\nabla}_{\mathrm{s}}\boldsymbol{w})-\boldsymbol{\sigma}(\cdot,\boldsymbol{\nabla}_{\mathrm{s}}\boldsymbol{w})\Big)\boldsymbol{n}_{TF},\end{aligned}$$

where we have used the definition (1.11) of $\boldsymbol{\pi}_h^k$ together with the fact that $\boldsymbol{\nabla}_{\mathrm{s},h}\boldsymbol{v}_h\in\mathbb{P}^{k-1}(\mathcal{T}_h,\mathbb{R}_{\mathrm{s}}^{d\times d})\subset\mathbb{P}^k(\mathcal{T}_h,\mathbb{R}_{\mathrm{s}}^{d\times d})$ to cancel the term in the first line, and we have inserted (1.62) and rearranged to conclude. Therefore, applying the Hölder inequality together with the bound $h_F\le h_T$, we infer

$$\begin{aligned}|\mathcal{T}_1|&\le\left(\sum_{T\in\mathcal{T}_h}h_T\|\boldsymbol{\sigma}(\cdot,\boldsymbol{\nabla}_{\mathrm{s}}\boldsymbol{w})-\boldsymbol{\pi}_T^k\boldsymbol{\sigma}(\cdot,\boldsymbol{\nabla}_{\mathrm{s}}\boldsymbol{w})\|_{L^{r'}(\partial T)^{d\times d}}^{r'}\right)^{\frac{1}{r'}}\\&\quad\times\left(\sum_{T\in\mathcal{T}_h}\sum_{F\in\mathcal{F}_T}h_F^{1-r}\|\boldsymbol{v}_F-\boldsymbol{v}_T\|_{L^r(F)^d}^r\right)^{\frac{1}{r}}\\&\lesssim h^{(k+1)(\tilde r-1)}|\boldsymbol{\sigma}(\cdot,\boldsymbol{\nabla}_{\mathrm{s}}\boldsymbol{w})|_{W^{(k+1)(\tilde r-1),r'}(\mathcal{T}_h)^{d\times d}}\|\underline{\boldsymbol{v}}_h\|_{\boldsymbol{\varepsilon},r,h},\end{aligned}\tag{1.63}$$

where the conclusion follows using the $((k+1)(\tilde r-1),r')$-trace approximation properties (1.12b) of $\boldsymbol{\pi}_T^k$ along with $h_T\le h$ for the first factor and the definition (1.14) of the $\|\cdot\|_{\boldsymbol{\varepsilon},r,h}$-norm for the second.

For the second term, using the Hölder inequality and again (1.42), we get

$$|\mathcal{T}_2|\le\|\boldsymbol{\sigma}(\cdot,\mathbf{G}_{\mathrm{s},h}^k\underline{\hat{\boldsymbol{w}}}_h)-\boldsymbol{\sigma}(\cdot,\boldsymbol{\nabla}_{\mathrm{s}}\boldsymbol{w})\|_{L^{r'}(\Omega)^{d\times d}}\|\underline{\boldsymbol{v}}_h\|_{\boldsymbol{\varepsilon},r,h}.\tag{1.64}$$

We estimate the first factor as follows:

$$\begin{aligned}&\|\boldsymbol{\sigma}(\cdot,\mathbf{G}_{\mathrm{s},h}^k\underline{\hat{\boldsymbol{w}}}_h)-\boldsymbol{\sigma}(\cdot,\boldsymbol{\nabla}_{\mathrm{s}}\boldsymbol{w})\|_{L^{r'}(\Omega)^{d\times d}}\\&\quad\le\sigma_{\mathrm{hc}}\left\|\left(\delta^r+|\mathbf{G}_{\mathrm{s},h}^k\underline{\hat{\boldsymbol{w}}}_h|_{d\times d}^r+|\boldsymbol{\nabla}_{\mathrm{s}}\boldsymbol{w}|_{d\times d}^r\right)^{\frac{r-\tilde r}{r}}|\mathbf{G}_{\mathrm{s},h}^k\underline{\hat{\boldsymbol{w}}}_h-\boldsymbol{\nabla}_{\mathrm{s}}\boldsymbol{w}|_{d\times d}^{\tilde r-1}\right\|_{L^{r'}(\Omega)}\\&\quad\lesssim\sigma_{\mathrm{hc}}\left(\delta^r+\|\mathbf{G}_{\mathrm{s},h}^k\underline{\hat{\boldsymbol{w}}}_h\|_{L^r(\Omega)^{d\times d}}^r+\|\boldsymbol{\nabla}_{\mathrm{s}}\boldsymbol{w}\|_{L^r(\Omega)^{d\times d}}^r\right)^{\frac{r-\tilde r}{r}}\|\mathbf{G}_{\mathrm{s},h}^k\underline{\hat{\boldsymbol{w}}}_h-\boldsymbol{\nabla}_{\mathrm{s}}\boldsymbol{w}\|_{L^r(\Omega)^{d\times d}}^{\tilde r-1}\\&\quad\lesssim\sigma_{\mathrm{hc}}\left(\delta^r+\|\underline{\hat{\boldsymbol{w}}}_h\|_{\boldsymbol{\varepsilon},r,h}^r+|\boldsymbol{w}|_{W^{1,r}(\Omega)^d}^r\right)^{\frac{r-\tilde r}{r}}\|\boldsymbol{\pi}_h^k(\boldsymbol{\nabla}_{\mathrm{s}}\boldsymbol{w})-\boldsymbol{\nabla}_{\mathrm{s}}\boldsymbol{w}\|_{L^r(\Omega)^{d\times d}}^{\tilde r-1}\\&\quad\lesssim h^{(k+1)(\tilde r-1)}\sigma_{\mathrm{hc}}\left(\delta^r+|\boldsymbol{w}|_{W^{1,r}(\Omega)^d}^r\right)^{\frac{r-\tilde r}{r}}|\boldsymbol{w}|_{W^{k+2,r}(\mathcal{T}_h)^d}^{\tilde r-1},\end{aligned}$$

where we have used the Hölder continuity (1.3c) of $\boldsymbol{\sigma}$ in the first bound, the $(r'; \frac{r}{r-\tilde{r}}, \frac{r}{\tilde{r}-1})$-Hölder inequality (1.40) in the second, the boundedness of Ω along with (1.42) and the commutation property (1.17) of $\mathbf{G}_{\mathrm{s},h}^k$ in the third, and we have concluded invoking the $(k+1, r, 0)$-approximation property (1.12a) of $\boldsymbol{\pi}_T^k$. Plugging this estimate into (1.64), we get

$$|\mathcal{T}_2| \lesssim h^{(k+1)(\tilde{r}-1)} \sigma_{\mathrm{hc}} \left(\delta^r + |\boldsymbol{w}|^r_{W^{1,r}(\Omega)^d} \right)^{\frac{r-\tilde{r}}{r}} |\boldsymbol{w}|^{\tilde{r}-1}_{W^{k+2,r}(\mathcal{T}_h)^d} \|\underline{\boldsymbol{v}}_h\|_{\boldsymbol{\varepsilon},r,h}. \tag{1.65}$$

Finally, using the fact that $\gamma \le \sigma_{\mathrm{hc}}$ together with the consistency (1.45) of s_h and the norm equivalence (1.42), we obtain for the third term

$$|\mathcal{T}_3| \lesssim h^{(k+1)(\tilde{r}-1)} \sigma_{\mathrm{hc}} |\boldsymbol{w}|^{r-\tilde{r}}_{W^{1,r}(\Omega)^d} |\boldsymbol{w}|^{\tilde{r}-1}_{W^{k+2,r}(\mathcal{T}_h)^d} \|\underline{\boldsymbol{v}}_h\|_{\boldsymbol{\varepsilon},r,h}. \tag{1.66}$$

Plug the bounds (1.63), (1.65), and (1.66) into (1.61) and pass to the supremum to conclude. □

1.7.3.2 Consistency of the pressure-velocity coupling bilinear form

Lemma 45 (Consistency of b_h)**.** *Let $q \in W^{1,r'}(\Omega) \cap W^{(k+1)(\tilde{r}-1),r'}(\mathcal{T}_h)$. Let $\mathcal{E}_{\mathrm{b},h}(q;\cdot) : \underline{\boldsymbol{U}}_h^k \to \mathbb{R}$ be the pressure consistency error linear form such that, for all $\underline{\boldsymbol{v}}_h \in \underline{\boldsymbol{U}}_h^k$,*

$$\mathcal{E}_{\mathrm{b},h}(q;\underline{\boldsymbol{v}}_h) \coloneqq \int_\Omega \boldsymbol{\nabla} q \cdot \boldsymbol{v}_h - \mathrm{b}_h(\underline{\boldsymbol{v}}_h, \pi_h^k q). \tag{1.67}$$

Then, we have that

$$\sup_{\underline{\boldsymbol{v}}_h \in \underline{\boldsymbol{U}}_{h,0}^k, \|\underline{\boldsymbol{v}}_h\|_{\boldsymbol{\varepsilon},r,h}=1} \mathcal{E}_{\mathrm{b},h}(q;\underline{\boldsymbol{v}}_h) \lesssim h^{(k+1)(\tilde{r}-1)} |q|_{W^{(k+1)(\tilde{r}-1),r'}(\mathcal{T}_h)}. \tag{1.68}$$

Proof. Let $\underline{\boldsymbol{v}}_h \in \underline{\boldsymbol{U}}_{h,0}^k$. Integrating by parts element by element, we can reformulate the first term in the right-hand side of (1.67) as follows:

$$\int_\Omega \boldsymbol{\nabla} q \cdot \boldsymbol{v}_h = -\sum_{T\in\mathcal{T}_h} \left(\int_T q(\boldsymbol{\nabla}\cdot\boldsymbol{v}_T) + \sum_{F\in\mathcal{F}_T} \int_F q(\boldsymbol{v}_F - \boldsymbol{v}_T)\cdot\boldsymbol{n}_{TF} \right), \tag{1.69}$$

where the introduction of $\boldsymbol{v}_F$ in the boundary term is justified by the fact that the jumps of q vanish across interfaces by the assumed regularity and that $\boldsymbol{v}_F = \mathbf{0}$ on every boundary face $F \in \mathcal{F}_h^{\mathrm{b}}$. On the other hand, expanding, for each $T \in \mathcal{T}_h$, D_T^k according to its definition (1.28), we get

$$-\mathrm{b}_h(\underline{\boldsymbol{v}}_h, \pi_h^k q) = \sum_{T\in\mathcal{T}_h} \left(\int_T \pi_T^k q\ (\boldsymbol{\nabla}\cdot\boldsymbol{v}_T) + \sum_{F\in\mathcal{F}_T} \int_F \pi_T^k q\ (\boldsymbol{v}_F - \boldsymbol{v}_T)\cdot\boldsymbol{n}_{TF} \right). \tag{1.70}$$

Summing (1.69) and (1.70) and observing that the first terms in parentheses cancel out by the definition (1.11) of π_T^k since $\boldsymbol{\nabla}\cdot\boldsymbol{v}_T \in \mathbb{P}^{k-1}(T) \subset \mathbb{P}^k(T)$ for all $T \in \mathcal{T}_h$, we can write

$$\begin{aligned}\mathcal{E}_{\mathrm{b},h}(q;\underline{\boldsymbol{v}}_h) &= \sum_{T\in\mathcal{T}_h}\left(\cancel{\int_T(\pi_T^k q - q)(\boldsymbol{\nabla}\cdot\boldsymbol{v}_T)} + \sum_{F\in\mathcal{F}_T}\int_F(\pi_T^k q - q)(\boldsymbol{v}_F - \boldsymbol{v}_T)\cdot\boldsymbol{n}_{TF}\right)\\ &\le \left(\sum_{T\in\mathcal{T}_h} h_T\|\pi_T^k q - q\|_{L^{r'}(\partial T)}^{r'}\right)^{\frac{1}{r'}}\left(\sum_{T\in\mathcal{T}_h}\sum_{F\in\mathcal{F}_T} h_F^{1-r}\|\boldsymbol{v}_F - \boldsymbol{v}_T\|_{L^r(F)^d}^r\right)^{\frac{1}{r}}\\ &\lesssim h^{(k+1)(\tilde r-1)}|q|_{W^{(k+1)(\tilde r-1),r'}(\mathcal{T}_h)}\|\underline{\boldsymbol{v}}_h\|_{\boldsymbol{\varepsilon},r,h},\end{aligned}$$

where we have used the Hölder inequality along with $h_F \ge h_T$ whenever $F \in \mathcal{F}_T$ in the second line and the $((k+1)(\tilde r-1), r')$-trace approximation property (1.12b) of π_T^k together with the bound $h_F \le h$ and the definition (1.14) of the $\|\cdot\|_{\boldsymbol{\varepsilon},r,h}$-norm to conclude. Passing to the supremum yields (1.68). □

1.7.3.3 Proof of Theorem 36

Proof of Theorem 36. Let $(\underline{\boldsymbol{e}}_h, \epsilon_h) \coloneqq (\underline{\boldsymbol{u}}_h - \underline{\hat{\boldsymbol{u}}}_h, p_h - \hat p_h) \in \underline{\boldsymbol{U}}_{h,0}^k \times P_h^k$ where $\underline{\hat{\boldsymbol{u}}}_h \coloneqq \underline{\boldsymbol{I}}_h^k\boldsymbol{u} \in \underline{\boldsymbol{U}}_{h,0}^k$ and $\hat p_h \coloneqq \pi_h^k p \in P_h^k$.

Step 1. *Consistency error.* Let $\mathcal{E}_h : \underline{\boldsymbol{U}}_{h,0}^k \to \mathbb{R}$ be the consistency error linear form such that, for all $\underline{\boldsymbol{v}}_h \in \underline{\boldsymbol{U}}_{h,0}^k$,

$$\mathcal{E}_h(\underline{\boldsymbol{v}}_h) \coloneqq \int_\Omega \boldsymbol{f}\cdot\boldsymbol{v}_h - \mathrm{a}_h(\underline{\hat{\boldsymbol{u}}}_h, \underline{\boldsymbol{v}}_h) - \mathrm{b}_h(\underline{\boldsymbol{v}}_h, \hat p_h). \tag{1.71}$$

Using in the above expression the fact that $\boldsymbol{f} = -\boldsymbol{\nabla}\cdot\boldsymbol{\sigma}(\cdot, \boldsymbol{\nabla}_{\mathrm{s}}\boldsymbol{u}) + \boldsymbol{\nabla}p$ almost everywhere in Ω to write $\mathcal{E}_h(\underline{\boldsymbol{v}}_h) = \mathcal{E}_{\mathrm{a},h}(\boldsymbol{u};\underline{\boldsymbol{v}}_h) + \mathcal{E}_{\mathrm{b},h}(p;\underline{\boldsymbol{v}}_h)$, and invoking the consistency properties (1.60) of a_h and (1.68) of b_h, we obtain

$$\$ \coloneqq \sup_{\underline{\boldsymbol{v}}_h\in\underline{\boldsymbol{U}}_{h,0}^k, \|\underline{\boldsymbol{v}}_h\|_{\boldsymbol{\varepsilon},r,h}=1} \mathcal{E}_h(\underline{\boldsymbol{v}}_h) \lesssim h^{(k+1)(\tilde r-1)}\mathcal{N}_{\boldsymbol{\sigma},\boldsymbol{u},p}. \tag{1.72}$$

Step 2. *Error estimate for the velocity.* Using the Hölder monotonicity (1.47) of a_h, we get

$$\begin{aligned}&\|\underline{\boldsymbol{e}}_h\|_{\boldsymbol{\varepsilon},r,h}^{r+2-\tilde r}\\ &\quad\lesssim \sigma_{\mathrm{hm}}^{-1}\left(\delta^r + \|\underline{\boldsymbol{u}}_h\|_{\boldsymbol{\varepsilon},r,h}^r + \|\underline{\hat{\boldsymbol{u}}}_h\|_{\boldsymbol{\varepsilon},r,h}^r\right)^{\frac{2-\tilde r}{r}}\left(\mathrm{a}_h(\underline{\boldsymbol{u}}_h, \underline{\boldsymbol{e}}_h) - \mathrm{a}_h(\underline{\hat{\boldsymbol{u}}}_h, \underline{\boldsymbol{e}}_h)\right)\\ &\quad\lesssim \sigma_{\mathrm{hm}}^{-1}\mathcal{N}_f^{2-\tilde r}\left(\mathrm{a}_h(\underline{\boldsymbol{u}}_h, \underline{\boldsymbol{e}}_h) - \mathrm{a}_h(\underline{\hat{\boldsymbol{u}}}_h, \underline{\boldsymbol{e}}_h)\right),\end{aligned} \tag{1.73}$$

where we have used the a priori bound (1.31a) on the discrete solution along with the boundedness (1.53a) of the global interpolator and the a priori bound (1.8) on the continuous solution to conclude. Using then the discrete mass equation (1.30b) along with (1.53b) (written for $\boldsymbol{v} = \boldsymbol{u}$) and the continuous mass equation (1.6b) to write $\mathrm{b}_h(\underline{\boldsymbol{I}}_h^k \boldsymbol{u}, q_h) = b(\boldsymbol{u}, q_h) = 0$, we get $\mathrm{b}_h(\underline{\boldsymbol{e}}_h, q_h) = 0$ for all $q_h \in P_h^k$. Hence, combining this result with (1.71) and the discrete momentum equation (1.30a) (with $\underline{\boldsymbol{v}}_h = \underline{\boldsymbol{e}}_h$), we obtain

$$\mathrm{a}_h(\underline{\boldsymbol{u}}_h, \underline{\boldsymbol{e}}_h) - \mathrm{a}_h(\underline{\hat{\boldsymbol{u}}}_h, \underline{\boldsymbol{e}}_h) = \int_\Omega \boldsymbol{f} \cdot \boldsymbol{e}_h - \mathrm{a}_h(\underline{\hat{\boldsymbol{u}}}_h, \underline{\boldsymbol{e}}_h) - \cancel{\mathrm{b}_h(\underline{\boldsymbol{e}}_h, p_h)} = \mathcal{E}_h(\underline{\boldsymbol{e}}_h). \tag{1.74}$$

Plugging (1.74) into (1.73), we get

$$\|\underline{\boldsymbol{e}}_h\|_{\boldsymbol{\varepsilon},r,h}^{r+2-\tilde{r}} \le \sigma_{\mathrm{hm}}^{-1} \mathcal{N}_f^{2-\tilde{r}} \$ \|\underline{\boldsymbol{e}}_h\|_{\boldsymbol{\varepsilon},r,h}.$$

Simplifying, using (1.72), and taking the $(r+1-\tilde{r})$th root of the resulting inequality yields (1.32a).

Step 3. *Error estimate for the pressure.* Using the Hölder continuity (1.46) of a_h, we have, for all $\underline{\boldsymbol{v}}_h \in \underline{\boldsymbol{U}}_{h,0}^k$,

$$\begin{aligned}
&\left|\mathrm{a}_h(\underline{\hat{\boldsymbol{u}}}_h, \underline{\boldsymbol{v}}_h) - \mathrm{a}_h(\underline{\boldsymbol{u}}_h, \underline{\boldsymbol{v}}_h)\right| \\
&\qquad \lesssim \sigma_{\mathrm{hc}} \left(\delta^r + \|\underline{\hat{\boldsymbol{u}}}_h\|_{\boldsymbol{\varepsilon},r,h}^r + \|\underline{\boldsymbol{u}}_h\|_{\boldsymbol{\varepsilon},r,h}^r\right)^{\frac{r-\tilde{r}}{r}} \|\underline{\boldsymbol{e}}_h\|_{\boldsymbol{\varepsilon},r,h}^{\tilde{r}-1} \|\underline{\boldsymbol{v}}_h\|_{\boldsymbol{\varepsilon},r,h} \\
&\qquad \lesssim \sigma_{\mathrm{hc}} \mathcal{N}_f^{r-\tilde{r}} \|\underline{\boldsymbol{e}}_h\|_{\boldsymbol{\varepsilon},r,h}^{\tilde{r}-1} \|\underline{\boldsymbol{v}}_h\|_{\boldsymbol{\varepsilon},r,h},
\end{aligned} \tag{1.75}$$

where the first factor is estimated as in (1.73). Thus, using the inf-sup condition (1.52), we can write

$$\begin{aligned}
\|\epsilon_h\|_{L^{r'}(\Omega)} &\lesssim \sup_{\underline{\boldsymbol{v}}_h \in \underline{\boldsymbol{U}}_{h,0}^k, \|\underline{\boldsymbol{v}}_h\|_{\boldsymbol{\varepsilon},r,h}=1} \mathrm{b}_h(\underline{\boldsymbol{v}}_h, \epsilon_h) \\
&= \sup_{\underline{\boldsymbol{v}}_h \in \underline{\boldsymbol{U}}_{h,0}^k, \|\underline{\boldsymbol{v}}_h\|_{\boldsymbol{\varepsilon},r,h}=1} \left(\mathcal{E}_h(\underline{\boldsymbol{v}}_h) + \mathrm{a}_h(\underline{\hat{\boldsymbol{u}}}_h, \underline{\boldsymbol{v}}_h) - \mathrm{a}_h(\underline{\boldsymbol{u}}_h, \underline{\boldsymbol{v}}_h)\right) \\
&\lesssim \$ + \sigma_{\mathrm{hc}} \mathcal{N}_f^{r-\tilde{r}} \|\underline{\boldsymbol{e}}_h\|_{\boldsymbol{\varepsilon},r,h}^{\tilde{r}-1} \\
&\lesssim h^{(k+1)(\tilde{r}-1)} \mathcal{N}_{\boldsymbol{\sigma},\boldsymbol{u},p} + h^{(k+1)(\tilde{r}-1)^2} \sigma_{\mathrm{hc}} \mathcal{N}_f^{|r-2|(\tilde{r}-1)} \left(\sigma_{\mathrm{hm}}^{-1} \mathcal{N}_{\boldsymbol{\sigma},\boldsymbol{u},p}\right)^{\frac{\tilde{r}-1}{r+1-\tilde{r}}},
\end{aligned} \tag{1.76}$$

where we have used the definition (1.71) of the consistency error together with equation (1.30a) to pass to the second line, (1.75) to pass to the third line (recall that \$ denotes here the supremum in the left-hand side of (1.72)), and the bounds (1.72) and (1.32a) (proved in Step 2) to conclude. □

1.A Power-framed functions

In the following theorem, we introduce the notion of power-framed function and discuss sufficient conditions for this property to hold.

Theorem 46 (Power-framed function)**.** *Let U be a measurable subset of $\mathbb{R}^n$ with $n \geq 1$, $(W, (\cdot,\cdot)_W)$ an inner product space, and $\boldsymbol{\sigma} : U \times W \to W$. Assume that there exists a Carathéodory function $\varsigma : U \times [0,\infty) \to \mathbb{R}$ such that, for all $\boldsymbol{\tau} \in W$ and almost every $\boldsymbol{x} \in U$,*

$$\boldsymbol{\sigma}(\boldsymbol{x},\boldsymbol{\tau}) = \varsigma(\boldsymbol{x}, \|\boldsymbol{\tau}\|_W)\boldsymbol{\tau}, \tag{1.77a}$$

where $\|\cdot\|_W$ is the norm induced by $(\cdot,\cdot)_W$. Additionally assume that for almost every $\boldsymbol{x} \in U$, $\varsigma(\boldsymbol{x},\cdot)$ is differentiable on $(0,\infty)$ and there exist $r \in (1,\infty)$, $\delta \in [0,\infty)$, and $\varsigma_{\mathrm{hm}}, \varsigma_{\mathrm{hc}} \in (0,\infty)$ independent of $\boldsymbol{x}$ such that, for all $\alpha \in (0,\infty)$,

$$\varsigma_{\mathrm{hm}}(\delta^r + \alpha^r)^{\frac{r-2}{r}} \leq \frac{\partial(\alpha\varsigma(\boldsymbol{x},\alpha))}{\partial\alpha} \leq \varsigma_{\mathrm{hc}}(\delta^r + \alpha^r)^{\frac{r-2}{r}}. \tag{1.77b}$$

*Then, $\boldsymbol{\sigma}$ is an (r,δ)-*power-framed function*, i.e., for all $(\boldsymbol{\tau},\boldsymbol{\eta}) \in W^2$ with $\boldsymbol{\tau} \neq \boldsymbol{\eta}$ and almost every $\boldsymbol{x} \in U$, the function $\boldsymbol{\sigma}$ verifies the Hölder continuity property*

$$\|\boldsymbol{\sigma}(\boldsymbol{x},\boldsymbol{\tau}) - \boldsymbol{\sigma}(\boldsymbol{x},\boldsymbol{\eta})\|_W \leq \sigma_{\mathrm{hc}} \left(\delta^r + \|\boldsymbol{\tau}\|_W^r + \|\boldsymbol{\eta}\|_W^r\right)^{\frac{r-2}{r}} \|\boldsymbol{\tau} - \boldsymbol{\eta}\|_W, \tag{1.78a}$$

and the Hölder monotonicity property

$$(\boldsymbol{\sigma}(\boldsymbol{x},\boldsymbol{\tau}) - \boldsymbol{\sigma}(\boldsymbol{x},\boldsymbol{\eta}), \boldsymbol{\tau} - \boldsymbol{\eta})_W \geq \sigma_{\mathrm{hm}} \left(\delta^r + \|\boldsymbol{\tau}\|_W^r + \|\boldsymbol{\eta}\|_W^r\right)^{\frac{r-2}{r}} \|\boldsymbol{\tau} - \boldsymbol{\eta}\|_W^2, \tag{1.78b}$$

with $\sigma_{\mathrm{hc}} \coloneqq 2^{2-\tilde{r}+r^{-1}\lceil 2-\tilde{r}\rceil}(\tilde{r}-1)^{-1}\varsigma_{\mathrm{hc}}$, and $\sigma_{\mathrm{hm}} \coloneqq 2^{\tilde{r}-r-\lceil r^{-1}(r-\tilde{r})\rceil}(r+1-\tilde{r})^{-1}\varsigma_{\mathrm{hm}}$, where $\tilde{r}$ is given by (1.2) and $\lceil\cdot\rceil$ is the ceiling function.

Remark 47 (Notation). The boldface notation for the elements of W is reminiscent of the fact that Theorem 46 is used with $W = \mathbb{R}^{d\times d}_{\mathrm{s}}$ in Corollary 48 to characterize the Carreau–Yasuda law as an (r,δ)-power-framed function and in Lemma 32 with $W = \mathbb{R}^d$ to study the local stabilization function s_T.

Proof of Theorem 46. Let $\boldsymbol{x} \in U$ be such that (1.77) holds, and $\boldsymbol{\tau},\boldsymbol{\eta} \in W$. By symmetry of inequalities (1.78) and the fact that $\boldsymbol{\sigma}$ is continuous, we can assume, without loss of generality, that $\|\boldsymbol{\tau}\|_W > \|\boldsymbol{\eta}\|_W > 0$.

(i) *Hölder monotonicity.* Let $\beta \in (0,\infty)$ and let $g : [\beta,\infty) \to \mathbb{R}$ be such that, for all $\alpha \in [\beta,\infty)$,

$$g(\alpha) \coloneqq \alpha\varsigma(\boldsymbol{x},\alpha) - \beta\varsigma(\boldsymbol{x},\beta) - C_{\mathrm{hm}}(\delta^r + \alpha^r + \beta^r)^{\frac{r-2}{r}}(\alpha-\beta), \quad \text{with } C_{\mathrm{hm}} \coloneqq \tfrac{2^{\tilde{r}-r}}{r+1-\tilde{r}}\varsigma_{\mathrm{hm}}.$$

Differentiating g and using the first inequality in (1.77b), we obtain, for all $\alpha \in [\beta, \infty)$,

$$\begin{aligned}\frac{\partial}{\partial\alpha} g(\alpha) &\geq \varsigma_{\mathrm{hm}}(\delta^r + \alpha^r)^{\frac{r-2}{r}} \\ &\quad - C_{\mathrm{hm}}\left((r-2)(\delta^r + \alpha^r + \beta^r)^{-\frac{2}{r}}(\alpha-\beta)\alpha^{r-1} + (\delta^r + \alpha^r + \beta^r)^{\frac{r-2}{r}}\right) \\ &\geq \varsigma_{\mathrm{hm}}(\delta^r + \alpha^r)^{\frac{r-2}{r}} - (r+1-\tilde{r})C_{\mathrm{hm}}(\delta^r + \alpha^r + \beta^r)^{\frac{r-2}{r}} \\ &\geq \varsigma_{\mathrm{hm}} 2^{\tilde{r}-r}(\delta^r + \alpha^r + \beta^r)^{\frac{r-2}{r}} - (r+1-\tilde{r})C_{\mathrm{hm}}(\delta^r + \alpha^r + \beta^r)^{\frac{r-2}{r}} = 0,\end{aligned}$$

where, to pass to the second line, we have removed negative contributions if $r < 2$ and used the fact that $(\alpha-\beta)\alpha^{r-1} \leq \delta^r + \alpha^r + \beta^r$ if $r \geq 2$, to pass to the third line we have used the fact that $t \mapsto t^{r-2}$ is non-increasing if $r < 2$, and the fact that $\beta \leq \alpha$ otherwise, while the conclusion follows from the definition of C_{hm}. This shows that g is non-decreasing. Hence, for all $\alpha \in [\beta, \infty)$, $g(\alpha) \geq g(\beta) = 0$, i.e.

$$\alpha\varsigma(\boldsymbol{x}, \alpha) - \beta\varsigma(\boldsymbol{x}, \beta) \geq C_{\mathrm{hm}}(\delta^r + \alpha^r + \beta^r)^{\frac{r-2}{r}}(\alpha - \beta). \tag{1.79}$$

Moreover, for all $\alpha, \beta \in (0, \infty)$, using (1.79) (with $\beta = 0$) along with the fact that $t \mapsto t^{r-2}$ is decreasing if $r < 2$ and inequality (1.37) if $r \geq 2$, we infer that

$$\begin{aligned}\varsigma(\boldsymbol{x}, \alpha) + \varsigma(\boldsymbol{x}, \beta) &\geq C_{\mathrm{hm}}\left((\delta^r + \alpha^r)^{\frac{r-2}{r}} + (\delta^r + \beta^r)^{\frac{r-2}{r}}\right) \\ &\geq C_{\mathrm{hm}} 2^{1-\lceil\frac{r-\tilde{r}}{r}\rceil}(\delta^r + \alpha^r + \beta^r)^{\frac{r-2}{r}}.\end{aligned} \tag{1.80}$$

We conclude that $\boldsymbol{\sigma}$ verifies (1.78b) by using (1.79) and (1.80) with $\alpha = \|\boldsymbol{\tau}\|_W$ and $\beta = \|\boldsymbol{\eta}\|_W$ as follows:

$$\begin{aligned}&(\boldsymbol{\sigma}(\boldsymbol{x}, \boldsymbol{\tau}) - \boldsymbol{\sigma}(\boldsymbol{x}, \boldsymbol{\eta}), \boldsymbol{\tau} - \boldsymbol{\eta})_W \\ &\quad = (\boldsymbol{\tau}\varsigma(\boldsymbol{x}, \|\boldsymbol{\tau}\|_W) - \boldsymbol{\eta}\varsigma(\boldsymbol{x}, \|\boldsymbol{\eta}\|_W), \boldsymbol{\tau} - \boldsymbol{\eta})_W \\ &\quad = \|\boldsymbol{\tau}\|_W^2 \varsigma(\boldsymbol{x}, \|\boldsymbol{\tau}\|_W) + \|\boldsymbol{\eta}\|_W^2 \varsigma(\boldsymbol{x}, \|\boldsymbol{\eta}\|_W) - (\boldsymbol{\tau}, \boldsymbol{\eta})_W \left[\varsigma(\boldsymbol{x}, \|\boldsymbol{\tau}\|_W) + \varsigma(\boldsymbol{x}, \|\boldsymbol{\eta}\|_W)\right] \\ &\quad = \left[\|\boldsymbol{\tau}\|_W \varsigma(\boldsymbol{x}, \|\boldsymbol{\tau}\|_W) - \|\boldsymbol{\eta}\|_W \varsigma(\boldsymbol{x}, \|\boldsymbol{\eta}\|_W)\right](\|\boldsymbol{\tau}\|_W - \|\boldsymbol{\eta}\|_W) \\ &\qquad + \left[\varsigma(\boldsymbol{x}, \|\boldsymbol{\tau}\|_W) + \varsigma(\boldsymbol{x}, \|\boldsymbol{\eta}\|_W)\right](\|\boldsymbol{\tau}\|_W \|\boldsymbol{\eta}\|_W - (\boldsymbol{\tau}, \boldsymbol{\eta})_W) \\ &\quad \geq C_{\mathrm{hm}} 2^{-\lceil\frac{r-\tilde{r}}{r}\rceil}\left(\delta^r + \|\boldsymbol{\tau}\|_W^r + \|\boldsymbol{\eta}\|_W^r\right)^{\frac{r-2}{r}} \\ &\qquad \times \left[(\|\boldsymbol{\tau}\|_W - \|\boldsymbol{\eta}\|_W)^2 + 2(\|\boldsymbol{\tau}\|_W \|\boldsymbol{\eta}\|_W - (\boldsymbol{\tau}, \boldsymbol{\eta})_W)\right] \\ &\quad = C_{\mathrm{hm}} 2^{-\lceil\frac{r-\tilde{r}}{r}\rceil}\left(\delta^r + \|\boldsymbol{\tau}\|_W^r + \|\boldsymbol{\eta}\|_W^r\right)^{\frac{r-2}{r}} \|\boldsymbol{\tau} - \boldsymbol{\eta}\|_W^2.\end{aligned}$$

(ii) *Hölder continuity.* Now, setting $C_{\mathrm{hc}} := \frac{\varsigma_{\mathrm{hc}}}{\tilde{r}-1}$ and reasoning in a similar way as for the proof of (1.79) to leverage the second inequality in (1.77b), we have, for all $\alpha \in [\beta, \infty)$,

$$\alpha\varsigma(\boldsymbol{x}, \alpha) - \beta\varsigma(\boldsymbol{x}, \beta) \leq C_{\mathrm{hc}}\,(\delta^r + \alpha^r + \beta^r)^{\frac{r-2}{r}}\,(\alpha - \beta). \tag{1.81}$$

First, let $r \geq 2$. Using (1.81) (with $\beta = 0$) and the fact that $t \mapsto t^{r-2}$ is non-decreasing, we have, for all $\alpha, \beta \in (0, \infty)$,

$$\begin{aligned} \varsigma(\boldsymbol{x}, \alpha)\varsigma(\boldsymbol{x}, \beta) &\leq C_{\mathrm{hc}}^2 \left(\delta^r + \alpha^r\right)^{\frac{r-2}{r}} \left(\delta^r + \beta^r\right)^{\frac{r-2}{r}} \\ &\leq \left[C_{\mathrm{hc}} \left(\delta^r + \alpha^r + \beta^r\right)^{\frac{r-2}{r}}\right]^2. \end{aligned} \tag{1.82}$$

Thus, using inequalities (1.81) and (1.82) with $\alpha = \|\boldsymbol{\tau}\|_W$ and $\beta = \|\boldsymbol{\eta}\|_W$, we infer

$$\begin{aligned} &\|\boldsymbol{\sigma}(\boldsymbol{x}, \boldsymbol{\tau}) - \boldsymbol{\sigma}(\boldsymbol{x}, \boldsymbol{\eta})\|_W^2 \\ &\quad = (\boldsymbol{\tau}\varsigma(\boldsymbol{x}, \|\boldsymbol{\tau}\|_W) - \boldsymbol{\eta}\varsigma(\boldsymbol{x}, \|\boldsymbol{\eta}\|_W), \boldsymbol{\tau}\varsigma(\boldsymbol{x}, \|\boldsymbol{\tau}\|_W) - \boldsymbol{\eta}\varsigma(\boldsymbol{x}, \|\boldsymbol{\eta}\|_W))_W \\ &\quad = [\|\boldsymbol{\tau}\|_W\varsigma(\boldsymbol{x}, \|\boldsymbol{\tau}\|_W) - \|\boldsymbol{\eta}\|_W\varsigma(\boldsymbol{x}, \|\boldsymbol{\eta}\|_W)]^2 \\ &\qquad + 2\varsigma(\boldsymbol{x}, \|\boldsymbol{\tau}\|_W)\varsigma(\boldsymbol{x}, \|\boldsymbol{\eta}\|_W)\left[\|\boldsymbol{\tau}\|_W\|\boldsymbol{\eta}\|_W - (\boldsymbol{\tau}, \boldsymbol{\eta})_W\right] \\ &\quad \leq \left[C_{\mathrm{hc}} \left(\delta^r + \|\boldsymbol{\tau}\|_W^r + \|\boldsymbol{\eta}\|_W^r\right)^{\frac{r-2}{r}}\right]^2 \\ &\qquad \times \left[(\|\boldsymbol{\tau}\|_W - \|\boldsymbol{\eta}\|_W)^2 + 2(\|\boldsymbol{\tau}\|_W\|\boldsymbol{\eta}\|_W - (\boldsymbol{\tau}, \boldsymbol{\eta})_W)\right] \\ &\quad = \left[C_{\mathrm{hc}} \left(\delta^r + \|\boldsymbol{\tau}\|_W^r + \|\boldsymbol{\eta}\|_W^r\right)^{\frac{r-2}{r}} \|\boldsymbol{\tau} - \boldsymbol{\eta}\|_W\right]^2, \end{aligned} \tag{1.83}$$

hence $\boldsymbol{\sigma}$ verifies (1.78a) for $r \geq 2$. Assume now $r < 2$. Using a triangle inequality followed by (1.81) and the left inequality in (1.37), it is inferred that

$$\begin{aligned} \|\boldsymbol{\sigma}(\boldsymbol{x}, \boldsymbol{\tau}) - \boldsymbol{\sigma}(\boldsymbol{x}, \boldsymbol{\eta})\|_W &\leq \varsigma(\boldsymbol{x}, \|\boldsymbol{\tau}\|_W)\|\boldsymbol{\tau}\|_W + \varsigma(\boldsymbol{x}, \|\boldsymbol{\eta}\|_W)\|\boldsymbol{\eta}\|_W \\ &\leq C_{\mathrm{hc}} \left(\left(\delta^r + \|\boldsymbol{\tau}\|_W^r\right)^{\frac{r-1}{r}} + \left(\delta^r + \|\boldsymbol{\eta}\|_W^r\right)^{\frac{r-1}{r}}\right) \\ &\leq 2^{\frac{1}{r}} C_{\mathrm{hc}} (2\delta^r + \|\boldsymbol{\tau}\|_W^r + \|\boldsymbol{\eta}\|_W^r)^{\frac{r-1}{r}} \\ &= 2^{\frac{1}{r}} C_{\mathrm{hc}} (2\delta^r + \|\boldsymbol{\tau}\|_W^r + \|\boldsymbol{\eta}\|_W^r)^{\frac{r-2}{r}} (2\delta^r + \|\boldsymbol{\tau}\|_W^r + \|\boldsymbol{\eta}\|_W^r)^{\frac{1}{r}}, \\ &\leq 2^{\frac{1}{r}} C_{\mathrm{hc}} (\delta^r + \|\boldsymbol{\tau}\|_W^r + \|\boldsymbol{\eta}\|_W^r)^{\frac{r-2}{r}} (2\delta + \|\boldsymbol{\tau}\|_W + \|\boldsymbol{\eta}\|_W), \end{aligned}$$

where the last line follows from the fact that $t \mapsto t^{r-2}$ is decreasing and again (1.37). If $2\delta + \|\boldsymbol{\tau}\|_W + \|\boldsymbol{\eta}\|_W \leq 2^{2-r}\|\boldsymbol{\tau} - \boldsymbol{\eta}\|_W$, from the previous bound we directly get the conclusion, i.e. (1.78a) with $\sigma_{\mathrm{hc}} = 2^{2-r+\frac{1}{r}} C_{\mathrm{hc}}$. Otherwise, using (1.37) and a triangle inequality yields

$$\begin{aligned} &\left(\delta^r + \|\boldsymbol{\tau}\|_W^r\right)^{\frac{1}{r}} \left(\delta^r + \|\boldsymbol{\eta}\|_W^r\right)^{\frac{1}{r}} \geq 2^{-\frac{2}{r'}} (\delta + \|\boldsymbol{\tau}\|_W)(\delta + \|\boldsymbol{\eta}\|_W) \\ &\quad = 2^{-2(\frac{1}{r'}+1)} \left[(2\delta + \|\boldsymbol{\tau}\|_W + \|\boldsymbol{\eta}\|_W)^2 - (\|\boldsymbol{\tau}\|_W - \|\boldsymbol{\eta}\|_W)^2\right] \\ &\quad \geq 2^{-2(\frac{1}{r'}+1)} \left[(2\delta + \|\boldsymbol{\tau}\|_W + \|\boldsymbol{\eta}\|_W)^2 - \|\boldsymbol{\tau} - \boldsymbol{\eta}\|_W^2\right] \\ &\quad \geq 2^{-2(\frac{1}{r'}+1)} (1 - 4^{r-2}) (2\delta + \|\boldsymbol{\tau}\|_W + \|\boldsymbol{\eta}\|_W)^2 \\ &\quad \geq 2^{\frac{2}{(r-2)r} - 2} \left(\delta^r + \|\boldsymbol{\tau}\|_W^r + \|\boldsymbol{\eta}\|_W^r\right)^{\frac{2}{r}}, \end{aligned} \tag{1.84}$$

where we concluded with (1.37) together with the fact that $2^{-2(\frac{1}{r'}+1)}\left(1-4^{r-2}\right) \geq 2^{\frac{2}{(r-2)r}-2}$. Finally, raising both sides of (1.84) to the power $r-2$, we get a relation analogous to (1.82). Hence, proceeding as in (1.83), we infer (1.78a). □

Corollary 48 (Carreau–Yasuda)**.** *The strain rate-shear stress law of the* (μ, δ, a, r)*-Carreau–Yasuda fluid defined in Example 28 is an* (r, δ)*-power-framed function.*

Proof. Let $\boldsymbol{x} \in \Omega$ and $g : (0, \infty) \to \mathbb{R}$ be such that, for all $\alpha \in (0, \infty)$,

$$\begin{aligned} g(\alpha) &:= \frac{\partial}{\partial \alpha}\left[\alpha \mu(\boldsymbol{x})\left(\delta^{a(\boldsymbol{x})}+\alpha^{a(\boldsymbol{x})}\right)^{\frac{r-2}{a(\boldsymbol{x})}}\right] \\ &= \mu(\boldsymbol{x})\left(\delta^{a(\boldsymbol{x})}+\alpha^{a(\boldsymbol{x})}\right)^{\frac{r-2}{a(\boldsymbol{x})}-1}\left(\delta^{a(\boldsymbol{x})}+(r-1)\alpha^{a(\boldsymbol{x})}\right). \end{aligned}$$

We have for all $\alpha \in (0, \infty)$,

$$\mu_{-}(\tilde{r}-1)\left(\delta^{a(\boldsymbol{x})}+\alpha^{a(\boldsymbol{x})}\right)^{\frac{r-2}{a(\boldsymbol{x})}} \leq g(\alpha) \leq \mu_{+}(r+1-\tilde{r})\left(\delta^{a(\boldsymbol{x})}+\alpha^{a(\boldsymbol{x})}\right)^{\frac{r-2}{a(\boldsymbol{x})}},$$

and we conclude using (1.37) together with Theorem 46. □

Chapter 2

Improved error estimates for HHO discretizations of Leray–Lions problems

This chapter has been published in the following international journal (see [52]):

Calcolo, 2021.
Volume 58, Issue 19.

Abstract

We derive novel error estimates for Hybrid High-Order (HHO) discretizations of Leray–Lions problems set in $W^{1,p}$ with $p \in (1,2]$. Specifically, we prove that, depending on the degeneracy of the problem, the convergence rate may vary between $(k+1)(p-1)$ and $(k+1)$, with k denoting the degree of the HHO approximation. These regime-dependent error estimates are illustrated by a complete panel of numerical experiments.

2.1 Introduction

We consider Hybrid High-Order (HHO) approximations of Leray–Lions problems set in $W^{1,p}$ with $p \in (1,2]$. For this class of problems, negative powers of the gradient of the solution can appear in the flux. Depending on the expression of the latter, this can lead to a (local) degeneracy of the problem when the gradient of the solution vanishes or becomes large.

In this work, we prove novel error estimates that highlight the dependence of the convergence rate on the two possible cases of degeneracy simultaneously, and we do not differentiate these two degeneracies any longer. Specifically, we show that, for the

globally non-degenerate case, the energy-norm of the error converges as h^{k+1}, with h denoting the mesh size and k the degree of the HHO approximation. In the globally degenerate case, on the other hand, the energy-norm of the error converges as $h^{(k+1)(p-1)}$, coherently with the estimate originally proved in [47, Theorem 3.2]. We additionally introduce, for each mesh element T of diameter h_T, a dimensionless number η_T that captures the local degeneracy of the model in T and identifies the contribution of the element to the global error: from the fully degenerate regime, corresponding to a contribution in $O(h_T^{(k+1)(p-1)})$, to the non-degenerate regime, corresponding to a contribution in $O(h_T^{k+1})$, through all intermediate regimes. Estimates depending on local regimes have been established in linear settings (see, e.g., [53, 59] for advection–diffusion–reaction models and [26] for the Brinkman problem). Such work has also been done for the Leray–Lions problems with Adaptative Finite Element methods in [17]; to the best of our knowledge, their extension to HHO methods is entirely new.

Error estimates for the lowest-order conforming finite element approximation of the pure p-Laplacian have been known for quite some time; see, e.g., the founding work [74], in which $O(h^{1/(3-p)})$ error estimates are obtained in the case $p \leq 2$ considered here. These estimates were later improved in [10] to $O(h)$, for solutions of high (and global) regularity – in the space $W^{3,1}(\Omega) \cap C^{2,(2-p)/p}(\overline{\Omega})$. The above results have been extended to non-conforming finite elements in [90]. A glaciology model is considered in [75], corresponding to a non-degenerate p-Laplace equation (with flux satisfying (2.2) below with $\delta = 1$), and error estimates for the conforming finite element approximation have been obtained: $O(h)$ if the solution is in $H^2(\Omega)$, and $O(h^{p/2})$ if it belongs to $W^{2,p}(\Omega)$. A common feature of all these studies, in which sharp error estimates are derived (which do not degrade too much as p gets far from 2), is that they only consider low-order schemes on 2D triangular meshes and with continuity properties – either all along the edges for the conforming method, or at the edges midpoints for the non-conforming method. To our knowledge, for higher-order methods that may involve fully discontinuous functions and are applicable to generic polytopal meshes, such as HHO, no sharp error estimates are known and only convergence in $h^{(k+1)(p-1)}$ has been established so far. This paper therefore bridges a gap between the results available for the low-order finite element methods and HHO methods. Notice that, very recently, $O(h^{(k+1)/(3-p)})$ error estimates have been obtained in [33] for an HHO method on standard simplicial meshes based on a stable gradient inspired by [53]. In passing, even though we focus on the HHO method, our approach could in all likelihood be extended to other polytopal methods such as, e.g., the Mimetic Finite Difference method [6] or the Virtual Element method [104]; see the preface of [50] for an up-to-date literature review on this subject.

The rest of the paper is organized as follows. In Section 2.2 we establish the continuous setting, including novel assumptions on the flux function weaker than the ones considered in [47, Section 3.1]. In Section 2.3 we briefly recall the discrete setting upon which rests the HHO scheme described in Section 2.4. The main result of this paper

is contained Section 2.5. Finally, Section 2.6 contains a complete panel of numerical tests illustrating the effect of local degeneracy on the convergence rate.

2.2 Continuous setting

2.2.1 Flux function

Let $\Omega \subset \mathbb{R}^d$, $d \in \mathbb{N}^*$, denote a bounded, connected, polytopal open set with Lipschitz boundary $\partial\Omega$. We consider the Leray–Lions problem, which consist in finding $u : \Omega \to \mathbb{R}$ such that

$$-\boldsymbol{\nabla}\cdot\boldsymbol{\sigma}(\cdot, \boldsymbol{\nabla} u) = f \qquad \text{in } \Omega, \tag{2.1a}$$

$$u = 0 \qquad \text{on } \partial\Omega, \tag{2.1b}$$

where $f : \Omega \to \mathbb{R}$ represents a volumetric force term, while $\boldsymbol{\sigma} : \Omega \times \mathbb{R}^d \to \mathbb{R}^d$ is the *flux function*. The flux function is possibly variable in space and depends on the *potential* $u : \Omega \to \mathbb{R}$ only through its gradient. The following assumptions characterize $\boldsymbol{\sigma}$.

Assumption 3 (Flux function)**.** Let a real number $p \in (1, 2]$ be fixed and denote by

$$p' \coloneqq \frac{p}{p-1} \in [2, \infty)$$

the conjugate exponent of p. The flux function satisfies

$$\boldsymbol{\sigma}(\boldsymbol{x}, \boldsymbol{0}) = \boldsymbol{0} \text{ for almost every } \boldsymbol{x} \in \Omega, \tag{2.2a}$$

$$\boldsymbol{\sigma}(\cdot, \boldsymbol{\xi}) : \Omega \to \mathbb{R}^d \text{ is measurable for all } \boldsymbol{\xi} \in \mathbb{R}^d. \tag{2.2b}$$

Moreover, there exist a *degeneracy function* $\delta \in L^p(\Omega, [0, \infty))$ and two real numbers $\sigma_{\mathrm{hc}}, \sigma_{\mathrm{hm}} \in (0, \infty)$ such that, for all $\boldsymbol{\tau}, \boldsymbol{\eta} \in \mathbb{R}^d$ and almost every $\boldsymbol{x} \in \Omega$, we have the *continuity* property

$$|\boldsymbol{\sigma}(\boldsymbol{x}, \boldsymbol{\tau}) - \boldsymbol{\sigma}(\boldsymbol{x}, \boldsymbol{\eta})| \le \sigma_{\mathrm{hc}} \left(\delta(\boldsymbol{x})^p + |\boldsymbol{\tau}|^p + |\boldsymbol{\eta}|^p\right)^{\frac{p-2}{p}} |\boldsymbol{\tau} - \boldsymbol{\eta}|, \tag{2.2c}$$

and the *Hölder monotonicity* property

$$(\boldsymbol{\sigma}(\boldsymbol{x}, \boldsymbol{\tau}) - \boldsymbol{\sigma}(\boldsymbol{x}, \boldsymbol{\eta})) \cdot (\boldsymbol{\tau} - \boldsymbol{\eta}) \ge \sigma_{\mathrm{hm}} \left(\delta(\boldsymbol{x})^p + |\boldsymbol{\tau}|^p + |\boldsymbol{\eta}|^p\right)^{\frac{p-2}{p}} |\boldsymbol{\tau} - \boldsymbol{\eta}|^2. \tag{2.2d}$$

Some remarks are in order.

Remark 49 (Flux at rest). Assumption (2.2a) expresses the fact that the flux at rest is zero, and can be relaxed taking $\boldsymbol{\sigma}(\cdot, \boldsymbol{0}) \in L^{p'}(\Omega)^d$. This modification requires only minor changes in the analysis, not detailed for the sake of conciseness.

Remark 50 (Relations between the continuity and monotonicity constants). Inequalities (2.2c) and (2.2d) give

$$\sigma_{\mathrm{hm}} \le \sigma_{\mathrm{hc}}. \tag{2.3}$$

Indeed, let $\boldsymbol{\tau} \in \mathbb{R}^d$ be such that $|\boldsymbol{\tau}| > 0$. Using the Hölder monotonicity (2.2d) (with $\boldsymbol{\eta} = \mathbf{0}$) along with (2.2a), the Cauchy–Schwarz inequality, and the continuity (2.2c) (again with $\boldsymbol{\eta} = \mathbf{0}$) and (2.2a), we infer that

$$\sigma_{\mathrm{hm}} \left(\delta^p + |\boldsymbol{\tau}|^p\right)^{\frac{p-2}{p}} |\boldsymbol{\tau}|^2 \le \boldsymbol{\sigma}(\cdot,\boldsymbol{\tau}) \cdot \boldsymbol{\tau} \le |\boldsymbol{\sigma}(\cdot,\boldsymbol{\tau})||\boldsymbol{\tau}| \le \sigma_{\mathrm{hc}} \left(\delta^p + |\boldsymbol{\tau}|^p\right)^{\frac{p-2}{p}} |\boldsymbol{\tau}|^2$$

almost everywhere in Ω, hence (2.3).

Remark 51 (Degenerate case). We note the following inequality: For all $x, y \in \mathbb{R}^n$, $n \in \mathbb{N}^*$, and all $\alpha \in [0,\infty)$,

$$(\alpha + |x| + |y|)^{p-2}|x - y| \le |x - y|^{p-1}. \tag{2.4}$$

To prove (2.4), notice that, if $\alpha + |x| + |y| > 0$, using a triangle inequality to write $|x| + |y| \ge |x - y|$ together with the fact that $\mathbb{R} \ni t \mapsto t^{p-2} \in \mathbb{R}$ is non-increasing (since $p < 2$) and $\alpha \ge 0$, we infer that $(\alpha + |x| + |y|)^{p-2} \le |x - y|^{p-2}$, which, multiplying by $|x - y|$, gives (2.4). Since (2.4) is valid when $\alpha + |x| + |y| > 0$, we can extend the left-hand side by continuity (with value 0) in the singular case $\alpha + |x| + |y| = 0$ and this estimate remains valid.

Inequality (2.29) below together with (2.4) ensures that properties (2.2c)–(2.2d) are well-formulated by extension also when $\delta(\boldsymbol{x})^p + |\boldsymbol{\tau}|^p + |\boldsymbol{\eta}|^p$ vanishes. As a consequence, $\boldsymbol{\sigma}(\boldsymbol{x},\cdot) : \mathbb{R}^d \to \mathbb{R}^d$ is continuous for a.e. $\boldsymbol{x} \in \Omega$. The relation (2.4) will also play a key role in the proof of Theorem 59 below.

Remark 52 (Non-degenerate case). In [47], an error estimate is given for broader versions of inequalities (2.2c)–(2.2d). The novelty here lies in the introduction of the degeneracy function δ, since it directly affects the convergence rate of the method. The crux of its intervention is located in the proof of Theorem 59, and more precisely at (2.44) where it prevents singularities. See Remark 60 for more details, see also Figure 2.1 for a set of numerical results illustrating this phenomenon.

Example 53 (p-Laplace flux function)**.** A typical example of flux function is $\boldsymbol{\sigma}(\boldsymbol{x},\boldsymbol{\tau}) = |\boldsymbol{\tau}|^{p-2}\boldsymbol{\tau}$, for which (2.1) is the p-Laplace equation $-\boldsymbol{\nabla}\cdot(|\boldsymbol{\nabla} u|^{p-2}\boldsymbol{\nabla} u) = f$. This flux function satisfies Assumption 3 with degeneracy function $\delta = 0$, see e.g. [50, Lemma 6.26].

Example 54 (Carreau–Yasuda flux function)**.** Another example of function $\boldsymbol{\sigma}$ which satisfies Assumption 3, inspired by the rheology of Carreau–Yosida fluids, is obtained setting, for almost every $\boldsymbol{x} \in \Omega$ and all $\boldsymbol{\tau} \in \mathbb{R}^d$,

$$\boldsymbol{\sigma}(\boldsymbol{x},\boldsymbol{\tau}) = \mu(\boldsymbol{x}) \left(\delta(\boldsymbol{x})^{a(\boldsymbol{x})} + |\boldsymbol{\tau}|^{a(\boldsymbol{x})}\right)^{\frac{p-2}{a(\boldsymbol{x})}} \boldsymbol{\tau}, \tag{2.5}$$

where $\mu : \Omega \to [\mu_-, \mu_+]$ is a measurable function with $\mu_-, \mu_+ \in (0, \infty)$ corresponding to the *local flow consistency index*, $\delta \in L^p(\Omega, [0, \infty))$ is the *degeneracy parameter*, $a : \Omega \to [a_-, a_+]$ is a measurable function with $a_-, a_+ \in (0, \infty)$ expressing the *local transition flow behavior index*, and $p \in (1, 2]$ is the *flow behavior index*. It was proved in [27, Appendix A] that $\boldsymbol{\sigma}$ is an (p, δ)-power-framed function (with a straightforward analogy to generalize the degeneracy constant δ to a function) with

$$\sigma_{\mathrm{hc}} = \frac{\mu_+}{p-1} 2^{\left[-\left(\frac{1}{a_+}-\frac{1}{p}\right)^{\ominus}-1\right](p-2)+\frac{1}{p}} \quad \text{and} \quad \sigma_{\mathrm{hm}} = \mu_-(p-1)2^{\left(\frac{1}{a_-}-\frac{1}{p}\right)^{\oplus}(p-2)},$$

where $\xi^{\oplus} \coloneqq \max(0;\xi)$ and $\xi^{\ominus} \coloneqq -\min(0;\xi)$ denote, respectively, the positive and negative parts of a real number ξ. As a consequence, the flux function (2.5) matches Assumption 3.

2.2.2 Weak formulation

We define the following space for the potential embedding the homogeneous boundary condition:

$$U \coloneqq W_0^{1,p}(\Omega).$$

Assuming $f \in L^{p'}(\Omega)$, the weak formulation of problem (2.1) reads: Find $u \in U$ such that

$$a(u, v) = \int_\Omega fv \qquad \forall v \in U, \tag{2.6}$$

where the *diffusion function* $a : U \times U \to \mathbb{R}$ is defined such that, for all $v, w \in U$,

$$a(w, v) \coloneqq \int_\Omega \boldsymbol{\sigma}(\cdot, \boldsymbol{\nabla} w) \cdot \boldsymbol{\nabla} v. \tag{2.7}$$

Proposition 55 (Well-posedness and a priori estimate)**.** *Under Assumption 3, the continuous problem (2.6) admits a unique solution $u \in U$ that satisfies the following a priori bound:*

$$\begin{aligned}\|\boldsymbol{\nabla} u\|_{L^p(\Omega)^d} \le{}& \left(2^{\frac{2-p}{p}} C_{\mathrm{P}} \sigma_{\mathrm{hm}}^{-1} \|f\|_{L^{p'}(\Omega)}\right)^{\frac{1}{p-1}} \\ &+ \min\left(\|\delta\|_{L^p(\Omega)}; 2^{\frac{2-p}{p}} C_{\mathrm{P}} \sigma_{\mathrm{hm}}^{-1} \|\delta\|_{L^p(\Omega)}^{2-p} \|f\|_{L^{p'}(\Omega)}\right).\end{aligned} \tag{2.8}$$

where the real number $C_{\mathrm{P}} > 0$, only depending on Ω and on p, is such that, for all $v \in W_0^{1,p}(\Omega)$, the Poincaré inequality $\|v\|_{L^p(\Omega)} \le C_{\mathrm{P}} \|\boldsymbol{\nabla} v\|_{L^p(\Omega)^d}$ holds.

Proof. For the existence and uniqueness of a solution to (2.6) see, e.g., [76, Section 2.4]. To prove the a priori bound (2.8), use the Hölder monotonicity (2.2d) of $\boldsymbol{\sigma}$, (2.6) written for $v = u$, and invoke the Hölder and Poincaré inequalities to write

$$\sigma_{\mathrm{hm}}\left(\|\delta\|_{L^p(\Omega)}^p + \|\boldsymbol{\nabla} u\|_{L^p(\Omega)^d}^p\right)^{\frac{p-2}{p}} \|\boldsymbol{\nabla} u\|_{L^p(\Omega)^d}^2 \le a(u,u) = \int_\Omega fu \le C_{\mathrm{P}}\|f\|_{L^{p'}(\Omega)}\|\boldsymbol{\nabla} u\|_{L^p(\Omega)^d},$$

that is,

$$\mathcal{N} := \left(\|\delta\|_{L^p(\Omega)}^p + \|\boldsymbol{\nabla} u\|_{L^p(\Omega)^d}^p\right)^{\frac{p-2}{p}} \|\boldsymbol{\nabla} u\|_{L^p(\Omega)^d} \le C_{\mathrm{P}}\sigma_{\mathrm{hm}}^{-1}\|f\|_{L^{p'}(\Omega)}. \tag{2.9}$$

Observing that $\|\boldsymbol{\nabla} u\|_{L^p(\Omega)^d} \le 2^{\frac{2-p}{p}} \max\left(\|\boldsymbol{\nabla} u\|_{L^p(\Omega)^d}; \|\delta\|_{L^p(\Omega)}\right)^{2-p}\mathcal{N}$, we obtain, enumerating the cases for the maximum and summing the corresponding bounds,

$$\|\boldsymbol{\nabla} u\|_{L^p(\Omega)^d} \le (2^{\frac{2-p}{p}}\mathcal{N})^{\frac{1}{p-1}} + 2^{\frac{2-p}{p}}\|\delta\|_{L^p(\Omega)}^{2-p}\mathcal{N}. \tag{2.10}$$

On the other hand, we have $\mathcal{N} \ge 2^{\frac{p-2}{p}}\|\boldsymbol{\nabla} u\|_{L^p(\Omega)^d}^{p-1}$ if $\|\boldsymbol{\nabla} u\|_{L^p(\Omega)^d} \ge \|\delta\|_{L^p(\Omega)}$. Thus we have, for any value of $\|\boldsymbol{\nabla} u\|_{L^p(\Omega)^d}$,

$$\|\boldsymbol{\nabla} u\|_{L^p(\Omega)^d} \le (2^{\frac{2-p}{p}}\mathcal{N})^{\frac{1}{p-1}} + \|\delta\|_{L^p(\Omega)}. \tag{2.11}$$

Combining (2.9) with the minimum of inequalities (2.10) and (2.11) gives (2.8). □

2.3 Discrete setting

2.3.1 Mesh

For any set $X \subset \mathbb{R}^d$, denote by h_X its diameter. A polytopal mesh is defined as a couple $\mathcal{M}_h := (\mathcal{T}_h, \mathcal{F}_h)$, where $\mathcal{T}_h$ is a finite collection of polytopal elements $T \in \mathcal{T}_h$ such that $h = \max_{T\in\mathcal{T}_h} h_T$, while $\mathcal{F}_h$ is a finite collection of hyperplanar faces. It is assumed henceforth that the mesh $\mathcal{M}_h$ matches the geometrical requirements detailed in [50, Definition 1.7]. Boundary faces lying on $\partial\Omega$ and internal faces contained in Ω are collected in the sets $\mathcal{F}_h^{\mathrm{b}}$ and $\mathcal{F}_h^{\mathrm{i}}$, respectively. For every mesh element $T \in \mathcal{T}_h$, we denote by $\mathcal{F}_T$ the subset of $\mathcal{F}_h$ collecting the faces that lie on the boundary ∂T of T. For every face $F \in \mathcal{F}_h$, we denote by $\mathcal{T}_F$ the subset of $\mathcal{T}_h$ containing the one (if $F \in \mathcal{F}_h^{\mathrm{b}}$) or two (if $F \in \mathcal{F}_h^{\mathrm{i}}$) elements on whose boundary F lies. For each mesh element $T \in \mathcal{T}_h$ and face $F \in \mathcal{F}_T$, $\boldsymbol{n}_{TF}$ denotes the (constant) unit vector normal to F pointing out of T.

Our focus is on the h-convergence analysis, so we consider a sequence of refined meshes that is regular in the sense of [50, Definition 1.9], with regularity parameter uniformly bounded away from zero. The mesh regularity assumption implies, in particular, that the diameter of a mesh element and those of its faces are comparable uniformly in h, and that the number of faces of one element is bounded above by an integer independent of h.

2.3.2 Notation for inequalities up to a multiplicative constant

To avoid the proliferation of generic constants, we write henceforth $a \lesssim b$ (resp., $a \gtrsim b$) for the inequality $a \le Cb$ (resp., $a \ge Cb$) with real number $C > 0$ independent of h, of the parameters $\delta, \sigma_{\mathrm{hc}}, \sigma_{\mathrm{hm}}$ in Assumption 3, and, for local inequalities, of the mesh element or face on which the inequality holds. We also write $a \simeq b$ to mean $a \lesssim b$ and $b \lesssim a$. The dependencies of the hidden constants are further specified when needed.

2.3.3 Projectors and broken spaces

Given $X \in \mathcal{T}_h \cup \mathcal{F}_h$ and $l \in \mathbb{N}$, we denote by $\mathbb{P}^l(X)$ the space spanned by the restriction to X of scalar-valued, d-variate polynomials of total degree $\le l$. The local L^2-orthogonal projector $\pi_X^l : L^1(X) \to \mathbb{P}^l(X)$ is defined such that, for all $v \in L^1(X)$,

$$\int_X (\pi_X^l v - v) w = 0 \qquad \forall w \in \mathbb{P}^l(X). \tag{2.12}$$

When applied to vector-valued functions in $L^1(X)^d$, the L^2-orthogonal projector mapping on $\mathbb{P}^l(X)^d$ acts component-wise and is denoted in boldface font as $\boldsymbol{\pi}_X^l$. Let $T \in \mathcal{T}_h$, $n \in [0, l+1]$, and $m \in [0, n]$. The following (n, p, m)-approximation properties of π_T^l hold: For any $v \in W^{n,p}(T)$,

$$|v - \pi_T^l v|_{W^{m,p}(T)} \lesssim h_T^{n-m} |v|_{W^{n,p}(T)}. \tag{2.13a}$$

The above property will also be used in what follows with p replaced by its conjugate exponent p'. If, additionally, $n \ge 1$, we have the following (n, p')-trace approximation property:

$$\|v - \pi_T^l v\|_{L^{p'}(\partial T)} \lesssim h_T^{n-\frac{1}{p'}} |v|_{W^{n,p'}(T)}. \tag{2.13b}$$

The hidden constants in (2.13) are independent of h and T, but possibly depend on d, the mesh regularity parameter, l, n, and p. The approximation properties (2.13) are proved for integer n and m in [48, Appendix A.2] (see also [50, Theorem 1.45]), and can be extended to non-integer values using standard interpolation techniques (see, e.g., [89, Theorem 5.1]).

The additional regularity on the exact solution in the error estimates will be expressed in terms of the broken Sobolev spaces

$$W^{n,p}(\mathcal{T}_h) \coloneqq \left\{ v \in L^p(\Omega) \ : \ v_{|T} \in W^{n,p}(T) \quad \forall T \in \mathcal{T}_h \right\}.$$

The corresponding seminorm is such that $|v|_{W^{n,p}(\mathcal{T}_h)} \coloneqq \left(\sum_{T\in\mathcal{T}_h} |v|^p_{W^{n,p}(T)} \right)^{\frac{1}{p}}$ for all $v \in W^{n,p}(\mathcal{T}_h)$.

2.4 HHO discretization

2.4.1 Hybrid space and norms

Let an integer $k \geq 0$ be fixed. The HHO space is, with usual notation,

$$\underline{U}_h^k \coloneqq \left\{ \underline{v}_h \coloneqq ((v_T)_{T\in\mathcal{T}_h}, (v_F)_{F\in\mathcal{F}_h}) \ \middle| \ \begin{array}{l} v_T \in \mathbb{P}^k(T) \ \ \forall T \in \mathcal{T}_h \\ v_F \in \mathbb{P}^k(F) \ \ \forall F \in \mathcal{F}_h \end{array} \right\}.$$

The interpolation operator $\underline{I}_h^k : W^{1,1}(\Omega) \to \underline{U}_h^k$ maps a function $v \in W^{1,1}(\Omega)$ on the vector of discrete unknowns $\underline{I}_h^k v$ defined as follows:

$$\underline{I}_h^k v \coloneqq ((\pi_T^k v_{|T})_{T\in\mathcal{T}_h}, (\pi_F^k v_{|F})_{F\in\mathcal{F}_h}).$$

For all $T \in \mathcal{T}_h$, we denote by $\underline{U}_T^k$ and $\underline{I}_T^k$ the restrictions of $\underline{U}_h^k$ and $\underline{I}_h^k$ to T, respectively, and, for all $\underline{v}_h \in \underline{U}_h^k$, we let $\underline{v}_T \coloneqq (v_T, (v_F)_{F\in\mathcal{F}_T}) \in \underline{U}_T^k$ denote the vector collecting the discrete unknowns attached to T and its faces. Furthermore, for all $\underline{v}_h \in \underline{U}_h^k$, we define the broken polynomial field $v_h \in \mathbb{P}^k(\mathcal{T}_h)$ obtained patching element unknowns, that is,

$$(v_h)_{|T} \coloneqq v_T \qquad \forall T \in \mathcal{T}_h.$$

For all $q \in (1,\infty)$, we define on $\underline{U}_h^k$ the $W^{1,q}(\Omega)$-like seminorm $\|\cdot\|_{1,q,h}$ such that, for all $\underline{v}_h \in \underline{U}_h^k$,

$$\|\underline{v}_h\|_{1,q,h} \coloneqq \left(\sum_{T\in\mathcal{T}_h} \|\underline{v}_T\|^q_{1,q,T} \right)^{\frac{1}{q}}, \tag{2.14a}$$

with for all $T \in \mathcal{T}_h$,

$$\|\underline{v}_T\|_{1,q,T} \coloneqq \left(\|\boldsymbol{\nabla} v_T\|^q_{L^q(T)^d} + \sum_{F\in\mathcal{F}_T} h_F^{1-q} \|v_F - v_T\|^q_{L^q(F)} \right)^{\frac{1}{q}}. \tag{2.14b}$$

The following boundedness property for $\underline{I}_T^k$ is proved in [50, Proposition 6.24]: For all $T \in \mathcal{T}_h$ and all $v \in W^{1,p}(T)$,

$$\|\underline{I}_T^k v\|_{1,p,T} \lesssim |v|_{W^{1,p}(T)}, \tag{2.15}$$

where the hidden constant depends only on d, the mesh regularity parameter, p, and k.

The discrete potential is sought in the subspace of $\underline{U}_h^k$ embedding the homogeneous boundary condition:

$$\underline{U}_{h,0}^k \coloneqq \left\{\underline{v}_h = ((v_T)_{T\in\mathcal{T}_h}, (v_F)_{F\in\mathcal{F}_h}) \in \underline{U}_h^k \;:\; v_F = 0 \quad \forall F \in \mathcal{F}_h^{\mathrm{b}}\right\}.$$

The following discrete Poincaré inequality descends from [48, Proposition 5.4] (cf. Remark 5.5 therein): For all $\underline{v}_h \in \underline{U}_{h,0}^k$,

$$\|v_h\|_{L^p(\Omega)} \lesssim \|\underline{v}_h\|_{1,p,h}. \tag{2.16}$$

By virtue of this inequality, $\|\cdot\|_{1,p,h}$ is a norm on $\underline{U}_{h,0}^k$ (reason as in [50, Corollary 2.16]).

2.4.2 Reconstructions

For all $T \in \mathcal{T}_h$, we define the *local gradient reconstruction* $\mathbf{G}_T^k : \underline{U}_T^k \to \mathbb{P}^k(T)^d$ such that, for all $\underline{v}_T \in \underline{U}_T^k$, and all $\boldsymbol{\tau} \in \mathbb{P}^k(T)^d$,

$$\int_T \mathbf{G}_T^k \underline{v}_T \cdot \boldsymbol{\tau} = \int_T \boldsymbol{\nabla} v_T \cdot \boldsymbol{\tau} + \sum_{F\in\mathcal{F}_T} \int_F (v_F - v_T)\,(\boldsymbol{\tau}\cdot\boldsymbol{n}_{TF}). \tag{2.17}$$

By design, the following relation holds (see [50, Section 7.2.5]): For all $v \in W^{1,1}(T)$,

$$\mathbf{G}_T^k(\underline{I}_T^k v) = \boldsymbol{\pi}_T^k(\boldsymbol{\nabla} v). \tag{2.18}$$

The *local potential reconstruction* $\mathrm{r}_T^{k+1} : \underline{U}_T^k \to \mathbb{P}^{k+1}(T)$ is such that, for all $\underline{v}_T \in \underline{U}_T^k$,

$$\begin{aligned} &\int_T (\boldsymbol{\nabla}\mathrm{r}_T^{k+1}\underline{v}_T - \mathbf{G}_T^k\underline{v}_T)\cdot\boldsymbol{\nabla} w = 0 \qquad \forall w \in \mathbb{P}^{k+1}(T),\\ &\int_T \mathrm{r}_T^{k+1}\underline{v}_T = \int_T v_T. \end{aligned} \tag{2.19}$$

Composed with the local interpolator, this reconstruction commutes with the elliptic projector; see [50, Sections 1.3 and 2.1.1–2.1.3].

2.4.3 Discrete diffusion function

The *discrete diffusion function* $\mathrm{a}_h : \underline{U}_h^k \times \underline{U}_h^k \to \mathbb{R}$, discretizing the function a defined by (2.7), is such that, for all $\underline{v}_h, \underline{w}_h \in \underline{U}_h^k$,

$$\mathrm{a}_h(\underline{w}_h, \underline{v}_h) \coloneqq \sum_{T\in\mathcal{T}_h} \left(\int_T \boldsymbol{\sigma}(\cdot, \mathbf{G}_T^k\underline{w}_T)\cdot\mathbf{G}_T^k\underline{v}_T + \mathrm{s}_T(\underline{w}_T, \underline{v}_T)\right). \tag{2.20}$$

Above, for all $T \in \mathcal{T}_h$, $\mathrm{s}_T : \underline{U}_T^k \times \underline{U}_T^k \to \mathbb{R}$ is a local stabilization function. To state the assumptions on this function, we introduce the mesh skeleton $\partial\mathcal{M}_h \coloneqq \bigcup_{F\in\mathcal{F}_h} \overline{F}$ and set

$$\begin{aligned} L^p(\partial\mathcal{M}_h) &\coloneqq \left\{\mu \,:\, \partial\mathcal{M}_h \to \mathbb{R} \,:\, \mu_{|F} \in L^p(F) \quad \forall F \in \mathcal{F}_h\right\}, \\ \|\mu\|_{L^p(\partial\mathcal{M}_h)} &\coloneqq \left(\sum_{T\in\mathcal{T}_h} h_T \sum_{F\in\mathcal{F}_T} \|\mu_{|F}\|_{L^p(F)}^p\right)^{\frac{1}{p}}. \end{aligned} \tag{2.21}$$

Assumption 4 (Local stabilization functions)**.** There exists $\zeta \in L^p(\partial\mathcal{M}_h; [0,\infty))$ such that, for all $T \in \mathcal{T}_h$ and all $\underline{v}_T, \underline{w}_T \in \underline{U}_T^k$,

$$\mathrm{s}_T(\underline{w}_T, \underline{v}_T) \coloneqq h_T \int_{\partial T} \mathrm{S}_T(\cdot, \Delta_{\partial T}^k \underline{w}_T)\, \Delta_{\partial T}^k \underline{v}_T, \tag{2.22}$$

where $\mathrm{S}_T : \partial T \times \mathbb{R} \to \mathbb{R}$ is a measurable function satisfying, for all $v, w \in \mathbb{R}$ and almost every $\boldsymbol{x} \in \partial T$,

$$|\mathrm{S}_T(\boldsymbol{x}, w) - \mathrm{S}_T(\boldsymbol{x}, v)| \lesssim \sigma_{\mathrm{hc}} \left(\zeta(\boldsymbol{x})^p + |w|^p + |v|^p\right)^{\frac{p-2}{p}} |w - v|, \tag{2.23a}$$

$$(\mathrm{S}_T(\boldsymbol{x}, w) - \mathrm{S}_T(\boldsymbol{x}, v))\,(w - v) \gtrsim \sigma_{\mathrm{hm}} \left(\zeta(\boldsymbol{x})^p + |w|^p + |v|^p\right)^{\frac{p-2}{p}} |w - v|^2, \tag{2.23b}$$

$$\mathrm{S}_T(\boldsymbol{x}, 0) = 0, \tag{2.23c}$$

while the boundary residual operator $\Delta_{\partial T}^k : \underline{U}_T^k \to L^p(\partial T)$ is such that, for all $\underline{v}_T \in \underline{U}_T^k$,

$$(\Delta_{\partial T}^k \underline{v}_T)_{|F} \coloneqq \frac{1}{h_T}\left[\pi_F^k(\mathrm{r}_T^{k+1}\underline{v}_T - v_F) - \pi_T^k(\mathrm{r}_T^{k+1}\underline{v}_T - v_T)\right] \qquad \forall F \in \mathcal{F}_T \tag{2.24}$$

with potential reconstruction r_T^{k+1} defined by (2.19).

Example 56 (Stabilization function)**.** Local stabilization functions that match Assumption 4 can be obtained setting, for all $T \in \mathcal{T}_h$, all $w \in \mathbb{R}$, and all $\boldsymbol{x} \in \partial T$,

$$\mathrm{S}_T(\boldsymbol{x}, w) \coloneqq \gamma_T \left(\zeta(\boldsymbol{x})^p + |w|^p\right)^{\frac{p-2}{p}} w, \tag{2.25}$$

with $\gamma_T \in [\sigma_{\mathrm{hm}}, \sigma_{\mathrm{hc}}]$ (see (2.3)). It can be checked that S_T is a non-degenerate (p,ζ)-power-framed function satisfying (2.23); see [27, Appendix A] for a proof.

Leveraging the results in [47], and additionally using $h_F \simeq h_T$ for all $F \in \mathcal{F}_T$, it can be checked that, for all $q \in (1,\infty)$,

$$\|\mathbf{G}_T^k \underline{v}_T\|_{L^q(T)^d}^q + h_T \|\Delta_{\partial T}^k \underline{v}_T\|_{L^q(\partial T)}^q \simeq \|\underline{v}_T\|_{1,q,T}^q \qquad \forall \underline{v}_T \in \underline{U}_T^k. \tag{2.26}$$

Additionally, $\Delta_{\partial T}^k$ is polynomially consistent, i.e.,

$$\Delta_{\partial T}^k(\underline{I}_T^k w) = 0 \qquad \forall w \in \mathbb{P}^{k+1}(T). \tag{2.27}$$

2.4.4 Discrete problem

The discrete problem reads: Find $\underline{u}_h \in \underline{U}_{h,0}^k$ such that

$$\mathrm{a}_h(\underline{u}_h, \underline{v}_h) = \int_\Omega f v_h \qquad \forall \underline{v}_h \in \underline{U}_{h,0}^k. \tag{2.28}$$

2.5 Error analysis

In this section, after establishing a stability result for the discrete function a_h, we prove the error estimate that constitutes the main result of this paper.

2.5.1 Hölder monotonicity of the discrete diffusion function

We recall the following inequality between sums of power (see [27, Eq. (15)]): Let an integer $n \geq 1$ and a real number $m \in (0, \infty)$ be given. Then, for all $a_1, \ldots, a_n \in (0, \infty)$, we have

$$n^{-(m-1)^\ominus} \sum_{i=1}^n a_i^m \leq \left(\sum_{i=1}^n a_i \right)^m \leq n^{(m-1)^\oplus} \sum_{i=1}^n a_i^m. \tag{2.29}$$

Lemma 57 (Hölder monotonicity of a_h)**.** *For all $\underline{v}_h, \underline{w}_h \in \underline{U}_h^k$, setting $\underline{e}_h \coloneqq \underline{v}_h - \underline{w}_h$, it holds*

$$\begin{aligned} \|\underline{e}_h\|_{1,p,h}^2 \lesssim \sigma_{\mathrm{hm}}^{-1} \left(\|\delta\|_{L^p(\Omega)}^p + \|\zeta\|_{L^p(\partial\mathcal{M}_h)}^p + \|\underline{v}_h\|_{1,p,h}^p + \|\underline{w}_h\|_{1,p,h}^p \right)^{\frac{2-p}{p}} \\ \times \left(\mathrm{a}_h(\underline{v}_h, \underline{e}_h) - \mathrm{a}_h(\underline{w}_h, \underline{e}_h) \right). \end{aligned} \tag{2.30}$$

Proof. Let $T \in \mathcal{T}_h$. Using the Hölder monotonicity (2.2d) of $\boldsymbol{\sigma}$ and the $\left(\frac{2}{2-p}, \frac{2}{p}\right)$-Hölder inequality, we get

$$\begin{aligned} \sigma_{\mathrm{hm}}^{\frac{p}{2}} \|\mathbf{G}_T^k \underline{e}_T\|_{L^p(T)^d}^p &\leq \int_T \left(\delta^p + |\mathbf{G}_T^k \underline{v}_T|^p + |\mathbf{G}_T^k \underline{w}_T|^p \right)^{\frac{2-p}{2}} \\ &\quad \times \left[\left(\boldsymbol{\sigma}(\cdot, \mathbf{G}_T^k \underline{v}_T) - \boldsymbol{\sigma}(\cdot, \mathbf{G}_T^k \underline{w}_T) \right) \cdot \mathbf{G}_T^k \underline{e}_T \right]^{\frac{p}{2}} \\ &\leq \left(\|\delta\|_{L^p(T)}^p + \|\mathbf{G}_T^k \underline{v}_T\|_{L^p(T)^d}^p + \|\mathbf{G}_T^k \underline{w}_T\|_{L^p(T)^d}^p \right)^{\frac{2-p}{2}} \\ &\quad \times \left[\int_T \left(\boldsymbol{\sigma}(\cdot, \mathbf{G}_T^k \underline{v}_T) - \boldsymbol{\sigma}(\cdot, \mathbf{G}_T^k \underline{w}_T) \right) \cdot \mathbf{G}_T^k \underline{e}_T \right]^{\frac{p}{2}} \\ &\lesssim \left(\|\delta\|_{L^p(T)}^p + \|\underline{v}_T\|_{1,p,T}^p + \|\underline{w}_T\|_{1,p,T}^p \right)^{\frac{2-p}{2}} \\ &\quad \times \left[\int_T \left(\boldsymbol{\sigma}(\cdot, \mathbf{G}_T^k \underline{v}_T) - \boldsymbol{\sigma}(\cdot, \mathbf{G}_T^k \underline{w}_T) \right) \cdot \mathbf{G}_T^k \underline{e}_T \right]^{\frac{p}{2}}, \end{aligned} \tag{2.31}$$

where the conclusion follows from the seminorm equivalence (2.26). Similarly, the Hölder monotonicity (2.23b) of S_T followed by the same reasoning as above yields,

$$\begin{aligned}\sigma_{\mathrm{hm}}^{\frac{p}{2}} h_T \|\Delta_{\partial T}^k \underline{e}_T\|_{L^p(\mathcal{F}_T)}^p \lesssim \left(h_T\|\zeta\|_{L^p(\partial T)}^p + \|\underline{v}_T\|_{1,p,T}^p + \|\underline{w}_T\|_{1,p,T}^p\right)^{\frac{2-p}{2}} \\ \times \left(\mathrm{s}_T(\underline{v}_T, \underline{e}_T) - \mathrm{s}_T(\underline{w}_T, \underline{e}_T)\right)^{\frac{p}{2}}.\end{aligned} \tag{2.32}$$

Combining the norm equivalence (2.26) with (2.31) and (2.32) and using (2.29) yields

$$\begin{aligned}\sigma_{\mathrm{hm}}^{\frac{p}{2}} \|\underline{e}_T\|_{1,p,T}^p \lesssim \left(\|\delta\|_{L^p(T)}^p + h_T\|\zeta\|_{L^p(\partial T)}^p + \|\underline{v}_T\|_{1,p,T}^p + \|\underline{w}_T\|_{1,p,T}^p\right)^{\frac{2-p}{2}} \\ \times \left(\mathrm{a}_T(\underline{v}_T, \underline{e}_T) - \mathrm{a}_T(\underline{w}_T, \underline{e}_T)\right)^{\frac{p}{2}}.\end{aligned}$$

Summing over $T \in \mathcal{T}_h$, applying the discrete $\left(\frac{2}{2-p}, \frac{2}{p}\right)$-Hölder inequality, and raising to the power $\frac{2}{p}$ yields (2.30). □

Remark 58 (Well-posedness and a priori estimate). Using standard techniques (cf. [48, Theorem 4.5], see also [27, Theorem 17]), it can be proved that there exists a unique solution $\underline{u}_h \in \underline{U}_{h,0}^k$ to the discrete problem (2.28). Additionally, it can be shown in a similar way as for the continuous case (cf. Proposition 55) that the following a priori bound holds:

$$\begin{aligned}\|\underline{u}_h\|_{1,p,h} \lesssim \left(\sigma_{\mathrm{hm}}^{-1}\|f\|_{L^{p'}(\Omega)}\right)^{\frac{1}{p-1}} \\ + \min\left(\left(\|\delta\|_{L^p(\mathcal{T}_h)}^p + \|\zeta\|_{L^p(\partial\mathcal{M}_h)}^p\right)^{\frac{1}{p}}; \sigma_{\mathrm{hm}}^{-1}\left(\|\delta\|_{L^p(\mathcal{T}_h)}^p + \|\zeta\|_{L^p(\partial\mathcal{M}_h)}^p\right)^{\frac{2-p}{p}}\|f\|_{L^{p'}(\Omega)}\right).\end{aligned} \tag{2.33}$$

2.5.2 Error estimate

Theorem 59 (Error estimate)**.** *Let $u \in U$ and $\underline{u}_h \in \underline{U}_{h,0}^k$ solve (2.6) and (2.28), respectively. Assume $u \in W^{k+2,p}(\mathcal{T}_h)$ and $\boldsymbol{\sigma}(\cdot, \boldsymbol{\nabla} u) \in W^{1,p'}(\Omega)^d \cap W^{k+1,p'}(\mathcal{T}_h)^d$. Then, under Assumptions 3 and 4,*

$$\begin{aligned}\|\underline{u}_h - \underline{I}_h^k u\|_{1,p,h} \lesssim \mathcal{N}_f h^{k+1} |\boldsymbol{\sigma}(\cdot, \boldsymbol{\nabla} u)|_{W^{k+1,p'}(\mathcal{T}_h)^d} \\ + \mathcal{N}_f \sigma_{\mathrm{hc}} \left[\sum_{T\in\mathcal{T}_h} \left(\min(\eta_T; 1)^{2-p}\, h_T^{(k+1)(p-1)} |u|_{W^{k+2,p}(T)}^{p-1}\right)^{p'}\right]^{\frac{1}{p'}},\end{aligned} \tag{2.34}$$

where, for all $T \in \mathcal{T}_h$, defining

$$\mathfrak{D}_T \coloneqq \min\left(\operatorname*{ess\,inf}_{\boldsymbol{x}\in T}\left(\delta(\boldsymbol{x})+|\boldsymbol{\nabla} u(\boldsymbol{x})|\right); \operatorname*{ess\,inf}_{\boldsymbol{x}\in\partial T}\zeta(\boldsymbol{x})\right), \tag{2.35}$$

we have set

$$\eta_T \coloneqq \frac{h_T^{k+1}|u|_{W^{k+2,p}(T)}}{|T|^{\frac{1}{p}}\mathfrak{D}_T} \tag{2.36}$$

with the convention that $\eta_T = \infty$ if $\mathfrak{D}_T = 0 < |u|_{W^{k+2,p}(T)}$, and $\eta_T = 0$ if $\mathfrak{D}_T = |u|_{W^{k+2,p}(T)} = 0$, and where

$$\mathcal{N}_f \coloneqq \sigma_{\mathrm{hm}}^{-1}\left[\|\delta\|_{L^p(\Omega)} + \|\zeta\|_{L^p(\partial\mathcal{M}_h)} + \left(\sigma_{\mathrm{hm}}^{-1}\|f\|_{L^{p'}(\Omega)}\right)^{\frac{1}{p-1}}\right]^{2-p}.$$

Remark 60 (Convergence rates). For any $T \in \mathcal{T}_h$, the local *flux degeneracy parameter* $\mathfrak{D}_T$ defined in (2.35) is a measure of the local degeneracy of the flux and the stabilization function: the closer it is to zero, the more degenerate the model is. The dimensionless number η_T defined in (2.36) determines the convergence rate of the contribution to the approximation error stemming from T. If $\eta_T \geq 1$ (*locally degenerate case*), then the element T contributes to the error with a term in $h_T^{(k+1)(p-1)}$. If $\eta_T \leq h_T^{k+1}|u|_{W^{k+2,p}(T)}|T|^{-\frac{1}{p}}$, i.e. $\mathfrak{D}_T \geq 1$ (*locally non-degenerate case*), the contribution to the error is in h_T^{k+1}. The case $\eta_T \in (h_T^{k+1}|u|_{W^{k+2,p}(T)}|T|^{-\frac{1}{p}}, 1)$ corresponds to intermediate rates of convergence.

At the global level, defining the number $\eta_h \coloneqq \max_{T\in\mathcal{T}_h}\eta_T$, the bound $h_T \leq h$ together with the error estimate (2.34) yields

$$\begin{aligned}\|\underline{u}_h - \underline{I}_h^k u\|_{1,p,h} \lesssim \mathcal{N}_f\Big(&h^{k+1}|\boldsymbol{\sigma}(\cdot,\boldsymbol{\nabla} u)|_{W^{k+1,p'}(\mathcal{T}_h)^d}\\ &+ \sigma_{\mathrm{hc}}\min(\eta_h;1)^{2-p}\,h^{(k+1)(p-1)}|u|^{p-1}_{W^{k+2,p}(\mathcal{T}_h)}\Big).\end{aligned} \tag{2.37}$$

As a consequence, if $\eta_h \geq 1$ (*globally degenerate case*), then the convergence rate is $(k+1)(p-1)$. If $\eta_h \leq h^{k+1}|u|_{W^{k+2,p}(\mathcal{T}_h)}$ (*globally non-degenerate case*), the convergence rate is $k+1$. Finally, the case $\eta_h \in (h^{k+1}|u|_{W^{k+2,p}(\mathcal{T}_h)}, 1)$ corresponds to intermediate rates of convergence. This is the finest global estimate that can be obtained from the local one. However, for practical purposes, if $u \in W^{k+2,\infty}(\mathcal{T}_h)$ then we can replace η_h in (2.37) by the larger number

$$\tilde{\eta}_h \coloneqq \frac{|u|_{W^{k+2,\infty}(\mathcal{T}_h)}h^{k+1}}{\min_{T\in\mathcal{T}_h}\mathfrak{D}_T} = \frac{|u|_{W^{k+2,\infty}(\mathcal{T}_h)}h^{k+1}}{\min\left(\operatorname{ess\,inf}_\Omega(\delta+|\boldsymbol{\nabla} u|); \operatorname{ess\,inf}_{\partial\mathcal{M}_h}\zeta\right)}, \tag{2.38}$$

with the same convention as above regarding fractions $C/0$ and $0/0$. The convergence rate will result from the position of $\tilde{\eta}_h$ with respect to $h^{k+1}|u|_{W^{k+2,\infty}(\mathcal{T}_h)}$ and 1, and $\tilde{\eta}_h \le h^{k+1}|u|_{W^{k+2,\infty}(\mathcal{T}_h)}$ (non-degenerate case) is equivalent to

$$\min\left(\operatorname*{ess\,inf}_{\Omega}(\delta + |\boldsymbol{\nabla} u|)\,; \operatorname*{ess\,inf}_{\partial\mathcal{M}_h}\zeta\right) \ge 1,$$

which is consistent with the local requirement stated above.

Proof of Theorem 59. Define the consistency error as the linear form $\mathcal{E}_h : \underline{U}_h^k \to \mathbb{R}$ such that, for all $\underline{v}_h \in \underline{U}_h^k$,

$$\mathcal{E}_h(\underline{v}_h) \coloneqq \int_\Omega \boldsymbol{\nabla}\cdot\boldsymbol{\sigma}(\cdot,\boldsymbol{\nabla} u)\, v_h + \mathrm{a}_h(\underline{I}_h^k u, \underline{v}_h). \tag{2.39}$$

Let, for the sake of brevity, $\underline{\hat{u}}_h \coloneqq \underline{I}_h^k u$ and $\underline{e}_h \coloneqq \underline{u}_h - \underline{\hat{u}}_h \in \underline{U}_{h,0}^k$.

(i) *Estimate of the consistency error.* Expanding a_h according to its definition (2.20) in the expression (2.39) of $\mathcal{E}_h$, inserting

$$\sum_{T\in\mathcal{T}_h}\left(\int_T \boldsymbol{\pi}_T^k\boldsymbol{\sigma}(\cdot,\boldsymbol{\nabla} u)\cdot\mathbf{G}_T^k\underline{e}_T - \int_T \boldsymbol{\sigma}(\cdot,\boldsymbol{\nabla} u)\cdot\mathbf{G}_T^k\underline{e}_T\right) = 0$$

(the equality is a consequence of the definition of $\boldsymbol{\pi}_T^k$), and rearranging, we obtain

$$\begin{aligned}\mathcal{E}_h(\underline{e}_h) = \underbrace{\int_\Omega \boldsymbol{\nabla}\cdot\boldsymbol{\sigma}(\cdot,\boldsymbol{\nabla} u)\, e_h + \sum_{T\in\mathcal{T}_h}\int_T \boldsymbol{\pi}_T^k\boldsymbol{\sigma}(\cdot,\boldsymbol{\nabla} u)\cdot\mathbf{G}_T^k\underline{e}_T}_{\mathcal{T}_1}\\ + \underbrace{\sum_{T\in\mathcal{T}_h}\int_T\left[\boldsymbol{\sigma}(\cdot,\mathbf{G}_T^k\underline{\hat{u}}_T) - \boldsymbol{\sigma}(\cdot,\boldsymbol{\nabla} u)\right]\cdot\mathbf{G}_T^k\underline{e}_T}_{\mathcal{T}_2} + \underbrace{\sum_{T\in\mathcal{T}_h}\mathrm{s}_T(\underline{\hat{u}}_T,\underline{e}_T)}_{\mathcal{T}_3}.\end{aligned} \tag{2.40}$$

We proceed to estimate the terms in the right-hand side.

For the first term, we start by noticing that

$$\sum_{T\in\mathcal{T}_h}\sum_{F\in\mathcal{F}_T}\int_F e_F\,(\boldsymbol{\sigma}(\cdot,\boldsymbol{\nabla} u)\cdot\boldsymbol{n}_{TF}) = 0 \tag{2.41}$$

as a consequence of the continuity of the normal trace of $\boldsymbol{\sigma}(\cdot,\boldsymbol{\nabla} u)$ together with the single-valuedness of e_F across each interface $F \in \mathcal{F}_h^{\mathrm{i}}$ and the fact that $e_F = 0$ for every boundary face $F \in \mathcal{F}_h^{\mathrm{b}}$ (see [50, Corollary 1.19]). Using an element by element

integration by parts on the first term of $\mathcal{T}_1$ along with the definition (2.17) of $\mathbf{G}_T^k$, we can write

$$\begin{aligned}\mathcal{T}_1 &= \cancel{\sum_{T\in\mathcal{T}_h}\int_T \left[\boldsymbol{\pi}_T^k\boldsymbol{\sigma}(\cdot,\boldsymbol{\nabla}u) - \boldsymbol{\sigma}(\cdot,\boldsymbol{\nabla}u)\right]\cdot\boldsymbol{\nabla}e_T} \\ &\quad + \sum_{T\in\mathcal{T}_h}\sum_{F\in\mathcal{F}_T}\left[\int_F (e_F - e_T)\left(\boldsymbol{\pi}_T^k\boldsymbol{\sigma}(\cdot,\boldsymbol{\nabla}u)\cdot\boldsymbol{n}_{TF}\right) + \int_F e_T\left(\boldsymbol{\sigma}(\cdot,\boldsymbol{\nabla}u)\cdot\boldsymbol{n}_{TF}\right)\right] \\ &= \sum_{T\in\mathcal{T}_h}\sum_{F\in\mathcal{F}_T}\int_F (e_F - e_T)\left[\boldsymbol{\pi}_T^k\boldsymbol{\sigma}(\cdot,\boldsymbol{\nabla}u) - \boldsymbol{\sigma}(\cdot,\boldsymbol{\nabla}u)\right]\cdot\boldsymbol{n}_{TF},\end{aligned}$$

where we have used the definition of $\boldsymbol{\pi}_T^k$ together with the fact that $\boldsymbol{\nabla}e_T \in \mathbb{P}^{k-1}(T)^d \subset \mathbb{P}^k(T)^d$ to cancel the term in the first line, and we have inserted (2.41) and rearranged to conclude. Hölder inequalities give

$$\begin{aligned}|\mathcal{T}_1| &\lesssim \left(\sum_{T\in\mathcal{T}_h} h_T\|\boldsymbol{\sigma}(\cdot,\boldsymbol{\nabla}u) - \boldsymbol{\pi}_T^k\boldsymbol{\sigma}(\cdot,\boldsymbol{\nabla}u)\|_{L^{p'}(\partial T)^d}^{p'}\right)^{\frac{1}{p'}} \\ &\quad\times\left(\sum_{T\in\mathcal{T}_h}\sum_{F\in\mathcal{F}_T} h_F^{1-p}\|e_F - e_T\|_{L^p(F)}^p\right)^{\frac{1}{p}} \\ &\lesssim h^{k+1}|\boldsymbol{\sigma}(\cdot,\boldsymbol{\nabla}u)|_{W^{k+1,p'}(\mathcal{T}_h)^d}\|\underline{e}_h\|_{1,p,h},\end{aligned} \tag{2.42}$$

where we have used the $(k+1,p')$-trace approximation properties (2.13b) of $\boldsymbol{\pi}_T^k$ along with $h_T \le h$ for the first factor, and the definition (2.14) of $\|\cdot\|_{1,p,h}$ for the second.

We move on to the next term $\mathcal{T}_2$. Let an element $T \in \mathcal{T}_h$ be fixed. If $\eta_T \ge 1$, using the (p',p)-Hölder inequality together with the equivalence (2.26), we obtain

$$\begin{aligned}&\left|\int_T \left[\boldsymbol{\sigma}(\cdot,\mathbf{G}_T^k\underline{\hat{u}}_T) - \boldsymbol{\sigma}(\cdot,\boldsymbol{\nabla}u)\right]\cdot\mathbf{G}_T^k\underline{e}_T\right| \\ &\quad\le \|\boldsymbol{\sigma}(\cdot,\mathbf{G}_T^k\underline{\hat{u}}_T) - \boldsymbol{\sigma}(\cdot,\boldsymbol{\nabla}u)\|_{L^{p'}(T)^d}\|\underline{e}_T\|_{1,p,T} \\ &\quad\le \sigma_{\mathrm{hc}}\left\|\left(\delta + |\boldsymbol{\pi}_T^k(\boldsymbol{\nabla}u)| + |\boldsymbol{\nabla}u|\right)^{p-2}|\boldsymbol{\pi}_T^k(\boldsymbol{\nabla}u) - \boldsymbol{\nabla}u|\right\|_{L^{p'}(T)}\|\underline{e}_T\|_{1,p,T} \\ &\quad\le \sigma_{\mathrm{hc}}\|\boldsymbol{\pi}_T^k(\boldsymbol{\nabla}u) - \boldsymbol{\nabla}u\|_{L^p(T)^d}^{p-1}\|\underline{e}_T\|_{1,p,T} \\ &\quad\lesssim \sigma_{\mathrm{hc}}h_T^{(k+1)(p-1)}|u|_{W^{k+2,p}(T)}^{p-1}\|\underline{e}_T\|_{1,p,T} \\ &\quad= \sigma_{\mathrm{hc}}\min(\eta_T;1)^{2-p}\,h_T^{(k+1)(p-1)}|u|_{W^{k+2,p}(T)}^{p-1}\|\underline{e}_T\|_{1,p,T},\end{aligned} \tag{2.43}$$

where we have used the continuity (2.2c) of $\boldsymbol{\sigma}$ together with the commutation property (2.18) of the discrete gradient and (2.29) in the second bound, inequality (2.4) with

$x = \boldsymbol{\pi}_T^k(\boldsymbol{\nabla} u)$, $y = \boldsymbol{\nabla} u$, and $\alpha = \delta$ in the third bound, and the $(k+1, p, 0)$-approximation properties of π_T^k to conclude.

On the other hand, if $\eta_T < 1$ then, using the (p, p')-Hölder inequality together with the boundedness (2.26), we infer

$$\begin{aligned}
&\left|\int_T \left[\boldsymbol{\sigma}(\cdot, \mathbf{G}_T^k \hat{\underline{u}}_T) - \boldsymbol{\sigma}(\cdot, \boldsymbol{\nabla} u)\right] \cdot \mathbf{G}_T^k \underline{e}_T\right| \\
&\quad \le \|\boldsymbol{\sigma}(\cdot, \mathbf{G}_T^k \hat{\underline{u}}_T) - \boldsymbol{\sigma}(\cdot, \boldsymbol{\nabla} u)\|_{L^p(T)^d} \|\underline{e}_T\|_{1,p',T} \\
&\quad \lesssim \sigma_{\mathrm{hc}} \left\| \left(\delta + |\boldsymbol{\pi}_T^k(\boldsymbol{\nabla} u)| + |\boldsymbol{\nabla} u|\right)^{p-2} |\boldsymbol{\pi}_T^k(\boldsymbol{\nabla} u) - \boldsymbol{\nabla} u| \right\|_{L^p(T)} |T|^{\frac{p-2}{p}} \|\underline{e}_T\|_{1,p,T} \\
&\quad \le \sigma_{\mathrm{hc}} \mathfrak{D}_T^{p-2} |T|^{\frac{p-2}{p}} \|\boldsymbol{\pi}_T^k(\boldsymbol{\nabla} u) - \boldsymbol{\nabla} u\|_{L^p(T)^d} \|\underline{e}_T\|_{1,p,T} \\
&\quad \lesssim \sigma_{\mathrm{hc}} \mathfrak{D}_T^{p-2} |T|^{\frac{p-2}{p}} h_T^{k+1} |u|_{W^{k+2,p}(T)} \|\underline{e}_T\|_{1,p,T} \\
&\quad = \sigma_{\mathrm{hc}} \min(\eta_T; 1)^{2-p} h_T^{(k+1)(p-1)} |u|_{W^{k+2,p}(T)}^{p-1} \|\underline{e}_T\|_{1,p,T},
\end{aligned} \tag{2.44}$$

where we passed to the third line as in (2.43) additionally using the bound $\|\underline{e}_T\|_{1,p',T} \lesssim |T|^{\frac{p-2}{p}} \|\underline{e}_T\|_{1,p,T}$ (see [48, Lemmas 5.1 and 5.2]), used in the fourth line the fact that $\mathbb{R} \ni x \mapsto x^{p-2} \in \mathbb{R}$ is non-increasing to infer that $\left(\delta + |\boldsymbol{\pi}_T^k(\boldsymbol{\nabla} u)| + |\boldsymbol{\nabla} u|\right)^{p-2} \le (\delta + |\boldsymbol{\nabla} u|)^{p-2} \le \mathfrak{D}_T^{p-2}$ almost everywhere in T, and concluded as above.

Gathering the estimates (2.43) and (2.44) and using a discrete Hölder inequality yields

$$|\mathcal{T}_2| \lesssim \sigma_{\mathrm{hc}} \left[\sum_{T \in \mathcal{T}_h} \left(\min(\eta_T; 1)^{2-p} h_T^{(k+1)(p-1)} |u|_{W^{k+2,p}(T)}^{p-1}\right)^{p'}\right]^{\frac{1}{p'}} \|\underline{e}_h\|_{1,p,h}. \tag{2.45}$$

Let us finally consider $\mathcal{T}_3$. Let $T \in \mathcal{T}_h$, set $\check{\underline{u}}_T := \underline{I}_T^k(\pi_T^{k+1} u)$ for the sake of brevity, and observe that $\mathrm{S}_T\left(\cdot, \Delta_{\partial T}^k \check{\underline{u}}_T\right) = 0$ thanks to the polynomial consistency (2.27) of $\Delta_{\partial T}^k$ and the property (2.23c) of S_T.

If $\eta_T \ge 1$, using the (p', p)-Hölder inequality together with the boundedness property (2.26) (with $q = p$), we infer

$$\begin{aligned}
|\mathrm{s}_T(\hat{\underline{u}}_T, \underline{e}_T)| &\lesssim h_T^{\frac{1}{p'}} \left\|\mathrm{S}_T\left(\cdot, \Delta_{\partial T}^k \hat{\underline{u}}_T\right) - \mathrm{S}_T\left(\cdot, \Delta_{\partial T}^k \check{\underline{u}}_T\right)\right\|_{L^{p'}(\partial T)} \|\underline{e}_T\|_{1,p,T} \\
&\lesssim \sigma_{\mathrm{hc}} h_T^{\frac{1}{p'}} \left\| \left(\zeta + |\Delta_{\partial T}^k \hat{\underline{u}}_T| + |\Delta_{\partial T}^k \check{\underline{u}}_T|\right)^{p-2} \Delta_{\partial T}^k (\hat{\underline{u}}_T - \check{\underline{u}}_T) \right\|_{L^{p'}(\partial T)} \|\underline{e}_T\|_{1,p,T} \\
&\le \sigma_{\mathrm{hc}} h_T^{\frac{1}{p'}} \|\Delta_{\partial T}^k (\hat{\underline{u}}_T - \check{\underline{u}}_T)\|_{L^p(\partial T)}^{p-1} \|\underline{e}_T\|_{1,p,T} \\
&\lesssim \sigma_{\mathrm{hc}} h_T^{(k+1)(p-1)} |u|_{W^{k+2,p}(T)}^{p-1} \|\underline{e}_T\|_{1,p,T} \\
&= \sigma_{\mathrm{hc}} \min(\eta_T; 1)^{2-p} h_T^{(k+1)(p-1)} |u|_{W^{k+2,p}(T)}^{p-1} \|\underline{e}_T\|_{1,p,T},
\end{aligned} \tag{2.46}$$

where we have used the continuity (2.23a) of S_T together with (2.29) to pass to the second line, inequality (2.4) with $x = \Delta_{\partial T}^k \hat{\underline{u}}_T$, $y = \Delta_{\partial T}^k \check{\underline{u}}_T$ and $\alpha = \zeta$ in the third line, and the boundedness (2.26) of $\Delta_{\partial T}^k$ and (2.15) of $\underline{I}_T^k$ together with the $(k+1,p,1)$-approximation properties of π_T^{k+1} to conclude by writing $h_T^{\frac{1}{p}} \|\Delta_{\partial T}^k(\hat{\underline{u}}_T - \check{\underline{u}}_T)\|_{L^p(\partial T)} \lesssim \|\underline{I}_T^k(u - \pi_T^{k+1}u)\|_{1,p,T} \lesssim |u - \pi_T^{k+1}u|_{W^{1,p}(T)} \lesssim h_T^{k+1}|u|_{W^{k+2,p}(T)}$.

Otherwise, $\eta_T < 1$ and using the (p,p')-Hölder inequality together with boundedness property (2.26) (with $q = p'$), we infer as above that

$$
\begin{aligned}
|\mathrm{s}_T(\hat{\underline{u}}_T, \underline{e}_T)| &\lesssim h_T^{\frac{1}{p}} \left\| \mathrm{S}_T\big(\cdot, \Delta_{\partial T}^k \hat{\underline{u}}_T\big) - \mathrm{S}_T\big(\cdot, \Delta_{\partial T}^k \check{\underline{u}}_T\big) \right\|_{L^p(\partial T)} \|\underline{e}_T\|_{1,p',T} \\
&\lesssim \sigma_{\mathrm{hc}} h_T^{\frac{1}{p}} \left\| \Big(\zeta + |\Delta_{\partial T}^k \hat{\underline{u}}_T| + |\Delta_{\partial T}^k \check{\underline{u}}_T|\Big)^{p-2} \Delta_{\partial T}^k(\hat{\underline{u}}_T - \check{\underline{u}}_T) \right\|_{L^p(\partial T)} |T|^{\frac{p-2}{p}} \|\underline{e}_T\|_{1,p,T} \\
&\le \sigma_{\mathrm{hc}} \mathfrak{D}_T^{p-2} |T|^{\frac{p-2}{p}} h_T^{\frac{1}{p}} \|\Delta_{\partial T}^k(\hat{\underline{u}}_T - \check{\underline{u}}_T)\|_{L^p(\partial T)} \|\underline{e}_T\|_{1,p,T} \\
&\lesssim \sigma_{\mathrm{hc}} \mathfrak{D}_T^{p-2} |T|^{\frac{p-2}{p}} h_T^{k+1} |u|_{W^{k+2,p}(T)} \|\underline{e}_T\|_{1,p,T} \\
&= \sigma_{\mathrm{hc}} \min(\eta_T; 1)^{2-p} h_T^{(k+1)(p-1)} |u|_{W^{k+2,p}(T)}^{p-1} \|\underline{e}_T\|_{1,p,T},
\end{aligned}
\tag{2.47}
$$

where the second inequality follows as before from the bound $\|\underline{e}_T\|_{1,p',T} \lesssim |T|^{\frac{p-2}{p}} \|\underline{e}_T\|_{1,p,T}$ (see [48, Lemmas 5.1 and 5.2]), the third inequality is a consequence of the monotonicity of $\mathbb{R} \ni x \mapsto x^{p-2} \in \mathbb{R}$ that yields $\big(\zeta + |\Delta_{\partial T}^k \hat{\underline{u}}_T| + |\Delta_{\partial T}^k \check{\underline{u}}_T|\big)^{p-2} \le \zeta^{p-2} \le \mathfrak{D}_T^{p-2}$ almost everywhere in ∂T, and the conclusion is obtained as in (2.46).

Following then the same reasoning that lead to (2.45), we obtain for the third term

$$
|\mathcal{T}_3| \lesssim \sigma_{\mathrm{hc}} \left[\sum_{T \in \mathcal{T}_h} \Big(\min(\eta_T; 1)^{2-p} h_T^{(k+1)(p-1)} |u|_{W^{k+2,p}(T)}^{p-1} \Big)^{p'} \right]^{\frac{1}{p'}} \|\underline{e}_h\|_{1,p,h}. \tag{2.48}
$$

Plugging the bounds (2.42), (2.45), and (2.48) into (2.40) yields

$$
\begin{aligned}
|\mathcal{E}_h(\underline{e}_h)| &\lesssim h^{k+1} |\boldsymbol{\sigma}(\cdot, \boldsymbol{\nabla} u)|_{W^{k+1,p'}(\mathcal{T}_h)^d} \|\underline{e}_h\|_{1,p,h} \\
&\quad + \sigma_{\mathrm{hc}} \left[\sum_{T \in \mathcal{T}_h} \Big(\min(\eta_T; 1)^{2-p} h_T^{(k+1)(p-1)} |u|_{W^{k+2,p}(T)}^{p-1} \Big)^{p'} \right]^{\frac{1}{p'}} \|\underline{e}_h\|_{1,p,h}.
\end{aligned}
\tag{2.49}
$$

(ii) *Error estimate.* Using the Hölder monotonicity (2.30) of a_h, we get

$$
\begin{aligned}
\|\underline{e}_h\|_{1,p,h}^2 &\lesssim \sigma_{\mathrm{hm}}^{-1} \Big(\|\delta\|_{L^p(\Omega)}^p + \|\zeta\|_{L^p(\partial\mathcal{M}_h)}^p + \|\underline{u}_h\|_{1,p,h}^p + \|\hat{\underline{u}}_h\|_{1,p,h}^p \Big)^{\frac{2-p}{p}} \qquad (2.50) \\
&\qquad \times \big[\mathrm{a}_h(\underline{u}_h, \underline{e}_h) - \mathrm{a}_h(\hat{\underline{u}}_h, \underline{e}_h) \big] \\
&\lesssim \mathcal{N}_f \big[\mathrm{a}_h(\underline{u}_h, \underline{e}_h) - \mathrm{a}_h(\hat{\underline{u}}_h, \underline{e}_h) \big], \qquad (2.51)
\end{aligned}
$$

where we have used the a priori bound (2.33) on the discrete solution along with the boundedness (2.15) of the global interpolator, the a priori bound (2.8) on the continuous solution, and (2.29) to conclude. Furthermore, using the equation (2.28) (with $\underline{v}_h = \underline{e}_h$), and the fact that $f = -\boldsymbol{\nabla}\cdot\boldsymbol{\sigma}(\cdot, \boldsymbol{\nabla} u)$ almost everywhere in Ω, we see that

$$\mathrm{a}_h(\underline{u}_h, \underline{e}_h) - \mathrm{a}_h(\hat{\underline{u}}_h, \underline{e}_h) = \int_\Omega f e_h - \mathrm{a}_h(\hat{\underline{u}}_h, \underline{e}_h) = -\mathcal{E}_h(\underline{e}_h). \tag{2.52}$$

Hence, plugging (2.52) into (2.51), recalling the bound (2.49) on the consistency error, and simplifying, (2.34) follows. □

2.6 Numerical examples

In this section, we give some numerical results to confirm Theorem 59. We consider the domain $\Omega = (0,1)^2$ and define $\boldsymbol{\sigma}$ as the Carreau–Yasuda law of Example 54 with $p \in \{1.25, 1.5, 1.75\}$ and $\mu = a = 1$. The degeneracy parameter δ and the exact solution u will depend on the considered case. The stabilization functions are defined by (2.25) with ζ such that the local flux degeneracy number $\mathfrak{D}_T$ introduced in (2.36) is equal to the first argument of its min for all $T \in \mathcal{T}_h$, so that ζ does not influence the error estimates. The function f and the Dirichlet boundary condition are inferred from the exact solution. In all cases, except for the non-homogeneous boundary condition, these solutions match the assumptions required in Theorem 59. We consider the HHO scheme for $k \in \{1, 2, 3\}$ on a triangular mesh family.

2.6.1 Non-degenerate flux

We consider nonzero constant degeneracy parameters $\delta \in \{1, 0.1, 10^{-2}, 5\cdot 10^{-4}\}$, and the potential u is given by

$$u(x_1, x_2) = \sin(\pi x_1)\sin(\pi x_2) \quad \forall (x_1, x_2) \in \Omega.$$

Thus, the dimensionless number $\tilde{\eta}_h$ defined in (2.38) satisfies

$$\tilde{\eta}_h = \mu_h(\delta) \coloneqq \frac{2^{\frac{k-1}{2}}\pi^k h^{k+1}}{\delta}. \tag{2.53}$$

Therefore, we should observe a $(k+1)(p-1)$ pre-asymptotic order of convergence until the size of the mesh is small enough compared to δ so that the convergence rate switches to $k+1$ (see Remark 60).

Indeed, in Figure 2.1 and Table 2.1, we can see for $k \in \{1, 2\}$ in the first row of results (corresponding to the case $\delta = 1$) a constant convergence rate of $k+1$, which is in agreement with Remark 60 since $\tilde{\eta}_h \le h^{k+1}|u|_{W^{k+2,\infty}(\mathcal{T}_h)} \Leftrightarrow \delta \ge 1$. From row to row, we

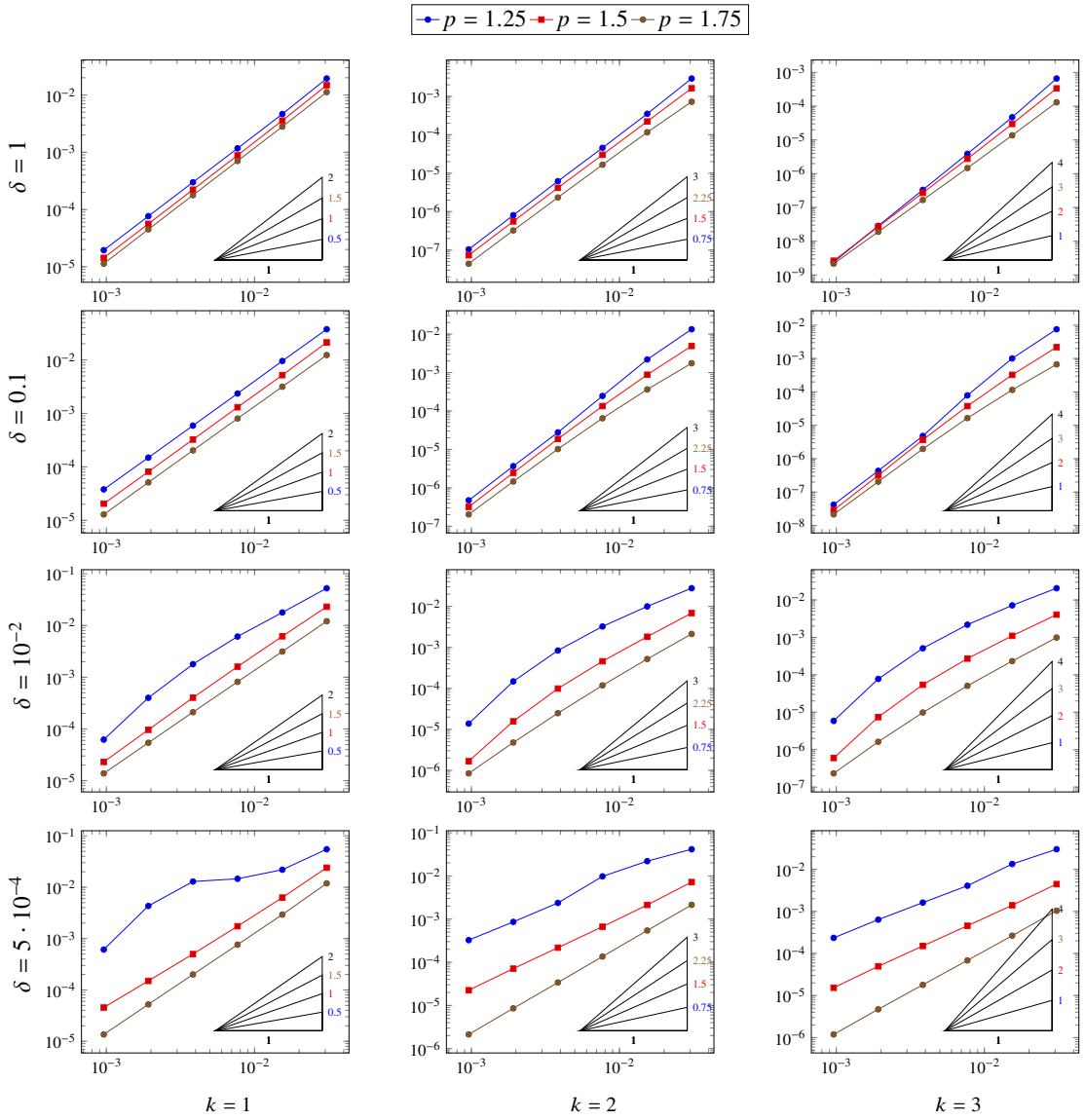

Figure 2.1: Numerical results for the test case of Section 2.6.1. The steeper slope (in black) indicates the $k+1$ convergence rate expected from Theorem 59 when the number δ is large enough compared to the mesh size. Otherwise the other slopes indicate the $(k+1)(p-1)$ convergence rate according to p.

Table 2.1: Convergence rates for the test case of Section 2.6.1. The bold numbers in each column correspond to the $(k+1)(p-1) \sim (k+1)$ convergence rates.

$\delta = 1$									
k	1			2			3		
h \ p	1.25	1.5	1.75	1.25	1.5	1.75	1.25	1.5	1.75
3.07e-02	**0.5 ~ 2**	**1 ~ 2**	**1.5 ~ 2**	**0.75 ~ 3**	**1.5 ~ 3**	**2.25 ~ 3**	**1 ~ 4**	**2 ~ 4**	**3 ~ 4**
1.54e-02	2.07	2.06	2.01	3.06	2.88	2.65	3.83	3.51	3.26
7.68e-03	1.98	2.01	1.98	2.94	2.87	2.79	3.59	3.41	3.21
3.84e-03	1.97	1.99	1.98	2.88	2.86	2.83	3.55	3.35	3.14
1.92e-03	1.97	1.98	1.99	2.94	2.90	2.85	3.54	3.33	3.13
9.60e-04	1.97	1.97	1.99	2.95	2.93	2.88	3.56	3.34	3.14
$\delta = 0.1$									
k	1			2			3		
h \ p	1.25	1.5	1.75	1.25	1.5	1.75	1.25	1.5	1.75
3.07e-02	**0.5 ~ 2**	**1 ~ 2**	**1.5 ~ 2**	**0.75 ~ 3**	**1.5 ~ 3**	**2.25 ~ 3**	**1 ~ 4**	**2 ~ 4**	**3 ~ 4**
1.54e-02	1.98	2.04	1.97	2.63	2.49	2.28	2.92	2.77	2.55
7.68e-03	2.01	1.99	1.97	3.14	2.70	2.48	3.67	3.10	2.79
3.84e-03	1.99	2.00	1.98	3.15	2.84	2.66	4.04	3.35	3.07
1.92e-03	1.99	2.00	1.98	2.92	2.93	2.80	3.47	3.54	3.26
9.60e-04	1.98	1.98	1.99	2.96	2.95	2.85	3.37	3.46	3.26
$\delta = 10^{-2}$									
k	1			2			3		
h \ p	1.25	1.5	1.75	1.25	1.5	1.75	1.25	1.5	1.75
3.07e-02	**0.5 ~ 2**	**1 ~ 2**	**1.5 ~ 2**	**0.75 ~ 3**	**1.5 ~ 3**	**2.25 ~ 3**	**1 ~ 4**	**2 ~ 4**	**3 ~ 4**
1.54e-02	1.57	1.91	1.96	1.48	1.93	2.04	1.53	1.89	2.10
7.68e-03	1.54	1.94	1.94	1.62	1.98	2.13	1.71	2.01	2.18
3.84e-03	1.77	1.99	1.95	1.95	2.21	2.25	2.09	2.32	2.37
1.92e-03	2.16	2.06	1.97	2.50	2.65	2.38	2.72	2.87	2.60
9.60e-04	2.69	2.07	1.97	3.42	3.23	2.50	3.73	3.63	2.80

$\delta = 5 \cdot 10^{-4}$									
k	1			2			3		
h \ p	1.25	1.5	1.75	1.25	1.5	1.75	1.25	1.5	1.75
3.07e-02	**0.5 ~ 2**	**1 ~ 2**	**1.5 ~ 2**	**0.75 ~ 3**	**1.5 ~ 3**	**2.25 ~ 3**	**1 ~ 4**	**2 ~ 4**	**3 ~ 4**
1.54e-02	1.33	1.94	2.03	0.92	1.77	1.98	1.17	1.68	1.98
7.68e-03	0.58	1.84	1.94	1.17	1.67	2.00	1.71	1.61	1.94
3.84e-03	0.18	1.80	1.93	2.04	1.61	2.00	1.33	1.59	1.93
1.92e-03	1.58	1.74	1.94	1.46	1.61	1.99	1.34	1.61	1.93
9.60e-04	2.82	1.72	1.94	1.40	1.66	2.01	1.44	1.69	1.98

can observe a lower pre-asymptotic convergence rate (still above $(k+1)(p-1)$, but close to it in certain cases) which becomes worse as δ decreases; this is expected since $\tilde{\eta}_h$ is proportional to $1/\delta$. We note that, as k increases, the asymptotic rates are lower than the expected h^{k+1}, which could be due to the asymptotic regime not being achieved yet for these high-order schemes (due to the constants involving higher derivatives of u in (60)). The saturation of convergence rate, for $k = 2, 3$, at a lower rate than $(k+1)(p-1)$ when δ is very small could also be explained by the fact that the $W^{k+1,p'}$ norm of $\boldsymbol{\sigma}(\cdot, \boldsymbol{\nabla} u)$ explodes as $\delta \to 0$.

2.6.2 Non-degenerate potential

We consider $\delta = 0$ (the p-Laplacian case), and the potential u is given by

$$u(x_1, x_2) = \sin(\pi x_1) \sin(\pi x_2) + (\pi + 1)(x_1 + x_2) \quad \forall (x_1, x_2) \in \Omega.$$

Since $|\boldsymbol{\nabla} u| \geq 1$ on Ω, $\tilde{\eta}_h = \mu_h(1)$ and we should observe a constant convergence rate of $k+1$, which is indeed the case (see Figure 2.2 and Table 2.2).

2.6.3 Non-degenerate flux-potential couple

The exact solution u is given by

$$u(x_1, x_2) = \sin(\pi x_1) \sin(\pi x_2) \quad \forall (x_1, x_2) \in \Omega.$$

Since $\boldsymbol{\nabla} u$ vanishes at points $(\boldsymbol{x}_i)_{1 \leq i \leq 5} := \{(0,0), (1,0), (0,1), (1,1), (0.5, 0.5)\}$, we consider a degeneracy parameter function δ as the sum of bump functions centered at these points with $\frac{1}{5}$ radius. Specifically, for all $\boldsymbol{x} \in \Omega$,

$$\delta(\boldsymbol{x}) = \sum_{i=1}^{5} \begin{cases} \exp\left(1 - \dfrac{1}{1 - 25|\boldsymbol{x} - \boldsymbol{x}_i|^2}\right) & \text{if } |\boldsymbol{x} - \boldsymbol{x}_i| < \frac{1}{5}, \\ 0 & \text{otherwise.} \end{cases} \tag{2.54}$$

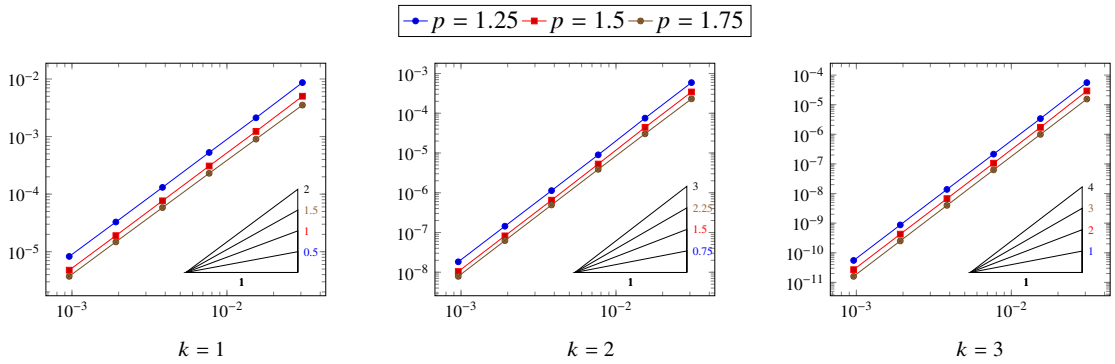

Figure 2.2: Numerical results for the test case of Section 2.6.2. The steeper slope (in black) indicates the $k+1$ convergence rate. The other slopes indicate the $(k+1)(p-1)$ convergence rate according to p.

Table 2.2: Convergence rates for the test case of Section 2.6.2. The bold numbers in each column correspond to the $(k+1)(p-1) \sim (k+1)$ convergence rates.

k	1			2			3		
h \ p	1.25	1.5	1.75	1.25	1.5	1.75	1.25	1.5	1.75
3.07e-02	**0.5 ~ 2**	**1 ~ 2**	**1.5 ~ 2**	**0.75 ~ 3**	**1.5 ~ 3**	**2.25 ~ 3**	**1 ~ 4**	**2 ~ 4**	**3 ~ 4**
1.54e-02	2.04	2.04	1.98	2.98	2.97	2.93	4.06	4.10	3.98
7.68e-03	2.00	1.99	1.96	3.05	3.06	2.96	3.97	4.01	3.96
3.84e-03	2.01	2.01	1.98	2.99	3.02	2.98	3.95	3.98	3.98
1.92e-03	2.00	2.01	1.98	2.97	2.98	2.98	3.98	3.98	3.98
9.60e-04	1.99	1.99	1.99	2.98	2.98	2.99	3.98	3.99	3.98

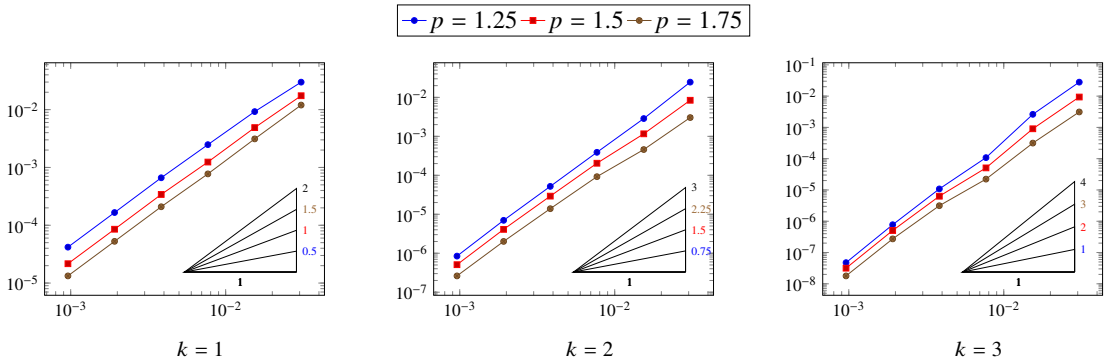

Figure 2.3: Numerical results for the test case of Section 2.6.3. The steeper slope (in black) indicates the $k+1$ convergence rate. The other slopes indicate the $(k+1)(p-1)$ convergence rate according to p.

Table 2.3: Convergence rates for the test case of Section 2.6.3. The bold numbers in each column correspond to the $(k+1)(p-1) \sim (k+1)$ convergence rates.

k	1			2			3		
h \ p	1.25	1.5	1.75	1.25	1.5	1.75	1.25	1.5	1.75
3.07e-02	**0.5 ~ 2**	**1 ~ 2**	**1.5 ~ 2**	**0.75 ~ 3**	**1.5 ~ 3**	**2.25 ~ 3**	**1 ~ 4**	**2 ~ 4**	**3 ~ 4**
1.54e-02	1.70	1.84	1.95	3.12	2.87	2.74	3.43	3.39	3.32
7.68e-03	1.89	1.97	2.00	2.87	2.50	2.30	4.58	4.14	3.81
3.84e-03	1.90	1.86	1.89	2.90	2.80	2.73	3.32	3.01	2.82
1.92e-03	2.00	2.00	1.99	2.90	2.83	2.79	3.80	3.64	3.52
9.60e-04	1.99	1.98	1.99	3.05	3.01	2.94	4.03	4.00	3.93

As a consequence, δ vanishes on about three quarters of Ω, however, $\tilde{\eta}_h = \mu_h(1)$ and we should observe a constant convergence rate of $k+1$. This is confirmed by the results presented in Figure 2.3 and Table 2.3.

2.6.4 Degenerate problem

We consider $\delta = 0$ (the p-Laplacian case), and the potential u is given such that,

$$u(x_1, x_2) = \frac{1}{10} \exp\left(-10\left(|x_1 - 0.5|^{p+\frac{k+2}{4}} + |x_2 - 0.5|^{p+\frac{k+2}{4}}\right)\right) \quad \forall (x_1, x_2) \in \Omega.$$

The particular choice of u, which changes with p and k, is driven by the need to ensure that the function and its flux have the required regularity for the error estimate in Theorem

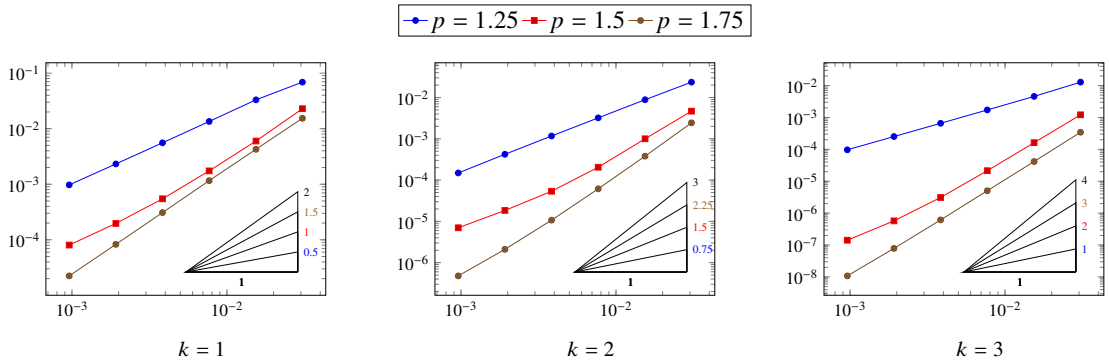

Figure 2.4: Numerical results for the test case of Section 2.6.4. The steeper slope (in black) indicates the $k+1$ convergence rate. The other slopes indicate the $(k+1)(p-1)$ convergence rate according to p.

59 to be valid (and thus to potentially avoid some of the issues observed in Section 2.6.1), all the while not being too smooth or with a simple structure, which might artificially generate a better convergence of the scheme. Since $\boldsymbol{\nabla} u$ vanishes on an entire region of the domain and $\delta = 0$, we have, $\tilde{\eta}_h = \infty$ and we should observe $(k+1)(p-1)$ asymptotic convergence rates. The results for this test are presented in Figure 2.4 and Table 2.4. In most cases, they do confirm that the asymptotic rate of convergence is closer to $(k+1)(p-1)$ than $k+1$, with major exceptions for $(p,k) = (1.25,1)$ and $(p,k) = (1.75,3)$, for which the observed rate is closer to $k+1$ – probably because, for the considered mesh sizes and parameter values, the first term in (2.34) might be dominant due to a larger multiplicative constant. Another explanation could be that the asymptotic regime is not reached yet for these tests, or, in view of the recent results in [33], that the error estimate in Theorem 59, which is valid in a more general setting, is actually sub-optimal for these particular test cases. In any case, these tests are outliers in the results presented here, which otherwise support rather well the theoretical error estimate.

2.7 Conclusion

We have presented and analysed a Hybrid High-Order scheme of arbitrary order k, for a non-linear model that generalises the p-Laplace equation (with $p \in (1,2]$) through the addition of an offset in the flux, that potentially remove its singularity at 0. Our error estimate highlights various convergence regimes for the scheme, depending on its degeneracy or lack thereof (the latter occurring in presence of a non-zero offset, or when the gradient of the continuous solution does not vanish); for a degenerate model we recover the known rates of convergence in $(k+1)(p-1)$, while an optimal rate of $(k+1)$, identical to the rate for linear models, is obtained when the model is not degenerate.

Table 2.4: Convergence rates for the test case of Section 2.6.4. The bold numbers in each column correspond to the $(k+1)(p-1) \sim (k+1)$ convergence rates.

k	1			2			3		
h \ p	1.25	1.5	1.75	1.25	1.5	1.75	1.25	1.5	1.75
3.07e-02	**0.5 ~ 2**	**1 ~ 2**	**1.5 ~ 2**	**0.75 ~ 3**	**1.5 ~ 3**	**2.25 ~ 3**	**1 ~ 4**	**2 ~ 4**	**3 ~ 4**
1.54e-02	1.06	1.94	1.86	1.42	2.24	2.70	1.49	2.91	3.98
7.68e-03	1.29	1.78	1.87	1.45	2.28	2.62	1.40	2.91	3.96
3.84e-03	1.28	1.67	1.91	1.46	1.93	2.52	1.39	2.79	3.98
1.92e-03	1.26	1.47	1.90	1.47	1.55	2.35	1.38	2.44	3.98
9.60e-04	1.25	1.29	1.89	1.50	1.39	2.14	1.38	2.01	3.98

These regimes are locally driven by a dimensionless number, and intermediate regimes are also identified.

Several numerical tests have been provided, and show a good agreement with the theoretical error estimate, except in a few cases where the convergence appears to be faster than expected (which could be due to the asymptotic regime not yet being attained in that case, or to the specifics of the particular degenerate test case considered here).

Chapter 3

A HHO method for incompressible flows of non-Newtonian fluids with power-like convective behaviour

This chapter has been published in the following international journal (see [35]):

IMA Journal of Numerical Analysis, 2021.
Published online.

Abstract

In this work, we design and analyze a Hybrid High-Order (HHO) discretization method for incompressible flows of non-Newtonian fluids with power-like convective behaviour. We work under general assumptions on the viscosity and convection laws, that are associated with possibly different Sobolev exponents $r \in (1, \infty)$ and $s \in (1, \infty)$. After providing a novel weak formulation of the continuous problem, we study its well-posedness highlighting how a subtle interplay between the exponents r and s determines the existence and uniqueness of a solution. We next design an HHO scheme based on this weak formulation and perform a comprehensive stability and convergence analysis, including convergence for general data and error estimates for shear-thinning fluids and small data. The HHO scheme is validated on a complete panel of model problems.

3.1 Introduction

In this paper, building on the results of [27], we design and analyze a Hybrid High-Order (HHO) method for incompressible flows of non-Newtonian fluids governed by the generalized Navier–Stokes equations. The formulation considered here encompasses general

viscosity and convection laws, possibly corresponding to different Sobolev exponents. The proposed numerical method aims at overcoming certain limitations of traditional (e.g., finite element or finite volume) schemes, particularly concerning the supported meshes and approximation orders. Notice, however, that the techniques introduced in this work can, in principle, be applied also to more classical discretizations.

Nonlinear rheologies are encountered in several fields, including ice sheet dynamics and glacier modelling [4, 78], mantle convection [101], chemical engineering [80], and biological fluids [70, 85]. Their mathematical study was pioneered in the work of Ladyzhenskaya [84]; detailed well-posedness and regularity analyses of the corresponding system of equations have been carried out in [13, 18, 64, 92, 96]. Recently, a variation of the classical trilinear convective term has been considered in [86] in relation to the computation of the Wasserstein distance for optimal transport applications (to the best of our knowledge, such generalizations haven't yet been considered in the context of fluid-mechanics). In this work, we propose a further generalization of this model encompassing power-like convective behaviours that satisfy non-dissipativity relations; see Assumption 6 below. The power-law behaviours of the viscous and convective terms are characterized by (possibly different) Sobolev exponents $r \in (1, \infty)$ and $s \in (1, \infty)$. In Theorem 66 below, we carry out a well-posedness analysis for the continuous problem showing that a subtle interplay of these exponents determines the existence and uniqueness of a solution (in the classical case $s = 2$, relevant in fluid mechanics, this translates into constraints on the Sobolev index r). Such an interplay, which reverberates at the discrete level, is required to leverage the Hölder continuity of the convective function that appears in the weak formulation of the problem. Notice that considering a general exponent $s \in (1, \infty)$ involves only (relatively) minor changes in the analysis with respect to the case $s = 2$, and has the advantage of making the proposed method suitable for applications in promising fields such as optimal transport. Also, to the best of our knowledge, both the analysis of this generalized Navier–Stokes problem and its numerical approximation are entirely new.

While a large body of literature deals with the numerical approximation of the Navier–Stokes equations, only a relatively small fraction of these works addresses nonlinear rheologies. Finite element methods for creeping (Stokes) flows of non-Newtonian fluids have been considered in [9, 16, 76]. Non-Newtonian fluid flows with standard convective behaviour have been considered in [44, 45]. This model is encountered in several other works: see, e.g., [65, 82] for finite element methods with implicit power-law-like rheologies; [80, 81] for generalized Newtonian fluids with space variable and concentration-dependent power-law index; [83] for a local discontinuous Galerkin method; [107] for a study of non-Newtonian polymer flows through porous media; [79] for simulations of transient flows of non-Newtonian fluids; [8] for a finite element approximation of non-Newtonian polymer aqueous solutions with fractional time-derivative.

Recent works have emphasized the importance of handling polytopal meshes in the

context of numerical fluid mechanics; see, e.g., the introduction of [50] for a broad discussion on this subject. General meshes, possibly combined with high order, can be used in this context to: adapt the shape of the elements to the local features of the flow, thus improving the resolution of boundary or internal layers; perform non-conforming local mesh refinement, which naturally preserves the mesh quality; reduce the computational cost while preserving the approximation of the domain geometry by mesh coarsening [11, 12]. Among recent methods for incompressible flows that natively support general polytopal meshes and arbitrary-order, we can cite discontinuous Galerkin methods [56] (see also [58, Chapter 6]), Virtual Element methods [15, 71, 77, 91] (see also [104]), and HHO methods [27, 28, 34, 62] (see also [50, Chapter 9]). While discontinuous Galerkin methods are commonly considered the golden standard in fluid mechanics, recent works have pointed out the potential of HHO methods in terms of overall efficiency and precision for real-life problems [23]. The developments of the present work show their ability to tackle complex, highly nonlinear physics.

In this paper, we extend the HHO method of [27] to the full generalized Navier–Stokes equations with power-law viscous and convective behaviours. The discretization of the convective term relies on the novel formulation devised at the continuous level, which guarantees non-dissipativity at the discrete level and is obtained replacing the continuous gradient by the classical HHO gradient reconstruction in full polynomial spaces; see [48, Eq. (4.3)] for the scalar case. For this novel discrete convective function we prove the key properties that intervene in the stability and consistency of the method. The former consist, in addition to non-dissipativity, in a Hölder continuity property expressed in terms of a discrete $W^{1,r}$-(semi)norm. The latter include consistency for smooth functions and sequential consistency. We perform complete stability and convergence analyses, highlighting the interplay between the exponents r and s. Specifically, existence and uniqueness of a discrete solution, established in Theorem 76, hold under the same conditions on r and s as for the continuous problem and a data smallness assumption where the constants of relevant continuous inequalities are replaced by their discrete counterparts. We then establish, in Theorem 77, various convergence results under minimal regularity of the solutions using compactness arguments. Finally, an error estimate for shear-thinning fluids displaying different orders of convergence according to the degeneracy of the problem in the spirit of [52] is proved in Theorem 78. When polynomials of degree $k \geq 1$ are used, denoting by h the meshsize, the error estimates give orders of convergence ranging from $h^{(k+1)(r-1)}$ to h^{k+1} for the velocity and from $h^{(k+1)(r-1)^2}$ to $h^{(k+1)(r-1)}$ for the pressure, depending on the degeneracy of the problem.

The rest of the paper is organized as follows. In Section 3.2 we introduce the strong and weak formulations of the generalized Navier–Stokes problem, discuss the assumptions on the viscosity and convection laws, and study existence and uniqueness of a weak solution. The construction of the HHO discretization is carried out in Section 3.3 by defining the discrete counterparts of the viscous, convective, and coupling terms.

In Section 3.4, we formulate the discrete problem and state the main stability and convergence results for the method. In Section 3.5, we investigate the performance of the method on a complete set of model problems. Finally, Section 3.6 collects the proofs of the consistency properties of the discrete convective function and of the main results.

3.2 Continuous setting

Let $\Omega \subset \mathbb{R}^d$, $d \in \{2, 3\}$, denote a bounded, connected, polyhedral open set with Lipschitz boundary $\partial\Omega$. We consider the incompressible flow of a fluid occupying Ω and subjected to a volumetric force field $\boldsymbol{f} : \Omega \to \mathbb{R}^d$, governed by the following generalized Navier–Stokes problem: Find the velocity field $\boldsymbol{u} : \Omega \to \mathbb{R}^d$ and the pressure field $p : \Omega \to \mathbb{R}$ such that

$$-\boldsymbol{\nabla}\cdot\boldsymbol{\sigma}(\cdot, \boldsymbol{\nabla}_{\mathrm{s}}\boldsymbol{u}) + (\boldsymbol{u}\cdot\boldsymbol{\nabla})\boldsymbol{\chi}(\cdot,\boldsymbol{u}) + \boldsymbol{\nabla}p = \boldsymbol{f} \qquad \text{in } \Omega, \tag{3.1a}$$

$$\boldsymbol{\nabla}\cdot\boldsymbol{u} = 0 \qquad \text{in } \Omega, \tag{3.1b}$$

$$\boldsymbol{u} = \boldsymbol{0} \qquad \text{on } \partial\Omega, \tag{3.1c}$$

$$\int_\Omega p = 0, \tag{3.1d}$$

where $\boldsymbol{\nabla}\cdot$ denotes the divergence operator applied to tensor-valued or vector-valued fields, $\boldsymbol{\nabla}_{\mathrm{s}}$ is the symmetric part of the gradient operator $\boldsymbol{\nabla}$ applied to vector fields, and, denoting by $\mathbb{R}^{d\times d}_{\mathrm{s}}$ the set of square, symmetric, real-valued $d\times d$ matrices, $\boldsymbol{\sigma} : \Omega\times\mathbb{R}^{d\times d}_{\mathrm{s}} \to \mathbb{R}^{d\times d}_{\mathrm{s}}$ is the viscosity law and $\boldsymbol{\chi} : \Omega\times\mathbb{R}^d \to \mathbb{R}^d$ is the convection law. In what follows, we formulate assumptions on $\boldsymbol{\sigma}$ and $\boldsymbol{\chi}$ that encompass common models for non-Newtonian fluids and state a weak formulation for problem (3.1) that will be used as a starting point for its discretization.

3.2.1 Viscosity law

For all $m \in [1,\infty]$, we define the *conjugate*, *Sobolev*, and *singular* exponents of m by

$$m' := \begin{cases} \frac{m}{m-1} & \text{if } m \in (1,\infty) \\ \infty & \text{if } m = 1 \\ 1 & \text{if } m = \infty \end{cases} \in [1,\infty], \qquad m^* := \begin{cases} \frac{dm}{d-m} & \text{if } m < d \\ \infty & \text{if } m \geq d \end{cases} \in [m,\infty], \tag{3.2}$$

$$\tilde{m} := \min(m, 2) \in [1, 2].$$

For all $\boldsymbol{\tau} = (\tau_{ij})_{1\leq i,j\leq d}$ and $\boldsymbol{\eta} = (\eta_{ij})_{1\leq i,j\leq d}$ in $\mathbb{R}^{d\times d}$, we also define the Frobenius inner product $\boldsymbol{\tau} : \boldsymbol{\eta} := \sum_{i,j=1}^d \tau_{ij}\eta_{ij}$ and the corresponding norm $|\boldsymbol{\tau}|_{d\times d} := \sqrt{\boldsymbol{\tau} : \boldsymbol{\tau}}$.

Assumption 5 (Viscosity law)**.** Let a real number $r \in (1, \infty)$ be fixed. The viscosity law satisfies

$$\boldsymbol{\sigma} : \Omega \times \mathbb{R}^{d\times d}_{\mathrm{s}} \to \mathbb{R}^{d\times d}_{\mathrm{s}} \text{ is measurable,} \tag{3.3}$$

$$\boldsymbol{\sigma}(\boldsymbol{x}, \mathbf{0}) \in L^{r'}(\Omega, \mathbb{R}^{d\times d}_{\mathrm{s}}) \text{ for almost every } \boldsymbol{x} \in \Omega. \tag{3.4}$$

Moreover, there exist real numbers $\delta \in [0, \infty)$ and $\sigma_{\mathrm{hc}}, \sigma_{\mathrm{hm}} \in (0, \infty)$ such that, for all $\boldsymbol{\tau}, \boldsymbol{\eta} \in \mathbb{R}^{d\times d}_{\mathrm{s}}$ and almost every $\boldsymbol{x} \in \Omega$, the following Hölder continuity and Hölder monotonicity properties hold

$$|\boldsymbol{\sigma}(\boldsymbol{x}, \boldsymbol{\tau}) - \boldsymbol{\sigma}(\boldsymbol{x}, \boldsymbol{\eta})|_{d\times d} \le \sigma_{\mathrm{hc}} \left(\delta^r + |\boldsymbol{\tau}|^r_{d\times d} + |\boldsymbol{\eta}|^r_{d\times d}\right)^{\frac{r-2}{r}} |\boldsymbol{\tau} - \boldsymbol{\eta}|_{d\times d}, \tag{3.5}$$

$$(\boldsymbol{\sigma}(\boldsymbol{x}, \boldsymbol{\tau}) - \boldsymbol{\sigma}(\boldsymbol{x}, \boldsymbol{\eta})) : (\boldsymbol{\tau} - \boldsymbol{\eta}) \ge \sigma_{\mathrm{hm}} \left(\delta^r + |\boldsymbol{\tau}|^r_{d\times d} + |\boldsymbol{\eta}|^r_{d\times d}\right)^{\frac{r-2}{r}} |\boldsymbol{\tau} - \boldsymbol{\eta}|^2_{d\times d}. \tag{3.6}$$

Remark 61 (Degeneracy function). The parameter δ in Assumption 5 is related to the degeneracy of the flux function when $r < 2$. Another possible choice, considered in [52], consists in taking $\delta \in L^r(\Omega, [0, \infty))$. This variation requires only minor changes in the analysis, not detailed here for the sake of conciseness.

Example 62 (Carreau–Yasuda stress)**.** An example of viscosity law satisfying Assumption 5 is the (μ, δ, a, r)-Carreau–Yasuda law such that, for almost every $\boldsymbol{x} \in \Omega$ and all $\boldsymbol{\tau} \in \mathbb{R}^{d\times d}_{\mathrm{s}}$,

$$\boldsymbol{\sigma}(\boldsymbol{x}, \boldsymbol{\tau}) = \mu(\boldsymbol{x}) \left(\delta^{a(\boldsymbol{x})} + |\boldsymbol{\tau}|^{a(\boldsymbol{x})}_{d\times d}\right)^{\frac{r-2}{a(\boldsymbol{x})}} \boldsymbol{\tau}, \tag{3.7}$$

where $\mu : \Omega \to [\mu_-, \mu_+]$ and $a : \Omega \to [a_-, a_+]$ are measurable functions with $\mu_\pm, a_\pm \in (0, \infty)$, $\delta \in [0, \infty)$, and $r \in (1, \infty)$. Notice that the case $\delta = 0$ corresponds to classical power-law fluids. See [27, Example 4] for a proof of the fact that this law matches Assumption 5 and also [52, Example 6] for the generalization of δ to a function.

Remark 63 (Traceless-stable assumption). Although we consider incompressible flows (which are characterized by traceless strain rate fields), our analysis does not require that $\operatorname{tr} \boldsymbol{\sigma}(\boldsymbol{x}, \boldsymbol{\tau}) = \mathbf{0}$ for almost every $\boldsymbol{x} \in \Omega$ and all $\boldsymbol{\tau} \in \mathbb{R}^{d\times d}_{\mathrm{s}}$ such that $\operatorname{tr} \boldsymbol{\tau} = 0$. In practice, however, this property holds for generalized Newtonian fluids, for which there exists a scalar function $\nu : \Omega \times \mathbb{R}^{d\times d}_{\mathrm{s}} \to \mathbb{R}$ such that $\boldsymbol{\sigma}(\boldsymbol{x}, \boldsymbol{\tau}) = \nu(\boldsymbol{x}, \boldsymbol{\tau})\boldsymbol{\tau}$ for almost every $\boldsymbol{x} \in \Omega$ and all $\boldsymbol{\tau} \in \mathbb{R}^{d\times d}_{\mathrm{s}}$; cf. Example 62.

3.2.2 Convection law

In what follows, $|\cdot|$ will denote both the absolute value of scalars and Euclidian norm of vectors, while $\otimes$ denotes the tensor product of two vectors such that, for all $\boldsymbol{x} = (x_i)_{1\le i\le d} \in \mathbb{R}^d$ and $\boldsymbol{y} = (y_j)_{1\le j\le d} \in \mathbb{R}^d$, $\boldsymbol{x} \otimes \boldsymbol{y} := (x_i y_j)_{1\le i,j\le d} \in \mathbb{R}^{d\times d}$.

Assumption 6 (Convection law)**.** Let a real number $s \in (1, \infty)$ be fixed. The convection law satisfies

$$\boldsymbol{\chi} : \Omega \times \mathbb{R}^d \to \mathbb{R}^d \text{ is measurable,} \tag{3.8a}$$
$$\boldsymbol{\chi}(\boldsymbol{x}, \boldsymbol{0}) = \boldsymbol{0} \text{ for almost every } \boldsymbol{x} \in \Omega. \tag{3.8b}$$

We also assume that, for all $\boldsymbol{w} \in \mathbb{R}^d$, the non-dissipativity relations hold:

$$(\boldsymbol{w} \cdot \boldsymbol{\nabla})\boldsymbol{\chi}(\cdot, \boldsymbol{w}) = (\boldsymbol{\chi}(\cdot, \boldsymbol{w}) \cdot \boldsymbol{\nabla})\boldsymbol{w} + (s-2)|\boldsymbol{w}|^{-2}[(\boldsymbol{\chi}(\cdot, \boldsymbol{w}) \cdot \boldsymbol{\nabla})\boldsymbol{w} \cdot \boldsymbol{w}]\boldsymbol{w}, \tag{3.8c}$$
$$\boldsymbol{w} \otimes \boldsymbol{\chi}(\cdot, \boldsymbol{w}) = \boldsymbol{\chi}(\cdot, \boldsymbol{w}) \otimes \boldsymbol{w}. \tag{3.8d}$$

Moreover, there exists a real number $\chi_{\mathrm{hc}} \in (0, \infty)$ such that, for all $\boldsymbol{v}, \boldsymbol{w} \in \mathbb{R}^d$ and almost every $\boldsymbol{x} \in \Omega$, the following Hölder continuity property holds:

$$|\boldsymbol{\chi}(\boldsymbol{x}, \boldsymbol{w}) - \boldsymbol{\chi}(\boldsymbol{x}, \boldsymbol{v})| \le \chi_{\mathrm{hc}} \left(|\boldsymbol{w}|^s + |\boldsymbol{v}|^s\right)^{\frac{s-\tilde{s}}{s}} |\boldsymbol{w} - \boldsymbol{v}|^{\tilde{s}-1}. \tag{3.8e}$$

Example 64 (Standard convection law)**.** The standard convection law is obtained taking $s = 2$ and $\boldsymbol{\chi}(\cdot, \boldsymbol{w}) \equiv \boldsymbol{w}$. According to Theorem 77 below, with this choice we can prove convergence provided that $r \in \left(\frac{3}{2}, \infty\right)$ if $d = 2$ and $r \in \left(\frac{9}{5}, \infty\right)$ if $d = 3$. Error estimates stated by Theorem 78, on the other hand, also require $r \le 2$, reducing the above intervals to $r \in \left[\frac{3}{2}, 2\right]$ if $d = 2$ and $r \in \left[\frac{9}{5}, 2\right]$ if $d = 3$; note that the additional regularity assumption allows the left limit points.

Example 65 ((ν, s)-Laplace convection law)**.** Another example of convection law satisfying Assumption 6 is the (ν, s)-Laplace law considered in [86] in the context of applications to optimal transport and such that, for almost every $\boldsymbol{x} \in \Omega$ and all $\boldsymbol{w} \in \mathbb{R}^d$,

$$\boldsymbol{\chi}(\boldsymbol{x}, \boldsymbol{w}) = \nu(\boldsymbol{x})|\boldsymbol{w}|^{s-2}\boldsymbol{w}, \tag{3.9}$$

where $\nu : \Omega \to [0, \nu_+]$ is a measurable function with $\nu_+ \in [0, \infty)$ corresponding to the local flow convection index, while $s \in (1, \infty)$ is the convection behaviour index. It can be proved as in [27, Example 4] that $\boldsymbol{\chi}$ is an $(s, 0)$-power-framed function, which implies (3.8e).

3.2.3 Weak formulation

The starting point for the HHO discretization of problem (3.1) is the weak formulation studied in this section. We define the following velocity and pressure spaces embedding, respectively, the homogeneous boundary condition for the velocity and the zero-average constraint for the pressure:

$$\boldsymbol{U} \coloneqq \left\{\boldsymbol{v} \in W^{1,r}(\Omega)^d \ : \ \boldsymbol{v}_{|\partial\Omega} = \boldsymbol{0}\right\}, \qquad P \coloneqq \left\{q \in L^{r'}(\Omega) \ : \ \int_\Omega q = 0\right\}.$$

Assuming $\boldsymbol{f} \in L^{r'}(\Omega)^d$, the weak formulation of problem (3.1) reads: Find $(\boldsymbol{u}, p) \in \boldsymbol{U} \times P$ such that

$$a(\boldsymbol{u}, \boldsymbol{v}) + c(\boldsymbol{u}, \boldsymbol{v}) + b(\boldsymbol{v}, p) = \int_\Omega \boldsymbol{f} \cdot \boldsymbol{v} \qquad \forall \boldsymbol{v} \in \boldsymbol{U}, \tag{3.10a}$$

$$-b(\boldsymbol{u}, q) = 0 \qquad \forall q \in P, \tag{3.10b}$$

where the function $a : \boldsymbol{U} \times \boldsymbol{U} \to \mathbb{R}$, the bilinear form $b : \boldsymbol{U} \times L^{r'}(\Omega) \to \mathbb{R}$, and the function $c : \boldsymbol{U} \times \boldsymbol{U} \to \mathbb{R}$ are defined such that, for all $\boldsymbol{v}, \boldsymbol{w} \in \boldsymbol{U}$ and all $q \in L^{r'}(\Omega)$,

$$a(\boldsymbol{w}, \boldsymbol{v}) \coloneqq \int_\Omega \boldsymbol{\sigma}(\cdot, \boldsymbol{\nabla}_{\mathrm{s}} \boldsymbol{w}) : \boldsymbol{\nabla}_{\mathrm{s}} \boldsymbol{v}, \qquad b(\boldsymbol{v}, q) \coloneqq -\int_\Omega (\boldsymbol{\nabla} \cdot \boldsymbol{v}) q, \tag{3.11}$$

$$\begin{aligned} c(\boldsymbol{w}, \boldsymbol{v}) \coloneqq \frac{1}{s} \int_\Omega (\boldsymbol{\chi}(\cdot, \boldsymbol{w}) \cdot \boldsymbol{\nabla}) \boldsymbol{w} \cdot \boldsymbol{v} - \frac{1}{s'} \int_\Omega (\boldsymbol{\chi}(\cdot, \boldsymbol{w}) \cdot \boldsymbol{\nabla}) \boldsymbol{v} \cdot \boldsymbol{w} \\ + \frac{s-2}{s} \int_\Omega \frac{\boldsymbol{v} \cdot \boldsymbol{w}}{|\boldsymbol{w}|^2} (\boldsymbol{\chi}(\cdot, \boldsymbol{w}) \cdot \boldsymbol{\nabla}) \boldsymbol{w} \cdot \boldsymbol{w}. \end{aligned} \tag{3.12}$$

In order to obtain the function c in (3.12), we have used (3.8c)–(3.8d) as follows: Denoting by $\boldsymbol{n}_{\partial\Omega}$ the unit normal vector pointing out of $\partial\Omega$ and observing that $1 = \frac{1}{s} + \frac{1}{s'}$, for smooth enough functions $\boldsymbol{v}, \boldsymbol{w} : \Omega \to \mathbb{R}^d$ such that $\boldsymbol{\nabla} \cdot \boldsymbol{w} = 0$ and $\boldsymbol{w}_{|\partial\Omega} = \boldsymbol{0}$ we can write

$$\begin{aligned} \int_\Omega (\boldsymbol{w} \cdot \boldsymbol{\nabla}) \boldsymbol{\chi}(\cdot, \boldsymbol{w}) \cdot \boldsymbol{v} &= \frac{1}{s} \int_\Omega (\boldsymbol{w} \cdot \boldsymbol{\nabla}) \boldsymbol{\chi}(\cdot, \boldsymbol{w}) \cdot \boldsymbol{v} + \frac{1}{s'} \int_\Omega (\boldsymbol{w} \cdot \boldsymbol{\nabla}) \boldsymbol{\chi}(\cdot, \boldsymbol{w}) \cdot \boldsymbol{v} \\ &= \frac{1}{s} \left(\int_\Omega (\boldsymbol{\chi}(\cdot, \boldsymbol{w}) \cdot \boldsymbol{\nabla}) \boldsymbol{w} \cdot \boldsymbol{v} + (s-2) \int_\Omega \frac{\boldsymbol{v} \cdot \boldsymbol{w}}{|\boldsymbol{w}|^2} (\boldsymbol{\chi}(\cdot, \boldsymbol{w}) \cdot \boldsymbol{\nabla}) \boldsymbol{w} \cdot \boldsymbol{w} \right) \\ &\quad - \frac{1}{s'} \left(\int_\Omega (\boldsymbol{w} \cdot \boldsymbol{\nabla}) \boldsymbol{v} \cdot \boldsymbol{\chi}(\cdot, \boldsymbol{w}) + \cancel{\int_\Omega (\boldsymbol{\chi}(\cdot, \boldsymbol{w}) \cdot \boldsymbol{v})(\boldsymbol{\nabla} \cdot \boldsymbol{w})} \right. \\ &\quad \left. \cancel{- \int_{\partial\Omega} (\boldsymbol{\chi}(\cdot, \boldsymbol{w}) \cdot \boldsymbol{v})(\boldsymbol{w} \cdot \boldsymbol{n}_{\partial\Omega})} \right), \end{aligned} \tag{3.13}$$

where the second equality follows from an integration by parts along with (3.8c), while the cancellations are a consequence of the assumptions on $\boldsymbol{w}$. Using (3.8d) on the last non-zero term of (3.13), we finally get the expression in the right-hand side of (3.12). This version of c satisfies, by construction, the following non-dissipativity property: For all $\boldsymbol{w} \in \boldsymbol{U}$,

$$c(\boldsymbol{w}, \boldsymbol{w}) = 0. \tag{3.14}$$

We now recall the following Korn inequality (see [72, Theorem 1]): For all $m \in (1, \infty)$, there is $C_{\mathrm{K},m} \in (0, \infty)$ only depending on m, d, and Ω such that, for all $\boldsymbol{v} \in \boldsymbol{U}$,

$$\|\boldsymbol{v}\|_{W^{1,m}(\Omega)^d} \le C_{\mathrm{K},m} \|\boldsymbol{\nabla}_{\mathrm{s}} \boldsymbol{v}\|_{L^m(\Omega)^{d \times d}}. \tag{3.15}$$

Theorem 66 (Existence and uniqueness for problem (3.10))**.** *Under Assumptions 5 and 6, there exists a solution* $(\boldsymbol{u}, p) \in \boldsymbol{U} \times P$ *to the weak formulation* (3.10)*, and any solution satisfies*

$$|\boldsymbol{u}|_{W^{1,r}(\Omega)^d} \le C_{\mathrm{v}} \left[\left(\sigma_{\mathrm{hm}}^{-1} \|\boldsymbol{f}\|_{L^{r'}(\Omega)^d} \right)^{r'} + \min\left(\delta^r ; \left(\delta^{2-\tilde{r}} \sigma_{\mathrm{hm}}^{-1} \|\boldsymbol{f}\|_{L^{r'}(\Omega)^d} \right)^{\frac{r}{r+1-\tilde{r}}} \right) \right]^{\frac{1}{r}} \tag{3.16}$$

with $C_{\mathrm{v}} > 0$ *depending only on* Ω*,* d*, and* r*. Moreover, assuming* $2 \le s \le \frac{\tilde{r}^*}{\tilde{r}'}$*, i.e.,*

$$s \in \begin{cases} \left[2, \frac{d(r-1)}{d-r}\right] & \text{if } d = 2 \text{ and } r \in \left[\frac{3}{2}, 2\right) \text{ or } d = 3 \text{ and } r \in \left[\frac{9}{5}, 2\right], \\ [2, 3] & \text{if } d = 3 \text{ and } r \in (2, 3), \\ [2, \infty) & \text{if } d = 2 \text{ and } r \in [2, \infty) \text{ or } d = 3 \text{ and } r \in [3, \infty), \end{cases} \tag{3.17}$$

and that the following data smallness condition holds:

$$\delta^r + \left(\sigma_{\mathrm{hm}}^{-1} \|\boldsymbol{f}\|_{L^{r'}(\Omega)^d} \right)^{r'} < \left(1 + 2C_{\mathrm{v}}^r\right)^{-1} \left(C_{\mathrm{c},\tilde{r}}^{-1} \chi_{\mathrm{hc}}^{-1} C_{\mathrm{a}} \sigma_{\mathrm{hm}} \delta^{r-\tilde{r}} \right)^{\frac{r}{s+1-\tilde{r}}}, \tag{3.18}$$

the solution of (3.10) *is unique.*

Remark 67 (Uniqueness). Uniqueness of the solution of (3.10) is not guaranteed for any value of r and s, and in particular when $r > 2$ in the degenerate case $\delta = 0$. The assumptions on r and s ensuring the uniqueness of the continuous weak solution will carry out to the discrete level, in both the well-posedness result of Theorem 76 and the error estimate of Theorem 78, where $r \le 2$ is additionally required.

Proof of Theorem 66. 1. *Existence.* Replacing the function a by the sum $a + c$ in [27, Remark 6] and using the non-dissipativity (3.14) of the convective function c yields the existence of a solution to the weak formulation (3.10) and the a priori estimate (3.16), see also [52, Proposition 6] for the min-term.

2. *Uniqueness.* Let $(\boldsymbol{u}, p), (\boldsymbol{u}', p') \in \boldsymbol{U} \times P$ be two solutions of (3.10). Taking the difference of (3.10a) written first for $(\boldsymbol{u}, p)$ and then for $(\boldsymbol{u}', p')$, we infer, for all $\boldsymbol{v} \in \boldsymbol{U}$,

$$a(\boldsymbol{u}, \boldsymbol{v}) - a(\boldsymbol{u}', \boldsymbol{v}) + c(\boldsymbol{u}, \boldsymbol{v}) - c(\boldsymbol{u}', \boldsymbol{v}) + b(\boldsymbol{v}, p - p') = 0. \tag{3.19}$$

If $\boldsymbol{u} = \boldsymbol{u}'$, (3.19) yields $b(\boldsymbol{v}, p - p') = 0$ for all $\boldsymbol{v} \in \boldsymbol{U}$. This relation combined with the inf-sup stability of b (c.f. [22, Theorem 1]) yields,

$$\|p - p'\|_{L^{r'}(\Omega)} \le C_{\mathrm{b}} \sup_{\boldsymbol{v} \in \boldsymbol{U}, |\boldsymbol{v}|_{W^{1,r}(\Omega)^d} = 1} b(\boldsymbol{v}, p - p') = 0.$$

Hence, uniqueness of the solution is equivalent to uniqueness of the velocity.

Assume now $2 \le s \le \frac{\tilde r^*}{\tilde r'}$ and $(\boldsymbol{u}, p) \neq (\boldsymbol{u}', p')$. Setting $\boldsymbol{e} \coloneqq \boldsymbol{u} - \boldsymbol{u}'$, the previous reasoning yields $\boldsymbol{u} \neq \boldsymbol{u}'$, hence $|\boldsymbol{e}|_{W^{1,\tilde r}(\Omega)^d} > 0$. Using the Hölder continuity (3.26) of c proved in Lemma 69 below with $(\boldsymbol{u}, \boldsymbol{w}, \boldsymbol{v}) = (\boldsymbol{u}, \boldsymbol{u}', \boldsymbol{e})$ and $m = \tilde r$, we infer

$$
\begin{aligned}
|\boldsymbol{e}|^2_{W^{1,\tilde r}(\Omega)^d} &\ge C_{\mathrm{c},\tilde r}^{-1}\chi_{\mathrm{hc}}^{-1}\left(|\boldsymbol{u}|^r_{W^{1,r}(\Omega)^d} + |\boldsymbol{u}'|^r_{W^{1,r}(\Omega)^d}\right)^{\frac{1-s}{r}}(c(\boldsymbol{u}', \boldsymbol{e}) - c(\boldsymbol{u}, \boldsymbol{e}))\\
&= C_{\mathrm{c},\tilde r}^{-1}\chi_{\mathrm{hc}}^{-1}\left(|\boldsymbol{u}|^r_{W^{1,r}(\Omega)^d} + |\boldsymbol{u}'|^r_{W^{1,r}(\Omega)^d}\right)^{\frac{1-s}{r}}(a(\boldsymbol{u}, \boldsymbol{e}) - a(\boldsymbol{u}', \boldsymbol{e}))\\
&\ge C_{\mathrm{c},\tilde r}^{-1}\chi_{\mathrm{hc}}^{-1}C_{\mathrm{a}}\sigma_{\mathrm{hm}}\left(\delta^r + |\boldsymbol{u}|^r_{W^{1,r}(\Omega)^d} + |\boldsymbol{u}'|^r_{W^{1,r}(\Omega)^d}\right)^{\frac{\tilde r-1-s}{r}}\delta^{r-\tilde r}|\boldsymbol{e}|^2_{W^{1,\tilde r}(\Omega)^d}\\
&\ge C_{\mathrm{c},\tilde r}^{-1}\chi_{\mathrm{hc}}^{-1}C_{\mathrm{a}}\sigma_{\mathrm{hm}}(1+2C_{\mathrm{v}}^r)^{\frac{\tilde r-1-s}{r}}\left[\delta^r + \left(\sigma_{\mathrm{hm}}^{-1}\|\boldsymbol{f}\|_{L^{r'}(\Omega)^d}\right)^{r'}\right]^{\frac{\tilde r-1-s}{r}}\delta^{r-\tilde r}|\boldsymbol{e}|^2_{W^{1,\tilde r}(\Omega)^d},
\end{aligned}
$$

where the equality in the second line is obtained using (3.19) with $\boldsymbol{v} = \boldsymbol{e}$ together with the fact that $b(\boldsymbol{e}, p - p') = 0$ thanks to (3.10b), the third line is obtained invoking the Hölder monotonicity (3.21) of a with $m = \tilde r$, while the conclusion follows using the a priori bound (3.16). Since $|\boldsymbol{e}|_{W^{1,\tilde r}(\Omega)^d} > 0$, simplifying and raising to the power $\frac{r}{\tilde r-1-s} < 0$, we infer the contrapositive of (3.18). □

We next prove the Hölder monotonicity of a used in the proof of Theorem 3.2.3 above after recalling the following result. Let $X \subset \mathbb{R}^d$ be measurable, $n \in \mathbb{N}^*$, and let $t, p_1, \dots, p_n \in (0, \infty]$ be such that $\sum_{i=1}^n \frac{1}{p_i} = \frac{1}{t}$. The continuous $(t; p_1, \dots, p_n)$-Hölder inequality reads: For any $(f_1, \dots, f_n) \in \bigtimes_{i=1}^n L^{p_i}(X)$,

$$
\left\|\prod_{i=1}^n f_i\right\|_{L^t(X)} \le \prod_{i=1}^n \|f_i\|_{L^{p_i}(X)}. \tag{3.20}
$$

Lemma 68 (Hölder monotonicity of a)**.** *For $m \in \{\tilde r, r\}$ and all $\boldsymbol{u}, \boldsymbol{w} \in \boldsymbol{U}$, it holds*

$$
\begin{aligned}
&a(\boldsymbol{u}, \boldsymbol{u} - \boldsymbol{w}) - a(\boldsymbol{w}, \boldsymbol{u} - \boldsymbol{w})\\
&\qquad \ge C_{\mathrm{a}}\sigma_{\mathrm{hm}}\left(\delta^r + |\boldsymbol{u}|^r_{W^{1,r}(\Omega)^d} + |\boldsymbol{w}|^r_{W^{1,r}(\Omega)^d}\right)^{\frac{\tilde r-2}{r}}\delta^{r-m}|\boldsymbol{u} - \boldsymbol{w}|^{m+2-\tilde r}_{W^{1,m}(\Omega)^d}.
\end{aligned} \tag{3.21}
$$

Proof. The case $m = r$ is obtained reasoning as in [27, Eq. (46)] and using the Korn inequality (3.15). It remains to prove the case $r > 2$ with $m = \tilde r = 2$. Let $\boldsymbol{e} \coloneqq \boldsymbol{u} - \boldsymbol{w}$. Using the Hölder monotonicity (3.6) of $\boldsymbol{\sigma}$ with $(\boldsymbol{\tau}, \boldsymbol{\eta}) = (\boldsymbol{\nabla}_{\mathrm{s}}\boldsymbol{u}, \boldsymbol{\nabla}_{\mathrm{s}}\boldsymbol{w})$ yields

$$
\begin{aligned}
&\sigma_{\mathrm{hm}}\|\boldsymbol{\nabla}_{\mathrm{s}}\boldsymbol{e}\|^2_{L^2(\Omega)^{d\times d}}\\
&\quad\le \int_\Omega \left(\delta^r + |\boldsymbol{\nabla}_{\mathrm{s}}\boldsymbol{u}|^r_{d\times d} + |\boldsymbol{\nabla}_{\mathrm{s}}\boldsymbol{w}|^r_{d\times d}\right)^{\frac{2-r}{r}}\left(\boldsymbol{\sigma}(\cdot, \boldsymbol{\nabla}_{\mathrm{s}}\boldsymbol{u}) - \boldsymbol{\sigma}(\cdot, \boldsymbol{\nabla}_{\mathrm{s}}\boldsymbol{w})\right) : \boldsymbol{\nabla}_{\mathrm{s}}\boldsymbol{e}\\
&\quad\le \delta^{2-r}\big(a(\boldsymbol{u}, \boldsymbol{e}) - a(\boldsymbol{w}, \boldsymbol{e})\big),
\end{aligned} \tag{3.22}
$$

where we used the monotonicity of $\mathbb{R} \ni x \mapsto x^{2-r} \in \mathbb{R}$ since $r > 2$, together with the definition (3.11) of a. Applying the Korn inequality (3.15) yields (3.21). □

We move to the Hölder continuity of c used in the proof of Theorem 3.2.3 above after recalling some preliminary results. For any $n \in \mathbb{N}^*$, the $(s,0)$-power framed function $\mathbb{R}^n \ni x \mapsto |x|^{s-2}x \in \mathbb{R}^n$ enjoys the following properties (see [27, Appendix A]): There exist $C_{\mathrm{hc}}, C_{\mathrm{hm}} \in (0,\infty)$ depending only on s, such that the following Hölder continuity and the Hölder monotonicity properties hold for all $x, y \in \mathbb{R}^n$,

$$||x|^{s-2}x - |y|^{s-2}y| \le C_{\mathrm{hc}}(|x|^s + |y|^s)^{\frac{s-\tilde{s}}{s}}|x-y|^{\tilde{s}-1}, \tag{3.23a}$$

$$(|x|^{s-2}x - |y|^{s-2}y)\cdot(x-y) \ge C_{\mathrm{hm}}(|x|^s + |y|^s)^{\frac{\tilde{s}-2}{s}}|x-y|^{s+2-\tilde{s}}. \tag{3.23b}$$

Finally, we recall the following Sobolev embeddings: For all $m \in [1,\infty)$ such that $m \le r^*$ and all $\boldsymbol{v} \in \boldsymbol{U}$,

$$\|\boldsymbol{v}\|_{L^m(\Omega)^d} \le C_{\mathrm{S},m}|\boldsymbol{v}|_{W^{1,r}(\Omega)^d}, \tag{3.24}$$

where $C_{\mathrm{S},m} > 0$ is a real number depending only on m, r, d, and Ω.

Lemma 69 (Hölder continuity of c)**.** *Under Assumption 6, for all $m \in [1,r]$ such that*

$$s \le \frac{m^*}{m'}, \tag{3.25}$$

and all $\boldsymbol{u},\boldsymbol{v},\boldsymbol{w} \in \boldsymbol{U}$,

$$|c(\boldsymbol{u},\boldsymbol{v}) - c(\boldsymbol{w},\boldsymbol{v})| \le C_{\mathrm{c},m}\chi_{\mathrm{hc}}\left(|\boldsymbol{u}|^r_{W^{1,r}(\Omega)^d} + |\boldsymbol{w}|^r_{W^{1,r}(\Omega)^d}\right)^{\frac{s+1-\tilde{s}}{r}} |\boldsymbol{u}-\boldsymbol{w}|^{\tilde{s}-1}_{W^{1,m}(\Omega)^d}|\boldsymbol{v}|_{W^{1,m}(\Omega)^d}, \tag{3.26}$$

where $C_{\mathrm{c},m} > 0$ depends only on m, r, s, d, and Ω.

Proof. Throughout the proof, $a \lesssim b$ (resp. $a \gtrsim b$) means $a \le Cb$ (resp. $a \ge Cb$) with $C > 0$ having the same dependencies as $C_{\mathrm{c},m}$.

Using the definition (3.12) of c and inserting $\pm\left(\frac{1}{s}\int_\Omega(\boldsymbol{\chi}(\cdot,\boldsymbol{u})\cdot\boldsymbol{\nabla})\boldsymbol{w}\cdot\boldsymbol{v}\right.$

$+\frac{s-2}{s}\int_\Omega \frac{\boldsymbol{v}\cdot\boldsymbol{u}}{|\boldsymbol{u}|^2}(\chi(\cdot,\boldsymbol{u})\cdot\boldsymbol{\nabla})\boldsymbol{w}\cdot\boldsymbol{u}+\frac{1}{s'}\int_\Omega(\chi(\cdot,\boldsymbol{u})\cdot\boldsymbol{\nabla})\boldsymbol{v}\cdot\boldsymbol{w}\big)$, we get

$$
\begin{aligned}
&c(\boldsymbol{u},\boldsymbol{v})-c(\boldsymbol{w},\boldsymbol{v})\\
&=\frac{1}{s}\Bigg(\underbrace{\int_\Omega(\chi(\cdot,\boldsymbol{u})\cdot\boldsymbol{\nabla})(\boldsymbol{u}-\boldsymbol{w})\cdot\boldsymbol{v}}_{\mathcal{T}_1}+\underbrace{\int_\Omega\big((\chi(\cdot,\boldsymbol{u})-\chi(\cdot,\boldsymbol{w}))\cdot\boldsymbol{\nabla}\big)\boldsymbol{w}\cdot\boldsymbol{v}}_{\mathcal{T}_2}\Bigg)\\
&+\frac{s-2}{s}\Bigg(\underbrace{\int_\Omega\frac{\boldsymbol{v}\cdot\boldsymbol{u}}{|\boldsymbol{u}|^2}(\chi(\cdot,\boldsymbol{u})\cdot\boldsymbol{\nabla})(\boldsymbol{u}-\boldsymbol{w})\cdot\boldsymbol{u}}_{\mathcal{T}_3}\\
&\qquad+\underbrace{\int_\Omega\left(\frac{\boldsymbol{v}\cdot\boldsymbol{u}}{|\boldsymbol{u}|^2}(\chi(\cdot,\boldsymbol{u})\cdot\boldsymbol{\nabla})\boldsymbol{w}\cdot\boldsymbol{u}-\frac{\boldsymbol{v}\cdot\boldsymbol{w}}{|\boldsymbol{w}|^2}(\chi(\cdot,\boldsymbol{w})\cdot\boldsymbol{\nabla})\boldsymbol{w}\cdot\boldsymbol{w}\right)}_{\mathcal{T}_4}\Bigg)\\
&-\frac{1}{s'}\Bigg(\underbrace{\int_\Omega(\chi(\cdot,\boldsymbol{u})\cdot\boldsymbol{\nabla})\boldsymbol{v}\cdot(\boldsymbol{u}-\boldsymbol{w})}_{\mathcal{T}_5}+\underbrace{\int_\Omega\big((\chi(\cdot,\boldsymbol{u})-\chi(\cdot,\boldsymbol{w}))\cdot\boldsymbol{\nabla}\big)\boldsymbol{v}\cdot\boldsymbol{w}}_{\mathcal{T}_6}\Bigg).
\end{aligned}
\tag{3.27}
$$

We start by writing

$$
\begin{aligned}
|\mathcal{T}_1|+|\mathcal{T}_3|&\lesssim\int_\Omega|\chi(\cdot,\boldsymbol{u})||\boldsymbol{\nabla}(\boldsymbol{u}-\boldsymbol{w})|_{d\times d}|\boldsymbol{v}|\\
&\le\chi_{\mathrm{hc}}\int_\Omega|\boldsymbol{u}|^{s-1}|\boldsymbol{\nabla}(\boldsymbol{u}-\boldsymbol{w})|_{d\times d}|\boldsymbol{v}|\\
&\le\chi_{\mathrm{hc}}\|\boldsymbol{u}\|^{s-1}_{L^{sm'}(\Omega)^d}|\boldsymbol{u}-\boldsymbol{w}|_{W^{1,m}(\Omega)^d}\|\boldsymbol{v}\|_{L^{sm'}(\Omega)^d}\\
&\lesssim\chi_{\mathrm{hc}}|\boldsymbol{u}|^{s-1}_{W^{1,r}(\Omega)^d}|\boldsymbol{u}-\boldsymbol{w}|^{2-\tilde{s}}_{W^{1,r}(\Omega)^d}|\boldsymbol{u}-\boldsymbol{w}|^{\tilde{s}-1}_{W^{1,m}(\Omega)^d}|\boldsymbol{v}|_{W^{1,m}(\Omega)^d}\\
&\lesssim\chi_{\mathrm{hc}}\Big(|\boldsymbol{u}|^r_{W^{1,r}(\Omega)^d}+|\boldsymbol{w}|^r_{W^{1,r}(\Omega)^d}\Big)^{\frac{s+1-\tilde{s}}{r}}|\boldsymbol{u}-\boldsymbol{w}|^{\tilde{s}-1}_{W^{1,m}(\Omega)^d}|\boldsymbol{v}|_{W^{1,m}(\Omega)^d},
\end{aligned}
\tag{3.28}
$$

where we have used the Hölder continuity (3.8e) of χ with $(\boldsymbol{w},\boldsymbol{v})=(\boldsymbol{u},\boldsymbol{0})$ to pass to the second line, the $(1;\frac{sm'}{s-1},m,sm')$-Hölder inequality (3.20) in the third line, the Sobolev embedding (3.24) (valid since $sm'\le m^*$ by (3.25) and $m\le r\implies m^*\le r^*$, so that $sm'\le r^*$) together with the $(1;\frac{r}{m},\frac{r}{r-m})$-Hölder inequality (3.20) (valid since $m\le r$) in the fourth line, while the conclusion follows writing first $|\boldsymbol{u}|^{s-1}_{W^{1,r}(\Omega)^d}\le(|\boldsymbol{u}|_{W^{1,r}(\Omega)^d}+|\boldsymbol{w}|_{W^{1,r}(\Omega)^d})^{s-1}$ by monotonicity of $\mathbb{R}\ni x\mapsto x^{s-1}\in\mathbb{R}$, then $|\boldsymbol{u}-\boldsymbol{w}|^{2-\tilde{s}}_{W^{1,r}(\Omega)^d}\le(|\boldsymbol{u}|_{W^{1,r}(\Omega)^d}+|\boldsymbol{w}|_{W^{1,r}(\Omega)^d})^{2-\tilde{s}}$ by a triangle inequality, and, finally, noticing that $(x+y)^r\lesssim x^r+y^r$ for all $x,y\in[0,\infty)$ (see [27, Eq. (36)]). Similar arguments give

for the fifth term

$$
\begin{aligned}
|\mathcal{T}_5| &\le \chi_{\mathrm{hc}} \int_\Omega |\boldsymbol{u}|^{s-1}|\boldsymbol{u}-\boldsymbol{w}||\boldsymbol{\nabla} \boldsymbol{v}|_{d\times d} \\
&\le \chi_{\mathrm{hc}} \|\boldsymbol{u}\|_{L^{sm'}(\Omega)^d}^{s-1} \|\boldsymbol{u}-\boldsymbol{w}\|_{L^{sm'}(\Omega)^d} |\boldsymbol{v}|_{W^{1,m}(\Omega)^d} \\
&\lesssim \chi_{\mathrm{hc}} \Big(|\boldsymbol{u}|_{W^{1,r}(\Omega)^d}^r + |\boldsymbol{w}|_{W^{1,r}(\Omega)^d}^r \Big)^{\frac{s+1-\tilde{s}}{r}} |\boldsymbol{u}-\boldsymbol{w}|_{W^{1,m}(\Omega)^d}^{\tilde{s}-1} |\boldsymbol{v}|_{W^{1,m}(\Omega)^d}.
\end{aligned}
\tag{3.29}
$$

We next estimate $\mathcal{T}_4$, which provides a paradigm for the remaining terms. Inserting $\pm\big(|\boldsymbol{u}|^{s-2}|\boldsymbol{w}|^{-1}\boldsymbol{u}\otimes\boldsymbol{w} + |\boldsymbol{w}|^{s-2}|\boldsymbol{u}|^{-1}\boldsymbol{w}\otimes\boldsymbol{u} + |\boldsymbol{u}|^{s-3}\boldsymbol{u}\otimes\boldsymbol{u}\big)$, rearranging the terms, and using a triangle inequality yields

$$
\begin{aligned}
&|\boldsymbol{w}|^{s-1} \big| |\boldsymbol{u}|^{-2}\boldsymbol{u}\otimes\boldsymbol{u} - |\boldsymbol{w}|^{-2}\boldsymbol{w}\otimes\boldsymbol{w}\big|_{d\times d} \\
&\quad \le \Big| |\boldsymbol{w}|^{-1} \Big(|\boldsymbol{u}|^{s-2}\boldsymbol{u} - |\boldsymbol{w}|^{s-2}\boldsymbol{w}\Big)\otimes\boldsymbol{w}\Big|_{d\times d} \\
&\qquad + \Big| |\boldsymbol{u}|^{-1} \Big(|\boldsymbol{u}|^{s-2}\boldsymbol{u} - |\boldsymbol{w}|^{s-2}\boldsymbol{w}\Big)\otimes\boldsymbol{u}\Big|_{d\times d} \\
&\qquad + \Big| |\boldsymbol{u}|^{-1} \Big(|\boldsymbol{w}|^{s-2}|\boldsymbol{w}| - |\boldsymbol{u}|^{s-2}|\boldsymbol{u}|\Big) \Big(|\boldsymbol{u}|^{-1}\boldsymbol{u} + |\boldsymbol{w}|^{-1}\boldsymbol{w}\Big)\otimes\boldsymbol{u}\Big|_{d\times d} \\
&\quad \le 4\big||\boldsymbol{u}|^{s-2}\boldsymbol{u} - |\boldsymbol{w}|^{s-2}\boldsymbol{w}\big| \le 4C_{\mathrm{hc}} \left(|\boldsymbol{u}|^s + |\boldsymbol{w}|^s\right)^{\frac{s-\tilde{s}}{s}} |\boldsymbol{u}-\boldsymbol{w}|^{\tilde{s}-1},
\end{aligned}
\tag{3.30}
$$

where the last line is obtained using Cauchy-Schwarz and triangle inequalities along with the Hölder continuity property (3.23a). Thus, inserting $\pm\frac{\boldsymbol{v}\cdot\boldsymbol{u}}{|\boldsymbol{u}|^2}(\boldsymbol{\chi}(\cdot,\boldsymbol{w})\cdot\boldsymbol{\nabla})\boldsymbol{w}\cdot\boldsymbol{u}$ and using a triangle inequality leads to

$$
\begin{aligned}
|\mathcal{T}_4| &\le \int_\Omega \Big(|\boldsymbol{\chi}(\cdot,\boldsymbol{u}) - \boldsymbol{\chi}(\cdot,\boldsymbol{w})| + |\boldsymbol{\chi}(\cdot,\boldsymbol{w})| \big||\boldsymbol{u}|^{-2}\boldsymbol{u}\otimes\boldsymbol{u} - |\boldsymbol{w}|^{-2}\boldsymbol{w}\otimes\boldsymbol{w}\big|_{d\times d}\Big) \\
&\qquad \times |\boldsymbol{\nabla}\boldsymbol{w}|_{d\times d}|\boldsymbol{v}| \\
&\le (1+4C_{\mathrm{hc}})\chi_{\mathrm{hc}} \int_\Omega \left(|\boldsymbol{u}|^s + |\boldsymbol{w}|^s\right)^{\frac{s-\tilde{s}}{s}} |\boldsymbol{u}-\boldsymbol{w}|^{\tilde{s}-1} |\boldsymbol{\nabla}\boldsymbol{w}|_{d\times d}|\boldsymbol{v}| \\
&\le (1+4C_{\mathrm{hc}})\chi_{\mathrm{hc}} \Big(\|\boldsymbol{u}\|_{L^{sm'}(\Omega)^d}^s + \|\boldsymbol{w}\|_{L^{sm'}(\Omega)^d}^s \Big)^{\frac{s-\tilde{s}}{s}} \|\boldsymbol{u}-\boldsymbol{w}\|_{L^{sm'}(\Omega)^d}^{\tilde{s}-1} \\
&\qquad \times |\boldsymbol{w}|_{W^{1,m}(\Omega)^d} \|\boldsymbol{v}\|_{L^{sm'}(\Omega)^d} \\
&\lesssim \chi_{\mathrm{hc}} \Big(|\boldsymbol{u}|_{W^{1,r}(\Omega)^d}^r + |\boldsymbol{w}|_{W^{1,r}(\Omega)^d}^r \Big)^{\frac{s+1-\tilde{s}}{r}} |\boldsymbol{u}-\boldsymbol{w}|_{W^{1,m}(\Omega)^d}^{\tilde{s}-1} |\boldsymbol{v}|_{W^{1,m}(\Omega)^d},
\end{aligned}
\tag{3.31}
$$

where we have used the Hölder continuity property (3.8e) of $\boldsymbol{\chi}$ together with (3.30) in the second inequality, the $(1; \frac{sm'}{s-\tilde{s}}, \frac{sm'}{\tilde{s}-1}, m, sm')$-Hölder inequality (3.20) in the third inequality, and the Sobolev embedding (3.24) (since, as showed above, $sm' \le m^* \le r^*$) together with the $(1; \frac{r}{m}, \frac{r}{r-m})$-Hölder inequality (3.20) (since $m \le r$) and the inequality [27, Eq. (36)] to conclude. Similar arguments give for the second and sixth terms an

analogous bound:

$$|\mathcal{T}_2| + |\mathcal{T}_6| \lesssim \chi_{\mathrm{hc}} \left(|\boldsymbol{u}|^r_{W^{1,r}(\Omega)^d} + |\boldsymbol{w}|^r_{W^{1,r}(\Omega)^d} \right)^{\frac{s+1-\tilde{s}}{r}} |\boldsymbol{u} - \boldsymbol{w}|^{\tilde{s}-1}_{W^{1,m}(\Omega)^d} |\boldsymbol{v}|_{W^{1,m}(\Omega)^d}. \tag{3.32}$$

Plugging (3.28), (3.29), (3.31), and (3.32) into (3.27) gives (3.26). □

Remark 70 (Role of condition (3.25)). In the proof of Lemma 69, condition (3.25) is used (along with $m \le r$) to control $L^{sm'}$-norms of functions in $\boldsymbol{U}$ with $W^{1,m}$-(semi)norms.

3.3 Discrete setting

In this section we establish the discrete setting.

3.3.1 Mesh and notation for inequalities up to a multiplicative constant

Let $\mathcal{H} \subset (0, \infty)$ be a countable set of meshsizes having 0 as its unique accumulation point. Given a set $X \subset \mathbb{R}^d$, we denote by $h_X := \sup_{(\boldsymbol{x},\boldsymbol{y})\in X^2} |\boldsymbol{x} - \boldsymbol{y}|$ its diameter. For all $h \in \mathcal{H}$, we define a mesh as a couple $\mathcal{M}_h := (\mathcal{T}_h, \mathcal{F}_h)$ where $\mathcal{T}_h$ is a finite collection of polyhedral elements such that $h = \max_{T\in\mathcal{T}_h} h_T$, while $\mathcal{F}_h$ is a finite collection of planar faces. Notice that, here and in what follows, we use the three-dimensional nomenclature also when $d = 2$, i.e., we speak of polyhedra and faces rather than polygons and edges. It is assumed henceforth that the mesh $\mathcal{M}_h$ matches the geometrical requirements detailed in [50, Definition 1.7]. In order to have the boundedness property (3.40) below for the interpolator, we additionally assume that the mesh elements are star-shaped with respect to every point of a ball of radius uniformly comparable to the element diameter. Boundary faces lying on $\partial\Omega$ and internal faces contained in Ω are collected in the sets $\mathcal{F}_h^{\mathrm{b}}$ and $\mathcal{F}_h^{\mathrm{i}}$, respectively. For every mesh element $T \in \mathcal{T}_h$, we denote by $\mathcal{F}_T$ the subset of $\mathcal{F}_h$ containing the faces that lie on the boundary ∂T of T. For every face $F \in \mathcal{F}_h$, we denote by $\mathcal{T}_F$ the subset of $\mathcal{T}_h$ containing the one (if $F \in \mathcal{F}_h^{\mathrm{b}}$) or two (if $F \in \mathcal{F}_h^{\mathrm{i}}$) elements on whose boundary F lies. For each mesh element $T \in \mathcal{T}_h$ and face $F \in \mathcal{F}_T$, $\boldsymbol{n}_{TF}$ denotes the (constant) unit vector normal to F pointing out of T.

Our focus is on the h-convergence analysis, so we assume that the mesh sequence $(\mathcal{M}_h)_{h\in\mathcal{H}}$ is regular in the sense of [50, Definition 1.9], with regularity parameter uniformly bounded away from zero. The mesh regularity assumption implies, in particular, that the diameter of a mesh element and those of its faces are comparable uniformly in h and that the number of faces of one element is bounded above by an integer independent of h.

To avoid the proliferation of generic constants, we write henceforth $a \lesssim b$ (resp., $a \gtrsim b$) for the inequality $a \le Cb$ (resp., $a \ge Cb$) with real number $C > 0$ independent

of h, of the constants $\delta, \sigma_{\mathrm{hc}}, \sigma_{\mathrm{hm}}, \chi_{\mathrm{hc}}$ in Assumptions 5 and 6, and, for local inequalities, of the mesh element or face on which the inequality holds. We also write $a \simeq b$ to mean $a \lesssim b$ and $b \lesssim a$. The dependencies of the hidden constants are further specified when needed.

3.3.2 Projectors and broken spaces

Given $X \in \mathcal{T}_h \cup \mathcal{F}_h$ and $l \in \mathbb{N}$, we denote by $\mathbb{P}^l(X)$ the space spanned by the restriction to X of scalar-valued, d-variate polynomials of total degree $\le l$. The local L^2-orthogonal projector $\pi_X^l : L^1(X) \to \mathbb{P}^l(X)$ is defined such that, for all $v \in L^1(X)$,

$$\int_X (\pi_X^l v - v) w = 0 \qquad \forall w \in \mathbb{P}^l(X). \tag{3.33}$$

When applied to vector-valued fields in $L^1(X)^d$ (resp., tensor-valued fields in $L^1(X)^{d\times d}$), the L^2-orthogonal projector mapping on $\mathbb{P}^l(X)^d$ (resp., $\mathbb{P}^l(X)^{d\times d}$) acts component-wise and is denoted in boldface font. Let $T \in \mathcal{T}_h$, $m \in [1,\infty]$, $i \in [0, l+1]$, and $j \in [0, i]$. The following (i, m, j)-approximation properties of π_T^l hold: For any $v \in W^{i,m}(T)$,

$$|v - \pi_T^l v|_{W^{j,m}(T)} \lesssim h_T^{i-j} |v|_{W^{i,m}(T)}. \tag{3.34a}$$

If, additionally, $i \ge j + 1$, we have the following (i, m, j)-trace approximation property:

$$|v - \pi_T^l v|_{W^{j,m}(\partial T)} \lesssim h_T^{i-j-\frac{1}{m}} |v|_{W^{i,m}(T)}. \tag{3.34b}$$

The hidden constants in (3.34) are independent of h and T, but possibly depend on d, the mesh regularity parameter, l, i, and m. The approximation properties (3.34) are proved for integer i and j in [48, Appendix A.2] (see also [50, Theorem 1.45]), and can be extended to non-integer values using standard interpolation techniques (see, e.g., [89, Theorem 5.1]).

At the global level, we define the broken polynomial space $\mathbb{P}^l(\mathcal{T}_h)$ spanned by functions in $L^1(\Omega)$ whose restriction to each mesh element $T \in \mathcal{T}_h$ lies in $\mathbb{P}^l(T)$, and we define the global L^2-orthogonal projector $\pi_h^l : L^1(\Omega) \to \mathbb{P}^l(\mathcal{T}_h)$ such that, for all $v \in L^1(\Omega)$ and all $T \in \mathcal{T}_h$,

$$(\pi_h^l v)_{|T} \coloneqq \pi_T^l v_{|T}.$$

Broken polynomial spaces are subspaces of the broken Sobolev spaces

$$W^{n,m}(\mathcal{T}_h) \coloneqq \left\{ v \in L^m(\Omega) \ : \ v_{|T} \in W^{n,m}(T) \quad \forall T \in \mathcal{T}_h \right\},$$

which we endow with the usual broken seminorm $|\cdot|_{W^{n,m}(\mathcal{T}_h)}$; see, e.g., [58, Section 1.2.5] for further details. As a consequence of the $(l+1, \cdot, \cdot)$-approximation properties (3.34a), for all $\phi \in C_c^\infty(\Omega)$,

$$\pi_h^l \phi \xrightarrow[h\to 0]{} \phi \text{ strongly in } W^{[0,l],[1,\infty)}(\mathcal{T}_h). \tag{3.35}$$

We define the broken gradient operator $\boldsymbol{\nabla}_h : W^{1,1}(\mathcal{T}_h) \to L^1(\Omega)^d$ such that, for all $v \in W^{1,1}(\mathcal{T}_h)$ and all $T \in \mathcal{T}_h$, $(\boldsymbol{\nabla}_h v)_{|T} \coloneqq \boldsymbol{\nabla} v_{|T}$. We define similarly the broken gradient acting on vector fields along with its symmetric part $\boldsymbol{\nabla}_{\mathrm{s},h}$, as well as the broken divergence operator $\boldsymbol{\nabla}_h\cdot$ acting (row-wise) on tensor fields. The global L^2-orthogonal projector $\boldsymbol{\pi}_h^l$ mapping vector-valued fields in $L^1(\Omega)^d$ (resp., tensor-valued fields in $L^1(\Omega)^{d\times d}$) on $\mathbb{P}^l(\mathcal{T}_h)^d$ (resp., $\mathbb{P}^l(\mathcal{T}_h)^{d\times d}$) is obtained applying π_h^l component-wise.

3.4 Discrete problem and main results

3.4.1 Discrete spaces and norms

Let an integer $k \geq 1$ be fixed. The HHO space of discrete velocities is

$$\underline{\boldsymbol{U}}_h^k \coloneqq \left\{ \underline{\boldsymbol{v}}_h \coloneqq ((\boldsymbol{v}_T)_{T\in\mathcal{T}_h}, (\boldsymbol{v}_F)_{F\in\mathcal{F}_h}) \;\middle|\; \begin{array}{l} \boldsymbol{v}_T \in \mathbb{P}^k(T)^d \quad \forall T \in \mathcal{T}_h \\ \boldsymbol{v}_F \in \mathbb{P}^k(F)^d \quad \forall F \in \mathcal{F}_h \end{array} \right\}.$$

The interpolation operator $\underline{\boldsymbol{I}}_h^k : W^{1,1}(\Omega)^d \to \underline{\boldsymbol{U}}_h^k$ maps a function $\boldsymbol{v} \in W^{1,1}(\Omega)^d$ on the vector of polynomials $\underline{\boldsymbol{I}}_h^k \boldsymbol{v}$ defined as follows:

$$\underline{\boldsymbol{I}}_h^k \boldsymbol{v} \coloneqq ((\boldsymbol{\pi}_T^k \boldsymbol{v}_{|T})_{T\in\mathcal{T}_h}, (\boldsymbol{\pi}_F^k \boldsymbol{v}_{|F})_{F\in\mathcal{F}_h}).$$

For all $T \in \mathcal{T}_h$, we denote by $\underline{\boldsymbol{U}}_T^k$ and $\underline{\boldsymbol{I}}_T^k$ the restrictions of $\underline{\boldsymbol{I}}_h^k$ and $\underline{\boldsymbol{U}}_h^k$ to T, respectively and, for all $\underline{\boldsymbol{v}}_h \in \underline{\boldsymbol{U}}_h^k$, we let $\underline{\boldsymbol{v}}_T \coloneqq (\boldsymbol{v}_T, (\boldsymbol{v}_F)_{F\in\mathcal{F}_T}) \in \underline{\boldsymbol{U}}_T^k$ denote the vector collecting the polynomial components of $\underline{\boldsymbol{v}}_h$ attached to T and its faces. Furthermore, for all $\underline{\boldsymbol{v}}_h \in \underline{\boldsymbol{U}}_h^k$, we define the broken polynomial field $\boldsymbol{v}_h \in \mathbb{P}^k(\mathcal{T}_h)^d$ obtained patching element unknowns, that is,

$$(\boldsymbol{v}_h)_{|T} \coloneqq \boldsymbol{v}_T \qquad \forall T \in \mathcal{T}_h. \tag{3.36}$$

For any $m \in (1,\infty)$, we define on $\underline{\boldsymbol{U}}_h^k$ the seminorms $\|\cdot\|_{1,m,h}$ and $\|\cdot\|_{\boldsymbol{\varepsilon},m,h}$ such that, for all $\underline{\boldsymbol{v}}_h \in \underline{\boldsymbol{U}}_h^k$,

$$\|\underline{\boldsymbol{v}}_h\|_{\bullet,m,h} \coloneqq \left(\sum_{T\in\mathcal{T}_h} \|\underline{\boldsymbol{v}}_T\|_{\bullet,m,T}^m \right)^{\frac{1}{m}} \qquad \forall \bullet \in \{1, \boldsymbol{\varepsilon}\}, \tag{3.37a}$$

with, for all $T \in \mathcal{T}_h$,

$$\begin{aligned} \|\underline{\boldsymbol{v}}_T\|_{1,m,T} &\coloneqq \left(\|\boldsymbol{\nabla}\boldsymbol{v}_T\|_{L^m(T)^{d\times d}}^m + \sum_{F\in\mathcal{F}_T} h_F^{1-m} \|\boldsymbol{v}_F - \boldsymbol{v}_T\|_{L^m(F)^d}^m \right)^{\frac{1}{m}}, \\ \|\underline{\boldsymbol{v}}_T\|_{\boldsymbol{\varepsilon},m,T} &\coloneqq \left(\|\boldsymbol{\nabla}_{\mathrm{s}}\boldsymbol{v}_T\|_{L^m(T)^{d\times d}}^m + \sum_{F\in\mathcal{F}_T} h_F^{1-m} \|\boldsymbol{v}_F - \boldsymbol{v}_T\|_{L^m(F)^d}^m \right)^{\frac{1}{m}}. \end{aligned} \tag{3.37b}$$

The difference between these seminorms lies in the fact that the symmetric part of the gradient replaces the gradient in $\|\cdot\|_{\boldsymbol{\varepsilon},m,T}$.

The discrete velocity and pressure are sought in the following spaces, which embed, respectively, the homogeneous boundary condition for the velocity and the zero-average constraint for the pressure:

$$\underline{\boldsymbol{U}}_{h,0}^k \coloneqq \left\{\underline{\boldsymbol{v}}_h = ((\boldsymbol{v}_T)_{T\in\mathcal{T}_h}, (\boldsymbol{v}_F)_{F\in\mathcal{F}_h}) \in \underline{\boldsymbol{U}}_h^k \;:\; \boldsymbol{v}_F = \boldsymbol{0} \quad \forall F \in \mathcal{F}_h^{\mathrm{b}}\right\},$$
$$P_h^k \coloneqq \mathbb{P}^k(\mathcal{T}_h) \cap P.$$

The following discrete Korn inequality was proved in [27, Lemma 15]:

$$\|\boldsymbol{v}_h\|_{L^m(\Omega)^d}^m + |\boldsymbol{v}_h|_{W^{1,m}(\mathcal{T}_h)^d}^m \lesssim \|\underline{\boldsymbol{v}}_h\|_{\boldsymbol{\varepsilon},m,h}^m \qquad \forall \underline{\boldsymbol{v}}_h \in \underline{\boldsymbol{U}}_{h,0}^k. \tag{3.38}$$

A first consequence of (3.38) is that $\|\cdot\|_{\boldsymbol{\varepsilon},m,h}$ is a norm on $\underline{\boldsymbol{U}}_{h,0}^k$. A second consequence is the following equivalence uniform in h:

$$\|\underline{\boldsymbol{v}}_h\|_{\boldsymbol{\varepsilon},m,h} \simeq \|\underline{\boldsymbol{v}}_h\|_{1,m,h} \qquad \forall \underline{\boldsymbol{v}}_h \in \underline{\boldsymbol{U}}_{h,0}^k. \tag{3.39}$$

The following boundedness property for $\underline{\boldsymbol{I}}_T^k$ is proved in [50, Proposition 6.24] and requires the star-shaped assumption on the mesh elements: For all $T \in \mathcal{T}_h$ and all $\boldsymbol{v} \in W^{1,r}(T)^d$,

$$\|\underline{\boldsymbol{I}}_T^k \boldsymbol{v}\|_{1,r,T} \le C_{\mathrm{I}} |\boldsymbol{v}|_{W^{1,r}(T)^d}, \tag{3.40}$$

where $C_{\mathrm{I}} \ge 1$ depends only on d, the mesh regularity parameter, r, and k.

Finally, we recall the following discrete Sobolev embeddings (see [48, Proposition 5.4]): For all $m \in [1,\infty)$ such that $m \le r^*$,

$$\|\boldsymbol{v}_h\|_{L^m(\Omega)^d} \lesssim \|\underline{\boldsymbol{v}}_h\|_{1,r,h} \lesssim \|\underline{\boldsymbol{v}}_h\|_{\boldsymbol{\varepsilon},r,h} \qquad \forall \underline{\boldsymbol{v}}_h \in \underline{\boldsymbol{U}}_{h,0}^k, \tag{3.41}$$

where the last inequality is a consequence of (3.39).

3.4.2 Local gradient reconstruction

For all $T \in \mathcal{T}_h$, we define the local gradient reconstruction $\mathbf{G}_T^k : \underline{\boldsymbol{U}}_T^k \to \mathbb{P}^k(T)^{d\times d}$ such that, for all $\underline{\boldsymbol{v}}_T \in \underline{\boldsymbol{U}}_T^k$, and for all $\boldsymbol{\tau} \in \mathbb{P}^k(T)^{d\times d}$,

$$\int_T \mathbf{G}_T^k \underline{\boldsymbol{v}}_T : \boldsymbol{\tau} = \int_T \boldsymbol{\nabla}\boldsymbol{v}_T : \boldsymbol{\tau} + \sum_{F\in\mathcal{F}_T} \int_F (\boldsymbol{v}_F - \boldsymbol{v}_T)\cdot(\boldsymbol{\tau}\boldsymbol{n}_{TF}). \tag{3.42}$$

A global gradient reconstruction $\mathbf{G}_h^k : \underline{\boldsymbol{U}}_h^k \to \mathbb{P}^k(\mathcal{T}_h)^{d\times d}$ is obtained patching the local contributions, that is, for all $\underline{\boldsymbol{v}}_h \in \underline{\boldsymbol{U}}_h^k$, we set

$$(\mathbf{G}_h^k \underline{\boldsymbol{v}}_h)_{|T} \coloneqq \mathbf{G}_T^k \underline{\boldsymbol{v}}_T \qquad \forall T \in \mathcal{T}_h. \tag{3.43}$$

By construction, the following commutation property holds (see [62, Eq. (23)]): For all $T \in \mathcal{T}_h$ and all $\boldsymbol{v} \in W^{1,1}(T)^d$,

$$\mathbf{G}_T^k(\underline{\boldsymbol{I}}_T^k \boldsymbol{v}) = \boldsymbol{\pi}_T^k(\boldsymbol{\nabla} \boldsymbol{v}). \tag{3.44}$$

Combined with the $(k+1, r, 0)$-approximation properties (3.34) of $\boldsymbol{\pi}_T^k$, this gives, for all $\boldsymbol{v} \in W^{k+2,r}(T)^d$,

$$\|\mathbf{G}_T^k(\underline{\boldsymbol{I}}_T^k \boldsymbol{v}) - \boldsymbol{\nabla} \boldsymbol{v}\|_{L^r(T)^{d\times d}} + \left(\sum_{F\in\mathcal{F}_T} h_F \|\mathbf{G}_T^k(\underline{\boldsymbol{I}}_T^k \boldsymbol{v}) - \boldsymbol{\nabla} \boldsymbol{v}\|_{L^r(F)^{d\times d}}^r\right)^{\frac{1}{r}} \lesssim h_T^{k+1} |\boldsymbol{v}|_{W^{k+2,r}(T)^d}. \tag{3.45}$$

As a consequence, for all $\boldsymbol{\phi} \in C_c^\infty(\Omega)^d$,

$$\mathbf{G}_h^k(\underline{\boldsymbol{I}}_h^k \boldsymbol{\phi}) \xrightarrow[h\to 0]{} \boldsymbol{\nabla} \boldsymbol{\phi} \text{ strongly in } L^{[1,\infty)}(\Omega)^{d\times d}. \tag{3.46}$$

Combining [62, Proposition 1.1] with the local Lebesgue embeddings of [50, Lemma 1.25] (see also [48, Lemma 5.1]) gives

$$\|\mathbf{G}_T^k \underline{\boldsymbol{v}}_T\|_{L^r(T)^{d\times d}} \lesssim \|\underline{\boldsymbol{v}}_T\|_{1,r,T} \qquad \forall \underline{\boldsymbol{v}}_T \in \underline{\boldsymbol{U}}_T^k. \tag{3.47}$$

3.4.3 Convective term

The convective term is discretized through the function $\mathrm{c}_h : \underline{\boldsymbol{U}}_h^k \times \underline{\boldsymbol{U}}_h^k \to \mathbb{R}$ such that, for all $(\underline{\boldsymbol{w}}_h, \underline{\boldsymbol{v}}_h) \in \underline{\boldsymbol{U}}_h^k \times \underline{\boldsymbol{U}}_h^k$,

$$\begin{aligned}\mathrm{c}_h(\underline{\boldsymbol{w}}_h, \underline{\boldsymbol{v}}_h) \coloneqq \frac{1}{s}\int_\Omega (\boldsymbol{\chi}(\cdot, \boldsymbol{w}_h)\cdot \mathbf{G}_h^k)\underline{\boldsymbol{w}}_h \cdot \boldsymbol{v}_h - \frac{1}{s'}\int_\Omega (\boldsymbol{\chi}(\cdot, \boldsymbol{w}_h)\cdot \mathbf{G}_h^k)\underline{\boldsymbol{v}}_h \cdot \boldsymbol{w}_h \\ + \frac{s-2}{s}\int_\Omega \frac{\boldsymbol{v}_h\cdot\boldsymbol{w}_h}{|\boldsymbol{w}_h|^2}(\boldsymbol{\chi}(\cdot, \boldsymbol{w}_h)\cdot \mathbf{G}_h^k)\underline{\boldsymbol{w}}_h \cdot \boldsymbol{w}_h.\end{aligned} \tag{3.48}$$

This expression is obtained replacing in (3.12) the continuous gradient by $\mathbf{G}_h^k$ and the functions by their broken polynomial counterparts obtained according to (3.36).

Remark 71 (Comparison with [62]). For the standard convection law corresponding to $s = 2$ and $\boldsymbol{\chi}(\cdot, \boldsymbol{w}) \equiv \boldsymbol{w}$, the convective function (3.48) becomes

$$\mathrm{c}_h(\underline{\boldsymbol{w}}_h, \underline{\boldsymbol{v}}_h) = \frac{1}{2}\int_\Omega (\boldsymbol{w}_h\cdot \mathbf{G}_h^k)\underline{\boldsymbol{w}}_h \cdot \boldsymbol{v}_h - \frac{1}{2}\int_\Omega (\boldsymbol{w}_h\cdot \mathbf{G}_h^k)\underline{\boldsymbol{v}}_h \cdot \boldsymbol{w}_h.$$

This expression differs from the one originally proposed in [62, Eq. (32)] in that a gradient reconstruction of degree k instead of $2k$ (noted $\mathbf{G}_h^{2k}$ therein and defined taking

$\mathbb{P}^{2k}(T)^{d\times d}$ instead of $\mathbb{P}^{k}(T)^{d\times d}$ both as a codomain for $\mathbf{G}_T^{2k}$ and as a test space in (3.42)) is used. The latter choice leads to a simpler expression in the standard case since, for all $\underline{\boldsymbol{v}}_h, \underline{\boldsymbol{w}}_h \in \underline{\boldsymbol{U}}_h^k$ and all $T \in \mathcal{T}_h$, the quantity $\boldsymbol{v}_T \otimes \boldsymbol{\chi}(\cdot, \boldsymbol{w}_T)$ is a polynomial of degree $2k$ inside T, and $\mathbf{G}_T^{2k}$ can thus be expanded according to its definition; cf. [62, Eq. (33)]. This is no longer the case when considering general convection laws, for which the quantity $\boldsymbol{v}_T \otimes \boldsymbol{\chi}(\cdot, \boldsymbol{w}_T)$ is possibly non-polynomial inside T (hence we cannot use its degree to design a discrete gradient allowing to mimic the trick of [62, Eq. (33)]). Additionally, the consistency property (3.45) of $\mathbf{G}_T^k$ is not valid for $\mathbf{G}_T^l$ with $l > k$. As a matter of fact, it is shown in [62, Proposition 1] that one order of convergence is lost in this case, which would result in a degradation of the error estimates if $\mathbf{G}_T^{2k}$ were used in place of $\mathbf{G}_T^k$ in the expression of c_T.

Lemma 72 (Properties of c_h)**.** *Under Assumption 6, the following properties for* c_h *hold:*

1. Non-dissipativity. *For all* $\underline{\boldsymbol{w}}_h \in \underline{\boldsymbol{U}}_h^k$,
$$\mathrm{c}_h(\underline{\boldsymbol{w}}_h, \underline{\boldsymbol{w}}_h) = 0. \tag{3.49}$$

2. Hölder continuity. *For m and s as in Lemma 69 (i.e., $m \in [1, r]$ and $s \le \frac{m^*}{m'}$) and all $\underline{\boldsymbol{u}}_h, \underline{\boldsymbol{v}}_h, \underline{\boldsymbol{w}}_h \in \underline{\boldsymbol{U}}_{h,0}^k$, it holds*
$$\begin{aligned}&\left|\mathrm{c}_h(\underline{\boldsymbol{u}}_h, \underline{\boldsymbol{v}}_h) - \mathrm{c}_h(\underline{\boldsymbol{w}}_h, \underline{\boldsymbol{v}}_h)\right| \\ &\qquad \le C_{\mathrm{dc},m}\chi_{\mathrm{hc}} \left(\|\underline{\boldsymbol{u}}_h\|_{\boldsymbol{\varepsilon},r,h}^r + \|\underline{\boldsymbol{w}}_h\|_{\boldsymbol{\varepsilon},r,h}^r\right)^{\frac{s+1-\tilde{s}}{r}} \|\underline{\boldsymbol{u}}_h - \underline{\boldsymbol{w}}_h\|_{\boldsymbol{\varepsilon},m,h}^{\tilde{s}-1} \|\underline{\boldsymbol{v}}_h\|_{\boldsymbol{\varepsilon},m,h},\end{aligned} \tag{3.50}$$
where $C_{\mathrm{dc},m} > 0$ is independent of h.

3. Consistency. *If*
$$s \le \frac{r^*}{r'}, \tag{3.51}$$
then, for all $\boldsymbol{w} \in \boldsymbol{U} \cap W^{k+2,r}(\mathcal{T}_h)^d \cap W^{k+1,sr'}(\mathcal{T}_h)^d$ (so that, in particular, $\boldsymbol{w} \in W^{1,sr'}(\Omega)^d$) such that $\boldsymbol{\nabla}\cdot\boldsymbol{w} = 0$, it holds
$$\begin{aligned}&\sup_{\underline{\boldsymbol{v}}_h \in \underline{\boldsymbol{U}}_{h,0}^k, \|\underline{\boldsymbol{v}}_h\|_{\boldsymbol{\varepsilon},r,h}=1} \left|\int_\Omega (\boldsymbol{w}\cdot\boldsymbol{\nabla})\boldsymbol{\chi}(\cdot,\boldsymbol{w})\cdot\boldsymbol{v}_h - \mathrm{c}_h(\underline{\boldsymbol{I}}_h^k\boldsymbol{w}, \underline{\boldsymbol{v}}_h)\right| \\ &\quad \lesssim h^{k+1}\left[|\boldsymbol{w}|^s_{W^{k+1,sr'}(\mathcal{T}_h)^d} + \left(|\boldsymbol{w}|^s_{W^{1,sr'}(\Omega)^d} + |\boldsymbol{w}|^s_{W^{1,r}(\Omega)^d}\right)^{\frac{s-1}{s}}\right. \\ &\qquad \left.\times\left(|\boldsymbol{w}|_{W^{k+1,sr'}(\mathcal{T}_h)^d} + |\boldsymbol{w}|_{W^{k+2,r}(\mathcal{T}_h)^d}\right)\right] \\ &\quad + h^{(k+1)(\tilde{s}-1)}\left(|\boldsymbol{w}|^s_{W^{1,sr'}(\Omega)^d} + |\boldsymbol{w}|^s_{W^{1,r}(\Omega)^d}\right)^{\frac{s+1-\tilde{s}}{s}} |\boldsymbol{w}|^{\tilde{s}-1}_{W^{k+1,sr'}(\mathcal{T}_h)^d}.\end{aligned} \tag{3.52}$$

4. Sequential consistency. *Let* $(\underline{\boldsymbol{v}}_h)_{h\in\mathcal{H}}$ *be a bounded sequence of* $(\underline{\boldsymbol{U}}_{h,0}^k, \|\cdot\|_{\boldsymbol{\varepsilon},r,h})_{h\in\mathcal{H}}$ *such that* $\boldsymbol{v}_h \xrightarrow[h\to 0]{} \boldsymbol{v} \in \boldsymbol{U}$ *strongly in* $L^{[1,r^*)}(\Omega)^d$, *and* $\mathbf{G}_h^k \underline{\boldsymbol{v}}_h \xrightarrow[h\to 0]{} \boldsymbol{\nabla} \boldsymbol{v}$ *weakly in* $L^r(\Omega)^{d\times d}$, *and assume*

$$s < \frac{r^*}{r'}. \tag{3.53}$$

Then, for all $\boldsymbol{\phi} \in C_{\mathrm{c}}^\infty(\Omega, \mathbb{R}^d)$, *it holds, up to a subsequence,*

$$\mathrm{c}_h(\underline{\boldsymbol{v}}_h, \underline{\boldsymbol{I}}_h^k \boldsymbol{\phi}) \xrightarrow[h\to 0]{} c(\boldsymbol{v}, \boldsymbol{\phi}). \tag{3.54}$$

Proof. The non-dissipativity (3.49) of c_h is an immediate consequence of its definition (3.48). The proof of the Hölder continuity (3.50) is analogous to that of the corresponding property (3.26) for c, replacing the relevant continuous Sobolev embeddings (see Remark 70 on the role of the condition $s \le \frac{m^*}{m'}$) with their discrete counterpart (3.41), and leveraging the norm equivalence (3.39). Properties (3.52) and (3.54) are proved in Section 3.6.1 below. □

3.4.4 Viscous term

For all $T \in \mathcal{T}_h$, we define the local symmetric gradient reconstruction $\mathbf{G}_{\mathrm{s},T}^k : \underline{\boldsymbol{U}}_T^k \to \mathbb{P}^k(T, \mathbb{R}_{\mathrm{s}}^{d\times d})$ by setting, for all $\underline{\boldsymbol{v}}_T \in \underline{\boldsymbol{U}}_T^k$,

$$\mathbf{G}_{\mathrm{s},T}^k \underline{\boldsymbol{v}}_T \coloneqq \frac{1}{2}\left[\mathbf{G}_T^k \underline{\boldsymbol{v}}_T + (\mathbf{G}_T^k \underline{\boldsymbol{v}}_T)^\top\right]. \tag{3.55}$$

Similarly, the global symmetric gradient reconstruction $\mathbf{G}_{\mathrm{s},h}^k : \underline{\boldsymbol{U}}_h^k \to \mathbb{P}^k(\mathcal{T}_h, \mathbb{R}_{\mathrm{s}}^{d\times d})$ is obtained setting, for all $\underline{\boldsymbol{v}}_h \in \underline{\boldsymbol{U}}_h^k$,

$$\mathbf{G}_{\mathrm{s},h}^k \underline{\boldsymbol{v}}_h \coloneqq \frac{1}{2}\left[\mathbf{G}_h^k \underline{\boldsymbol{v}}_h + (\mathbf{G}_h^k \underline{\boldsymbol{v}}_h)^\top\right]. \tag{3.56}$$

The discrete counterpart of the function a defined in (3.11) is the function $\mathrm{a}_h : \underline{\boldsymbol{U}}_h^k \times \underline{\boldsymbol{U}}_h^k \to \mathbb{R}$ such that, for all $\underline{\boldsymbol{v}}_h, \underline{\boldsymbol{w}}_h \in \underline{\boldsymbol{U}}_h^k$,

$$\mathrm{a}_h(\underline{\boldsymbol{w}}_h, \underline{\boldsymbol{v}}_h) \coloneqq \int_\Omega \boldsymbol{\sigma}(\cdot, \mathbf{G}_{\mathrm{s},h}^k \underline{\boldsymbol{w}}_h) : \mathbf{G}_{\mathrm{s},h}^k \underline{\boldsymbol{v}}_h + \mathrm{s}_h(\underline{\boldsymbol{w}}_h, \underline{\boldsymbol{v}}_h). \tag{3.57}$$

Taking inspiration from [27] and [52], we take the stabilization function $\mathrm{s}_h : \underline{\boldsymbol{U}}_h^k \times \underline{\boldsymbol{U}}_h^k \to \mathbb{R}$ such that

$$\mathrm{s}_h(\underline{\boldsymbol{w}}_h, \underline{\boldsymbol{v}}_h) \coloneqq \frac{\sigma_{\mathrm{hc}} + \sigma_{\mathrm{hm}}}{2} \sum_{T\in\mathcal{T}_h} h_T \int_{\partial T} \left(\delta^r + |\boldsymbol{\Delta}_{\partial T}^k \underline{\boldsymbol{w}}_T|^r\right)^{\frac{r-2}{r}} \boldsymbol{\Delta}_{\partial T}^k \underline{\boldsymbol{w}}_T \cdot \boldsymbol{\Delta}_{\partial T}^k \underline{\boldsymbol{v}}_T, \tag{3.58}$$

where, for all $T \in \mathcal{T}_h$, the boundary residual operator $\boldsymbol{\Delta}_{\partial T}^k : \underline{\boldsymbol{U}}_T^k \to L^r(\partial T)^d$ is such that, for all $\underline{\boldsymbol{v}}_T \in \underline{\boldsymbol{U}}_T^k$,

$$(\boldsymbol{\Delta}_{\partial T}^k \underline{\boldsymbol{v}}_T)_{|F} = \frac{1}{h_T}\left[\boldsymbol{\pi}_F^k(\mathbf{r}_T^{k+1}\underline{\boldsymbol{v}}_T - \boldsymbol{v}_F) - \boldsymbol{\pi}_T^k(\mathbf{r}_T^{k+1}\underline{\boldsymbol{v}}_T - \boldsymbol{v}_T)\right] \qquad \forall F \in \mathcal{F}_T,$$

with $\mathbf{r}_T^{k+1} : \underline{\boldsymbol{U}}_T^k \to \mathbb{P}^{k+1}(T)^d$ velocity reconstruction consistent for polynomials of degree $\le k+1$ (see [27, Section 4.1.3] for one possible definition). With this choice, it holds (see, e.g., [27, Lemma 8]):

$$\boldsymbol{\Delta}_{\partial T}^k(\underline{\boldsymbol{I}}_T^k \boldsymbol{v}) = \mathbf{0} \qquad \forall \boldsymbol{v} \in \mathbb{P}^{k+1}(T)^d. \tag{3.59}$$

We define the corresponding boundary residual seminorm $|\cdot|_{r,h}$ such that, for all $\underline{\boldsymbol{v}}_h \in \underline{\boldsymbol{U}}_h^k$,

$$|\underline{\boldsymbol{v}}_h|_{r,h} \coloneqq \left(\sum_{T\in\mathcal{T}_h} h_T \|\boldsymbol{\Delta}_{\partial T}^k \underline{\boldsymbol{v}}_T\|_{L^r(\partial T)^d}^r\right)^{\frac{1}{r}}. \tag{3.60}$$

For future use, we note for all $T \in \mathcal{T}_h$, the following local uniform seminorm equivalence:

$$\|\mathbf{G}_T^k \underline{\boldsymbol{v}}_T\|_{L^r(T)^{d\times d}}^r + h_T\|\boldsymbol{\Delta}_{\partial T}^k \underline{\boldsymbol{v}}_T\|_{L^r(\partial T)^d}^r \simeq \|\underline{\boldsymbol{v}}_T\|_{\boldsymbol{\varepsilon},r,T}^r \qquad \forall \underline{\boldsymbol{v}}_T \in \underline{\boldsymbol{U}}_T^k, \tag{3.61}$$

which, summed over $T \in \mathcal{T}_h$, gives

$$\|\mathbf{G}_h^k \underline{\boldsymbol{v}}_h\|_{L^r(\Omega)^{d\times d}}^r + |\underline{\boldsymbol{v}}_h|_{r,h}^r \simeq \|\underline{\boldsymbol{v}}_h\|_{\boldsymbol{\varepsilon},r,h}^r \qquad \forall \underline{\boldsymbol{v}}_h \in \underline{\boldsymbol{U}}_h^k. \tag{3.62}$$

Lemma 73 (Properties of s_h)**.** *Under Assumption 5, we have the following properties for* s_h*:*

1. Hölder continuity. *For all* $\underline{\boldsymbol{u}}_h, \underline{\boldsymbol{v}}_h, \underline{\boldsymbol{w}}_h \in \underline{\boldsymbol{U}}_h^k$*, it holds*

$$\left|\mathrm{s}_h(\underline{\boldsymbol{u}}_h, \underline{\boldsymbol{v}}_h) - \mathrm{s}_h(\underline{\boldsymbol{w}}_h, \underline{\boldsymbol{v}}_h)\right| \lesssim \sigma_{\mathrm{hc}}\left(\delta^r + |\underline{\boldsymbol{u}}_h|_{r,h}^r + |\underline{\boldsymbol{w}}_h|_{r,h}^r\right)^{\frac{r-\tilde{r}}{r}} |\underline{\boldsymbol{u}}_h - \underline{\boldsymbol{w}}_h|_{r,h}^{\tilde{r}-1}|\underline{\boldsymbol{v}}_h|_{r,h}. \tag{3.63}$$

2. Hölder monotonicity. *For all* $\underline{\boldsymbol{u}}_h, \underline{\boldsymbol{w}}_h \in \underline{\boldsymbol{U}}_h^k$*, it holds*

$$\left(\mathrm{s}_h(\underline{\boldsymbol{u}}_h, \underline{\boldsymbol{u}}_h - \underline{\boldsymbol{w}}_h) - \mathrm{s}_h(\underline{\boldsymbol{w}}_h, \underline{\boldsymbol{u}}_h - \underline{\boldsymbol{w}}_h)\right)\left(\delta^r + |\underline{\boldsymbol{u}}_h|_{r,h}^r + |\underline{\boldsymbol{w}}_h|_{r,h}^r\right)^{\frac{2-\tilde{r}}{r}} \gtrsim \sigma_{\mathrm{hm}}|\underline{\boldsymbol{u}}_h - \underline{\boldsymbol{w}}_h|_{r,h}^{r+2-\tilde{r}}. \tag{3.64}$$

3. Sequential consistency. *Let* $(\underline{\boldsymbol{v}}_h)_{h\in\mathcal{H}}$ *denote a bounded sequence of* $(\underline{\boldsymbol{U}}_{h,0}^k, \|\cdot\|_{\boldsymbol{\varepsilon},r,h})_{h\in\mathcal{H}}$*. Then, for all* $\boldsymbol{\phi} \in C_{\mathrm{c}}^\infty(\Omega)^d$*,*

$$\mathrm{s}_h(\underline{\boldsymbol{v}}_h, \underline{\boldsymbol{I}}_h^k \boldsymbol{\phi}) \xrightarrow[h\to 0]{} 0. \tag{3.65}$$

Proof. Properties (3.63)–(3.64) can be proved reasoning as in [27] and proceeding as in [52] for the addition of δ. It remains to prove (3.65). Using the Hölder continuity (3.63) of s_h with $(\underline{\boldsymbol{u}}_h, \underline{\boldsymbol{v}}_h, \underline{\boldsymbol{w}}_h) = (\underline{\boldsymbol{v}}_h, \underline{\boldsymbol{I}}_h^k\boldsymbol{\phi}, \underline{\boldsymbol{0}})$, we infer

$$|\mathrm{s}_h(\underline{\boldsymbol{v}}_h, \underline{\boldsymbol{I}}_h^k\boldsymbol{\phi})| \lesssim \sigma_{\mathrm{hc}} \left(\delta^r + |\underline{\boldsymbol{v}}_h|_{r,h}^r+\right)^{\frac{r-\tilde{r}}{r}} |\underline{\boldsymbol{v}}_h|_{r,h}^{\tilde{r}-1} |\underline{\boldsymbol{I}}_h^k\boldsymbol{\phi}|_{r,h}. \tag{3.66}$$

Recalling the definition (3.60) of the boundary residual seminorm, we get

$$\begin{aligned}
|\underline{\boldsymbol{I}}_h^k\boldsymbol{\phi}|_{r,h}^r &= \sum_{T\in\mathcal{T}_h} h_T \|\boldsymbol{\Delta}_{\partial T}^k(\underline{\boldsymbol{I}}_h^k\boldsymbol{\phi})\|_{L^r(\partial T)^d}^r \\
&= \sum_{T\in\mathcal{T}_h} h_T \|\boldsymbol{\Delta}_{\partial T}^k[\underline{\boldsymbol{I}}_T^k(\boldsymbol{\phi} - \boldsymbol{\pi}_T^{k+1}\boldsymbol{\phi})]\|_{L^r(\partial T)^d}^r \\
&\lesssim \sum_{T\in\mathcal{T}_h} \|\underline{\boldsymbol{I}}_T^k(\boldsymbol{\phi} - \boldsymbol{\pi}_T^{k+1}\boldsymbol{\phi})\|_{\boldsymbol{\varepsilon},r,T}^r \lesssim |\boldsymbol{\phi} - \boldsymbol{\pi}_h^{k+1}\boldsymbol{\phi}|_{W^{1,r}(\Omega)^d}^r,
\end{aligned}$$

where we have used the polynomial consistency (3.59) of the boundary residual to insert $\boldsymbol{\pi}_T^{k+1}\boldsymbol{\phi}$ in the second line, the local seminorm equivalence (3.61) to pass to the third line, and the boundedness (3.40) of $\underline{\boldsymbol{I}}_T^k$ to conclude. Plugging this bound into (3.66) and using (3.35) along with the boundedness of $(\|\underline{\boldsymbol{v}}_h\|_{\boldsymbol{\varepsilon},r,h})_{h\in\mathcal{H}}$ (which implies that of $(|\underline{\boldsymbol{v}}_h|_{r,h})_{h\in\mathcal{H}}$ by virtue of (3.62)) yields (3.65). □

Lemma 74 (Properties of a_h)**.** *Under Assumption 5, we have the following properties for* a_h*:*

1. Hölder continuity. *For all* $\underline{\boldsymbol{u}}_h, \underline{\boldsymbol{v}}_h, \underline{\boldsymbol{w}}_h \in \underline{\boldsymbol{U}}_h^k$*, it holds*

$$\begin{aligned}
&\left|\mathrm{a}_h(\underline{\boldsymbol{u}}_h, \underline{\boldsymbol{v}}_h) - \mathrm{a}_h(\underline{\boldsymbol{w}}_h, \underline{\boldsymbol{v}}_h)\right| \\
&\qquad \lesssim \sigma_{\mathrm{hc}} \left(\delta^r + \|\underline{\boldsymbol{u}}_h\|_{\boldsymbol{\varepsilon},r,h}^r + \|\underline{\boldsymbol{w}}_h\|_{\boldsymbol{\varepsilon},r,h}^r\right)^{\frac{r-\tilde{r}}{r}} \|\underline{\boldsymbol{u}}_h - \underline{\boldsymbol{w}}_h\|_{\boldsymbol{\varepsilon},r,h}^{\tilde{r}-1} \|\underline{\boldsymbol{v}}_h\|_{\boldsymbol{\varepsilon},r,h}.
\end{aligned} \tag{3.67}$$

2. Hölder monotonicity. *For* $m \in \{\tilde{r}, r\}$ *and all* $\underline{\boldsymbol{u}}_h, \underline{\boldsymbol{w}}_h \in \underline{\boldsymbol{U}}_h^k$*, it holds, with* $C_{\mathrm{da}} > 0$ *independent of* h*,*

$$\begin{aligned}
&\mathrm{a}_h(\underline{\boldsymbol{u}}_h, \underline{\boldsymbol{u}}_h - \underline{\boldsymbol{w}}_h) - \mathrm{a}_h(\underline{\boldsymbol{w}}_h, \underline{\boldsymbol{u}}_h - \underline{\boldsymbol{w}}_h) \\
&\qquad \geq C_{\mathrm{da}}\sigma_{\mathrm{hm}} \left(\delta^r + \|\underline{\boldsymbol{u}}_h\|_{\boldsymbol{\varepsilon},r,h}^r + \|\underline{\boldsymbol{w}}_h\|_{\boldsymbol{\varepsilon},r,h}^r\right)^{\frac{\tilde{r}-2}{r}} \delta^{r-m} \|\underline{\boldsymbol{u}}_h - \underline{\boldsymbol{w}}_h\|_{\boldsymbol{\varepsilon},m,h}^{m+2-\tilde{r}}.
\end{aligned} \tag{3.68}$$

3. Consistency. *Let* $\boldsymbol{w} \in \boldsymbol{U} \cap W^{k+2,r}(\mathcal{T}_h)^d$ *be such that* $\boldsymbol{\sigma}(\cdot, \boldsymbol{\nabla}_{\mathrm{s}}\boldsymbol{w}) \in W^{1,r'}(\Omega)^{d\times d} \cap W^{k+1,r'}(\mathcal{T}_h)^{d\times d}$*. Then,*

$$\begin{aligned}
&\sup_{\underline{\boldsymbol{v}}_h\in\underline{\boldsymbol{U}}_{h,0}^k, \|\underline{\boldsymbol{v}}_h\|_{\boldsymbol{\varepsilon},r,h}=1} \left|\int_\Omega (\boldsymbol{\nabla}\cdot\boldsymbol{\sigma}(\cdot, \boldsymbol{\nabla}_{\mathrm{s}}\boldsymbol{w})) \cdot \boldsymbol{v}_h + \mathrm{a}_h(\underline{\boldsymbol{I}}_h^k\boldsymbol{w}, \underline{\boldsymbol{v}}_h)\right| \\
&\lesssim h^{k+1} |\boldsymbol{\sigma}(\cdot, \boldsymbol{\nabla}_{\mathrm{s}}\boldsymbol{w})|_{W^{k+1,r'}(\mathcal{T}_h)^{d\times d}} \\
&\quad + h^{(k+1)(\tilde{r}-1)} \min\left(\zeta_h(\boldsymbol{w}); 1\right)^{2-\tilde{r}} \sigma_{\mathrm{hc}} \left(\delta^r + |\boldsymbol{w}|_{W^{1,r}(\Omega)^d}^r\right)^{\frac{r-\tilde{r}}{r}} |\boldsymbol{w}|_{W^{k+2,r}(\mathcal{T}_h)^d}^{\tilde{r}-1},
\end{aligned} \tag{3.69}$$

where $\zeta_h(\boldsymbol{w}) \coloneqq \delta^{-1} \max_{T\in\mathcal{T}_h} \left(|T|^{-\frac{1}{p}} |\boldsymbol{w}|_{W^{k+2,r}(T)^d}\right) h^{k+1}$ *if* $\delta \neq 0$, $\zeta_h(\boldsymbol{w}) \coloneqq \infty$ *otherwise.*

Proof. Properties (3.67) is proved in [27] (with (3.63) replacing [27, Eq. (41b)]). Similarly, (3.68) is shown replacing [27, Eq. (41c)] by (3.64) when $r \leq 2$, and the proof of the case $r > 2$ is analogous to that of the corresponding property (3.21) for a, replacing the continuous Korn inequality (3.15) by its discrete counterpart (3.38). Finally, (3.69) is obtained modifying the reasoning of [27] according to [52, Theorem 10] in order to introduce the term involving $\zeta_h(\boldsymbol{w})$. □

3.4.5 Pressure-velocity coupling

We define the global divergence reconstruction $\mathrm{D}_h^k : \underline{\boldsymbol{U}}_h^k \to \mathbb{P}^k(\mathcal{T}_h)$ by setting for all $\underline{\boldsymbol{v}}_h \in \underline{\boldsymbol{U}}_h^k$,

$$\mathrm{D}_h^k \underline{\boldsymbol{v}}_h \coloneqq \mathrm{tr}(\mathbf{G}_h^k \underline{\boldsymbol{v}}_h). \tag{3.70}$$

The pressure-velocity coupling is realized by the bilinear form $\mathrm{b}_h : \underline{\boldsymbol{U}}_h^k \times \mathbb{P}^k(\mathcal{T}_h) \to \mathbb{R}$ such that, for all $(\underline{\boldsymbol{v}}_h, q_h) \in \underline{\boldsymbol{U}}_h^k \times \mathbb{P}^k(\mathcal{T}_h)$,

$$\mathrm{b}_h(\underline{\boldsymbol{v}}_h, q_h) \coloneqq -\int_\Omega \mathrm{D}_h^k \underline{\boldsymbol{v}}_h \, q_h. \tag{3.71}$$

Lemma 75 (Properties of b_h)**.** *We have the following properties for* b_h*:*

1. Inf-sup stability. *It holds, for all* $q_h \in P_h^k$,

$$\|q_h\|_{L^{r'}(\Omega)} \lesssim \sup_{\underline{\boldsymbol{v}}_h \in \underline{\boldsymbol{U}}_{h,0}^k, \|\underline{\boldsymbol{v}}_h\|_{\varepsilon,r,h}=1} \mathrm{b}_h(\underline{\boldsymbol{v}}_h, q_h). \tag{3.72}$$

2. Fortin operator. *For all* $\boldsymbol{v} \in W^{1,r}(\Omega)^d$ *and all* $q_h \in \mathbb{P}^k(\mathcal{T}_h)$,

$$\mathrm{b}_h(\underline{\boldsymbol{I}}_h^k \boldsymbol{v}, q_h) = b(\boldsymbol{v}, q_h). \tag{3.73}$$

3. Consistency. *For all* $q \in W^{1,r'}(\Omega) \cap W^{k+1,r'}(\mathcal{T}_h)$,

$$\sup_{\underline{\boldsymbol{v}}_h \in \underline{\boldsymbol{U}}_{h,0}^k, \|\underline{\boldsymbol{v}}_h\|_{\varepsilon,r,h}=1} \left| \int_\Omega \boldsymbol{\nabla} q \cdot \boldsymbol{v}_h - \mathrm{b}_h(\underline{\boldsymbol{v}}_h, \pi_h^k q) \right| \lesssim h^{k+1} |q|_{W^{k+1,r'}(\mathcal{T}_h)}. \tag{3.74}$$

4. Sequential consistency/1. *Let* $(q_h)_{h\in\mathcal{H}} \in (P_h^k)_{h\in\mathcal{H}}$ *be such that* $q_h \xrightarrow[h\to 0]{} q \in P$ *weakly in* $L^{r'}(\Omega)$*. Then, for all* $\boldsymbol{\phi} \in C_c^\infty(\Omega)^d$*, it holds*

$$\mathrm{b}_h(\underline{\boldsymbol{I}}_h^k \boldsymbol{\phi}, q_h) \xrightarrow[h\to 0]{} b(\boldsymbol{\phi}, q). \tag{3.75}$$

5. Sequential consistency/2. *Let* $(\underline{\boldsymbol{v}}_h)_{h\in\mathcal{H}} \in (\underline{\boldsymbol{U}}_{h,0}^k)_{h\in\mathcal{H}}$ *be such that* $\mathrm{D}_h^k\underline{\boldsymbol{v}}_h \xrightarrow[h\to 0]{} \boldsymbol{\nabla}\cdot\boldsymbol{v}$ *weakly in* $L^r(\Omega)$. *Then, for all* $\psi \in C_{\mathrm{c}}^\infty(\Omega)$, *it holds*

$$\mathrm{b}_h(\underline{\boldsymbol{v}}_h, \pi_h^k\psi) \xrightarrow[h\to 0]{} b(\boldsymbol{v},\psi). \tag{3.76}$$

Proof. Properties (3.72)–(3.74) are proved in [27]. Let us prove (3.75). Given $\boldsymbol{\phi} \in C_{\mathrm{c}}^\infty(\Omega)^d$, (3.46) combined with the definition (3.70) of D_h^k yields $\mathrm{D}_h^k(\underline{\boldsymbol{I}}_h^k\boldsymbol{\phi}) \xrightarrow[h\to 0]{} \boldsymbol{\nabla}\cdot\boldsymbol{\phi}$ strongly in $L^r(\Omega)$. Hence, $\mathrm{b}_h(\underline{\boldsymbol{I}}_h^k\boldsymbol{\phi}, q_h) = -\int_\Omega \mathrm{D}_h^k(\underline{\boldsymbol{I}}_h^k\boldsymbol{\phi})\, q_h \xrightarrow[h\to 0]{} -\int_\Omega(\boldsymbol{\nabla}\cdot\boldsymbol{\phi})\, q = b(\boldsymbol{\phi},q)$. Let now $\psi \in C_{\mathrm{c}}^\infty(\Omega)$. Combining the fact that $\mathrm{D}_h^k\underline{\boldsymbol{v}}_h \xrightarrow[h\to 0]{} \boldsymbol{\nabla}\cdot\boldsymbol{v}$ weakly in $L^r(\Omega)$ by assumption with (3.35), we obtain (3.76) by writing $\mathrm{b}_h(\underline{\boldsymbol{v}}_h, \pi_h^k\psi) = -\int_\Omega \mathrm{D}_h^k\underline{\boldsymbol{v}}_h\, \pi_h^k\psi \xrightarrow[h\to 0]{} -\int_\Omega(\boldsymbol{\nabla}\cdot\boldsymbol{v})\,\psi = b(v,\psi)$. □

3.4.6 Discrete problem and main results

The discrete problem reads: Find $(\underline{\boldsymbol{u}}_h, p_h) \in \underline{\boldsymbol{U}}_{h,0}^k \times P_h^k$ such that

$$\mathrm{a}_h(\underline{\boldsymbol{u}}_h,\underline{\boldsymbol{v}}_h) + \mathrm{c}_h(\underline{\boldsymbol{u}}_h,\underline{\boldsymbol{v}}_h) + \mathrm{b}_h(\underline{\boldsymbol{v}}_h, p_h) = \int_\Omega \boldsymbol{f}\cdot\boldsymbol{v}_h \qquad \forall \underline{\boldsymbol{v}}_h \in \underline{\boldsymbol{U}}_{h,0}^k, \tag{3.77a}$$

$$-\mathrm{b}_h(\underline{\boldsymbol{u}}_h, q_h) = 0 \qquad \forall q_h \in P_h^k. \tag{3.77b}$$

The following theorem states the existence of a discrete solution to problem (3.77) and provide conditions for uniqueness.

Theorem 76 (Existence and uniqueness for problem (3.77))**.** *Under Assumptions 5 and 6, there exists a solution* $(\underline{\boldsymbol{u}}_h, p_h) \in \underline{\boldsymbol{U}}_{h,0}^k \times P_h^k$ *to the discrete problem* (3.77), *and any solution satisfies*

$$\|\underline{\boldsymbol{u}}_h\|_{\boldsymbol{\varepsilon},r,h} \le C_{\mathrm{dv}}\left[\left(\sigma_{\mathrm{hm}}^{-1}\|\boldsymbol{f}\|_{L^{r'}(\Omega)^d}\right)^{r'} + \min\left(\delta^r; \left(\delta^{2-\tilde r}\sigma_{\mathrm{hm}}^{-1}\|\boldsymbol{f}\|_{L^{r'}(\Omega)^d}\right)^{\frac{r}{r+1-\tilde r}}\right)\right]^{\frac{1}{r}}, \tag{3.78a}$$

$$\|p_h\|_{L^{r'}(\Omega)} \lesssim \sigma_{\mathrm{hc}}\left[\sigma_{\mathrm{hm}}^{-1}\|\boldsymbol{f}\|_{L^{r'}(\Omega)^d} + \delta^{|r-2|(\tilde r-1)}\left(\sigma_{\mathrm{hm}}^{-1}\|\boldsymbol{f}\|_{L^{r'}(\Omega)^d}\right)^{\frac{\tilde r-1}{r+1-\tilde r}}\right], \tag{3.78b}$$

where $C_{\mathrm{dv}} > 0$ *is independent of* h. *Moreover, assuming* $2 \le s \le \frac{\tilde r^*}{\tilde r'}$ *(cf.* (3.17)*) and that the following data smallness condition holds:*

$$\delta^r + \left(\sigma_{\mathrm{hm}}^{-1}\|\boldsymbol{f}\|_{L^{r'}(\Omega)^d}\right)^{r'} < \left(1+2C_{\mathrm{dv}}^r\right)^{-1}\left(C_{\mathrm{dc},\tilde r}^{-1}\chi_{\mathrm{hc}}^{-1}C_{\mathrm{da}}\sigma_{\mathrm{hm}}\delta^{r-\tilde r}\right)^{\frac{r}{s+1-\tilde r}}, \tag{3.79}$$

the solution of (3.77) *is unique.*

Proof. Replacing a_h by $a_h + c_h$ in the proof of [27, Theorem 11] and using the non-dissipativity (3.49) of c_h, yields the existence of a solution to problem (3.77) and the a priori estimates (3.78), noticing that the Hölder monotonicity (3.68) of a_h with $m = r$ is the key property leveraged in the proof. Uniqueness of the solution under the above assumptions on s and r and the data smallness condition (3.79) can be proved as its continuous counterpart in Theorem 66 leveraging the inf-sup stability (3.72) of b_h, the Hölder monotonicity (3.68) of a_h with $m = \tilde{r}$, and the Hölder continuity (3.50) of c_h. □

We next state convergence results and error estimates.

Theorem 77 (Convergence to minimal regularity solutions)**.** *Let $((\underline{\boldsymbol{u}}_h, p_h))_{h\in\mathcal{H}}$ be a sequence of $(\underline{\boldsymbol{U}}_{h,0}^k \times P_h^k)_{h\in\mathcal{H}}$ such that, for all $h \in \mathcal{H}$, $(\underline{\boldsymbol{u}}_h, p_h)$ solves (3.77). Assume (3.53), namely $s < \frac{r^*}{r'}$, i.e.,*

$$s \in \begin{cases} \left(1, \frac{d(r-1)}{d-r}\right) & \text{if } d = 2 \text{ and } r \in (1,2) \text{ or } d = 3 \text{ and } r \in (1,3), \\ (1,\infty) & \text{if } d = 2 \text{ and } r \in [2,\infty) \text{ or } d = 3 \text{ and } r \in [3,\infty). \end{cases} \tag{3.80}$$

Then, under Assumptions 5 and 6, there exists $(\boldsymbol{u}, p) \in \boldsymbol{U} \times P$ solving (3.10) such that up to a subsequence,

- $\boldsymbol{u}_h \xrightarrow[h\to 0]{} \boldsymbol{u}$ *strongly in* $L^{[1,r^*)}(\Omega)^d$;
- $\mathbf{G}_{\mathrm{s},h}^k \underline{\boldsymbol{u}}_h \xrightarrow[h\to 0]{} \boldsymbol{\nabla}_{\mathrm{s}} \boldsymbol{u}$ *strongly in* $L^r(\Omega)^{d\times d}$;
- $|\underline{\boldsymbol{u}}_h|_{r,h} \xrightarrow[h\to 0]{} 0$;
- $p_h \xrightarrow[h\to 0]{} p$ *strongly in* $L^{r'}(\Omega)$.

Moreover, if the solution to (3.10) is unique (cf. Theorem 66), the convergences extend to the whole sequence.

Proof. See Section 3.6.2. □

Theorem 78 (Error estimate)**.** *Assume $r \le 2 \le s \le \frac{r^*}{r'}$ so that, in particular, the fluid is shear-thinning and*

$$s \in \begin{cases} \left[2, \frac{d(r-1)}{d-r}\right] & \text{if } d = 2 \text{ and } r \in \left[\frac{3}{2}, 2\right) \text{ or } d = 3 \text{ and } r \in \left[\frac{9}{5}, 2\right], \\ [2,\infty) & \text{if } d = 2 \text{ and } r = 2. \end{cases} \tag{3.81}$$

Let $(\boldsymbol{u}, p) \in \boldsymbol{U}\times P$ and $(\underline{\boldsymbol{u}}_h, p_h) \in \underline{\boldsymbol{U}}_{h,0}^k \times P_h^k$ solve (3.10) and (3.77), respectively. Assume the uniqueness of such solutions (which is verified, under (3.81), if the data smallness conditions (3.18) and (3.79) hold), and the additional regularity $\boldsymbol{u} \in W^{k+2,r}(\mathcal{T}_h)^d \cap W^{k+1,sr'}(\mathcal{T}_h)^d$ (so that, in particular, $\boldsymbol{u} \in W^{1,sr'}(\Omega)^d$), $\boldsymbol{\sigma}(\cdot, \boldsymbol{\nabla}_{\mathrm{s}}\boldsymbol{u}) \in W^{1,r'}(\Omega)^{d\times d} \cap$

$W^{k+1,r'}(\mathcal{T}_h)^{d\times d}$, *and* $p \in W^{1,r'}(\Omega) \cap W^{k+1,r'}(\mathcal{T}_h)$. *Let, furthermore, the following data smallness condition be verified:*

$$\mathcal{N}_1 \coloneqq \delta^r + \left(\sigma_{\mathrm{hm}}^{-1}\|\boldsymbol{f}\|_{L^{r'}(\Omega)^d}\right)^{r'} \le \left(1 + C_{\mathrm{v}}^r + C_{\mathrm{I}}^r C_{\mathrm{dv}}^r\right)^{-1} \left(\frac{C_{\mathrm{da}}\sigma_{\mathrm{hm}}}{2C_{\mathrm{dc},r}\chi_{\mathrm{hc}}}\right)^{\frac{r}{s+1-r}}. \tag{3.82}$$

Then, under Assumptions 5 and 6, it holds

$$\|\underline{\boldsymbol{u}}_h - \underline{\boldsymbol{I}}_h^k \boldsymbol{u}\|_{\boldsymbol{\varepsilon},r,h} \lesssim \sigma_{\mathrm{hm}}^{-1}\mathcal{N}_1^{\frac{2-r}{r}} \left(h^{(k+1)(r-1)} \min\left(\zeta_h(\boldsymbol{u}); 1\right)^{2-r} \mathcal{N}_2 + h^{k+1}\mathcal{N}_3\right), \tag{3.83a}$$

$$\begin{aligned}\|p_h - \pi_h^k p\|_{L^{r'}(\Omega)} \lesssim{}& \sigma_{\mathrm{hc}}\sigma_{\mathrm{hm}}^{1-r}\mathcal{N}_1^{\frac{2-r}{r'}} \left(h^{(k+1)(r-1)^2} \min\left(\zeta_h(\boldsymbol{u}); 1\right)^{(2-r)(r-1)} \mathcal{N}_2^{r-1}\right.\\ &\left. + h^{(k+1)(r-1)}\mathcal{N}_3^{r-1}\right) + \left(1 + \chi_{\mathrm{hc}}\sigma_{\mathrm{hm}}^{-1}\mathcal{N}_1^{\frac{s+1-r}{r}}\right)\\ &\times \left(h^{(k+1)(r-1)} \min\left(\zeta_h(\boldsymbol{u}); 1\right)^{2-r} \mathcal{N}_2 + h^{k+1}\mathcal{N}_3\right),\end{aligned} \tag{3.83b}$$

with ζ_h *introduced in* (3.69) *and where we have set, for the sake of brevity,*

$$\mathcal{N}_2 \coloneqq \sigma_{\mathrm{hc}}|\boldsymbol{u}|_{W^{k+2,r}(\mathcal{T}_h)^d}^{r-1},$$

$$\begin{aligned}\mathcal{N}_3 \coloneqq{}& |\boldsymbol{\sigma}(\cdot, \boldsymbol{\nabla}_{\mathrm{s}}\boldsymbol{u})|_{W^{k+1,r'}(\mathcal{T}_h)^{d\times d}} + |p|_{W^{(k+1)(r-1),r'}(\mathcal{T}_h)} + |\boldsymbol{u}|_{W^{k+1,sr'}(\mathcal{T}_h)^d}^s\\ &+ \left(|\boldsymbol{u}|_{W^{1,sr'}(\Omega)^d}^s + |\boldsymbol{u}|_{W^{1,r}(\Omega)^d}^s\right)^{\frac{s-1}{s}} \left(|\boldsymbol{u}|_{W^{k+1,sr'}(\mathcal{T}_h)^d} + |\boldsymbol{u}|_{W^{k+2,r}(\mathcal{T}_h)^d}\right).\end{aligned}$$

Proof. See Section 3.6.3. □

Remark 79 (Orders of convergence). From (3.83), neglecting higher-order terms, we infer asymptotic convergence rates of $O_{\mathrm{vel}}^k \in [(k+1)(r-1), k+1]$ for the velocity, and $O_{\mathrm{pre}}^k \in [(k+1)(r-1)^2, (k+1)(r-1)]$ for the pressure, according to the dimensionless number $\zeta_h(\boldsymbol{u})$. Notice that, owing to the presence of higher-order terms in the right-hand sides of (3.83), higher convergence rates may be observed in practice before attaining the asymptotic ones.

In the case $s = 2$, the error estimate given in [76, Theorem 3.1] for the approximation of the p-Stokes equations with conforming finite elements (to be compared with the case $k = 0$ in the present work) gives an order of convergence of the velocity coinciding with our upper bound irrespectively of the degeneracy of the problem. This difference with respect to conforming finite elements had already been observed in the context of the p-Laplacian, cf. [47, Remark 3.3], with improvements on the original HHO estimate recently made in [52]. On the other hand, the order of convergence for the pressure given by [76, Theorem 3.1] seems higher than the one derived in the present work. This point will make the object of future investigations.

3.5 Numerical examples

The method (3.77) was implemented within the SpaFEDTe library (cf. https://spafedte.github.io). We used a Picard method for the solution of the nonlinear algebraic problem corresponding to the HHO discretization with a tolerance of 10^{-10}. The linear systems at each iteration were solved using the sparse direct solver PardisoLU. In this section we present a numerical validation including a verification of the convergence rates in dimensions $d = 2$ and $d = 3$, as well as the more physical two-dimensional lid-driven cavity problem.

3.5.1 Numerical verification of the convergence rates

We consider manufactured solutions of problem (3.1) with diffusion law corresponding to the $(1, 1, r, r)$-Carreau–Yasuda model (3.7) and convection law given by the $(1, s)$-Laplace formula (3.9). The corresponding Sobolev exponents are the couples $(r, s) \in \left\{\frac{3}{2}, \frac{9}{5}, 2, \frac{5}{2}, 3\right\}^2$ that match the condition $s \leq \frac{r^*}{r'}$. The volumetric load $\boldsymbol{f}$ and the Dirichlet boundary conditions are inferred from the exact solution. Polynomial degrees ranging from 1 to 3 are considered. For each value of $d \in \{2, 3\}$, we let $\Omega = (0, 1)^d$, and consider the exact velocity $\boldsymbol{u}$ and pressure p such that, for all $\boldsymbol{x} = (x_i)_{1\leq i\leq d} \in \Omega$,

$$\boldsymbol{u}(\boldsymbol{x}) = \left(\prod_{j=1, j\neq i}^{d} \sin\left(\tfrac{\pi}{2}x_j\right)\right)_{1\leq i\leq d} \quad \text{and} \quad p(\boldsymbol{x}) = \prod_{i=1}^{d} \sin\left(\tfrac{\pi}{2}x_i\right) - \tfrac{2^d}{\pi^d}. \tag{3.84}$$

We consider the HHO scheme on distorted triangular (if $d = 2$) and cubic (if $d = 3$) mesh families. For the case $\frac{r^*}{r'} = 2$, i.e. $r = \frac{3}{2}$ if $d = 2$ and $r = \frac{9}{5}$ if $d = 3$, we display detailed convergence results in Figures 3.1 and 3.2, respectively. Table 3.1 collects the asymptotic convergence rates predicted by Theorem 78 with the interval for s in which the assumptions of Theorem 78 hold; when the interval is empty, we display the asymptotic convergence rates given by [27, Theorem 12] for the (generalized) Stokes problem, i.e. the same convergence rates if $r \leq 2$ and $O^k_{\mathrm{vel}} = O^k_{\mathrm{pre}} = \frac{k+1}{r-1}$ otherwise. When $r < 2$, the convergence rates are expected over an interval depending on the degeneracy of the problem (cf. [52, Theorem 11]); since $\delta = 1$, the expected convergence rates should correspond to the maximum of these intervals. In Tables 3.2 and 3.3 we provide an overview of the experimental convergence rates obtained for $d = 2$ and $d = 3$, respectively. Overall, the results are in agreement with the theoretical predictions. The expected asymptotic orders of convergence of the pressure are exceeded for $r < 2$, where the experimental convergence rates is closer to $k + 1$ (i.e., the same rate as the velocity). One explanation could be the partial nature of the error estimate (3.83b) involving only the L^2-orthogonal projection of the continuous solution. Should this behaviour be confirmed by further numerical evidence, it could suggest that the error estimate for the

Table 3.1: Asymptotic convergence rates predicted by Theorem 78 (cf. Remark 79) according to r and k. We also indicate, for the sake of completeness, the interval for s in which the assumptions of Theorem 78 hold; when the interval is empty, the asymptotic convergence rates correspond to the predictions of [27, Theorem 12] valid for the corresponding generalized Stokes problem.

r		$\frac{3}{2}$		$\frac{9}{5}$		2		$\frac{5}{2}$		3	
s	$d=2$	2		$[2,8]$		$[2,\infty)$		$\emptyset$		$\emptyset$	
	$d=3$	$\emptyset$		2		$[2,3]$		$\emptyset$		$\emptyset$	
k		O^k_{vel}	O^k_{pre}	O^k_{vel}	O^k_{pre}	O^k_{vel}	O^k_{pre}	O^k_{vel}	O^k_{pre}	O^k_{vel}	O^k_{pre}
1		$[1,2]$	$[\frac{1}{2},1]$	$[\frac{8}{5},2]$	$[\frac{32}{25},\frac{8}{5}]$	2	2	$\frac{4}{3}$	$\frac{4}{3}$	1	1
2		$[\frac{3}{2},3]$	$[\frac{3}{4},\frac{3}{2}]$	$[\frac{12}{5},3]$	$[\frac{48}{25},\frac{12}{5}]$	3	3	2	2	$\frac{3}{2}$	$\frac{3}{2}$
3		$[2,4]$	$[1,2]$	$[\frac{16}{5},4]$	$[\frac{64}{25},\frac{16}{5}]$	4	4	$\frac{8}{3}$	$\frac{8}{3}$	2	2

pressure can be improved. When the assumption $r \leq 2 \leq s$ of Theorem 78 is not met, the convergence rates seem to coincide with the predictions of [27, Theorem 12] for the corresponding Stokes problem with no convective terms when $s \geq 2$. However, in the case $s < 2$, we notice that the presence of the convective term seems to influence the convergence rates of the velocity and the pressure which are often lower than expected. This could be explained by the consistency (3.52) of c_h, which involves a term in $h^{(k+1)(s-1)}$ when $s < 2$. While the assumption $r \leq 2 \leq s$ seems necessary to obtain estimates of the convergence rates in the present setting, we do not exclude that it could be lifted using different techniques (notice that convergence is guaranteed by Theorem 77 under significantly milder assumptions).

3.5.2 Lid-driven cavity flow

We next consider the lid-driven cavity flow, a well-known problem in fluid mechanics. While this problem has been solved with a large variety of numerical methods for Newtonian fluids with standard convection law, some of the combinations of general viscosity and convection laws considered here appear to be entirely new. The domain is the unit square $\Omega = (0,1)^2$, and we enforce a unit tangential velocity $\boldsymbol{u} = (1,0)$ on the top edge (of equation $x_2 = 1$) and wall boundary conditions on the other edges. This boundary condition is incompatible with the formulation (3.10), even generalized to non-homogeneous boundary conditions, since $\boldsymbol{u} \notin \boldsymbol{U}$. However, this is a very classical test that demonstrates the performance of the method in situations closer to real-life problems.

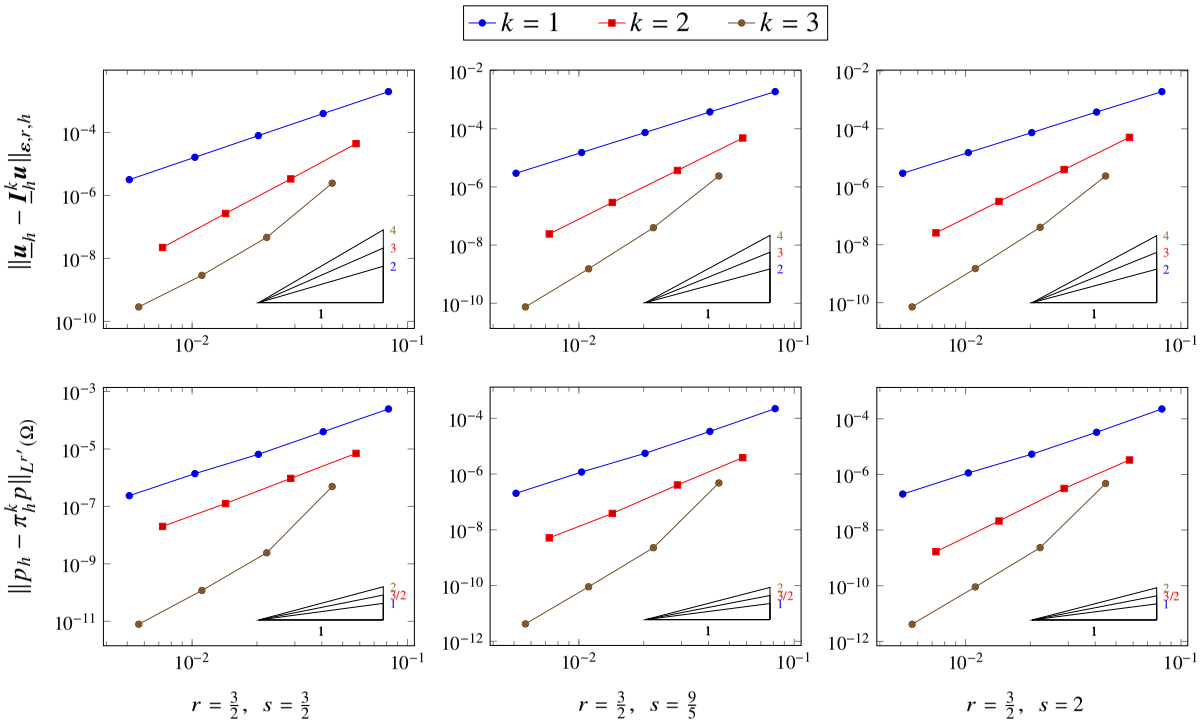

Figure 3.1: 2D-Numerical results for the test cases of Section 3.5.1 where $\frac{r^*}{r'} = 2$. The slopes indicate the convergence rates expected from Theorem 78 when $s = 2$, and [27, Theorem 12] otherwise.

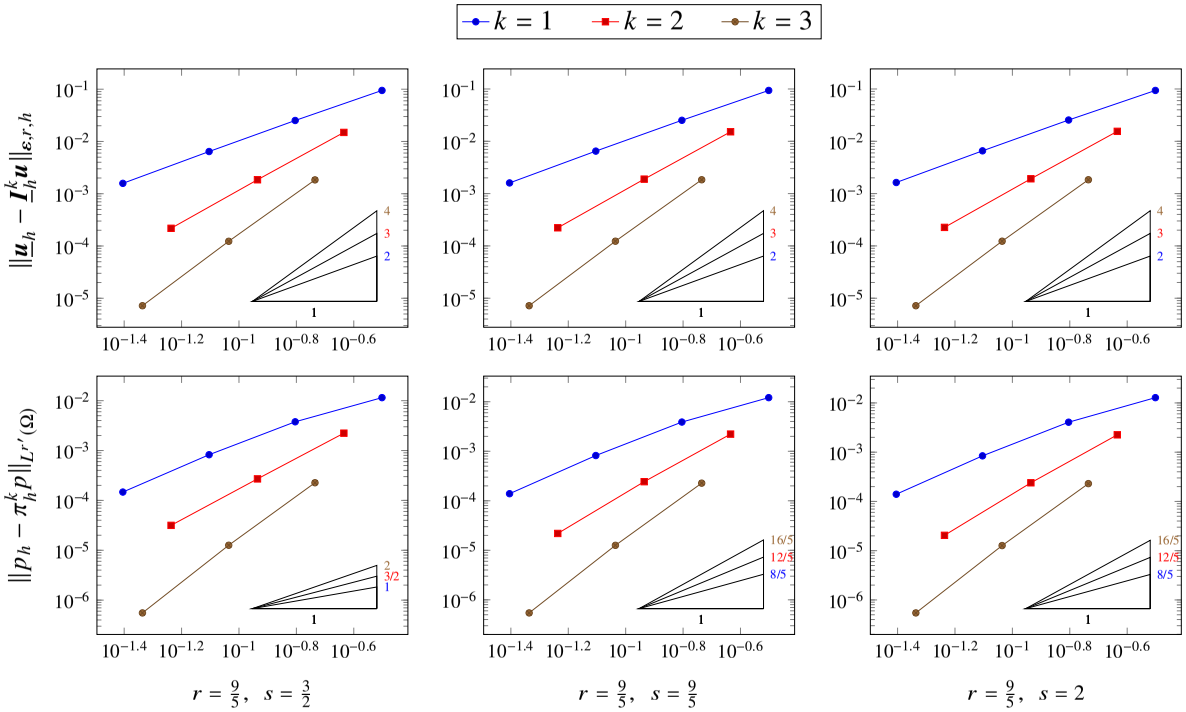

Figure 3.2: 3D-Numerical results for the test cases of Section 3.5.1 where $\frac{r^*}{r'} = 2$. The slopes indicate the convergence rates expected from Theorem 78 when $s = 2$, and [27, Theorem 12] otherwise.

Table 3.2: Convergence rates of the numerical tests of Section 3.5.1 with $d = 2$ and $r \in \{\frac{9}{5}, 2, \frac{5}{2}\}$.

$r = \frac{9}{5}$

	s	$\frac{3}{2}$		$\frac{9}{5}$		2		$\frac{5}{2}$		3	
k	h	$\boldsymbol{u}$	p	$\boldsymbol{u}$	p	$\boldsymbol{u}$	p	$\boldsymbol{u}$	p	$\boldsymbol{u}$	p
1	4.06e-02	2.06	1.95	2.07	1.99	2.09	2.06	2.14	2.19	2.18	2.17
	2.03e-02	2.11	2.32	2.12	2.34	2.13	2.35	2.14	2.33	2.14	2.29
	1.03e-02	2.06	1.99	2.05	1.97	2.05	1.96	2.05	1.99	2.04	2.04
	5.11e-03	2.12	2.23	2.13	2.21	2.13	2.20	2.14	2.16	2.15	2.16
2	4.06e-02	3.31	2.32	3.30	2.67	3.29	2.94	3.26	2.50	3.23	2.34
	2.03e-02	3.20	2.36	3.21	2.65	3.22	3.13	3.22	2.47	3.23	2.38
	1.03e-02	3.12	2.19	3.14	2.37	3.14	3.22	3.14	2.26	3.15	2.22
3	4.06e-02	4.50	6.13	4.77	6.42	4.74	6.42	4.64	6.29	4.49	6.07
	2.03e-02	3.31	3.36	4.20	3.71	4.25	3.72	4.29	3.76	4.32	3.83
	1.03e-02	2.83	3.09	4.05	3.87	4.21	3.93	4.21	3.99	4.22	4.07

$r = 2$

	s	$\frac{3}{2}$		$\frac{9}{5}$		2		$\frac{5}{2}$		3	
k	h	$\boldsymbol{u}$	p	$\boldsymbol{u}$	p	$\boldsymbol{u}$	p	$\boldsymbol{u}$	p	$\boldsymbol{u}$	p
1	4.06e-02	1.95	1.72	1.96	1.74	1.97	1.79	2.04	1.90	2.07	1.94
	2.03e-02	2.01	2.09	2.01	2.10	2.01	2.11	2.01	2.13	2.00	2.10
	1.03e-02	1.95	1.88	1.94	1.88	1.93	1.87	1.93	1.86	1.92	1.88
	5.11e-03	2.01	2.03	2.01	2.02	2.01	2.01	2.01	1.98	2.01	1.97
2	4.06e-02	3.05	2.08	3.04	2.49	3.03	2.80	3.01	2.37	2.99	2.20
	2.03e-02	2.99	2.11	3.00	2.37	3.00	2.82	3.00	2.24	3.01	2.16
	1.03e-02	2.91	1.97	2.92	2.13	2.93	2.99	2.93	2.04	2.93	2.00
3	4.06e-02	3.83	3.55	4.07	3.80	4.08	3.87	4.09	4.00	4.09	4.06
	2.03e-02	3.11	3.15	3.86	3.90	3.89	3.90	3.90	3.80	3.91	3.73
	1.03e-02	2.66	2.63	3.80	3.71	3.92	3.92	3.90	3.96	3.88	3.98

We consider the diffusion law corresponding to the $(\mu, 1, r, r)$-Carreau–Yasuda model (3.7) with a moderate Reynolds number $\mathrm{Re} := \frac{2}{\mu} = 1000$, and the convection law given by the $(1, s)$-Laplace formula (3.9). In order to compare the flow behavior with respect to both r and s, with (r, s) in $\{\frac{3}{2}, 2, 3\} \times \{2\}$ and $\{\frac{5}{2}\} \times \{\frac{3}{2}, 2, \frac{9}{2}\}$, we solve the discrete problem on a Cartesian mesh of size 32×32 for $k = 3$, corresponding to 15872 degrees of freedom. In Figure 3.3 we display the velocity magnitude, while in Figure 3.4 we plot the horizontal component u_1 of the velocity along the vertical centreline $x_1 = \frac{1}{2}$ (resp., vertical component u_2 along the horizontal centreline $x_2 = \frac{1}{2}$). When $r = s = 2$,

$r = \frac{5}{2}$											
s		$\frac{3}{2}$		$\frac{9}{5}$		2		$\frac{5}{2}$		3	
k	h	$\boldsymbol{u}$	p	$\boldsymbol{u}$	p	$\boldsymbol{u}$	p	$\boldsymbol{u}$	p	$\boldsymbol{u}$	p
1	4.06e-02	1.68	1.43	1.79	1.47	1.79	1.49	1.79	1.53	1.80	1.55
	2.03e-02	1.64	1.58	1.78	1.61	1.78	1.62	1.76	1.63	1.75	1.64
	1.03e-02	1.50	1.59	1.67	1.60	1.66	1.59	1.65	1.57	1.64	1.55
	5.11e-03	1.46	1.60	1.65	1.61	1.65	1.61	1.66	1.61	1.67	1.61
2	4.06e-02	2.68	2.22	2.68	2.60	2.67	2.68	2.65	2.47	2.64	2.26
	2.03e-02	2.64	1.83	2.64	2.28	2.64	2.54	2.64	2.07	2.64	1.89
	1.03e-02	2.53	1.61	2.55	1.86	2.55	2.39	2.55	1.71	2.55	1.63
3	4.06e-02	3.62	3.59	3.65	3.62	3.65	3.62	3.65	3.61	3.64	3.59
	2.03e-02	2.97	2.78	3.14	2.92	3.15	2.92	3.15	2.93	3.15	2.94
	1.03e-02	2.62	2.48	3.09	2.90	3.10	2.91	3.10	2.92	3.11	2.93

reference solutions from the literature [68, 73] are also plotted for the sake of comparison. We observe significant differences in the behavior of the flow according to the viscous exponent r and the convective exponent s, coherent with the expected physical behavior. In particular, the viscous effects increase with r, as reflected by the size of the central vortex and the inclination of the centrelines. We observed the same phenomenon on the Stokes problem, cf. [27, Sec. 5.2]. Moreover, the turbulent effects increase with s as shown by the circular nature of the central vortex and the sharpness of the centrelines.

3.6 Proofs of the main results

In this section we first give the proof of the properties (3.52) and (3.54) of the discrete convective function c_h, then prove, in this order, Theorems 77 and 78.

3.6.1 Consistency of c_h

Proof of (3.52) *(Consistency).* Let, for the sake of conciseness, $\underline{\hat{\boldsymbol{w}}}_h \coloneqq \underline{\boldsymbol{I}}_h^k \boldsymbol{w}$. Using the single-valuedness of $(\boldsymbol{w} \cdot \boldsymbol{n}_{TF})\boldsymbol{\chi}(\cdot, \boldsymbol{w})$ across any interface $F \in \mathcal{F}_h^{\mathrm{i}}$ together with the fact that $\boldsymbol{v}_F = \boldsymbol{0}$ on any boundary face $F \in \mathcal{F}_h^{\mathrm{b}}$, we get

$$\sum_{T \in \mathcal{T}_h} \sum_{F \in \mathcal{F}_T} \int_F (\boldsymbol{w} \cdot \boldsymbol{n}_{TF})\boldsymbol{\chi}(\cdot, \boldsymbol{w}) \cdot \boldsymbol{v}_F = 0.$$

Table 3.3: Convergence rates of the numerical tests of Section 3.5.1 with $d = 3$ and $r \in \{2, \frac{5}{2}, 3\}$.

$r = 2$

	s	$\frac{3}{2}$		$\frac{9}{5}$		2		$\frac{5}{2}$		3	
k	h	$\boldsymbol{u}$	p	$\boldsymbol{u}$	p	$\boldsymbol{u}$	p	$\boldsymbol{u}$	p	$\boldsymbol{u}$	p
1	1.57e-01	1.87	1.52	1.85	1.56	1.84	1.58	1.81	1.64	1.76	1.71
	7.87e-02	1.92	2.08	1.91	2.15	1.90	2.18	1.88	2.22	1.86	2.26
	3.94e-02	1.95	2.33	1.95	2.46	1.95	2.49	1.94	2.48	1.93	2.45
2	1.57e-01	2.88	2.86	2.87	3.01	2.87	3.06	2.86	3.09	2.87	3.10
	7.87e-02	2.91	2.77	2.92	3.23	2.92	3.34	2.92	3.04	2.92	2.74
3	1.57e-01	3.88	3.88	3.87	3.90	3.86	3.91	3.85	3.94	3.83	4.00
	7.87e-02	3.92	4.24	3.92	4.27	3.92	4.28	3.91	4.29	3.91	4.29

$r = \frac{5}{2}$

	s	$\frac{3}{2}$		$\frac{9}{5}$		2		$\frac{5}{2}$		3	
k	h	$\boldsymbol{u}$	p	$\boldsymbol{u}$	p	$\boldsymbol{u}$	p	$\boldsymbol{u}$	p	$\boldsymbol{u}$	p
1	1.57e-01	1.77	1.38	1.75	1.42	1.74	1.43	1.72	1.47	1.68	1.53
	7.87e-02	1.88	1.78	1.87	1.95	1.86	1.99	1.83	2.03	1.80	2.06
	3.94e-02	1.92	1.90	1.91	2.21	1.90	2.29	1.88	2.17	1.85	2.04
2	1.57e-01	2.46	2.61	2.46	2.71	2.46	2.73	2.46	2.70	2.46	2.65
	7.87e-02	2.57	2.31	2.57	2.89	2.57	3.05	2.57	2.64	2.57	2.32
3	1.57e-01	3.08	3.21	3.08	3.22	3.07	3.22	3.06	3.22	3.05	3.22
	7.87e-02	3.32	3.51	3.32	3.52	3.32	3.52	3.31	3.52	3.31	3.52

$r = 3$

	s	$\frac{3}{2}$		$\frac{9}{5}$		2		$\frac{5}{2}$		3	
k	h	$\boldsymbol{u}$	p	$\boldsymbol{u}$	p	$\boldsymbol{u}$	p	$\boldsymbol{u}$	p	$\boldsymbol{u}$	p
1	1.57e-01	1.63	1.29	1.62	1.31	1.62	1.31	1.60	1.31	1.59	1.35
	7.87e-02	1.73	1.61	1.72	1.82	1.72	1.88	1.71	1.90	1.69	1.90
	3.94e-02	1.17	1.56	1.18	1.89	1.19	2.03	1.21	1.80	1.25	1.61
3	1.57e-01	2.16	2.42	2.16	2.45	2.16	2.45	2.16	2.43	2.16	2.39
	7.87e-02	2.30	2.21	2.30	2.57	2.30	2.64	2.30	2.43	2.30	2.20
2	1.57e-01	2.76	2.84	2.76	2.84	2.75	2.83	2.75	2.83	2.75	2.83
	7.87e-02	2.93	2.89	2.93	2.89	2.93	2.89	2.93	2.89	2.92	2.89

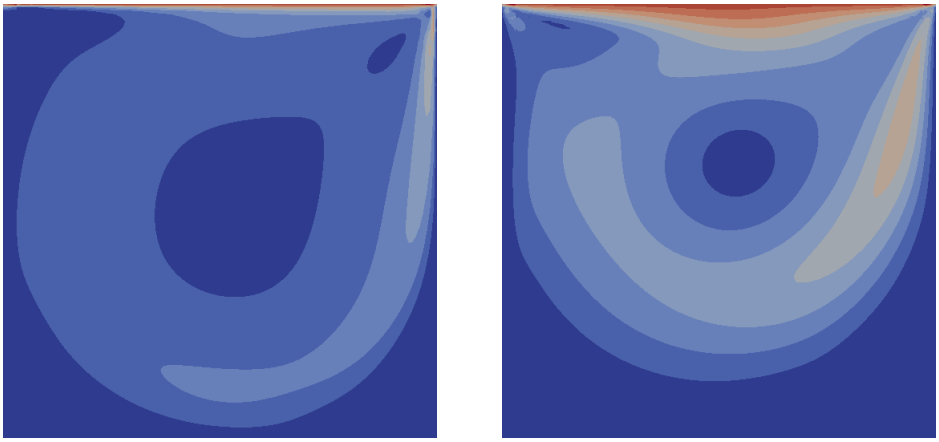

$r = \frac{3}{2},\ s = 2$

$r = \frac{5}{2},\ s = \frac{3}{2}$

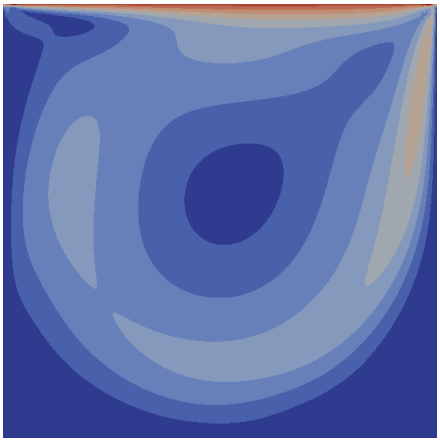

$r = 2,\ s = 2$

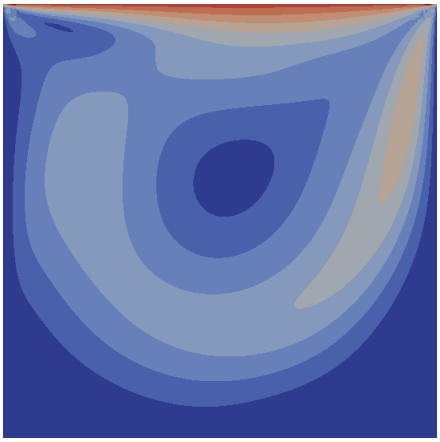

$r = \frac{5}{2},\ s = 2$

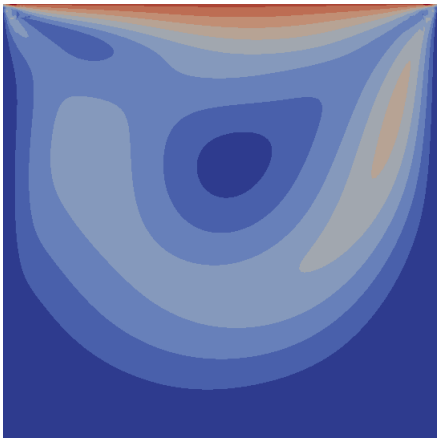

$r = 3,\ s = 2$

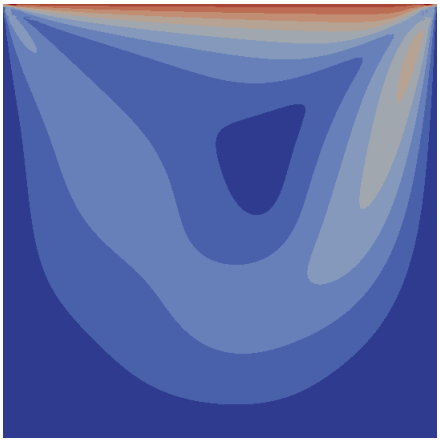

$r = \frac{5}{2},\ s = \frac{9}{2}$

Figure 3.3: Numerical results for the test case of Section 3.5.2. Velocity magnitude contours (10 equispaced values in the range $[0, 1]$).

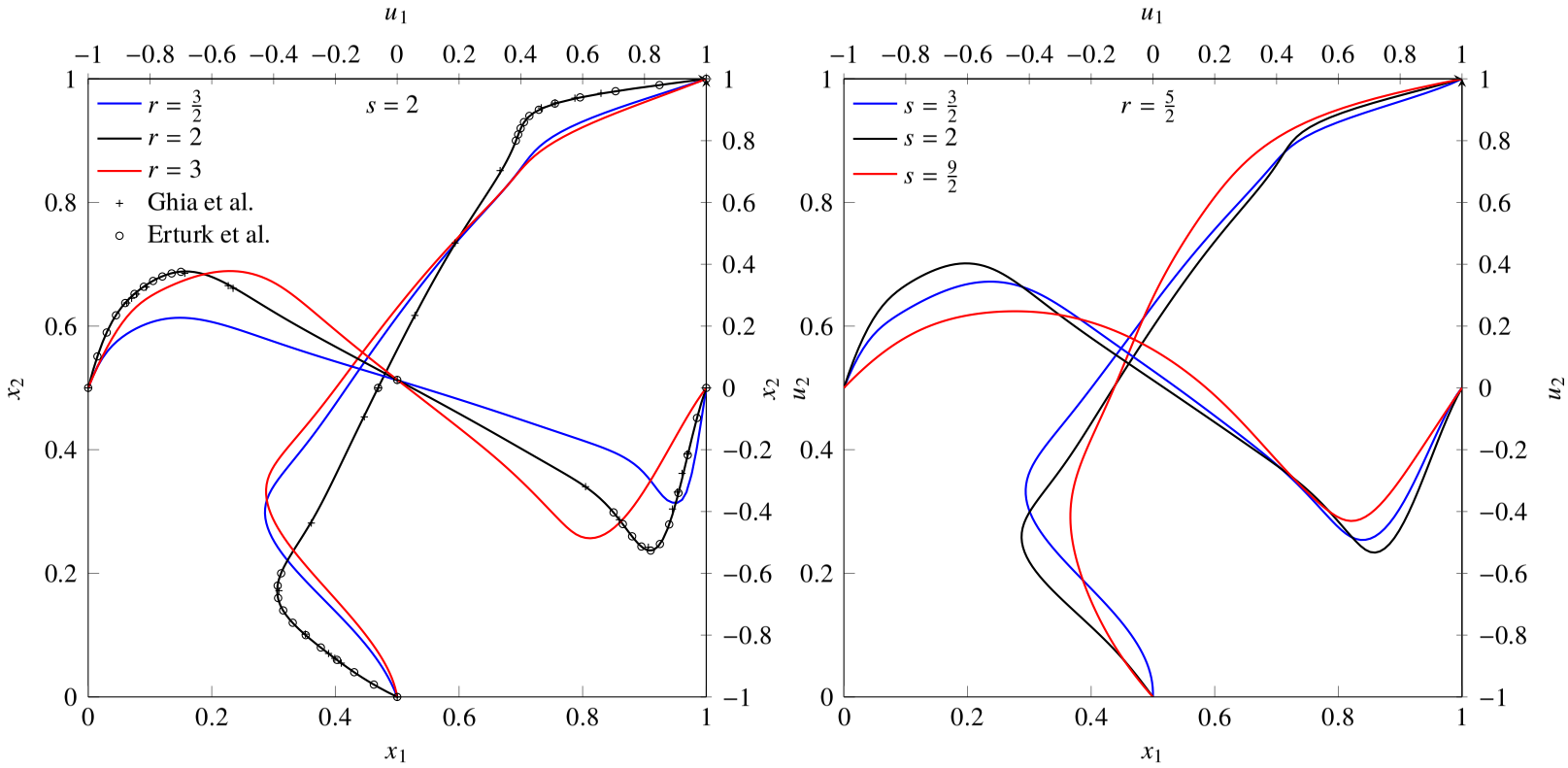

Figure 3.4: Numerical results for the test case of Section 3.5.2. Horizontal component u_1 of the velocity along the vertical centreline $x_1 = \frac{1}{2}$ and vertical component u_2 of the velocity along the horizontal centreline $x_2 = \frac{1}{2}$. *Top:* Results with $(r, s) \in \left\{\frac{3}{2}, 2, 3\right\} \times \{2\}$. *Bottom:* Results with $(r, s) \in \left\{\frac{5}{2}\right\} \times \left\{\frac{3}{2}, 2, \frac{9}{2}\right\}$.

Proceeding as in (3.13) but with an element-by-element integration by parts, and using the previous relation to insert $\boldsymbol{v}_F$ into the boundary term, we infer

$$\int_\Omega (\boldsymbol{w}\cdot\boldsymbol{\nabla})\boldsymbol{\chi}(\cdot,\boldsymbol{w})\cdot\boldsymbol{v}_h = \frac{1}{s}\int_\Omega (\boldsymbol{\chi}(\cdot,\boldsymbol{w})\cdot\boldsymbol{\nabla})\boldsymbol{w}\cdot\boldsymbol{v}_h + \frac{s-2}{s}\int_\Omega \frac{\boldsymbol{v}_h\cdot\boldsymbol{w}}{|\boldsymbol{w}|^2}(\boldsymbol{\chi}(\cdot,\boldsymbol{w})\cdot\boldsymbol{\nabla})\boldsymbol{w}\cdot\boldsymbol{w} - \frac{1}{s'}\left(\int_\Omega (\boldsymbol{\chi}(\cdot,\boldsymbol{w})\cdot\boldsymbol{\nabla}_h)\boldsymbol{v}_h\cdot\boldsymbol{w} + \sum_{T\in\mathcal{T}_h}\sum_{F\in\mathcal{F}_T}\int_F (\boldsymbol{w}\cdot\boldsymbol{n}_{TF})\boldsymbol{\chi}(\cdot,\boldsymbol{w})\cdot(\boldsymbol{v}_F-\boldsymbol{v}_T)\right). \tag{3.85}$$

Using the definitions (3.33) of $\boldsymbol{\pi}_T^k$, (3.43) of $\mathbf{G}_h^k$, and (3.42) of $\mathbf{G}_T^k$ (the latter with $\boldsymbol{\tau} = \boldsymbol{\pi}_T^k(\boldsymbol{\chi}(\cdot,\hat{\boldsymbol{w}}_T)\otimes\hat{\boldsymbol{w}}_T)$), we get

$$\begin{aligned}\int_\Omega (\boldsymbol{\chi}(\cdot,\hat{\boldsymbol{w}}_h)\cdot\mathbf{G}_h^k)\underline{\boldsymbol{v}}_h\cdot\hat{\boldsymbol{w}}_h &= \sum_{T\in\mathcal{T}_h}\int_T \mathbf{G}_T^k\underline{\boldsymbol{v}}_T : \boldsymbol{\pi}_T^k(\boldsymbol{\chi}(\cdot,\hat{\boldsymbol{w}}_T)\otimes\hat{\boldsymbol{w}}_T)\\ &= \sum_{T\in\mathcal{T}_h}\int_T \boldsymbol{\nabla}\boldsymbol{v}_T : \cancel{\boldsymbol{\pi}_T^k}(\boldsymbol{\chi}(\cdot,\hat{\boldsymbol{w}}_T)\otimes\hat{\boldsymbol{w}}_T)\\ &\quad + \sum_{T\in\mathcal{T}_h}\sum_{F\in\mathcal{F}_T}\int_F \left(\boldsymbol{\pi}_T^k(\boldsymbol{\chi}(\cdot,\hat{\boldsymbol{w}}_T)\otimes\hat{\boldsymbol{w}}_T)\,\boldsymbol{n}_{TF}\right)\cdot(\boldsymbol{v}_F-\boldsymbol{v}_T),\end{aligned} \tag{3.86}$$

where the removal of $\boldsymbol{\pi}_T^k$ is justified by its definition after observing that $\boldsymbol{\nabla}\boldsymbol{v}_T \in \mathbb{P}^{k-1}(T)^{d\times d} \subset \mathbb{P}^k(T)^{d\times d}$. Plugging (3.86) into the definition (3.48) of c_h, we obtain

$$\begin{aligned}\mathrm{c}_h(\underline{\hat{\boldsymbol{w}}}_h,\underline{\boldsymbol{v}}_h) &= \frac{1}{s}\int_\Omega (\boldsymbol{\chi}(\cdot,\hat{\boldsymbol{w}}_h)\cdot\mathbf{G}_h^k)\underline{\hat{\boldsymbol{w}}}_h\cdot\boldsymbol{v}_h\\ &\quad + \frac{s-2}{s}\int_\Omega \frac{\boldsymbol{v}_h\cdot\hat{\boldsymbol{w}}_h}{|\boldsymbol{w}_h|^2}(\boldsymbol{\chi}(\cdot,\hat{\boldsymbol{w}}_h)\cdot\mathbf{G}_h^k)\underline{\hat{\boldsymbol{w}}}_h\cdot\hat{\boldsymbol{w}}_h\\ &\quad - \frac{1}{s'}\left(\int_\Omega (\boldsymbol{\chi}(\cdot,\hat{\boldsymbol{w}}_h)\cdot\boldsymbol{\nabla}_h)\boldsymbol{v}_h\cdot\hat{\boldsymbol{w}}_h\right.\\ &\qquad \left. + \sum_{T\in\mathcal{T}_h}\sum_{F\in\mathcal{F}_T}\int_F \left(\boldsymbol{\pi}_T^k(\boldsymbol{\chi}(\cdot,\hat{\boldsymbol{w}}_T)\otimes\hat{\boldsymbol{w}}_T)\,\boldsymbol{n}_{TF}\right)\cdot(\boldsymbol{v}_F-\boldsymbol{v}_T)\right).\end{aligned} \tag{3.87}$$

Subtracting (3.87) from (3.85), then adding and subtracting to the right-hand side of the resulting expression the quantity

$$\begin{aligned}&\frac{1}{s}\int_\Omega (\boldsymbol{\chi}(\cdot,\boldsymbol{w})\cdot\mathbf{G}_h^k)\underline{\hat{\boldsymbol{w}}}_h\cdot\boldsymbol{v}_h + \frac{s-2}{s}\int_\Omega \frac{\boldsymbol{v}_h\cdot\boldsymbol{w}}{|\boldsymbol{w}|^2}(\boldsymbol{\chi}(\cdot,\boldsymbol{w})\cdot\mathbf{G}_h^k)\underline{\hat{\boldsymbol{w}}}_h\cdot\boldsymbol{w}\\ &+ \frac{1}{s'}\left[\int_\Omega (\boldsymbol{\chi}(\cdot,\boldsymbol{w})\cdot\boldsymbol{\nabla}_h)\boldsymbol{v}_h\cdot\hat{\boldsymbol{w}}_h + \sum_{T\in\mathcal{T}_h}\sum_{F\in\mathcal{F}_T}\left(\int_F ((\boldsymbol{\chi}(\cdot,\hat{\boldsymbol{w}}_T)\otimes\hat{\boldsymbol{w}}_T)\,\boldsymbol{n}_{TF})\cdot(\boldsymbol{v}_F-\boldsymbol{v}_T)\right.\right.\\ &\qquad \left.\left. + \int_F (\hat{\boldsymbol{w}}_T\cdot\boldsymbol{n}_{TF})\boldsymbol{\chi}(\cdot,\boldsymbol{w})\cdot(\boldsymbol{v}_F-\boldsymbol{v}_T)\right)\right],\end{aligned}$$

we obtain

$$\int_\Omega (\boldsymbol{w}\cdot\boldsymbol{\nabla})\boldsymbol{\chi}(\cdot,\boldsymbol{w})\cdot\boldsymbol{v}_h - \mathrm{c}_h(\underline{\boldsymbol{I}}_h^k\boldsymbol{w},\underline{\boldsymbol{v}}_h) = \frac{1}{s}\left(\mathcal{T}_1+\mathcal{T}_2\right)+\frac{s-2}{s}\left(\mathcal{T}_3+\mathcal{T}_4\right) - \frac{1}{s'}\left(\mathcal{T}_5+\mathcal{T}_6+\mathcal{T}_7+\mathcal{T}_8+\mathcal{T}_9\right), \quad (3.88)$$

with

$$\begin{aligned}
\mathcal{T}_1 &\coloneqq \int_\Omega (\boldsymbol{\chi}(\cdot,\boldsymbol{w})\cdot(\boldsymbol{\nabla}-\mathbf{G}_h^k\underline{\boldsymbol{I}}_h^k))\boldsymbol{w}\cdot\boldsymbol{v}_h,\\
\mathcal{T}_2 &\coloneqq \int_\Omega \left((\boldsymbol{\chi}(\cdot,\boldsymbol{w})-\boldsymbol{\chi}(\cdot,\hat{\boldsymbol{w}}_h))\cdot\mathbf{G}_h^k\right)\underline{\hat{\boldsymbol{w}}}_h\cdot\boldsymbol{v}_h,\\
\mathcal{T}_3 &\coloneqq \int_\Omega \frac{\boldsymbol{v}_h\cdot\boldsymbol{w}}{|\boldsymbol{w}|^2}\left(\boldsymbol{\chi}(\cdot,\boldsymbol{w})\cdot(\boldsymbol{\nabla}-\mathbf{G}_h^k\underline{\boldsymbol{I}}_h^k)\right)\boldsymbol{w}\cdot\boldsymbol{w},\\
\mathcal{T}_4 &\coloneqq \int_\Omega \left(\frac{\boldsymbol{v}_h\cdot\boldsymbol{w}}{|\boldsymbol{w}|^2}(\boldsymbol{\chi}(\cdot,\boldsymbol{w})\cdot\mathbf{G}_h^k)\underline{\hat{\boldsymbol{w}}}_h\cdot\boldsymbol{w}-\frac{\boldsymbol{v}_h\cdot\hat{\boldsymbol{w}}_h}{|\hat{\boldsymbol{w}}_h|^2}(\boldsymbol{\chi}(\cdot,\hat{\boldsymbol{w}}_h)\cdot\mathbf{G}_h^k)\underline{\hat{\boldsymbol{w}}}_h\cdot\hat{\boldsymbol{w}}_h\right),\\
\mathcal{T}_5 &\coloneqq \int_\Omega (\boldsymbol{\chi}(\cdot,\boldsymbol{w})\cdot\boldsymbol{\nabla}_h)\boldsymbol{v}_h\cdot(\boldsymbol{w}-\hat{\boldsymbol{w}}_h),\\
\mathcal{T}_6 &\coloneqq \int_\Omega \left((\boldsymbol{\chi}(\cdot,\boldsymbol{w})-\boldsymbol{\chi}(\cdot,\hat{\boldsymbol{w}}_h))\cdot\boldsymbol{\nabla}_h\right)\boldsymbol{v}_h\cdot\hat{\boldsymbol{w}}_h,\\
\mathcal{T}_7 &\coloneqq \sum_{T\in\mathcal{T}_h}\sum_{F\in\mathcal{F}_T}\int_F((\boldsymbol{w}-\hat{\boldsymbol{w}}_T)\cdot\boldsymbol{n}_{TF})\boldsymbol{\chi}(\cdot,\boldsymbol{w})\cdot(\boldsymbol{v}_F-\boldsymbol{v}_T),\\
\mathcal{T}_8 &\coloneqq \sum_{T\in\mathcal{T}_h}\sum_{F\in\mathcal{F}_T}\int_F(\hat{\boldsymbol{w}}_T\cdot\boldsymbol{n}_{TF})\left(\boldsymbol{\chi}(\cdot,\boldsymbol{w})-\boldsymbol{\chi}(\cdot,\hat{\boldsymbol{w}}_T)\right)\cdot(\boldsymbol{v}_F-\boldsymbol{v}_T),\\
\mathcal{T}_9 &\coloneqq \sum_{T\in\mathcal{T}_h}\sum_{F\in\mathcal{F}_T}\int_F\left(\left(\boldsymbol{\chi}(\cdot,\hat{\boldsymbol{w}}_T)\otimes\hat{\boldsymbol{w}}_T-\boldsymbol{\pi}_T^k(\boldsymbol{\chi}(\cdot,\hat{\boldsymbol{w}}_T)\otimes\hat{\boldsymbol{w}}_T)\right)\boldsymbol{n}_{TF}\right)\cdot(\boldsymbol{v}_F-\boldsymbol{v}_T).
\end{aligned}$$

We proceed to estimate these terms. For $\mathcal{T}_1$ and $\mathcal{T}_3$, using the $(1;s'r',r,sr')$-Hölder inequality (3.20) together with the Hölder continuity (3.8e) of $\boldsymbol{\chi}$, we get

$$\begin{aligned}
|\mathcal{T}_1|+|\mathcal{T}_3| &\lesssim \chi_{\mathrm{hc}}\|\boldsymbol{w}\|_{L^{sr'}(\Omega)^d}^{s-1}\|\boldsymbol{\nabla}\boldsymbol{w}-\mathbf{G}_h^k(\underline{\boldsymbol{I}}_h^k\boldsymbol{w})\|_{L^r(\Omega)^{d\times d}}\|\boldsymbol{v}_h\|_{L^{sr'}(\Omega)^d}\\
&\lesssim h^{k+1}\chi_{\mathrm{hc}}|\boldsymbol{w}|_{W^{1,r}(\Omega)^d}^{s-1}|\boldsymbol{w}|_{W^{k+2,r}(\mathcal{T}_h)^d}\|\underline{\boldsymbol{v}}_h\|_{\boldsymbol{\varepsilon},r,h},
\end{aligned}$$

where we concluded with the consistency (3.45) of the gradient reconstruction together with the continuous (3.24) and discrete (3.41) Sobolev embeddings (valid since $sr'\le r^*$ by (3.51)) and the norm equivalence (3.39).

Moving to $\mathcal{T}_2$ and $\mathcal{T}_4$, using a Cauchy–Schwarz inequality together with the Hölder

continuity (3.8e) of χ on $\mathcal{T}_2$ and the same reasoning as in (3.31) on $\mathcal{T}_4$ yields

$$\begin{aligned}
|\mathcal{T}_2| + |\mathcal{T}_4| &\le \chi_{\mathrm{hc}} \int_\Omega (|\boldsymbol{w}|^s + |\hat{\boldsymbol{w}}_h|^s)^{\frac{s-\tilde{s}}{s}} |\boldsymbol{w} - \hat{\boldsymbol{w}}_h|^{\tilde{s}-1} |\mathbf{G}_h^k \underline{\hat{\boldsymbol{w}}}_h|_{d\times d} |\boldsymbol{v}_h| \\
&\le \chi_{\mathrm{hc}} \left(\|\boldsymbol{w}\|^s_{L^{sr'}(\Omega)^d} + \|\hat{\boldsymbol{w}}_h\|^s_{L^{sr'}(\Omega)^d} \right)^{\frac{s-\tilde{s}}{s}} \|\boldsymbol{w} - \hat{\boldsymbol{w}}_h\|^{\tilde{s}-1}_{L^{sr'}(\Omega)^d} \\
&\quad \times \|\mathbf{G}_h^k \underline{\hat{\boldsymbol{w}}}_h\|_{L^r(\Omega)^{d\times d}} \|\boldsymbol{v}_h\|_{L^{sr'}(\Omega)^d} \\
&\lesssim h^{(k+1)(\tilde{s}-1)} \chi_{\mathrm{hc}} |\boldsymbol{w}|^{s+1-\tilde{s}}_{W^{1,r}(\Omega)^d} |\boldsymbol{w}|^{\tilde{s}-1}_{W^{k+1,sr'}(\mathcal{T}_h)^d} \|\underline{\boldsymbol{v}}_h\|_{\boldsymbol{\varepsilon},r,h},
\end{aligned}$$

where we have used the $(1; \frac{sr'}{s-\tilde{s}}, \frac{sr'}{\tilde{s}-1}, r, sr')$-Hölder inequality (3.20) in the second line, while the conclusion follows from the continuous (3.24) and discrete (3.41) Sobolev embeddings (again valid since $sr' \le r^*$ by (3.51)) along with the boundedness (3.47) of $\mathbf{G}_h^k$ and (3.40) of $\underline{\boldsymbol{I}}_h^k$, and the $(k+1, sr', 0)$-approximation properties (3.34a) of $\boldsymbol{\pi}_h^k$.

With a similar reasoning as for $\mathcal{T}_2$, we get the following bounds for $\mathcal{T}_5$ and $\mathcal{T}_6$:

$$\begin{aligned}
|\mathcal{T}_5| &\lesssim h^{k+1} \chi_{\mathrm{hc}} |\boldsymbol{w}|^{s-1}_{W^{1,r}(\Omega)^d} |\boldsymbol{w}|_{W^{k+1,sr'}(\mathcal{T}_h)^d} \|\underline{\boldsymbol{v}}_h\|_{\boldsymbol{\varepsilon},r,h}, \\
|\mathcal{T}_6| &\lesssim h^{(k+1)(\tilde{s}-1)} \chi_{\mathrm{hc}} |\boldsymbol{w}|^{s+1-\tilde{s}}_{W^{1,r}(\Omega)^d} |\boldsymbol{w}|^{\tilde{s}-1}_{W^{k+1,sr'}(\mathcal{T}_h)^d} \|\underline{\boldsymbol{v}}_h\|_{\boldsymbol{\varepsilon},r,h}.
\end{aligned}$$

Moving to $\mathcal{T}_8$, the Hölder continuity (3.8e) of χ, the $(1; sr', \frac{sr'}{s-\tilde{s}}, \frac{sr'}{\tilde{s}-1}, r)$-Hölder inequality (3.20), and the bound $h_F \lesssim h_T$ yield

$$\begin{aligned}
|\mathcal{T}_8| &\le \chi_{\mathrm{hc}} \left(\sum_{T\in\mathcal{T}_h} h_T \|\hat{\boldsymbol{w}}_T\|^{sr'}_{L^{sr'}(\partial T)^d} \right)^{\frac{1}{sr'}} \left(\sum_{T\in\mathcal{T}_h} h_T \left(\|\boldsymbol{w}\|^{sr'}_{L^{sr'}(\partial T)^d} + \|\hat{\boldsymbol{w}}_T\|^{sr'}_{L^{sr'}(\partial T)^d} \right) \right)^{\frac{s-\tilde{s}}{sr'}} \\
&\quad \times \left(\sum_{T\in\mathcal{T}_h} h_T \|\boldsymbol{w} - \hat{\boldsymbol{w}}_T\|^{sr'}_{L^{sr'}(\partial T)^d} \right)^{\frac{\tilde{s}-1}{sr'}} \left(\sum_{T\in\mathcal{T}_h} \sum_{F\in\mathcal{F}_T} h_F^{1-r} \|\boldsymbol{v}_F - \boldsymbol{v}_T\|^r_{L^r(F)^d} \right)^{\frac{1}{r}} \\
&\lesssim h^{(k+1)(\tilde{s}-1)} \chi_{\mathrm{hc}} \left(|\boldsymbol{w}|^s_{W^{1,sr'}(\Omega)^d} + \|\boldsymbol{w}\|^s_{L^{sr'}(\Omega)^d} + \|\hat{\boldsymbol{w}}_h\|^s_{L^{sr'}(\Omega)^d} \right)^{\frac{s+1-\tilde{s}}{s}} \\
&\quad \times |\boldsymbol{w}|^{\tilde{s}-1}_{W^{k+1,sr'}(\mathcal{T}_h)^d} \|\underline{\boldsymbol{v}}_h\|_{\boldsymbol{\varepsilon},r,h} \\
&\lesssim h^{(k+1)(\tilde{s}-1)} \chi_{\mathrm{hc}} \left(|\boldsymbol{w}|^s_{W^{1,sr'}(\Omega)^d} + |\boldsymbol{w}|^s_{W^{1,r}(\Omega)^d} \right)^{\frac{s+1-\tilde{s}}{s}} |\boldsymbol{w}|^{\tilde{s}-1}_{W^{k+1,sr'}(\mathcal{T}_h)^d} \|\underline{\boldsymbol{v}}_h\|_{\boldsymbol{\varepsilon},r,h},
\end{aligned}$$

where, to pass to the second line, we have used the discrete trace inequality [50, Eq. (1.55)], the continuous trace inequality [50, Eq. (1.51)] together with the bound $h_T \lesssim 1$, the $(k+1, sr', 0)$-trace approximation properties (3.34b) of $\boldsymbol{\pi}_T^k$, and the definition (3.37) of $\|\cdot\|_{\boldsymbol{\varepsilon},r,h}$, while the conclusion is obtained using the Sobolev embedding (3.24) (again valid since $sr' \le r^*$ by (3.51)).

With a similar reasoning, we get the following bound for $\mathcal{T}_7$:

$$|\mathcal{T}_7| \lesssim h^{k+1} \chi_{\mathrm{hc}} \left(|\boldsymbol{w}|^s_{W^{1,sr'}(\Omega)^d} + |\boldsymbol{w}|^s_{W^{1,r}(\Omega)^d} \right)^{\frac{s-1}{s}} |\boldsymbol{w}|_{W^{k+1,sr'}(\mathcal{T}_h)^d} \|\underline{\boldsymbol{v}}_h\|_{\boldsymbol{\varepsilon},r,h}.$$

Moving to $\mathcal{T}_9$, the Hölder inequality together with the bound $h_F \lesssim h_T$ and the definition (3.37) of $\|\cdot\|_{\boldsymbol{\varepsilon},r,h}$ yield

$$\begin{aligned}|\mathcal{T}_9| &\lesssim \left(\sum_{T\in\mathcal{T}_h} h_T \left\|\boldsymbol{\chi}(\cdot,\hat{\boldsymbol{w}}_T)\otimes\hat{\boldsymbol{w}}_T - \boldsymbol{\pi}_T^k\left(\boldsymbol{\chi}(\cdot,\hat{\boldsymbol{w}}_T)\otimes\hat{\boldsymbol{w}}_T\right)\right\|_{L^{r'}(\partial T)^{d\times d}}^{r'}\right)^{\frac{1}{r'}} \|\underline{\boldsymbol{v}}_h\|_{\boldsymbol{\varepsilon},r,h}\\ &\lesssim h^{k+1}\chi_{\mathrm{hc}}\,|\hat{\boldsymbol{w}}_T|^s_{W^{k+1,sr'}(\mathcal{T}_h)^d}\,\|\underline{\boldsymbol{v}}_h\|_{\boldsymbol{\varepsilon},r,h} \lesssim h^{k+1}\chi_{\mathrm{hc}}\,|\boldsymbol{w}|^s_{W^{k+1,sr'}(\mathcal{T}_h)^d}\,\|\underline{\boldsymbol{v}}_h\|_{\boldsymbol{\varepsilon},r,h},\end{aligned}$$

where we passed to the second line using the $(k+1,r',0)$-trace approximation properties (3.34b) of $\boldsymbol{\pi}_T^k$ together with a triangle inequality and the Hölder continuity (3.8e) of $\boldsymbol{\chi}$ (with $(\boldsymbol{v},\boldsymbol{w}) = (\boldsymbol{0},\hat{\boldsymbol{w}}_T)$), while the conclusion follows using a triangle inequality and the $(k+1,sr',k+1)$-approximation properties (3.34a) of $\boldsymbol{\pi}_T^k$ to write $|\hat{\boldsymbol{w}}_T|_{W^{k+1,sr'}(\mathcal{T}_h)^d} \le |\hat{\boldsymbol{w}}_T-\boldsymbol{w}|_{W^{k+1,sr'}(\mathcal{T}_h)^d} + |\boldsymbol{w}|_{W^{k+1,sr'}(\mathcal{T}_h)^d} \lesssim |\boldsymbol{w}|_{W^{k+1,sr'}(\mathcal{T}_h)^d}$.

Plugging the above bounds for $\mathcal{T}_1,\dots,\mathcal{T}_9$ into (3.88) and passing to the supremum, (3.52) follows. □

Proof of (3.54) *(Sequential consistency).* Let $\boldsymbol{\phi}\in C_{\mathrm{c}}^\infty(\Omega)^d$ and set $\underline{\hat{\boldsymbol{\phi}}}_h := \underline{\boldsymbol{I}}_h^k\boldsymbol{\phi}$. Writing the definition (3.48) of c_h with $(\underline{\boldsymbol{w}}_h,\underline{\boldsymbol{v}}_h)$ replaced by $(\underline{\boldsymbol{v}}_h,\underline{\hat{\boldsymbol{\phi}}}_h)$, we have

$$\begin{aligned}\mathrm{c}_h(\underline{\boldsymbol{v}}_h,\underline{\hat{\boldsymbol{\phi}}}_h) := \frac{1}{s}\underbrace{\int_\Omega(\boldsymbol{\chi}(\cdot,\boldsymbol{v}_h)\cdot\mathbf{G}_h^k)\underline{\boldsymbol{v}}_h\cdot\hat{\boldsymbol{\phi}}_h}_{\mathcal{T}_1} + \frac{s-2}{s}\underbrace{\int_\Omega\frac{\hat{\boldsymbol{\phi}}_h\cdot\boldsymbol{v}_h}{|\boldsymbol{v}_h|^2}(\boldsymbol{\chi}(\cdot,\boldsymbol{v}_h)\cdot\mathbf{G}_h^k)\underline{\boldsymbol{v}}_h\cdot\boldsymbol{v}_h}_{\mathcal{T}_2}\\ - \frac{1}{s'}\underbrace{\int_\Omega(\boldsymbol{\chi}(\cdot,\boldsymbol{v}_h)\cdot\mathbf{G}_h^k)\underline{\hat{\boldsymbol{\phi}}}_h\cdot\boldsymbol{v}_h}_{\mathcal{T}_3}.\end{aligned} \tag{3.89}$$

Inserting $\pm|\boldsymbol{v}_h|^{-2}(\boldsymbol{v}_h\otimes\boldsymbol{v}_h)\boldsymbol{\chi}(\cdot,\boldsymbol{v})$, then using a triangle inequality, we get

$$\begin{aligned}&\left\||\boldsymbol{v}_h|^{-2}(\boldsymbol{v}_h\otimes\boldsymbol{v}_h)\boldsymbol{\chi}(\cdot,\boldsymbol{v}_h) - |\boldsymbol{v}|^{-2}(\boldsymbol{v}\otimes\boldsymbol{v})\boldsymbol{\chi}(\cdot,\boldsymbol{v})\right\|_{L^{s'r'}(\Omega)^d}\\ &\quad\le \|\boldsymbol{\chi}(\cdot,\boldsymbol{v}_h)-\boldsymbol{\chi}(\cdot,\boldsymbol{v})\|_{L^{s'r'}(\Omega)^d}\\ &\qquad + \left\||\boldsymbol{\chi}(\cdot,\boldsymbol{v})|\left(|\boldsymbol{v}_h|^{-2}\boldsymbol{v}_h\otimes\boldsymbol{v}_h - |\boldsymbol{v}|^{-2}\boldsymbol{v}\otimes\boldsymbol{v}\right)\right\|_{L^{s'r'}(\Omega)^{d\times d}}\\ &\quad\le \chi_{\mathrm{hc}}\left(\|\boldsymbol{v}_h\|^s_{L^{sr'}(\Omega)^d} + \|\boldsymbol{v}\|^s_{L^{sr'}(\Omega)^d}\right)^{\frac{s-\tilde{s}}{s}}\|\boldsymbol{v}_h-\boldsymbol{v}\|^{\tilde{s}-1}_{L^{sr'}(\Omega)^d},\end{aligned} \tag{3.90}$$

where we have concluded proceeding as in (3.30) and using the Hölder continuity (3.8e) of $\boldsymbol{\chi}$ and the $(s'r';\frac{sr'}{s-\tilde{s}},\frac{sr'}{\tilde{s}-1})$-Hölder inequality (3.20). Thus, recalling that $\boldsymbol{v}_h \xrightarrow[h\to 0]{} \boldsymbol{v}$ strongly in $L^{sr'}(\Omega)^d$ (since $sr' < r^*$ by (3.53)), which implies that $\|\boldsymbol{v}_h\|^s_{L^{sr'}(\Omega)^d} +$

$\|\boldsymbol{v}\|^s_{L^{sr'}(\Omega)^d}$ is bounded uniformly in h, we infer from (3.90) that,

$$|\boldsymbol{v}_h|^{-2}(\boldsymbol{v}_h\otimes\boldsymbol{v}_h)\boldsymbol{\chi}(\cdot,\boldsymbol{v}_h)\xrightarrow[h\to 0]{}|\boldsymbol{v}|^{-2}(\boldsymbol{v}\otimes\boldsymbol{v})\boldsymbol{\chi}(\cdot,\boldsymbol{v})\text{ strongly in }L^{s'r'}(\Omega)^d, \tag{3.91}$$

$$\boldsymbol{\chi}(\cdot,\boldsymbol{v}_h)\xrightarrow[h\to 0]{}\boldsymbol{\chi}(\cdot,\boldsymbol{v})\text{ strongly in }L^{s'r'}(\Omega)^d. \tag{3.92}$$

Hence, observing that $\frac{1}{sr'}+\frac{1}{r}+\frac{1}{s'r'}=1$, the strong convergence (3.35) of $\hat{\boldsymbol{\phi}}_h$ in $L^{sr'}(\Omega)^d$ together with the fact that $\mathbf{G}^k_h\underline{\boldsymbol{v}}_h\xrightarrow[h\to 0]{}\boldsymbol{\nabla}\boldsymbol{v}$ weakly in $L^r(\Omega)^{d\times d}$ by assumption, along with (3.91) for $\mathcal{T}_1$ and (3.92) for $\mathcal{T}_2$ yield

$$\mathcal{T}_2\xrightarrow[h\to 0]{}\int_\Omega\frac{\boldsymbol{\phi}\cdot\boldsymbol{v}}{|\boldsymbol{v}|^2}(\boldsymbol{\chi}(\cdot,\boldsymbol{v})\cdot\boldsymbol{\nabla})\boldsymbol{v}\cdot\boldsymbol{v}\quad\text{and}\quad\mathcal{T}_1\xrightarrow[h\to 0]{}\int_\Omega(\boldsymbol{\chi}(\cdot,\boldsymbol{v})\cdot\boldsymbol{\nabla})\boldsymbol{v}\cdot\boldsymbol{\phi}. \tag{3.93}$$

Moving to $\mathcal{T}_3$, the fact that $\boldsymbol{v}_h\xrightarrow[h\to 0]{}\boldsymbol{v}$ strongly in $L^{sr'}(\Omega)^d$ (since $sr'<r^*$ by (3.53)) together with the strong convergence (3.46) of $\mathbf{G}^k_h\hat{\boldsymbol{\phi}}_h$ in $L^r(\Omega)^{d\times d}$ (notice that the weak convergence would suffice to infer the result in (3.107) below) and (3.92) give

$$\mathcal{T}_3\xrightarrow[h\to 0]{}\int_\Omega(\boldsymbol{\chi}(\cdot,\boldsymbol{v})\cdot\boldsymbol{\nabla})\boldsymbol{\phi}\cdot\boldsymbol{v}. \tag{3.94}$$

Hence passing to the limit in (3.89), using (3.93)–(3.94), and recalling the definition (3.12) of c, we infer (3.54). □

3.6.2 Convergence

Proof of Theorem 77. **Step 1.** *Existence of a limit.* Since, for all $h\in\mathcal{H}$, $(\underline{\boldsymbol{u}}_h,p_h)\in\underline{\boldsymbol{U}}^k_{h,0}\times P^k_h$ solves (3.77), the a priori bounds (3.78) implies that the sequences $(\|\underline{\boldsymbol{u}}_h\|_{\boldsymbol{\varepsilon},r,h})_{h\in\mathcal{H}}$ (hence also $(\|\underline{\boldsymbol{u}}_h\|_{1,r,h})_{h\in\mathcal{H}}$ by (3.39)) and $(\|p_h\|_{L^{r'}(\Omega)})_{h\in\mathcal{H}}$ are bounded uniformly in h. Thus, invoking the discrete compactness result of [50, Theorem 9.29], we infer the existence of $(\boldsymbol{u},p)\in\boldsymbol{U}\times P$ such that, up to a subsequence,

- $\boldsymbol{u}_h\xrightarrow[h\to 0]{}\boldsymbol{u}$ strongly in $L^{[1,r^*)}(\Omega)^d$;
- $\mathbf{G}^k_h\underline{\boldsymbol{u}}_h\xrightarrow[h\to 0]{}\boldsymbol{\nabla}\boldsymbol{u}$ weakly in $L^r(\Omega)^{d\times d}$;
- $p_h\xrightarrow[h\to 0]{}p$ weakly in $L^{r'}(\Omega)$.

Step 2. *Identification of the limit.* The discrete mass equation (3.77b) along with the sequential consistency (3.76) of b_h yield, for all $\psi\in C^\infty_c(\Omega)$,

$$0=\mathrm{b}_h(\underline{\boldsymbol{u}}_h,\pi^k_h\psi)\xrightarrow[h\to 0]{}b(\boldsymbol{u},\psi)=0.$$

By density of $C^\infty_c(\Omega)$ in $L^{r'}(\Omega)$, this shows that $\boldsymbol{u}$ satisfies the mass equation (3.10b).

Let us show now that $(\boldsymbol{u}, p)$ satisfy the momentum equation (3.10a). Since the sequence $(\|\underline{\boldsymbol{u}}_h\|_{\boldsymbol{\varepsilon},r,h})_{h\in\mathcal{H}}$ is bounded uniformly in h, (3.62) along with the fact that $\|\mathbf{G}^k_{\mathrm{s},h}\underline{\boldsymbol{u}}_h\|_{L^r(\Omega)^{d\times d}} \le \|\mathbf{G}^k_h\underline{\boldsymbol{u}}_h\|_{L^r(\Omega)^{d\times d}}$ imply that the sequence $(\|\mathbf{G}^k_{\mathrm{s},h}\underline{\boldsymbol{u}}_h\|_{L^r(\Omega)^{d\times d}})_{h\in\mathcal{H}}$ is also bounded uniformly in h. Combined with the Hölder continuity (3.5) of $\boldsymbol{\sigma}$, this result implies that the sequence $(\|\boldsymbol{\sigma}(\cdot,\mathbf{G}^k_{\mathrm{s},h}\underline{\boldsymbol{u}}_h)\|_{L^{r'}(\Omega)^{d\times d}})_{h\in\mathcal{H}}$ is also bounded uniformly in h. Therefore, $(\boldsymbol{\sigma}(\cdot,\mathbf{G}^k_{\mathrm{s},h}\underline{\boldsymbol{u}}_h))_{h\in\mathcal{H}}$ weakly converges to some $\boldsymbol{\sigma}_{\boldsymbol{u}} \in L^{r'}(\Omega,\mathbb{R}^{d\times d}_{\mathrm{s}})$ up to a subsequence. Furthermore, using the discrete momentum equation (3.77a) together with the definition (3.57) of a_h, for all $\boldsymbol{\phi} \in C^\infty_{\mathrm{c}}(\Omega)^d$, letting $\underline{\hat{\boldsymbol{\phi}}}_h := \underline{\boldsymbol{I}}^k_h\boldsymbol{\phi}$, we get

$$\int_\Omega \boldsymbol{\sigma}(\cdot,\mathbf{G}^k_{\mathrm{s},h}\underline{\boldsymbol{u}}_h) : \mathbf{G}^k_{\mathrm{s},h}\underline{\hat{\boldsymbol{\phi}}}_h = \int_\Omega \boldsymbol{f}\cdot\boldsymbol{\pi}^k_h\boldsymbol{\phi} - \mathrm{s}_h(\underline{\boldsymbol{u}}_h,\underline{\hat{\boldsymbol{\phi}}}_h) - \mathrm{c}_h(\underline{\boldsymbol{u}}_h,\underline{\hat{\boldsymbol{\phi}}}_h) - \mathrm{b}_h(\underline{\hat{\boldsymbol{\phi}}}_h, p_h). \quad (3.95)$$

So, since $\mathbf{G}^k_{\mathrm{s},h}\underline{\hat{\boldsymbol{\phi}}}_h \xrightarrow[h\to 0]{} \boldsymbol{\nabla}_{\mathrm{s}}\boldsymbol{\phi}$ strongly in $L^r(\Omega)^{d\times d}$ thanks to (3.46) and $\boldsymbol{\sigma}(\cdot,\mathbf{G}^k_h\underline{\boldsymbol{u}}_h) \xrightarrow[h\to 0]{} \boldsymbol{\sigma}_{\boldsymbol{u}}$ weakly in $L^{r'}(\Omega)^{d\times d}$, passing to the sub-limit equality (3.95) yields

$$\int_\Omega \boldsymbol{\sigma}_{\boldsymbol{u}} : \boldsymbol{\nabla}_{\mathrm{s}}\boldsymbol{\phi} = \int_\Omega \boldsymbol{f}\cdot\boldsymbol{\phi} - c(\boldsymbol{u},\boldsymbol{\phi}) - b(\boldsymbol{\phi},p), \quad (3.96)$$

where we used (3.35) together with the sequential consistencies (3.65) of s_h, (3.54) of c_h, and (3.75) of b_h in the right-hand side. By density, (3.96) is valid for $\boldsymbol{\phi} \in \boldsymbol{U}$. On the other hand, using the definition (3.57) of a_h, the fact that $\mathrm{s}_h(\boldsymbol{u}_h,\boldsymbol{u}_h) \ge 0$, and (3.77) together with the non-dissipativity (3.49) of c_h, we infer

$$\int_\Omega \boldsymbol{\sigma}(\cdot,\mathbf{G}^k_{\mathrm{s},h}\underline{\boldsymbol{u}}_h) : \mathbf{G}^k_{\mathrm{s},h}\underline{\boldsymbol{u}}_h = \mathrm{a}_h(\boldsymbol{u}_h,\boldsymbol{u}_h) - \mathrm{s}_h(\boldsymbol{u}_h,\boldsymbol{u}_h) \le \mathrm{a}_h(\boldsymbol{u}_h,\boldsymbol{u}_h) = \int_\Omega \boldsymbol{f}\cdot\boldsymbol{u}_h. \quad (3.97)$$

Hence, using the Hölder monotonicity (3.6) of $\boldsymbol{\sigma}$ and inequality (3.97) we obtain, for all $\boldsymbol{\Lambda} \in L^r(\Omega,\mathbb{R}^{d\times d}_{\mathrm{s}})$,

$$\begin{aligned} 0 &\le \int_\Omega \Big(\boldsymbol{\sigma}(\cdot,\mathbf{G}^k_{\mathrm{s},h}\underline{\boldsymbol{u}}_h) - \boldsymbol{\sigma}(\cdot,\boldsymbol{\Lambda})\Big) : \Big(\mathbf{G}^k_{\mathrm{s},h}\underline{\boldsymbol{u}}_h - \boldsymbol{\Lambda}\Big) \\ &\le \int_\Omega \boldsymbol{f}\cdot\boldsymbol{u}_h - \int_\Omega \boldsymbol{\sigma}(\cdot,\mathbf{G}^k_{\mathrm{s},h}\underline{\boldsymbol{u}}_h) : \boldsymbol{\Lambda} - \int_\Omega \boldsymbol{\sigma}(\cdot,\boldsymbol{\Lambda}) : \Big(\mathbf{G}^k_{\mathrm{s},h}\underline{\boldsymbol{u}}_h - \boldsymbol{\Lambda}\Big) \\ &\xrightarrow[h\to 0]{} \int_\Omega \boldsymbol{f}\cdot\boldsymbol{u} - \int_\Omega \boldsymbol{\sigma}_{\boldsymbol{u}} : \boldsymbol{\Lambda} - \int_\Omega \boldsymbol{\sigma}(\cdot,\boldsymbol{\Lambda}) : (\boldsymbol{\nabla}_{\mathrm{s}}\boldsymbol{u} - \boldsymbol{\Lambda}), \end{aligned} \quad (3.98)$$

where the limit of the third term is justified by the fact that $\boldsymbol{\sigma}(\cdot,\boldsymbol{\Lambda}) \in L^{r'}(\Omega,\mathbb{R}^{d\times d}_{\mathrm{s}})$ thanks to the Hölder continuity (3.5) of $\boldsymbol{\sigma}$ and the weak convergence of $\mathbf{G}^k_{\mathrm{s},h}\underline{\boldsymbol{u}}_h \xrightarrow[h\to 0]{} \boldsymbol{\nabla}_{\mathrm{s}}\boldsymbol{u}$ in $L^r(\Omega)^{d\times d}$ (consequence of the analogous property for $\mathbf{G}^k_h\underline{\boldsymbol{u}}_h$). It follows from the classical Minty's trick [87, 94] (see [48, Theorem 4.6] concerning its application to HHO methods) that $(\boldsymbol{u}, p)$ satisfies (3.10a). Indeed, taking $\boldsymbol{\Lambda} = \boldsymbol{\nabla}_{\mathrm{s}}\boldsymbol{u} \pm t\boldsymbol{\nabla}_{\mathrm{s}}\boldsymbol{v}$

with $t > 0$ and $\boldsymbol{v} \in \boldsymbol{U}$ into (3.98), and using (3.97) with $\boldsymbol{\phi} = \boldsymbol{u} \pm t\boldsymbol{v}$, we get

$$t \int_\Omega \boldsymbol{\sigma}(\boldsymbol{\nabla}_s \boldsymbol{u} \pm t\boldsymbol{\nabla}_s \boldsymbol{v}, \boldsymbol{\Lambda}) : \boldsymbol{\nabla}_s \boldsymbol{v} = t \int_\Omega \boldsymbol{f} \cdot \boldsymbol{v} + \cancel{c(\boldsymbol{u}, \boldsymbol{u})} - tc(\boldsymbol{u}, \boldsymbol{v}) + \cancel{b(\boldsymbol{u}, p)} - tb(\boldsymbol{v}, p), \quad (3.99)$$

where we have used the fact that $\boldsymbol{u}$ satisfies the mass equation (3.10b) (proved above) and the non-dissipativity property (3.14) of c, respectively, in the cancellations. Dividing (3.99) by t, letting $t \to 0$, and using a dominated convergence argument made possible by the Hölder continuity (3.5) of $\boldsymbol{\sigma}$ gives (3.10a).

Hence, $(\boldsymbol{u}, p) \in \boldsymbol{U} \times P$ is a solution of the weak formulation (3.10).

Step 3. *Strong convergence of the velocity gradient and convergence of the boundary residual seminorm.* Passing to the upper limit inequality (3.97), and using (3.96) with $\boldsymbol{\phi}$ replaced by $\boldsymbol{u}$ together with the mass equation (3.10b) and the non-dissipativity property (3.14) of c to cancel the two rightmost terms in the resulting equation, we obtain

$$\limsup_{h\to 0} \int_\Omega \boldsymbol{\sigma}(\cdot, \mathbf{G}^k_{s,h}\underline{\boldsymbol{u}}_h) : \mathbf{G}^k_{s,h}\underline{\boldsymbol{u}}_h \le \int_\Omega \boldsymbol{f} \cdot \boldsymbol{u} = \int_\Omega \boldsymbol{\sigma}_{\boldsymbol{u}} : \boldsymbol{\nabla}_s \boldsymbol{u}. \quad (3.100)$$

Thus, the Hölder monotonicity (3.6) of $\boldsymbol{\sigma}$ together with the $(r, \frac{r}{r+2-\tilde{r}}, \frac{r+2-\tilde{r}}{2-\tilde{r}})$-Hölder inequality (3.20) yields,

$$\begin{aligned} &\limsup_{h\to 0} \left(\sigma_{\mathrm{hm}} \|\mathbf{G}^k_{s,h}\underline{\boldsymbol{u}}_h - \boldsymbol{\nabla}_s \boldsymbol{u}\|^{r+2-\tilde{r}}_{L^r(\Omega)^{d\times d}} \left(\delta^r + \|\underline{\boldsymbol{u}}_h\|^r_{\boldsymbol{\varepsilon},r,h} + \|\boldsymbol{\nabla}_s \boldsymbol{u}\|^r_{L^r(\Omega)^{d\times d}} \right)^{\frac{\tilde{r}-2}{r}} \right) \\ &\lesssim \limsup_{h\to 0} \int_\Omega (\boldsymbol{\sigma}(\cdot, \mathbf{G}^k_{s,h}\underline{\boldsymbol{u}}_h) - \boldsymbol{\sigma}(\cdot, \boldsymbol{\nabla}_s \boldsymbol{u})) : (\mathbf{G}^k_{s,h}\underline{\boldsymbol{u}}_h - \boldsymbol{\nabla}_s \boldsymbol{u}) \\ &\le 0, \end{aligned} \quad (3.101)$$

where we concluded by strategically separating the terms in order to use inequality (3.100) along with the weak convergences of $\boldsymbol{\sigma}(\cdot, \mathbf{G}^k_{s,h}\underline{\boldsymbol{u}}_h) \xrightarrow[h\to 0]{} \boldsymbol{\sigma}_{\boldsymbol{u}}$ in $L^{r'}(\Omega)^{d\times d}$ and $\mathbf{G}^k_{s,h}\underline{\boldsymbol{u}}_h \xrightarrow[h\to 0]{} \boldsymbol{\nabla}_s \boldsymbol{u}$ in $L^r(\Omega)^{d\times d}$. Hence, since $(\|\underline{\boldsymbol{u}}_h\|_{\boldsymbol{\varepsilon},r,h})_{h\in\mathcal{H}}$ is bounded uniformly in h, $\mathbf{G}^k_{s,h}\underline{\boldsymbol{u}}_h \xrightarrow[h\to 0]{} \boldsymbol{\nabla}_s \boldsymbol{u}$ strongly in $L^r(\Omega)^{d\times d}$ up to a subsequence. Now, using the Hölder continuity (3.5) of $\boldsymbol{\sigma}$ together with the $(r'; \frac{r}{r-\tilde{r}}, \frac{r}{\tilde{r}-1})$-Hölder inequality, we get

$$\begin{aligned} &\|\boldsymbol{\sigma}(\cdot, \mathbf{G}^k_{s,h}\underline{\boldsymbol{u}}_h) - \boldsymbol{\sigma}(\cdot, \boldsymbol{\nabla}_s \boldsymbol{u})\|_{L^{r'}(\Omega)^{d\times d}} \\ &\lesssim \sigma_{\mathrm{hc}} \left(\delta^r + \|\mathbf{G}^k_{s,h}\underline{\boldsymbol{u}}_h\|^r_{L^r(\Omega)^{d\times d}} + \|\boldsymbol{\nabla}_s \boldsymbol{u}\|^r_{L^r(\Omega)^{d\times d}} \right)^{\frac{r-\tilde{r}}{r}} \|\mathbf{G}^k_{s,h}\underline{\boldsymbol{u}}_h - \boldsymbol{\nabla}_s \boldsymbol{u}\|^{\tilde{r}-1}_{L^r(\Omega)^{d\times d}} \\ &\xrightarrow[h\to 0]{} 0. \end{aligned}$$

Thus, $\boldsymbol{\sigma}(\cdot,\mathbf{G}_{\mathrm{s},h}^k\underline{\boldsymbol{u}}_h)\xrightarrow[h\to 0]{}\boldsymbol{\sigma}(\cdot,\boldsymbol{\nabla}_{\mathrm{s}}\boldsymbol{u})$ strongly in $L^{r'}(\Omega)^{d\times d}$ up to a subsequence. In particular, we have

$$\sigma_{\mathrm{hm}}\left(\delta^r+|\underline{\boldsymbol{u}}_h|_{r,h}^r\right)^{\frac{\tilde r-2}{r}}|\underline{\boldsymbol{u}}_h|_{r,h}^{r+2-\tilde r}\lesssim \mathrm{s}_h(\underline{\boldsymbol{u}}_h,\underline{\boldsymbol{u}}_h)$$
$$=\int_\Omega \boldsymbol{f}\cdot\boldsymbol{u}_h-\int_\Omega\boldsymbol{\sigma}(\cdot,\mathbf{G}_{\mathrm{s},h}^k\underline{\boldsymbol{u}}_h):\mathbf{G}_{\mathrm{s},h}^k\underline{\boldsymbol{u}}_h\xrightarrow[h\to 0]{}0,\quad(3.102)$$

thanks to the Hölder monotonicity (3.64) of s_h and the definition (3.57) of a_h. Hence, $|\underline{\boldsymbol{u}}_h|_{r,h}\xrightarrow[h\to 0]{}0$.

Step 4. *Strong convergence of the pressure.* Set $p_{h,\Omega}\coloneqq\int_\Omega|p_h|^{r'-2}p_h$. Reasoning as in [27, Eq. (50)], we infer the existence of $\boldsymbol{v}_{p_h}\in W_0^{1,r}(\Omega)^d$ such that

$$\boldsymbol{\nabla}\cdot\boldsymbol{v}_{p_h}=|p_h|^{r'-2}p_h-p_{h,\Omega}\quad\text{and}\quad\|\boldsymbol{v}_{p_h}\|_{W^{1,r}(\Omega)^d}\lesssim\|p_h\|_{L^{r'}(\Omega)}^{r'-1}.\quad(3.103)$$

Furthermore, letting $\underline{\hat{\boldsymbol{v}}}_{p_h}\coloneqq\underline{\boldsymbol{I}}_h^k\boldsymbol{v}_{p_h}$, and using the boundedness (3.40) of $\underline{\boldsymbol{I}}_h^k$ together with (3.39), we get

$$\|\underline{\hat{\boldsymbol{v}}}_{p_h}\|_{\boldsymbol{\varepsilon},r,h}\lesssim|\boldsymbol{v}_{p_h}|_{W^{1,r}(\Omega)^d}\lesssim\|p_h\|_{L^{r'}(\Omega)}^{r'-1}.$$

Since $(\|p_h\|_{L^{r'}(\Omega)})_{h\in\mathcal{H}}$ is bounded uniformly in h, by [50, Theorem 9.29] there exists $\boldsymbol{v}_p\in\boldsymbol{U}$ such that $\hat{\boldsymbol{v}}_{p_h}\xrightarrow[h\to 0]{}\boldsymbol{v}_p$ strongly in $L^{[1,r^*)}(\Omega)^d$ and $\mathbf{G}_h^k\underline{\hat{\boldsymbol{v}}}_{p_h}\xrightarrow[h\to 0]{}\boldsymbol{\nabla}\boldsymbol{v}_p$ weakly in $L^r(\Omega)^{d\times d}$. Therefore, recalling that $\boldsymbol{\sigma}(\cdot,\mathbf{G}_{\mathrm{s},h}^k\underline{\boldsymbol{u}}_h)\xrightarrow[h\to 0]{}\boldsymbol{\sigma}(\cdot,\boldsymbol{\nabla}_{\mathrm{s}}\boldsymbol{u})$ strongly in $L^{r'}(\Omega)^{d\times d}$, we get

$$\int_\Omega\boldsymbol{\sigma}(\cdot,\mathbf{G}_{\mathrm{s},h}^k\underline{\boldsymbol{u}}_h):\mathbf{G}_{\mathrm{s},h}^k\underline{\hat{\boldsymbol{v}}}_{p_h}\xrightarrow[h\to 0]{}\int_\Omega\boldsymbol{\sigma}(\cdot,\boldsymbol{\nabla}_{\mathrm{s}}\boldsymbol{u}):\boldsymbol{\nabla}_{\mathrm{s}}\boldsymbol{v}_p.\quad(3.104)$$

Using the Hölder continuity (3.63) of s_h with $\underline{\boldsymbol{w}}_h=\underline{\mathbf{0}}$, we next infer

$$|\mathrm{s}_h(\underline{\boldsymbol{u}}_h,\underline{\hat{\boldsymbol{v}}}_{p_h})|\lesssim\sigma_{\mathrm{hc}}\left(\delta^r+|\underline{\boldsymbol{u}}_h|_{r,h}^r\right)^{\frac{r-\tilde r}{r}}|\underline{\boldsymbol{u}}_h|_{r,h}^{\tilde r-1}|\underline{\hat{\boldsymbol{v}}}_{p_h}|_{r,h}\xrightarrow[h\to 0]{}0,\quad(3.105)$$

since $|\underline{\boldsymbol{u}}_h|_{r,h}\xrightarrow[h\to 0]{}0$ by (3.102) and noticing that the sequence $(|\underline{\hat{\boldsymbol{v}}}_{p_h}|_{r,h})_{h\in\mathcal{H}}$ is bounded uniformly in h by (3.62). Thus, recalling the definition (3.57) of a_h, (3.104) and (3.105) yields

$$\mathrm{a}_h(\underline{\boldsymbol{u}}_h,\underline{\hat{\boldsymbol{v}}}_{p_h})\xrightarrow[h\to 0]{}a(\boldsymbol{u},\boldsymbol{v}_p).\quad(3.106)$$

Furthermore, replacing $\boldsymbol{\phi}$ by $\boldsymbol{v}_{p_h}$ in the reasoning that gives (3.93)–(3.94) after recalling that $\mathbf{G}_h^k\underline{\hat{\boldsymbol{v}}}_{p_h}\xrightarrow[h\to 0]{}\boldsymbol{\nabla}\boldsymbol{v}_p$ weakly in $L^r(\Omega)^{d\times d}$ and that $\hat{\boldsymbol{v}}_{p_h}\xrightarrow[h\to 0]{}\boldsymbol{v}_p$ strongly in $L^{sr'}(\Omega)^d$ (since $sr'<r^*$ by (3.80)), we infer

$$\mathrm{c}_h(\underline{\boldsymbol{u}}_h,\underline{\hat{\boldsymbol{v}}}_{p_h})\xrightarrow[h\to 0]{}c(\boldsymbol{u},\boldsymbol{v}_p).\quad(3.107)$$

Moreover, since $\boldsymbol{f} \in L^{r'}(\Omega)^d$ and $\hat{\boldsymbol{v}}_{p_h} \xrightarrow[h\to 0]{} \boldsymbol{v}_p$ strongly in $L^r(\Omega)^d$, we get

$$\int_\Omega \boldsymbol{f}\cdot\hat{\boldsymbol{v}}_{p_h} \xrightarrow[h\to 0]{} \int_\Omega \boldsymbol{f}\cdot\boldsymbol{v}_p. \tag{3.108}$$

Hence, using the fact that p_h has zero mean value over Ω together with the equality in (3.103), the definition (3.11) of b, the Fortin property (3.73) of b_h, and equality (3.77a) yields

$$\begin{aligned}\int_\Omega (|p_h|^{r'-2}p_h)p_h &= \int_\Omega (\boldsymbol{\nabla}\cdot\boldsymbol{v}_{p_h})p_h = -b(\boldsymbol{v}_{p_h},p_h) = -\mathrm{b}_h(\underline{\hat{\boldsymbol{v}}}_{p_h},p_h)\\ &= \mathrm{a}_h(\underline{\boldsymbol{u}}_h,\underline{\hat{\boldsymbol{v}}}_{p_h}) + \mathrm{c}_h(\underline{\boldsymbol{u}}_h,\underline{\hat{\boldsymbol{v}}}_{p_h}) - \int_\Omega \boldsymbol{f}\cdot\hat{\boldsymbol{v}}_{p_h}\\ &\xrightarrow[h\to 0]{} a(\boldsymbol{u},\boldsymbol{v}_p) + c(\boldsymbol{u},\boldsymbol{v}_p) - \int_\Omega \boldsymbol{f}\cdot\boldsymbol{v}_p\\ &= -b(\boldsymbol{v}_p,p) = \int_\Omega (\boldsymbol{\nabla}\cdot\boldsymbol{v}_p)p,\end{aligned} \tag{3.109}$$

where we have used the discrete momentum equation (3.77a) in the second line, applied the limits (3.106), (3.107), and (3.108) in the third line, used the continuous momentum equation (3.10a) to pass to the fourth line, and invoked the mass equation (3.77b) to conclude. Meanwhile, since $(\||p_h|^{r'-2}p_h\|_{L^r(\Omega)})_{h\in\mathcal{H}} = (\|p_h\|_{L^{r'}(\Omega)})_{h\in\mathcal{H}}$ is bounded uniformly in h, $|p_h|^{r'-2}p_h$ weakly converges to $p_r \in L^r(\Omega)$ up to a subsequence. In particular, $p_{h,\Omega} \xrightarrow[h\to 0]{} p_{r,\Omega} \coloneqq \int_\Omega p_r$, and we deduce that $\boldsymbol{\nabla}\cdot\boldsymbol{v}_{p_h} \xrightarrow[h\to 0]{} p_r - p_{r,\Omega}$ weakly in $L^r(\Omega)$ and, by uniqueness of the limit in the distributional sense, that $\boldsymbol{\nabla}\cdot\boldsymbol{v}_p = p_r - p_{r,\Omega}$. Therefore, using (3.109) together with the fact that p has zero mean value over Ω, we infer

$$\int_\Omega (|p_h|^{r'-2}p_h)p_h \xrightarrow[h\to 0]{} \int_\Omega p_r p. \tag{3.110}$$

Moreover, using the Hölder monotonicity property (3.23b) (with $(n,x,y,s) = (1,p_h,p,r')$) together with the $(r', \frac{r'}{r'+2-\widetilde{r'}}, \frac{r'+2-\widetilde{r'}}{2-\widetilde{r'}})$-Hölder inequality, and passing to the limit with (3.110), we obtain

$$\begin{aligned}&\|p_h - p\|_{L^r(\Omega)}^{r'+2-\widetilde{r'}} \left(\|p_h\|_{L^{r'}(\Omega)}^{r'} + \|p\|_{L^{r'}(\Omega)}^{r'}\right)^{\frac{\widetilde{r'}-2}{r'}}\\ &\qquad\lesssim \int_\Omega (|p_h|^{r'-2}p_h - |p|^{r'-2}p)(p_h - p) \xrightarrow[h\to 0]{} 0.\end{aligned} \tag{3.111}$$

Hence, $p_h \xrightarrow[h\to 0]{} p$ strongly in $L^r(\Omega)$ up to a subsequence. □

3.6.3 Error estimate

Proof of Theorem 78. Let $(\underline{\boldsymbol{e}}_h, \epsilon_h) \coloneqq (\underline{\boldsymbol{u}}_h - \underline{\hat{\boldsymbol{u}}}_h, p_h - \hat{p}_h) \in \underline{\boldsymbol{U}}_{h,0}^k \times P_h^k$ where $\underline{\hat{\boldsymbol{u}}}_h \coloneqq \underline{\boldsymbol{I}}_h^k \boldsymbol{u}$ and $\hat{p}_h \coloneqq \pi_h^k p$.

Step 1. *Consistency error.* Let $\mathcal{E}_h : \underline{\boldsymbol{U}}_{h,0}^k \to \mathbb{R}$ be the consistency error linear form such that, for all $\underline{\boldsymbol{v}}_h \in \underline{\boldsymbol{U}}_{h,0}^k$,

$$\mathcal{E}_h(\underline{\boldsymbol{v}}_h) \coloneqq \int_\Omega \boldsymbol{f} \cdot \boldsymbol{v}_h - \mathrm{a}_h(\underline{\hat{\boldsymbol{u}}}_h, \underline{\boldsymbol{v}}_h) - \mathrm{c}_h(\underline{\hat{\boldsymbol{u}}}_h, \underline{\boldsymbol{v}}_h) - \mathrm{b}_h(\underline{\boldsymbol{v}}_h, \hat{p}_h). \tag{3.112}$$

Using in (3.112) the fact that $\boldsymbol{f} = -\boldsymbol{\nabla}\cdot\boldsymbol{\sigma}(\cdot, \boldsymbol{\nabla}_{\mathrm{s}}\boldsymbol{u}) + (\boldsymbol{u}\cdot\boldsymbol{\nabla})\boldsymbol{\chi}(\cdot, \boldsymbol{u}) + \boldsymbol{\nabla} p$ almost everywhere in Ω together with the consistency properties (3.69) of a_h, (3.74) of b_h, and (3.52) of c_h (since $s \le \frac{r^*}{r'}$), we obtain

$$\$ \coloneqq \sup_{\underline{\boldsymbol{v}}_h \in \underline{\boldsymbol{U}}_{h,0}^k, \|\underline{\boldsymbol{v}}_h\|_{\boldsymbol{\varepsilon},r,h}=1} \mathcal{E}_h(\underline{\boldsymbol{v}}_h) \lesssim h^{(k+1)(r-1)} \min\left(\zeta_h(\boldsymbol{u}); 1\right)^{2-r} \mathcal{N}_2 + h^{k+1}\mathcal{N}_3. \tag{3.113}$$

Step 2. *Error estimate for the velocity.* Replacing a_h by $\mathrm{a}_h + \mathrm{c}_h$ in the reasoning of [27, Eq. (70)] yields,

$$\begin{aligned}
\mathcal{E}_h(\underline{\boldsymbol{e}}_h) &= \mathrm{a}_h(\underline{\boldsymbol{u}}_h, \underline{\boldsymbol{e}}_h) - \mathrm{a}_h(\underline{\hat{\boldsymbol{u}}}_h, \underline{\boldsymbol{e}}_h) + \mathrm{c}_h(\underline{\boldsymbol{u}}_h, \underline{\boldsymbol{e}}_h) - \mathrm{c}_h(\underline{\hat{\boldsymbol{u}}}_h, \underline{\boldsymbol{e}}_h) \\
&\ge \left(C_{\mathrm{da}}\sigma_{\mathrm{hm}} - C_{\mathrm{dc},r}\chi_{\mathrm{hc}}\left(\delta^r + \|\underline{\boldsymbol{u}}_h\|_{\boldsymbol{\varepsilon},r,h}^r + \|\underline{\hat{\boldsymbol{u}}}_h\|_{\boldsymbol{\varepsilon},r,h}^r\right)^{\frac{s+1-r}{r}}\right) \\
&\qquad \times \left(\delta^r + \|\underline{\boldsymbol{u}}_h\|_{\boldsymbol{\varepsilon},r,h}^r + \|\underline{\hat{\boldsymbol{u}}}_h\|_{\boldsymbol{\varepsilon},r,h}^r\right)^{\frac{r-2}{r}} \|\underline{\boldsymbol{e}}_h\|_{\boldsymbol{\varepsilon},r,h}^2 \\
&\gtrsim \left(C_{\mathrm{da}}\sigma_{\mathrm{hm}} - C_{\mathrm{dc},r}\chi_{\mathrm{hc}}\mathcal{N}_1^{\frac{s+1-r}{r}}\right)\mathcal{N}_1^{\frac{r-2}{r}} \|\underline{\boldsymbol{e}}_h\|_{\boldsymbol{\varepsilon},r,h}^2 \\
&\gtrsim \sigma_{\mathrm{hm}}\mathcal{N}_1^{\frac{r-2}{r}} \|\underline{\boldsymbol{e}}_h\|_{\boldsymbol{\varepsilon},r,h}^2,
\end{aligned} \tag{3.114}$$

where, noting that $\tilde{r} = r$ and $\tilde{s} = 2$ since $r \le 2 \le s$, we have used the Hölder monotonicity (3.68) of a_h together with the Hölder continuity (3.50) of c_h (since $s \le \frac{r^*}{r'}$) in the second line, the a priori bound (3.78a) on the discrete solution along with the boundedness (3.40) of the global interpolator and the a priori bound (3.16) on the continuous solution in the penultimate line, and the small data assumption (3.82) to conclude. Hence, the fact that $\mathcal{E}_h(\underline{\boldsymbol{e}}_h) \le \$\|\underline{\boldsymbol{e}}_h\|_{\boldsymbol{\varepsilon},r,h}$ together with (3.113) yields (3.83a).

Step 3. *Error estimate for the pressure.* Using the Hölder continuity (3.50) of c_h together with the same raisoning giving the penultimate line of (3.114) we infer, for all $\underline{\boldsymbol{v}}_h \in \underline{\boldsymbol{U}}_{h,0}^k$,

$$\left|\mathrm{c}_h(\underline{\hat{\boldsymbol{u}}}_h, \underline{\boldsymbol{v}}_h) - \mathrm{c}_h(\underline{\boldsymbol{u}}_h, \underline{\boldsymbol{v}}_h)\right| \lesssim \chi_{\mathrm{hc}}\mathcal{N}_1^{\frac{s-1}{r}} \|\underline{\boldsymbol{e}}_h\|_{\boldsymbol{\varepsilon},r,h}\|\underline{\boldsymbol{v}}_h\|_{\boldsymbol{\varepsilon},r,h}. \tag{3.115}$$

Thus, replacing a_h with $a_h + c_h$ in the reasoning of [27, Eq. (72)], we obtain

$$\begin{aligned}\|\epsilon_h\|_{L^{r'}(\Omega)} &\lesssim \sup_{\underline{\boldsymbol{v}}_h \in \underline{\boldsymbol{U}}_{h,0}^k, \|\underline{\boldsymbol{v}}_h\|_{\boldsymbol{\varepsilon},r,h}=1} \big(\mathcal{E}_h(\underline{\boldsymbol{v}}_h) + a_h(\hat{\underline{\boldsymbol{u}}}_h, \underline{\boldsymbol{v}}_h) - a_h(\underline{\boldsymbol{u}}_h, \underline{\boldsymbol{v}}_h) \\ &\qquad + c_h(\hat{\underline{\boldsymbol{u}}}_h, \underline{\boldsymbol{v}}_h) - c_h(\underline{\boldsymbol{u}}_h, \underline{\boldsymbol{v}}_h)\big) \\ &\lesssim \$ + \sigma_{\mathrm{hc}} \|\underline{\boldsymbol{e}}_h\|_{\boldsymbol{\varepsilon},r,h}^{r-1} + \chi_{\mathrm{hc}} \mathcal{N}_1^{\frac{s-1}{r}} \|\underline{\boldsymbol{e}}_h\|_{\boldsymbol{\varepsilon},r,h},\end{aligned} \tag{3.116}$$

where we have used the Hölder continuity (3.67) of a_h together with (3.115) to conclude. Finally, the bounds (3.113) and (3.83a) (proved in Step 2) give (3.83b). □

List of Figures

List of Tables

Bibliography

[1] J. Aghili, S. Boyaval, and D. A. Di Pietro. "Hybridization of mixed high-order methods on general meshes and application to the Stokes equations". In: *Comput. Meth. Appl. Math.* 15.2 (2015), pp. 111–134. DOI: 10.1515/cmam-2015-0004.

[2] J. Aghili and D. A. Di Pietro. "An advection-robust Hybrid High-Order method for the Oseen problem". In: *J. Sci. Comput.* 77.3 (2018), pp. 1310–1338. DOI: 10.1007/s10915-018-0681-2.

[3] J. Aghili, D. A. Di Pietro, and B. Ruffini. "An hp-Hybrid High-Order method for variable diffusion on general meshes". In: *Comput. Meth. Appl. Math.* 17.3 (2017), pp. 359–376. DOI: 10.1515/cmam-2017-0009.

[4] J. Ahlkrona and D. Elfverson. "A cut finite element method for non-Newtonian free surface flows in 2D - application to glacier modelling". In: *Journal of Computational Physics: X* 11 (2021), p. 100090. ISSN: 2590-0552. DOI: 10.1016/j.jcpx.2021.100090.

[5] M. Amara, E. Vera, and D. Trujillo. "Vorticity–velocity–pressure formulation for Stokes problem". In: *Math. Comput.* 73 (Oct. 2004), pp. 1673–1697. DOI: 10.1090/S0025-5718-03-01615-6.

[6] P. F. Antonietti, N. Bigoni, and M. Verani. "Mimetic finite difference approximation of quasilinear elliptic problems". In: *Calcolo* 52 (1 2014), pp. 45–67. DOI: 10.1007/s10092-014-0107-y.

[7] E. Armelin, M. Martí, E. Rudé, J. Labanda, J. Llorens, and C. Alemán. "A simple model to describe the thixotropic behavior of paints". In: *Progress in Organic Coatings - PROG ORG COATING* 57 (Nov. 2006), pp. 229–235. DOI: 10.1016/j.porgcoat.2006.09.002.

[8] S. Azoug, H. Bakhti, L. Azrar, and T. Ali Ziane. "Stability and convergence analysis of a semi-implicit fractional FEM-scheme for non-Newtonian fluid flows of polymer aqueous solutions with fractional time-derivative". In: *Computational and Applied Mathematics* 39 (Feb. 2020), p. 84. DOI: 10.1007/s40314-020-1110-3.

[9] J. W. Barrett and W. B. Liu. "Quasi-norm error bounds for the finite element approximation of a non-Newtonian flow". In: *Numer. Math.* 68.4 (1994), pp. 437–456. DOI: 10.1007/s002110050071.

[10] John W. Barrett and W. B. Liu. "Finite element approximation of the p-Laplacian". In: *Math. Comp.* 61.204 (1993), pp. 523–537. ISSN: 0025-5718. DOI: 10.2307/2153239.

[11] F. Bassi, L. Botti, and A. Colombo. "Agglomeration-based physical frame dG discretizations: an attempt to be mesh free". In: *Math. Models Methods Appl. Sci.* 24.8 (2014), pp. 1495–1539. DOI: 10.1142/S0218202514400028.

[12] F. Bassi, L. Botti, A. Colombo, D. A. Di Pietro, and P. Tesini. "On the flexibility of agglomeration based physical space discontinuous Galerkin discretizations". In: *J. Comput. Phys.* 231.1 (2012), pp. 45–65. DOI: 10.1016/j.jcp.2011.08.018.

[13] H. Beirão da Veiga. "On the global regularity of shear thinning flows in smooth domains". In: *J. Math. Anal. Appl.* 349.2 (2009), pp. 335–360. DOI: 10.1016/j.jmaa.2008.09.009.

[14] L. Beirão da Veiga, C. Lovadina, and G. Vacca. "Divergence free Virtual Elements for the Stokes problem on polygonal meshes". In: *ESAIM: Math. Model. Numer. Anal. (M2AN)* 51.2 (2017), pp. 509–535. DOI: 10.1051/m2an/2016032.

[15] L. Beirão da Veiga, C. Lovadina, and G. Vacca. "Virtual Elements for the Navier–Stokes Problem on Polygonal Meshes". In: *SIAM J. Numer. Anal.* 56.3 (2018), pp. 1210–1242. DOI: 10.1137/17M1132811.

[16] L. Belenki, L. C. Berselli, L. Diening, and M. Růžička. "On the finite element approximation of p-Stokes systems". In: *SIAM J. Numer. Anal.* 50.2 (2012), pp. 373–397. DOI: 10.1137/10080436X.

[17] L. Belenki, L. Diening, and C. Kreuzer. "Optimality of an adaptive finite element method for the p-Laplacian equation". In: *IMA Journal of Numerical Analysis* 32.2 (2012), pp. 484–510.

[18] L. C. Berselli and M. Růžička. "Global regularity for systems with p-structure depending on the symmetric gradient". In: *Adv. Nonlinear Anal.* 9.1 (2020), pp. 176–192. DOI: 10.1515/anona-2018-0090.

[19] R. B. Bird, R. C. Armstrong, and O. Hassager. *Dynamics of Polymeric Liquids*. 2nd ed. Vol. 1. John Wiley, New York, 1987, p. 672. ISBN: 978-0-471-80245-7.

[20] D. Boffi, M. Botti, and D. A. Di Pietro. "A nonconforming high-order method for the Biot problem on general meshes". In: *SIAM J. Sci. Comput.* 38.3 (2016), A1508–A1537. DOI: 10.1137/15M1025505.

[21] D. Boffi, F. Brezzi, and M. Fortin. *Mixed finite element methods and applications*. Vol. 44. Springer Series in Computational Mathematics. Springer, Heidelberg, 2013, pp. xiv+685. DOI: 10.1007/978-3-642-36519-5.

[22] M. Bogovskiĭ. "Solution of the first boundary value problem for an equation of continuity of an incompressible medium". In: *Dokl. Akad. Nauk SSSR* 248.5 (1979), pp. 1037–1040.

[23] L. Botti and D. A. Di Pietro. "p-Multilevel preconditioners for HHO discretizations of the Stokes equations with static condensation". In: *Commun. Appl. Math. Comput.* (2021). To appear. DOI: 10.1007/s42967-021-00142-5.

[24] L. Botti and D. A. Di Pietro. "Assessment of Hybrid High-Order methods on curved meshes and comparison with discontinuous Galerkin methods". In: *J. Comput. Phys.* 370 (2018), pp. 58–84. DOI: 10.1016/j.jcp.2018.05.017.

[25] L. Botti, D. A. Di Pietro, and J. Droniou. "A Hybrid High-Order discretisation of the Brinkman problem robust in the Darcy and Stokes limits". In: *Comput. Meth. Appl. Mech. Engrg.* 341 (2018), pp. 278–310. DOI: 10.1016/j.cma.2018.07.004.

[26] L. Botti, D. A. Di Pietro, and J. Droniou. "A Hybrid High-Order discretisation of the Brinkman problem robust in the Darcy and Stokes limits". In: *Comput. Methods Appl. Mech. Engrg.* 341 (2018), pp. 278–310. DOI: 10.1016/j.cma.2018.07.004.

[27] M. Botti, D. Castanon Quiroz, D. A. Di Pietro, and A. Harnist. "A Hybrid High-Order method for creeping flows of non-Newtonian fluids". In: *ESAIM: Math. Model. Numer. Anal.* 55.5 (2021), pp. 2045–2073. DOI: 10.1051/m2an/2021051.

[28] M. Botti, D. A. Di Pietro, and A. Guglielmana. "A low-order nonconforming method for linear elasticity on general meshes". In: *Comput. Meth. Appl. Mech. Engrg.* 354 (2019), pp. 96–118. DOI: 10.1016/j.cma.2019.05.031.

[29] M. Botti, D. A. Di Pietro, and P. Sochala. "A Hybrid High-Order discretisation method for nonlinear poroelasticity". In: *Comput. Meth. Appl. Math.* 20.2 (2020), pp. 227–249. DOI: 10.1515/cmam-2018-0142.

[30] M. Botti, D. A. Di Pietro, and P. Sochala. "A hybrid high-order method for nonlinear elasticity". In: *SIAM J. Numer. Anal.* 55.6 (2017), pp. 2687–2717. DOI: 10.1137/16M1105943.

[31] E. Burman, M. Cicuttin, G. Delay, and A. Ern. "An unfitted Hybrid High-Order method with cell agglomeration for elliptic interface problems". In: *SIAM Journal on Scientific Computing* (2021). DOI: 10.1137/19M1285901.

[32] V. Calo, M. Cicuttin, Q. Deng, and A. Ern. "Spectral approximation of elliptic operators by the Hybrid High-Order method". In: *Mathematics of Computation* 88.318 (2019), pp. 1559–1586. DOI: 10.1090/mcom/3405.

[33] C. Carstensen and N. T. Tran. *Unstabilized Hybrid High-Order method for a class of degenerate convex minimization problems*. 2020. arXiv: 2011.15059 [math.NA].

[34] D. Castanon Quiroz and D. A. Di Pietro. "A Hybrid High-Order method for the incompressible Navier–Stokes problem robust for large irrotational body forces". In: *Comput. Math. Appl.* 79.8 (2020), pp. 2655–2677. DOI: 10.1016/j.camwa.2019.12.005.

[35] D. Castanon Quiroz, D. A. Di Pietro, and A. Harnist. "A Hybrid High-Order method for incompressible flows of non-Newtonian fluids with power-like convective behaviour". In: *IMA Journal of Numerical Analysis* (Dec. 2021). Published online. DOI: 10.1093/imanum/drab087.

[36] M. Čermák, F. Hecht, Z. Tang, and M. Vohralík. "Adaptive inexact iterative algorithms based on polynomial-degree-robust a posteriori estimates for the Stokes problem". In: *Numerische Mathematik* 138.4 (Feb. 2018), pp. 1027–1065. DOI: 10.1007/s00211-017-0925-3.

[37] F. Chave, D. A. Di Pietro, and L. Formaggia. "A Hybrid High-Order method for Darcy flows in fractured porous media". In: *SIAM J. Sci. Comput.* 40.2 (2018), A1063–A1094. DOI: 10.1137/17M1119500.

[38] F. Chave, D. A. Di Pietro, and L. Formaggia. "A Hybrid High-Order method for passive transport in fractured porous media". In: *Int. J. Geomath.* 10.12 (2019). DOI: 10.1007/s13137-019-0114-x.

[39] F. Chave, D. A. Di Pietro, and S. Lemaire. *A discrete Weber inequality on three-dimensional hybrid spaces with application to the HHO approximation of magnetostatics*. Submitted. July 2020. URL: https://hal.archives-ouvertes.fr/hal-02892526.

[40] F. Chave, D. A. Di Pietro, and S. Lemaire. "A three-dimensional Hybrid High-Order method for magnetostatics". In: *Finite Volumes for Complex Applications IX – Methods, Theoretical Aspects, Examples*. Ed. by R. Klöfkorn, E. Keilegavlen, F. A. Radu, and J. Fuhrmann. 2020, pp. 255–263. DOI: 10.1007/978-3-030-43651-3_22.

[41] F. Chave, D. A. Di Pietro, and F. Marche. "A Hybrid High-Order method for the convective Cahn–Hilliard problem in mixed form". In: *Finite Volumes for Complex Applications VIII – Hyperbolic, Elliptic and Parabolic Problems*. Ed. by C. Cancès and P. Omnes. 2017, pp. 517–526. DOI: 10.1007/978-3-319-57397-7.

[42] F. Chave, D. A. Di Pietro, F. Marche, and F. Pigeonneau. "A Hybrid High-Order method for the Cahn–Hilliard problem in mixed form". In: *SIAM J. Numer. Anal.* 54.3 (2016), pp. 1873–1898. DOI: 10.1137/15M1041055.

[43] M. Cicuttin, A. Ern, and S. Lemaire. "A Hybrid High-Order Method for Highly Oscillatory Elliptic Problems". In: *Computational Methods in Applied Mathematics* 19.4 (2019), pp. 723–748. DOI: doi:10.1515/cmam-2018-0013.

[44] M. J. Crochet, A. R. Davies, and K. Walters. *Numerical simulation of non-Newtonian flow*. Elsevier, 2012.

[45] M. J. Crochet and K. Walters. "Numerical methods in non-Newtonian fluid mechanics". In: *Annual Review of Fluid Mechanics* 15.1 (1983), pp. 241–260.

[46] K. Deimling. *Nonlinear functional analysis*. Springer-Verlag, Berlin, 1985, pp. xiv+450. ISBN: 3-540-13928-1. DOI: 10.1007/978-3-662-00547-7.

[47] D. A. Di Pietro and J. Droniou. "$W^{s,p}$-approximation properties of elliptic projectors on polynomial spaces, with application to the error analysis of a hybrid high-order discretisation of Leray-Lions problems". In: *Math. Models Methods Appl. Sci.* 27.5 (2017), pp. 879–908. DOI: 10.1142/S0218202517500191.

[48] D. A. Di Pietro and J. Droniou. "A Hybrid High-Order method for Leray-Lions elliptic equations on general meshes". In: *Math. Comp.* 86.307 (2017), pp. 2159–2191. DOI: 10.1090/mcom/3180.

[49] D. A. Di Pietro and J. Droniou. *An arbitrary-order discrete de Rham complex on polyhedral meshes: Exactness, Poincaré inequalities, and consistency*. submitted. Jan. 2021.

[50] D. A. Di Pietro and J. Droniou. *The Hybrid High-Order method for polytopal meshes. Design, analysis, and applications*. Modeling, Simulation and Application 19. Springer International Publishing, 2020. ISBN: 978-3-030-37202-6 (Hardcover) 978-3-030-37203-3 (eBook). DOI: 10.1007/978-3-030-37203-3.

[51] D. A. Di Pietro, J. Droniou, and A. Ern. "A discontinuous-skeletal method for advection-diffusion-reaction on general meshes". In: *SIAM J. Numer. Anal.* 53.5 (2015), pp. 2135–2157. DOI: 10.1137/140993971.

[52] D. A. Di Pietro, J. Droniou, and A. Harnist. "Improved error estimates for Hybrid High-Order discretizations of Leray–Lions problems". In: *Calcolo* 58.19 (2021). DOI: 10.1007/s10092-021-00410-z.

[53] D. A. Di Pietro, J. Droniou, and G. Manzini. "Discontinuous Skeletal Gradient Discretisation methods on polytopal meshes". In: *J. Comput. Phys.* 355 (2018), pp. 397–425. DOI: 10.1016/j.jcp.2017.11.018.

[54] D. A. Di Pietro, J. Droniou, and F. Rapetti. "Fully discrete polynomial de Rham sequences of arbitrary degree on polygons and polyhedra". In: *Math. Models Methods Appl. Sci.* 30.9 (2020), pp. 1809–1855. DOI: 10.1142/S0218202520500372.

[55] D. A. Di Pietro and A. Ern. "A hybrid high-order locking-free method for linear elasticity on general meshes". In: *Computer Methods in Applied Mechanics and Engineering* 283 (2015), pp. 1–21. DOI: 10.1016/j.cma.2014.09.009.

[56] D. A. Di Pietro and A. Ern. "Discrete functional analysis tools for discontinuous Galerkin methods with application to the incompressible Navier–Stokes equations". In: *Math. Comp.* 79 (2010), pp. 1303–1330. DOI: 10.1090/S0025-5718-10-02333-1.

[57] D. A. Di Pietro and A. Ern. "Equilibrated tractions for the Hybrid High-Order method". In: *C. R. Acad. Sci. Paris, Ser. I* 353 (2015), pp. 279–282. DOI: 10.1016/j.crma.2014.12.009.

[58] D. A. Di Pietro and A. Ern. *Mathematical aspects of discontinuous Galerkin methods*. Vol. 69. Mathématiques & Applications (Berlin) [Mathematics & Applications]. Springer, Heidelberg, 2012, pp. xviii+384. DOI: 10.1007/978-3-642-22980-0.

[59] D. A. Di Pietro, A. Ern, and J.-L. Guermond. "Discontinuous Galerkin methods for anisotropic semi-definite diffusion with advection". In: *SIAM J. Numer. Anal.* 46.2 (2008), pp. 805–831. DOI: 10.1137/060676106.

[60] D. A. Di Pietro, A. Ern, A. Linke, and F. Schieweck. "A discontinuous skeletal method for the viscosity-dependent Stokes problem". In: *Comput. Methods Appl. Mech. Engrg.* 306 (2016), pp. 175–195. DOI: 10.1016/j.cma.2016.03.033.

[61] D. A. Di Pietro, B. Kapidani, R. Specogna, and F. Trevisan. "An arbitrary-order discontinuous skeletal method for solving electrostatics on general polyhedral meshes". In: *IEEE Transactions on Magnetics* 53.6 (2017), pp. 1–4. DOI: 10.1109/TMAG.2017.2666546.

[62] D. A. Di Pietro and S. Krell. "A Hybrid High-Order method for the steady incompressible Navier–Stokes problem". In: *J. Sci. Comput.* 74.3 (2018), pp. 1677–1705. DOI: 10.1007/s10915-017-0512-x.

[63] D. A. Di Pietro and R. Specogna. "An a posteriori-driven adaptive Mixed High-Order method with application to electrostatics". In: *J. Comput. Phys.* 326.1 (2016), pp. 35–55. DOI: 10.1016/j.jcp.2016.08.041.

[64] L. Diening and F. Ettwein. "Fractional estimates for non-differentiable elliptic systems with general growth". In: *Forum Math.* 20.3 (2008), pp. 523–556. DOI: 10.1515/FORUM.2008.027.

[65] L. Diening, C. Kreuzer, and E. Süli. "Finite Element Approximation of Steady Flows of Incompressible Fluids with Implicit Power-Law-Like Rheology". In: *SIAM J. Numer. Anal.* 51.2 (2013), pp. 984–1015. DOI: 10.1137/120873133.

[66] J. Droniou, R. Eymard, T. Gallouët, C. Guichard, and R. Herbin. *The gradient discretisation method*. Vol. 82. Mathématiques & Applications (Berlin) [Mathematics & Applications]. Springer, Cham, 2018, pp. xxiv+497. ISBN: 978-3-319-79042-8; 978-3-319-79041-1.

[67] R. Duran, M. A. Muschietti, E. Russ, and P. Tchamitchian. "Divergence operator and Poincaré inequalities on arbitrary bounded domains". In: *Complex Var. Elliptic Equ.* 55.8-10 (2010), pp. 795–816. DOI: 10.1080/17476931003786659.

[68] E. Erturk, T. C. Corke, and C. Gökçöl. "Numerical solutions of 2-D steady incompressible driven cavity flow at high Reynolds numbers". In: *International Journal for Numerical Methods in Fluids* 48.7 (2005), pp. 747–774. DOI: 10.1002/fld.953.

[69] G. P. Galdi, R. Rannacher, A. M. Robertson, and S. Turek. "Hemodynamical flows". In: vol. 37. Oberwolfach Seminars 3. Birkhäuser, 2008. Chap. Mathematical Problems in Classical and Non-Newtonian Fluid Mechanics.

[70] G. P. Galdi, R. Rannacher, A. M. Robertson, and S. Turek. "Hemodynamical flows". In: vol. 37. Oberwolfach Seminars 3. Birkhäuser, 2008. Chap. Mathematical Problems in Classical and Non-Newtonian Fluid Mechanics.

[71] G. N. Gatica, Ma. Munar, and F. A. Sequeira. "A mixed virtual element method for the Navier-Stokes equations". In: *Math. Models Methods Appl. Sci.* 28.14 (2018), pp. 2719–2762. DOI: 10.1142/S0218202518500598.

[72] G. Geymonat and P. M. Suquet. “Functional spaces for Norton-Hoff materials”. In: *Math. Methods Appl. Sci.* 8.2 (1986), pp. 206–222. DOI: 10.1002/mma.1670080113.

[73] U. Ghia, K. N. Ghia, and C. T. Shin. “High-Re solutions for incompressible flow using the Navier-Stokes equations and a multigrid method”. In: *Journal of Computational Physics* 48.3 (1982), pp. 387–411. DOI: 10.1016/0021-9991(82)90058-4.

[74] R. Glowinski and A. Marrocco. “Sur l’approximation, par éléments finis d’ordre un, et la résolution, par pénalisation-dualité, d’une classe de problèmes de Dirichlet non linéaires”. In: *Rev. Française Automat. Informat. Recherche Opérationnelle Sér. Rouge Anal. Numér.* 9.R-2 (1975), pp. 41–76. ISSN: 0397-9342.

[75] R. Glowinski and J. Rappaz. “Approximation of a nonlinear elliptic problem arising in a non-Newtonian fluid flow model in glaciology”. In: *M2AN Math. Model. Numer. Anal.* 37.1 (2003), pp. 175–186. DOI: 10.1051/m2an:2003012.

[76] A. Hirn. “Approximation of the p-Stokes equations with equal-order finite elements”. In: *J. Math. Fluid Mech.* 15.1 (2013), pp. 65–88. DOI: 10.1007/s00021-012-0095-0.

[77] D. Irisarri and G. Hauke. “Stabilized virtual element methods for the unsteady incompressible Navier-Stokes equations”. In: *Calcolo* 56.4 (2019), Paper No. 38, 21. DOI: 10.1007/s10092-019-0332-5.

[78] T. Isaac, G. Stadler, and O. Ghattas. “Solution of nonlinear Stokes equations discretized by high-order finite elements on nonconforming and anisotropic meshes, with application to ice sheet dynamics”. In: *SIAM J. Sci. Comput.* 37.6 (2015), B804–B833. DOI: 10.1137/140974407.

[79] A. Janecka, J. Málek, V. Průša, and G. Tierra. “Numerical scheme for simulation of transient flows of non-Newtonian fluids characterised by a non-monotone relation between the symmetric part of the velocity gradient and the Cauchy stress tensor”. In: *Acta Mechanica* 230 (Mar. 2019), pp. 1–19. DOI: 10.1007/s00707-019-2372-y.

[80] S. Ko, P. Pustejovská, and E. Süli. “Finite element approximation of an incompressible chemically reacting non-Newtonian fluid”. In: *M2AN Math. Model. Numer. Anal.* 52.2 (2018), pp. 509–541. DOI: 10.1051/m2an/2017043.

[81] S. Ko and E. Süli. “Finite element approximation of steady flows of generalized Newtonian fluids with concentration-dependent power-law index”. In: *Math. Comp.* 88.6 (2018), pp. 1061–1090. DOI: 10.1090/mcom/3379.

[82] C. Kreuzer and E. Süli. “Adaptive finite element approximation of steady flows of incompressible fluids with implicit power-law-like rheology”. In: *M2AN Math. Model. Numer. Anal.* 50.5 (2016), pp. 1333–1369. DOI: 10.1051/m2an/2015085.

[83] D. Kröner, M. Růžička, and I. Toulopoulos. “Local discontinuous Galerkin numerical solutions of non-Newtonian incompressible flows modeled by p-Navier–Stokes equations”. In: *Journal of Computational Physics* 270 (2014), pp. 182–202. ISSN: 0021-9991. DOI: 10.1016/j.jcp.2014.03.045.

[84] O. A. Ladyzhenskaya. *The Mathematical Theory of Viscous Incompressible Flow*. 2nd ed. Gordon Breach, New York, 1969, pp. xiv+184. DOI: 10.1137/1006075.

[85] W. M. Lai, S. C. Kuei, and V. C. Mow. “Rheological Equations for Synovial Fluids”. In: *J. Biomech. Eng.* 100.4 (Nov. 1978), pp. 169–186. DOI: 10.1115/1.3426208.

[86] L. Lei and L. Jian-Guo. "p-Euler equations and p-Navier–Stokes equations". In: *Journal of Differential Equations* 264.7 (2018), pp. 4707–4748. ISSN: 0022-0396. DOI: 10.1016/j.jde.2017.12.023.

[87] J. Leray and J.-L. Lions. "Quelques résultats de Višik sur les problèmes elliptiques nonlinéaires par les méthodes de Minty-Browder". In: *Bull. Soc. Math. France* 93 (1965), pp. 97–107. URL: http://www.numdam.org/item?id=BSMF_1965__93__97_0.

[88] K. Lewandowska, A. Dabrowska, and H. Kaczmarek. "Rheological properties of pectin, poly(vinyl alcohol) and their blends in aqueous solutions". In: *E-Polymers* 016 (Jan. 2012), p. 1. DOI: 10.1515/epoly.2012.12.1.160.

[89] J.-L. Lions and E. Magenes. *Non-homogeneous boundary value problems and applications. Vol. I*. Translated from the French by P. Kenneth, Die Grundlehren der mathematischen Wissenschaften, Band 181. Springer-Verlag, New York-Heidelberg, 1972, pp. xvi+357.

[90] W. Liu and N. Yan. "Quasi-norm a priori and a posteriori error estimates for the nonconforming approximation of p-Laplacian". In: *Numer. Math.* 89 (2001), pp. 341–378.

[91] X. Liu and Z. Chen. "The nonconforming virtual element method for the Navier-Stokes equations". In: *Adv. Comput. Math.* 45.1 (2019), pp. 51–74. DOI: 10.1007/s10444-018-9602-z.

[92] J. Málek and K. R. Rajagopal. "Mathematical issues concerning the Navier–Stokes equations and some of their generalizations". In: *Evolutionary Equations*. Vol. 2. Handbook of Differential Equations. Elsevier/North-Holland, Amsterdam, 2005, pp. 371–459.

[93] J. Málek, K. R. Rajagopal, and M. Růžička. "Existence and regularity of solutions and the stability of the rest state for fluids with shear dependent viscosity". In: *Math. Models Methods Appl. Sci.* 5.6 (1995), pp. 789–812. DOI: 10.1142/S0218202595000449.

[94] G. J. Minty. "On a "monotonicity" method for the solution of non-linear equations in Banach spaces". In: *Proc. Nat. Acad. Sci. U.S.A.* 50 (1963), pp. 1038–1041.

[95] I. Pérez-Reyes, R. Vargas, S. Perez-Vega, and A. S. Ortiz-Perez. "Applications of Viscoelastic Fluids Involving Hydrodynamic Stability and Heat Transfer". In: Oct. 2018. DOI: 10.5772/intechopen.76122.

[96] M. Růžička and L. Diening. "Non-Newtonian fluids and function spaces". In: *Nonlinear Analysis, Function Spaces and Applications*. Praha: Institute of Mathematics of the Academy of Sciences of the Czech Republic, 2007, pp. 95–143.

[97] D. Sandri. "Numerical analysis of a four-field model for the approximation of a fluid obeying the power law or Carreau's law". In: *Japan Journal of Industrial and Applied Mathematics* 31.3 (2014), pp. 633–663. DOI: 10.1007/s13160-014-0155-3.

[98] D. Sandri. "Sur l'approximation numérique des écoulements quasi-newtoniens dont la viscosité suit la loi puissance ou la loi de Carreau". In: *M2AN Math. Model. Numer. Anal.* 27.2 (1993), pp. 131–155. URL: http://www.numdam.org/item/M2AN_1993__27_2_131_0.

[99] P. Saramito. *Complex fluids : modeling and algorithms*. Springer, 2016. DOI: 10.1007/978-3-319-44362-1.

[100] L. Schmitt, G. Ghnassia, J. J. Bimbenet, and G. Cuvelier. "Flow properties of stirred yogurt: Calculation of the pressure drop for a thixotropic fluid". In: *Journal of Food Engineering* 37 (1998). 7 graph., pp. 367–388.

[101] G. Schubert, D. L. Turcotte, and P. Olson. *Mantle Convection in the Earth and Planets*. Cambridge University Press, 2001. DOI: 10.1017/CBO9781051161287.

[102] V. Suja and A. Barakat. "A Mathematical Model for the Sounds Produced by Knuckle Cracking". In: *Scientific Reports* 8 (Mar. 2018). DOI: 10.1038/s41598-018-22664-4.

[103] H. D. Ursell. "Inequalities between sums of powers". In: *Proc. London Math. Soc. (3)* 9 (1959), pp. 432–450. DOI: 10.1112/plms/s3-9.3.432.

[104] L. Veiga, F. Brezzi, A. Cangiani, G. Manzini, L. Marini, and A. Russo. "Basic principles of Virtual Element Methods". In: *Mathematical Models and Methods in Applied Sciences* 23 (Nov. 2012). DOI: 10.1142/S0218202512500492.

[105] K. Yasuda, R.C. Armstrong, and R.E. Cohen. "Shear flow properties of concentrated solutions of linear and star branched polystyrenes". In: *Rheologica Acta* 20.2 (Mar. 1981), pp. 163–178. DOI: 10.1007/BF01513059.

[106] K. Yeleswarapu. "Evaluation of Continuum Models for Characterizing the Constitutive Behavior of Blood". In: *PhD Thesis* (Jan. 1996).

[107] N. Zamani, R. Kaufmann, P. Kosinski, and A. Skauge. "Mechanisms of Non-Newtonian Polymer Flow Through Porous Media Using Navier–Stokes Approach". In: *Journal of Dispersion Science and Technology* 36.3 (2015), pp. 310–325. DOI: 10.1080/01932691.2014.896221.

[108] Z. Żołek-Tryznowska. "Rheology of Printing Inks". In: Dec. 2016, pp. 87–99. DOI: 10.1016/B978-0-323-37468-2.00006-3.